PETROLOGICAL STUDIES WITHIN THE IRON MASK BATHOLITH, SOUTH CENTRAL BRITISH COLUMBIA

By

LORI D. SNYDER

B.S., Colorado State University, 1990

A THESIS SUBMITTED IN PARTIAL FULFILLMENT OF THE REQUIREMENTS FOR THE DEGREE OF MASTER OF SCIENCE

in

THE FACULTY OF GRADUATE STUDIES
DEPARTMENT OF GEOLOGICAL SCIENCES

We accept this thesis as conforming to the required standard

THE UNIVERSITY OF BRITISH COLUMBIA

June, 1994

In presenting this thesis in partial fulfilment of the requirements for an advanced degree at the University of British Columbia, I agree that the Library shall make it freely available for reference and study. I further agree that permission for extensive copying of this thesis for scholarly purposes may be granted by the head of my department or by his or her representatives. It is understood that copying or publication of this thesis for financial gain shall not be allowed without my written permission.

Department of GEOLOGICAL SCIENCES

The University of British Columbia
Vancouver, Canada

Date 14 June 1994

DE-6 (2/88)

ABSTRACT

The alkalic Early Jurassic Iron Mask batholith (204 ± 5 Ma) intrudes Late Triassic Nicola Group volcanic rocks of the Quesnellia terrane in south-central British Columbia. The batholith consists of three intrusive rock units which are, from oldest to youngest, Pothook diorite, Cherry Creek monzodiorite to monzonite and Sugarloaf diorite and one "hybrid" unit (Iron Mask hybrid). Pothook and Cherry Creek rocks are locally gradational, contain clinopyroxene or biotite as the major mafic phase and define a chemical trend in major element space. Sugarloaf rocks intrude all other Iron Mask units, contain abundant hornblende and sparse clinopyroxene and do not follow the linear major-element trends defined by the other units. Primary quartz is rarely found in a few samples from the Cherry Creek and Sugarloaf units. REE profiles from the intrusive units are very similar, showing slight enrichment of LREE's and no evidence of plagioclase fractionation. These intrusive units are part of a complex magmatic system and appear not to be related through simple fractionation processes.

The Iron Mask hybrid unit is highly variable in texture and composition; it is divided into three types. Type I and II are characterized by abundant (partially digested) xenoliths, many of which are derived from Nicola Group rocks. Type III is xenolith-poor and exhibits extreme textual variation on an outcrop scale. The Iron Mask hybrid is postulated to represent the effects of progressive assimilation of Nicola Group rocks by Pothook magma. This postulate is supported by REE data. One consequence of selective assimilation processes is the potential for increasing the volatile content of the melt. It is shown that thermal dehydration and partial assimilation of Nicola Group rocks by Pothook magma is a valid method for promoting early volatile saturation in the melt.

Xenoliths and blocks of serpentinized picritic basalt are found within the Iron Mask batholith. These exposures are correlated with relatively well-preserved picritic basalt from three localities outside of the Iron Mask batholith on the basis of texture, mineralogy and chemistry. The Kamloops Lake picritic basalts represent an episode of ultramafic volcanism during the latter stages of Nicola volcanism. The rocks are olivine ± clinopyroxene porphyritic. Olivine compositions range from $Fo_{89.5}$ to $Fo_{92.9}$. Clinopyroxene MG#'s [$100 \cdot Mg/(Mg + Fe^{2+}$] range from 87.1 to 99.7 with calculated Fe_2O_3 contents of 1.44 to 6.66 wt% and Cr-spinel is also highly oxidized ($100 \cdot Fe^{3+}/(Fe^{3+} + Al + Cr)$ from 13.7 to 82.9). Mineral compositions, as well as incompatible element patterns for bulk rocks indicate crystallization from an island-arc primary magma under oxidizing conditions. REE profiles indicated olivine control on the pattern and abundances.

Calculation of T-$\ln fO_2$ paths, primary melt compositions and olivine crystallization suggest that the Kamloops Lake rocks contain a significant cumulate component. The results support crystallization under high oxygen fugacity from a magma with 14.9 to 20.5 wt% MgO.

TABLE OF CONTENTS

LIST OF FIGURES

LIST OF TABLES

LIST OF PLATES

ACKNOWLEDGEMENTS

I wish to thank J.K. Russell, my supervisor, for his endless enthusiasm and innovative approaches to evaluating petrologic processes. This document was greatly improved by his numerous edits, helpful discussions and mathematical expertise. Constructive comments from and discussions with J.F.H. Thompson, J.R. Lang, C.R. Stanley and B.R. Edwards are gratefully appreciated. Thanks are also extended to M. Raudsepp, whose electron microprobe expertise was invaluable in collecting and analyzing mineral compositions. Technical support from M. Baker is appreciated.

Special appreciation is extended to J. Brian Mahoney for his constructive review of this document and for his encouragement, understanding and patience throughout the process.

Normative mineralogy was calculated with NEWPET provided by Daryl Clarke at the Memorial University of Newfoundland. Error propagation for Pearce Element Ratio diagrams was performed by a Turbo Pascal program PRATIO provided by J. Nicholls at the University of Calgary and modified by Y. Cui.

Funding for this project was provided by Natural Sciences and Engineering Research Council of Canada, the Science Council of British Columbia and industry sponsors through The Mineral Deposit Research Unit at The University of British Columbia on the research project "Copper-Gold Porphyry Deposits of British Columbia". A University Graduate Fellowship grant is gratefully acknowledged. Thanks are extended to Afton Operating Corporation and Teck Corporation for access to their property and records.

1.0 INTRODUCTION

1.1 STUDY AREA AND REGIONAL SETTING

The Iron Mask batholith is located in the Quesnellia terrane of the Intermontane Belt in south-central British Columbia (Figure 1.1). It is composed of two separate bodies, the Cherry Creek pluton in the north and the Iron Mask batholith in the south. The batholith is a composite alkaline intrusive of Early Jurassic age (205 ± 4 Ma; Mortensen and Ghosh, in review) which hosts numerous porphyry style copper-gold deposits, some of which have produced significant quantities of these metals (Kwong, 1987). The batholith also hosts magnetite-apatite lodes in vein structures (Cann, 1979). The batholith consists of three intrusive rock units (Pothook, Cherry Creek and Sugarloaf) and one hybridized unit (Iron Mask hybrid).

The Iron Mask batholith intrudes the Late Triassic Nicola Group which comprises an extensive sequence of volcanic, volcaniclastic and subordinate sedimentary rocks in the Quesnellia terrane. Nicola Group rocks are interpreted as a volcanic arc which was accreted onto the western margin of North America in the Late Triassic (Monger, et al. 1982, Monger 1989a). Eocene Kamloops Group volcanic rocks are also exposed in the area of the Iron Mask batholith (Ewing, 1981a, 1981b, 1982). Alkali basalt flows and minor sediments are exposed in a graben structure separating the two Iron Mask masses and as small, flat-lying erosional remnants in the Iron Mask batholith.

The Iron Mask batholith is geographically located in southwestern British Columbia approximately 10km southwest of the city of Kamloops. The area is characterized by an arid climate with annual rainfall averaging about 26cm. Broad, rolling hills with elevations between 610 and 1100m are dominated by sagebrush and sparse Ponderosa pine and Douglas fir. Glacial overburden reaches 100m in thickness in some locations. Access to the Iron Mask batholith is excellent with major thoroughfares and

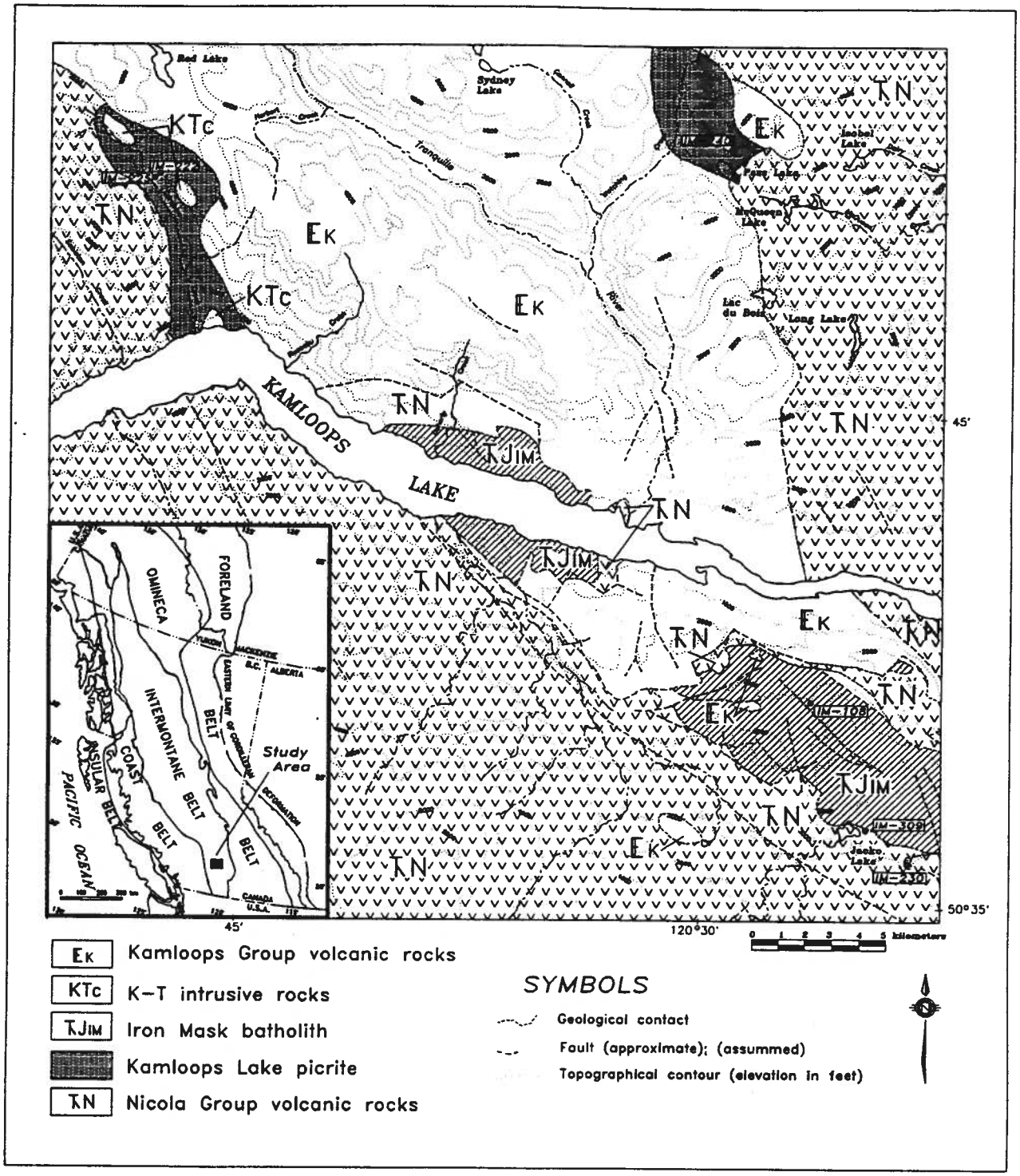

Figure 1.1 Location of the Iron Mask batholith and the Kamloops Lake picritic basalts in the southern Canadian Cordillera.

abundant secondary ranching and mining roads. Outcrop is poor, especially in the southern portion of the batholith.

Within the Iron Mask batholith, lenticular bodies of serpentinite are found. These rocks have been interpreted as intrusive into the batholith during the middle stages of formation (see Figure 2.3) (Northcote, 1977, Kwong, 1987). Bodies of picritic basalt found outside of the batholith have been previously identified (Mathews, 1941; Cockfield, 1948; Monger, 1989b) and investigation of these localities suggested that they may be equivalent to the serpentinite in the Iron Mask batholith. Thus, documentation and characterization of these ultramafic rocks is important in interpreting the magmatic history of the study area.

The Kamloops Lake picritic basalts outcrop within an area of approximately 35km^2 with the Iron Mask batholith at the southeastern corner (Figure 1.1). Relatively fresh rocks are found in three localities while the fourth locality is serpentinite blocks within the Iron Mask batholith. The exact stratigraphic position and age of the Kamloops Lake picrites is unclear. The exposures lie stratigraphically on top of Nicola Group rocks and are found within the Iron Mask batholith. These relationships constrain the age of the ultramafic volcanic event to be Latest Triassic or Earliest Jurassic.

1.2 SCOPE OF RESEARCH

This thesis is presented in two parts. The first section addresses the petrology, geochemistry and magmatic history of the Iron Mask batholith and the second addresses the geochemistry, magmatic conditions and tectonic affinity of the Kamloops Lake picritic basalts.

The Iron Mask batholith is composed of three distinct intrusive rock units and one hybrid rock unit; the first section of this document describes field relationships, texture, mineralogy, mineral chemistry and major, trace and REE chemistry of these rock units. These data test whether the intrusive

units are cogenetic. In addition, these data elucidate processes involved in formation of the Iron Mask hybrid unit. Specifically, this process involves the selective dehydration and assimilation of material derived from the surrounding Nicola Group volcanic rocks into the Iron Mask magma. Effects of these processes in terms of volatile budget in the system are addressed.

The second part of this thesis describes and classifies the Kamloops Lake picritic basalts. These ultramafic rocks are investigated in light of new information on their origin, occurrence and significance. The Kamloops Lake picritic basalts consist of small, disconnected exposures which have been correlated on the basis of stratigraphic position, mineralogy, mineral chemistry and major, minor and REE chemistry. Mineralogical and chemical data obtained from the Kamloops Lake picritic basalts are compared to data from other ultramafic rock suites to infer origin, magmatic processes and tectonic affinity. Pearce element ratio plots test cogenetic relationships and constrain fractionation processes. Oxygen fugacity during crystallization is modeled through equilibrium calculation of bulk-rock chemistry and observed olivine composition.

Together, these two lines of research elucidate the magmatic history of part of the southern Quesnellia terrane in the Late Triassic and Early Jurassic. The petrochemical data obtained from the Iron Mask batholith and the magmatic processes they document may be used in evaluating the relative timing and style of mineralization at the different deposits within the batholith. The identification and characterization of a previously unrecognized ultramafic volcanic event may aid in interpretation of the tectonic history of this part of the Canadian Cordillera.

2.0 IRON MASK BATHOLITH

2.1 INTRODUCTION

The Iron Mask batholith, located in the Quesnellia Terrane of the southern Intermontane Belt (Figure 2.1), is one of several Early Jurassic (205 ± 4 Ma; Mortensen and Ghosh, in review) alkalic intrusions in British Columbia. Porphyry-style copper-gold mineralization is found throughout the

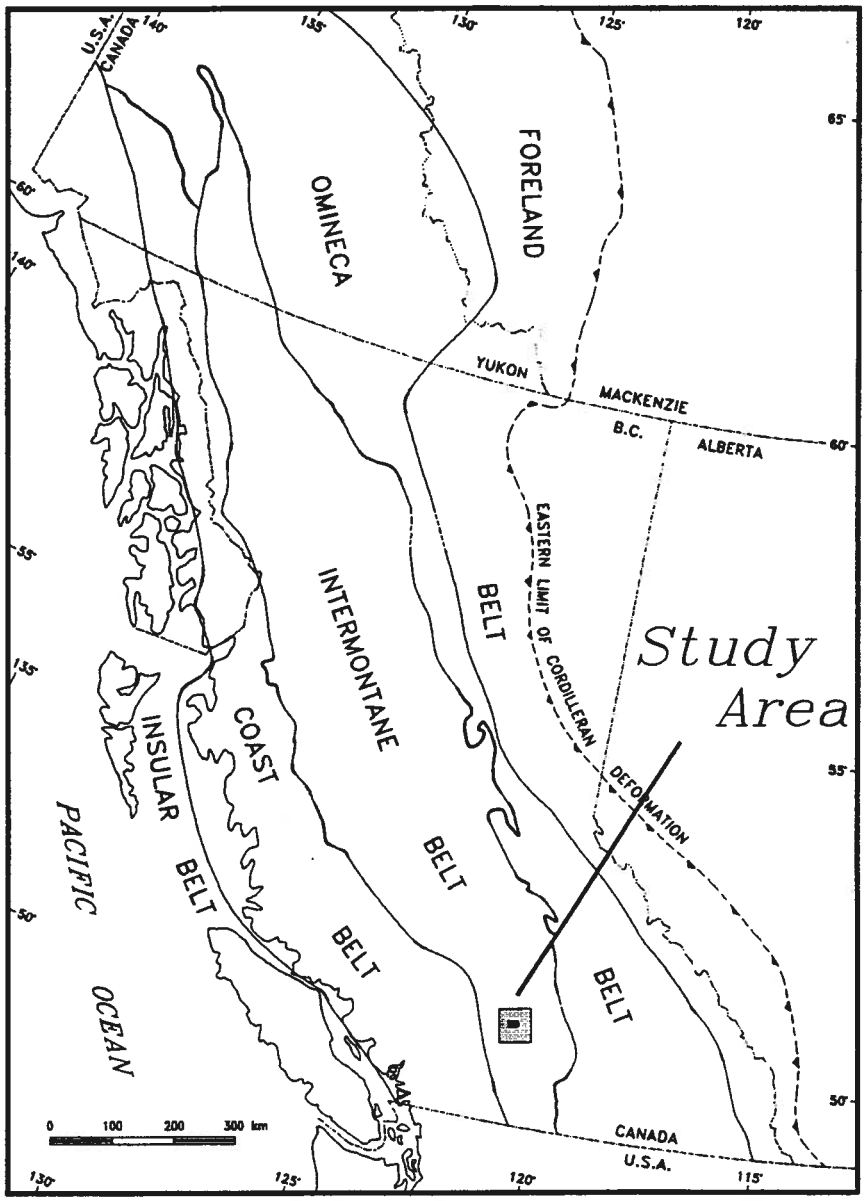

Figure 2.1. Location of the Iron Mask batholith in south-central British Columbia.

batholith (Carr and Reed, 1976; Ross, et al., in review; Lang and Stanley, in review) and the Afton, Ajax, Crescent and Pothook deposits have produced significant quantities of these metals (Kwong, 1987; Ross et al., in review). The Iron Mask batholith also hosts vein-style magnetite/apatite lode deposits (Cann, 1979).

This paper describes the texture, mineralogy, chemistry and origins of the intrusive rock types comprising the Iron Mask batholith. We summarize the geochemical evolution and intrusive styles of the Iron Mask batholith and investigate magmatic relationships, magmatic differentiation and temporal evolution. Processes and consequences of selective magmatic assimilation and melt contamination are also addressed. These igneous processes are particularly important in resolving the genesis of the enigmatic Iron Mask hybrid unit which comprises a significant portion of the exposures within the batholith. Our analysis provides a template upon which to investigate and classify the individual porphyry copper-gold deposits within the batholith (Ajax, Pothook, Crescent).

2.2 REGIONAL GEOLOGY

The Iron Mask batholith is located approximately 10km southwest of the city of Kamloops. This area is characterized by an arid climate and consists mainly of broad, rolling hills which are dominated by sagebrush and sparse pine forest vegetation. Access is excellent with major thoroughfares and abundant secondary ranching and mining roads. Outcrop exposure is poor, especially in the southern portion of the Iron Mask pluton.

Mathews (1941) and Cockfield (1948) were the first to describe the geology of the Iron Mask batholith. More detailed petrologic descriptions are provided by Carr (1956) and Preto (1967) with emphasis on exploration activities within the batholith. Northcote (1974, 1976, 1977) remapped the batholith and documented the major textural and mineralogical characteristics of the intrusive units. Kwong (1987) produced a geological map of the Iron Mask batholith compiled from previous workers.

This paper and previous work of Snyder and Russell (1993) revises the age relationships between the intrusive rock units and the origins of several map units.

The Iron Mask batholith intrudes rocks of the Upper Triassic Nicola Group which comprise an areally extensive (70km x 190km) and thick (7000m) sequence of volcanic, volcaniclastic and related sedimentary rocks distributed across the Quesnellia terrane (Schau, 1970; Preto, 1977, 1979; Mortimer, 1987). Nicola Group rocks have been interpreted to represent a volcanic arc which was accreted onto the western margin of North America in the Middle Jurassic (Monger et al., 1982; Monger, 1989a). They have been subdivided by Preto (1977) into three distinct, sub-parallel, north-trending belts. The Iron Mask batholith intrudes the eastern-most Nicola volcanic belt which comprises a sequence of alkalic flows, flow breccias and related sediments. The Nicola rocks are broadly folded and regionally metamorphosed to zeolite, prehnite-pumpellyite, and greenschist facies (Mortimer, 1987).

Adjacent to the Iron Mask batholith, Nicola Group rocks consist of green to purple coloured basaltic and andesitic clinopyroxene-phyric flows and flow breccias, light green massive tuffs, and green andesite to dacite bedded ash to lapilli tuffs. Minor amounts of hematitic, poorly bedded chert and dark grey plagioclase-phyric flows and dykes are also present. Nicola Group rocks are commonly foliated near the margin of the batholith and copper mineralization is observed in many outcrops (Cockfield, 1948; Carr, 1956). Olivine porphyritic picritic basalt is found outside the western margin of the batholith near Jacko Lake (Mathews, 1941).

The Iron Mask batholith intruded Nicola Group rocks along deep-seated structures (Preto, 1967; Northcote, 1974, 1976, 1977). It consists of two separate masses; 1) the northwest trending 5 x 20km Iron Mask batholith in the south, and 2) the smaller (5 x 5km) Cherry Creek pluton to the north (Figure 2.2; Plate 2.1). Contacts between the Iron Mask batholith and Nicola Group are either faulted (on the eastern margin), intrusive (observed along the western contact) or not exposed. Locally, Nicola Group rocks are hornfelsed up to 50m from intrusive contacts and recrystallized clasts of Nicola origin are found within

Iron Mask rock units, being particularly abundant along the western margin. Larger screens and pods of sheared, altered and metamorphosed Nicola Group rocks are also present, especially in mineralized areas (Ross, et al., 1993; Stanley, 1994). The association between mineralization and screens of country rock may reflect either common control along permeable shear zones or bias imposed by extensive mapping around mineralized zones.

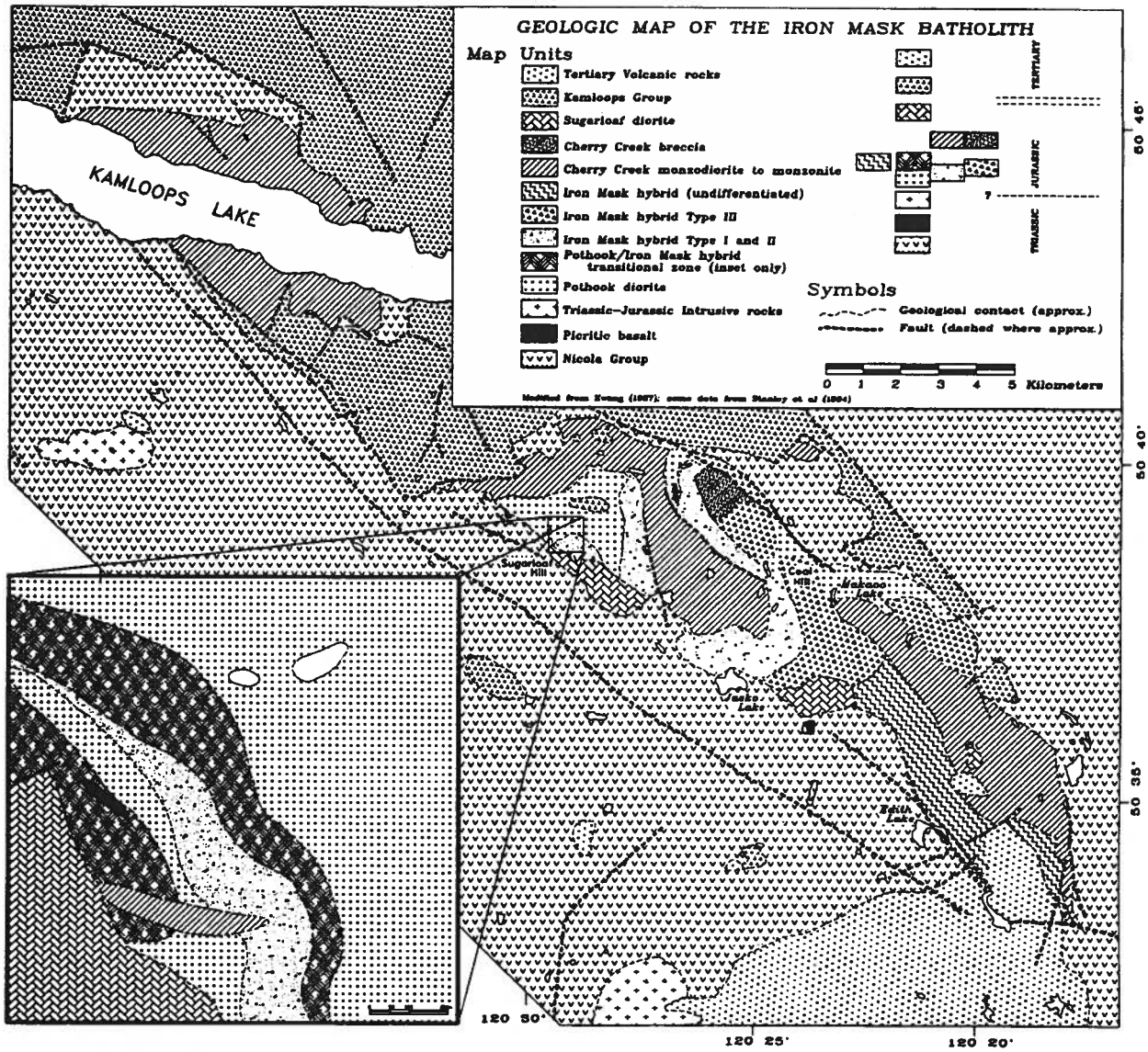

Figure 2.2. Geologic map of the Iron Mask batholith. Modified from Kwong (1987) and Stanley et al., 1994. Inset illustrates the transitional zone between the Pothook suite and the Iron Mask hybrid unit (Type II).

Eocene Kamloops Group volcanic rocks are exposed as small, flat-lying erosional remnants atop the Iron Mask batholith and within an east-west trending graben which separates the batholith from the Cherry Creek pluton (Figure 2.2; Northcote, 1977; Ewing, 1982; Kwong, 1987). The Kamloops Group consists dominantly of alkali olivine basalt flows with minor intercalated sediments (Ewing, 1981a, 1981b). Kwong (1987) reports small exposures of other Tertiary volcanic rocks within the Iron Mask pluton.

2.3 ROCK TYPES IN THE IRON MASK BATHOLITH

Five areas within the Iron Mask batholith were chosen for detailed study to investigate the relationships among the units. These maps and their location within the batholith are shown in Appendix A. The Iron Mask batholith comprises three distinct intrusive rock types (Figure 2.2, Plate 2.1). Based on the revised stratigraphy (Figure 2.3), the intrusive units are, from oldest to youngest: gabbro and diorite of the Pothook phase, Cherry Creek monzodiorite to monzonite and Sugarloaf diorite. The Iron Mask batholith also contains an enigmatic rock unit characterized by abundant partially digested xenoliths and extreme compositional and textural variability. Previous workers have called this rock type the Iron Mask hybrid unit and identified it as an agmatite (Northcote, 1977). Defined by Mehnert (1971), agmatite is a migmatite structure derived solely from the brecciation of pre-existing metamorphic rocks by magma, wherein breccia fragments experience minimal transport and can be rejoined without gaps. In this paper, the name 'Iron Mask hybrid' is retained but an 'agmatite' origin will be shown as invalid for the majority of the unit. Hybrid rocks are interpreted to be coeval with intrusion of the Pothook diorite.

Pods and screens of serpentinized picritic basalt up to 250m in exposed length are scattered throughout the Iron Mask batholith. Previously, these ultramafic rocks were interpreted to have been intruded into the batholith (Figure 2.3) although not genetically related (Preto, 1967, Kwong, 1987). Relatively unaltered picritic basalt occurs outside the batholith margin near Jacko Lake and on the north side of Kamloops Lake near Watching Creek and Carabine Creek (Cockfield, 1948). These rocks were

grouped by Monger (1989b) with the Iron Mask intrusive suite. These exposures, however, are shown to represent arc-derived ultramafic volcanic rocks stratigraphically at the top of the Nicola Group and they are unrelated to the Iron Mask batholith rocks.

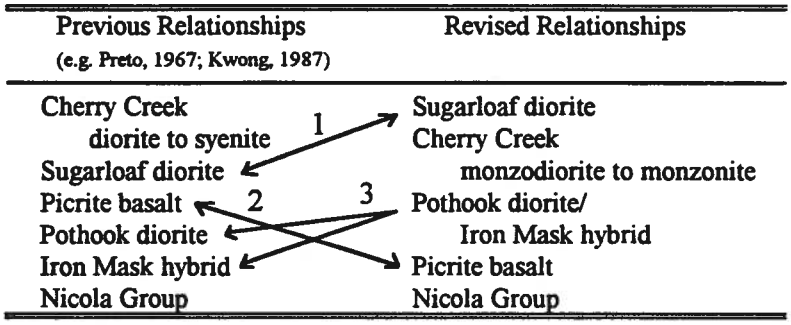

Figure 2.3. Age relationships of the igneous units of the Iron Mask batholith. The major revisions are: Sugarloaf intrusive rocks are the youngest magmatic event, serpentinized picritic basalt is pre-Iron Mask, and the Iron Mask hybrid is contemporaneous and genetically associated with the Pothook diorite.

2.3.1 Pothook Diorite

Pothook diorite comprises a large portion of the northern part of the Iron Mask batholith. It is a greenish coloured, equigranular, slightly to moderately foliated, medium to coarse-grained biotite-pyroxene diorite. Subhedral, 0.5 to 2mm plagioclase feldspar comprises 40 to 65% of Pothook rocks. It is commonly sericitized but, where preserved, exhibits compositions ranging from An_{43} to An_{52}; zoning is rarely observed. Euhedral to subhedral clinopyroxene accounts for 15 to 25% of the rock and ranges in size from 0.2 to 3mm. It is colourless or light green; grains are weakly pleochroic from pale yellow to pale green. Clinopyroxene commonly contains opaque inclusions and in some samples, exsolution 'crosses' of spinel are observed. Pothook diorite was originally defined by the presence of poikilitic biotite (Northcote, 1974), which occurs from 5 to 15% as subhedral to anhedral grains enclosing plagioclase and clinopyroxene. Commonly, the biotite is corroded and intergrown with epidote ± clinopyroxene along cleavage planes (Plate 2.2). Magnetite, which comprises 5 to 15% of the rock, is subhedral to anhedral and ranges from 0.2 to 0.4mm. It is both disseminated and concentrated in centimetre-sized veinlets. Locally, metre-sized veins of magnetite ± apatite occur creating lode deposits such as the Magnet showing

(Cann, 1979). Primary K-feldspar is a minor constituent in some samples; it may range up to a few percent as subhedral to anhedral, interstitial crystals and large poikilitic grains enclosing plagioclase and clinopyroxene.

Apatite is an abundant accessory mineral; euhedral grains which are closely associated with clinopyroxene may comprise up to 3% of Pothook rocks. Titanite and rare zircon are present in trace amounts. Alteration minerals found in Pothook rocks include K-feldspar, sericite, epidote and chlorite.

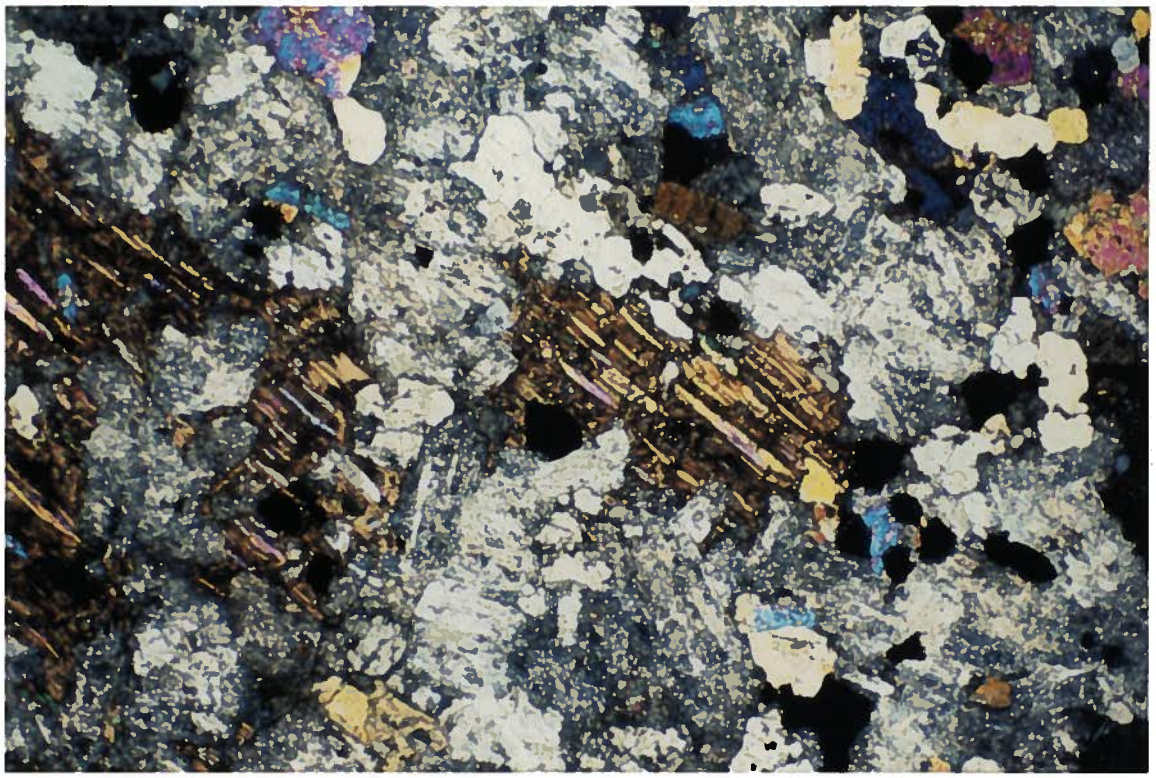

Plate 2.2. Photomicrograph of typical poikilitic biotite characteristic of the Pothook diorite unit. The grain is intergrown with secondary epidote. FOV=5mm.

Near contacts with the Cherry Creek unit, the Pothook diorite has commonly been affected by potassic alteration. This metasomatism is manifested by potassium feldspar veinlets with coalescing alteration envelopes and, less commonly, as truly pervasive alteration (Stanley, 1994; Lang, 1994; Lang and Stanley, in review). Locally, the K-feldspar metasomatism is intense, obliterating primary minerals and textures (Stanley, 1994; Lang, 1994).

2.3.2 Cherry Creek Monzodiorite to Monzonite

The Cherry Creek unit was defined by early workers to span the compositional range from diorite to syenite (Kwong, 1987), however, the 'Cherry Creek syenite' appears to be a manifestation of extreme potassium metasomatism of Pothook and Cherry Creek phases along their contacts. Because of this phenomenon, previous maps of the batholith have tended to over-represent Cherry Creek rocks and under-estimate exposed Pothook rocks.

Cherry Creek rocks range from monzodiorite to monzonite. They are fine to medium grained and characterized by subhedral, interlocking plagioclase feldspar. Plagioclase makes up 45 to 65% of the rock, is commonly sub-trachytic to trachytic and, where preserved, has compositions ranging from An_{35} to An_{45}. Both unzoned and strongly normal-zoned plagioclase are observed and a few samples contain unzoned, well-twinned crystals with thin, discontinuous, untwinned, zoned plagioclase overgrowths. Clinopyroxene is the major ferromagnesian mineral (5 to 25%) in most Cherry Creek rocks. It ranges from 0.2 to 0.5mm and forms euhedral to subhedral, colourless to very light green, slightly aligned crystals containing sparse inclusions of opaque minerals. Cherry Creek rocks contain up to 20% biotite as well-preserved, light brown, weakly aligned crystals locally enclosing plagioclase and pyroxene. A few samples contain minor amounts of a second population similar to 'Pothook' biotite (corroded, strongly poikilitic, and intergrown with epidote ± clinopyroxene). Modal K-feldspar content of Cherry Creek is highly variable, ranging from 3 to 15%, and occurring as anhedral interstitial crystals commonly altered to clay minerals. Subhedral to anhedral magnetite disseminated throughout the groundmass comprises 5 to 10% of Cherry Creek rocks. Locally, minor chloritized primary hornblende is observed. It is a medium green with a pleochroic scheme of green-light brown-light yellow. Rare primary quartz is present up to 5% as interstitial grains.

Accessory minerals in the Cherry Creek include apatite, zircon and titanite. Abundant anhedral, ragged titanite is found in a few samples and is interpreted to be secondary in origin. Epidote, sericite and K-feldspar are other common alteration minerals. Stanley (1994) reported secondary quartz in miarolitic cavities at the Pothook Pit in the northwestern part of the Iron Mask batholith.

Excellent exposures of a monzonite intrusion breccia occur in the north-central portion of the batholith (Figure 2.2; Figure A.4; Plate 2.1; Plate 2.3). Originally identified as Iron Mask hybrid unit (Northcote, 1977; Kwong, 1987), these rocks are interpreted as an intrusion breccia associated with emplacement of the Cherry Creek phase. Clasts ranging in size from 0.03 to 1 metre are set in a matrix of fine to medium grained biotite monzonite. The clasts consist of rocks derived from the Iron Mask hybrid unit as well as recrystallized rock fragments interpreted as Nicola Group. The boundaries between the clasts and matrix are diffuse or sharp with the sharpest contacts found at the higher elevations. The breccia zone is intruded by abundant northwest and northeast oriented, 0.5 to 15m, fine-grained, light grey biotite monzonite dykes interpreted as part of the Cherry Creek phase. Several similar localities of intrusion breccia are located to the west of the large breccia zone, but are not at mappable scale.

2.3.3 Sugarloaf diorite

The Sugarloaf unit comprises a suite of hornblende-phyric dioritic rocks exposed as lenticular bodies and dykes in the western part of the batholith and in adjacent Nicola Group. Rocks of the Sugarloaf phase are distinctive for their porphyritic nature, manifested by abundant, locally trachytic phenocrysts of amphibole in a fine-grained groundmass. Locally, lesser subhedral to anhedral phenocrystic plagioclase is present.

Sugarloaf diorite contains 25 to 55%, 0.5 to 1mm, euhedral to subhedral plagioclase grains which are locally trachytic and commonly altered to sericite or saussurite. Where preserved, plagioclase has compositions ranging from An_{32} to An_{38}. Amphibole, commonly altered to chlorite, makes up 15 to

Plate 2.3. Field photograph of monzonite intrusion breccia with clasts of Iron Mask hybrid and recrystallized Nicola Group rocks. Intrusion is assumed to have a Cherry Creek affinity.

55% of the rock as euhedral to subhedral, locally aligned crystals up to 3mm in length. Minor clinopyroxene occurs as 0.5mm rounded, corroded grains. Magnetite is present in minor amounts as euhedral to subhedral grains up to 0.5mm. Rarely, primary K-feldspar comprises up to 10% of Sugarloaf rocks.

Accessory minerals in Sugarloaf rocks include apatite, titanite and rare quartz. Secondary minerals include epidote, chlorite and minor calcite. The secondary K-feldspar occurs rarely as small veinlets, large poikilitic grains, and interstitial grains. Albitization is the most prominent style of alteration in Sugarloaf rocks and is especially intense near mineralized zones (Lang and Stanley, in review). At the Ajax East pit, secondary albite has destroyed much of the original texture (Ross et al., 1993; Ross et al., in review).

Rocks assigned to the Sugarloaf unit span a variety of hornblende-phyric rocks. At Sugarloaf Hill, the outcrops are light grey and are characterized by stubby, aligned hornblende phenocrysts, trachytic tabular plagioclase and lesser rounded pyroxene in an aphanitic groundmass. Near Jacko Lake at the southwest margin of the batholith, the rocks are light tan and contain abundant bladed hornblende phenocrysts, commonly in radial aggregates, and sparse anhedral plagioclase phenocrysts. These exposures are intruded by abundant northwest-trending dark grey, fine-grained dykes containing abundant disseminated magnetite and chalcopyrite interpreted to belong to the Sugarloaf phase.

2.3.4 Iron Mask Hybrid

The Iron Mask hybrid unit accounts for approximately 45% of the mappable exposure of the Iron Mask batholith. It is mineralogically and texturally diverse and is subdivided on the basis of texture and clast abundance into three main types. Type I Iron Mask hybrid is confined to thin (50 to 75m) discontinuous zones along contacts between the Iron Mask batholith and the Nicola Group. It is an intrusive breccia characterized by abundant (60 to 80%) angular fragments which are themselves derived from immediately adjacent Nicola Group. Matrix in Type I hybrid is fine to medium grained pyroxene ± hornblende diorite. Type II Iron Mask hybrid is characterized by abundant xenoliths (10 to 80%) of volcanic, plutonic and recrystallized sedimentary rocks (Plate 2.4). This heterolithic variety is exposed near the margins of Pothook dioritic stocks in the western and central portions of the batholith. Within Type II hybrid, the clasts have reacted to varying degrees with the enclosing magma. Some clasts are angular with sharp boundaries where as others are rounded with diffuse boundaries and plagioclase crystals spanning the xenolith-matrix interface. The igneous matrix of Type II is texturally variable on an outcrop scale. In many areas the matrix consists predominantly of fine to coarse grained interlocking, randomly oriented grains of pyroxene, biotite, plagioclase, euhedral magnetite and rare hornblende. In other locations, it consists of fine to medium grained, trachytic hornblende and plagioclase with euhedral magnetite and lesser amounts of subhedral pyroxene and subhedral to anhedral biotite. Mineral abundances are characteristically non-uniform and locally the matrix is anorthositic.

Plate 2.4. Typical Type II Iron Mask hybrid showing recrystallized and partially digested clasts.

Type III Iron Mask hybrid dominates the northeastern portion of the batholith. These rocks have fewer (<10%) xenoliths which are generally highly recrystallized and digested. Type III hybrid varies from fine-grained to almost pegmatitic on an outcrop scale with and pods and dykelets of different compositional and textural characteristics randomly distributed. Modal mineral proportions vary greatly between outcrops, however, there is some relationship between grain size and mineralogy. Coarser grained patches in Type III are characterized by subhedral, equant grains of clinopyroxene and plagioclase with disseminated coarse magnetite. The clinopyroxene is commonly chloritized and rimmed by dark brown amphibole. Locally, some coarser grained rocks contain trachytic, acicular megacrysts (up to 15 cm in length) of amphibole which encloses clinopyroxene and plagioclase. Finer grained material in Type III is dominantly trachytic hornblende and normally zoned plagioclase with lesser amounts of pyroxene and disseminated magnetite.

Type III Iron Mask hybrid can be texturally and compositionally homogeneous over areas of approximately 250m. These zones are either coarse or fine grained and each contains distinctive, internally consistent mineral assemblages. At their margins, these homogenous patches grade into more typical Type III rocks where outcrop-scale textural and compositional heterogeneity dominates. For example, at the top of Coal Hill, a 200m zone of fine-grained amphibole diorite is found. This zone grades laterally into a texturally diverse pyroxene diorite.

Accessory minerals are apatite and rare titanite and zircon. Primary K-feldspar is absent, although areas of faint K-feldspar overprinting near contacts with the Cherry Creek suite have been observed. Secondary minerals in the Iron Mask hybrid rocks include chlorite and epidote in addition to hornblende overgrowths on clinopyroxene.

2.3.5 Contact Relationships

Locally, a 50 to 250m wide transitional zone is exposed between Pothook diorite and Type II Iron Mask hybrid. The inset map in Figure 2.2 illustrates the geometry of this gradational contact. A transect across the transitional unit from Pothook into Iron Mask hybrid on the north slope of Sugarloaf Hill reveals the following changes. Pothook diorite incorporates clasts of plutonic, volcanic and recrystallized sedimentary rocks while characteristic magnetite veining and weak foliation of this rock unit becomes less prominent. Rounded and partially digested and disaggregated xenoliths increase in abundance and magnetite occurs as discrete euhedral to subhedral grains in the matrix. The Pothook matrix varies from fine to medium grained on a scale of several centimetres and mineralogical heterogeneity is manifested by zones of dominantly felsic or mafic minerals. Finally, poikilitic biotite, characteristic of Pothook intrusive rocks, disappears, hornblende occurs locally in the matrix and grain-size and mineralogical heterogeneity of the matrix increases.

Contacts between the Pothook and Cherry Creek rocks are locally ambiguous. In many areas, especially in the northern part of the batholith, extreme K-feldspar metasomatism has rendered identification uncertain. Further ambiguity arises through apparently contrasting intrusive relationships between Cherry Creek rocks and the coeval Pothook and hybrid rock units. For example, near Makaoo Lake in the central part of the batholith coarse-grained, foliated Pothook diorite has a gradational contact with medium to fine-grained, non-foliated pyroxene-monzodiorite of the Cherry Creek unit over a distance of approximately 100m. Conversely, clasts of Iron Mask hybrid are found within an intrusion breccia with a biotite monzonite matrix (described previously) interpreted to belong to the Cherry Creek phase. There is no evidence to suggest that the Pothook rocks themselves are younger than the Cherry Creek phases and Lang (1994) has described the presence of Cherry Creek-like dykes brecciating the Pothook phase in the Crescent pit.

This apparent temporal overlap between the Cherry Creek and Pothook/hybrid rocks is permissible. The Iron Mask hybrid unit, formed from the interaction of Pothook magma and Nicola Group country rocks, is concentrated at the top and sides of the magma chamber, and thus formed a brittle shell around hotter, deeper uncontaminated Pothook magma. A phase of the Cherry Creek unit may have intruded and brecciated the hybridized carapace and outer margins of the Pothook magma chamber and contemporaneously interacted with unsolidified Pothook magma at depth. Additionally, the compositional range of the Cherry Creek unit (monzodiorite to monzonite) and random variability in the dominant ferromagnesian mineral between localities suggests that the Cherry Creek unit may be comprised of more than one intrusive phase (Hoiles, 1978) and Stanley (1994) identified two phases of Pothook diorite intrusion at the Pothook pit. The multi-phase nature of the magmatic rocks and the geometry of the Iron Mask system allows for various styles of interaction between the Pothook and Cherry Creek units.

Sugarloaf rocks consistently crosscut the other rock units in the Iron Mask batholith indicating that they are the youngest intrusive phase. They are commonly found near exposures of serpentinized

picritic basalt both inside the batholith (near the Iron Mask mine and in the Ajax East pit) and outside of the batholith near Jacko Lake.

2.4 CLINOPYROXENE CHEMISTRY

Clinopyroxene is the most common ferromagnesian mineral in most rocks of the Iron Mask batholith. In Pothook and Cherry Creek rocks, pyroxene occurs as subhedral crystals which are either colourless or very light green. The Iron Mask hybrid unit contains dominantly greenish coloured clinopyroxene in both the matrix as well as the recrystallized xenoliths whereas Sugarloaf rocks locally contain rounder, colourless clinopyroxene.

The occurrence of green-coloured clinopyroxene in mafic alkaline rocks is well documented (Scott, 1976; Brooks and Printzlau, 1978; Barton and van Bergen, 1981) and a variety of processes have been proposed for their origin including xenocrystic material, magma mixing and melt contamination by crustal rocks. Clinopyroxene is a useful petrogenetic indicator (Bedard, 1988). For example, tholeiitic, calc-alkaline and alkaline suites can be distinguished on the basis of Al^{IV} contents in clinopyroxene (LeBas, 1962). Clinopyroxene compositions are useful in tracking the extent of fractionation (Scott, 1976). Zoning patterns in clinopyroxene have been used to recognize magmatic contamination or infer changes in pressure and temperature (Bedard, 1988). Clinopyroxene from rocks of the Iron Mask batholith was analyzed by electron microprobe for major and minor elements and used for investigations of differentiation trends.

2.4.1 Analytical Methods

Clinopyroxene compositions were measured using the Cameca SX-50 electron microprobe at The University of British Columbia. Grains were analyzed with a focused, spot-fixed beam at operating conditions of 15 kV and 20 nA and peak counting times of 30 seconds. Background concentrations were

counted for 10 seconds. Calibration standards included: diopside (Si, Mg, Ca), aegirine (Fe, Na), grossularite (Al), pyromangite (Mn), rutile (Ti), chromite (Cr) and nickel-olivine (Ni).

2.4.2 Results

Representative clinopyroxene analyses from rocks in the Iron Mask batholith are shown in Table 2.1. Complete analyses are given in appendix C. Chromium was analyzed but is below detection in most samples. Clinopyroxene from the Iron Mask batholith spans a narrow compositional range. Grains from Cherry Creek rocks plot as diopside and augite in the pyroxene quadrilateral (Figure 2.4), while clinopyroxene from all of the other units are primarily restricted to the diopside field (Morimoto, 1988). MG#'s range from 72.8 to 96.03, with a significant amount of overlap between all of the rock units. Clinopyroxene from the Iron Mask batholith contain a significant amount of calculated Fe_2O_3 (0.69-5.21 wt%) based on charge balance considerations (e.g., 4 cations and 6 oxygens).

Clinopyroxene in the Pothook diorite has MG#'s ranging from 82.5 to 98.1; zoning averages 3 MG units from core to rim (n=30). In 55 out of 111 analyses of Pothook unit clinopyroxene the Al content, which ranges from 0.25 to 3.88 wt% Al_2O_3, is not sufficient to fill the tetrahedral site vacancy when added to Si. Pothook rocks are shown to be relatively depleted in Al^{IV} (Al in the tetrahedral site) compared to clinopyroxene from Sugarloaf rocks and the Iron Mask dykes (Figure 2.5a). However, the majority of clinopyroxene from Cherry Creek rocks, although showing lower MG#'s (72.8 to 92.9) and less zoning (2.1 MG units from core to rim; n=54) are similar in Al^{IV} content to clinopyroxene from the Pothook diorite. Many of the Cherry Creek grains (74 out of 160) also exhibited tetrahedral site vacancy. Where there is insufficient Al to fill the tetrahedral site, Ti^{4+} or Fe^{3+} may also occupy this location (Bedard, 1988; Cundari and Salviulo, 1989). TiO_2 concentrations in Pothook clinopyroxene ranges from below detection to 0.64 wt% and in Cherry Creek grains from 0.02 to 0.47 wt%.

Table 2.1. Representative electron microprobe analyses of clinopyroxene from rock units in the Iron Mask batholith.

Unit	PH	PH	PH	PH	PH	PH	PH	PH	PH	PH	PH-TZ	PH-TZ	CC	CC	CC	CC
Sample	IM-251	IM-251	IM-119	IM-119	IM-257	IM-257	IM-265	IM-265	IM-124	IM-124	IM-242	IM-242	IM-237	IM-237	IM-171	IM-171
Position	c	r	i	c	r	i	r	i	c	c	i	i	c	c	i	r
SiO_2	49.34	50.27	51.46	52.89	51.98	52.97	52.20	53.33	52.36	53.54	51.57	52.05	53.04	51.88	51.00	52.02
TiO_2	0.57	0.57	0.30	0.23	0.20	0.02	0.18	0.19	0.26	0.00	0.24	0.11	0.20	0.20	0.14	0.13
Al_2O_3	3.88	2.64	1.42	1.12	1.22	0.24	1.23	0.69	1.05	0.60	0.94	0.60	0.92	0.94	1.36	0.63
Fe_2O_3	3.67	3.44	2.42	2.33	1.59	1.34	1.79	2.14	2.94	1.72	3.49	4.06	1.40	3.15	2.92	2.81
FeO	4.47	3.82	4.63	2.93	5.49	3.24	5.68	2.44	4.18	2.11	3.96	1.22	5.77	3.99	6.23	4.83
MnO	0.36	0.49	0.43	0.30	0.56	0.42	0.70	0.49	0.32	0.00	0.60	0.27	0.81	0.80	0.68	0.75
MgO	13.87	14.95	14.51	15.43	14.51	15.87	15.04	16.55	14.99	16.30	14.67	15.88	14.90	14.92	14.70	15.17
CaO	21.92	21.80	22.35	23.75	22.28	23.81	21.44	23.46	22.50	24.59	22.65	23.87	22.49	22.64	20.28	22.04
Na_2O	0.41	0.38	0.49	0.50	0.41	0.20	0.42	0.32	0.61	0.30	0.47	0.43	0.36	0.40	0.44	0.32
TOTAL	98.49	98.36	98.01	99.48	98.24	98.11	98.68	99.61	99.21	99.16	98.59	98.49	99.89	98.92	97.75	98.70
FeO_T	7.77	6.92	6.81	5.03	6.92	4.45	7.29	4.37	6.83	3.66	7.10	4.87	7.03	6.82	8.86	7.36
MG #	84.69	87.47	84.84	90.33	82.49	89.67	82.53	92.36	86.49	93.24	86.81	95.87	82.15	86.95	80.80	84.83

Unit	CC	CC	CC	CC	CC	CC	CC	CC	CC	CC	dike	dike	dike	dike	dike	dike
Sample	IM-303	IM-303	IM-27G	IM-27G	IM-253	IM-253	IM-11	IM-11	IM-269	IM-269	IM-254	IM-254	IM-208	IM-208	IM-308	IM-308
Position	i	r	r	c	i	i	i	i	r	r	r	i	r	r	i	c
SiO_2	52.91	49.34	52.16	51.72	51.52	50.79	51.76	52.24	52.59	49.96	52.09	51.80	52.69	50.89	49.85	52.78
TiO_2	0.13	0.44	0.34	0.26	0.34	0.37	0.13	0.13	0.19	0.18	0.15	0.16	0.21	0.24	0.35	0.17
Al_2O_3	0.70	2.15	1.74	1.32	1.75	1.71	0.97	0.80	0.92	0.85	0.79	0.89	1.54	1.48	2.50	1.14
Fe_2O_3	0.69	5.21	1.09	2.88	1.29	4.18	1.47	1.98	1.41	5.33	1.92	3.10	0.89	3.59	3.49	1.76
FeO	6.16	2.04	6.18	4.73	5.74	3.53	8.14	5.22	5.74	1.96	5.45	3.85	5.81	3.06	5.09	2.39
MnO	0.75	0.45	0.82	0.69	0.80	0.70	1.14	0.65	0.89	0.79	0.91	0.94	0.66	0.73	0.37	0.18
MgO	14.65	15.05	14.34	14.81	13.98	14.40	12.20	14.73	14.47	14.73	14.44	15.16	14.67	14.76	13.26	17.20
CaO	22.41	22.12	21.93	22.12	21.33	22.50	22.50	22.38	22.19	22.43	22.38	22.27	22.40	22.82	22.49	22.89
Na_2O	0.36	0.38	0.44	0.42	0.68	0.51	0.47	0.39	0.48	0.47	0.36	0.38	0.41	0.38	0.44	0.16
TOTAL	98.76	97.18	99.04	98.95	97.43	98.69	98.78	98.52	98.88	96.70	98.49	98.55	99.28	97.95	97.84	98.98
FeO(T)	6.78	6.73	7.16	7.32	6.90	7.29	9.46	7.00	7.01	6.76	7.18	6.64	6.61	6.29	8.23	3.97
MG #	80.93	92.93	80.56	84.82	81.31	87.92	72.77	83.43	81.80	93.04	82.52	87.53	81.83	89.55	82.30	92.75

MG# = 100•Mg/(Mg + Fe^{2+}) TZ=Pothook/Hybrid Transitional Zone

Table 2.1 (continued)

Unit	HY-I	HY-I	HY-II	HY-II	HY-III	HY-III	HY-III	HY-III	HY-XE	HY-XE	HY-XE	HY-XE	SL	SL	SL	SL
Sample	IM-173	IM-173	IM-306	IM-306	IM-120	IM-120	IM-256	IM-256	IM-121	IM-121	IM-268	IM-268	IM-274	IM-274	IM-272	IM-272
Position	i	r	i	i	r	i	i	r	i	i	c	i	r	r	i	i
SiO_2	50.96	50.70	51.71	50.25	49.80	48.50	50.78	51.35	50.81	49.92	48.53	50.25	50.63	52.01	53.05	48.95
TiO_2	0.44	0.42	0.27	0.44	0.62	0.78	0.58	0.44	0.39	0.40	0.70	0.66	0.29	0.13	0.06	0.38
Al_2O_3	2.84	2.97	1.90	2.23	3.78	4.32	2.65	2.61	3.04	3.29	4.88	3.68	2.36	1.08	0.20	3.00
Fe_2O_3	2.95	4.15	2.28	4.65	2.92	4.94	3.22	4.47	2.73	4.36	4.16	3.61	2.80	2.73	0.90	4.56
FeO	3.98	2.85	5.06	2.94	4.28	2.65	4.26	1.66	3.59	2.38	3.41	2.35	5.24	1.26	6.14	4.58
MnO	0.31	0.28	0.48	0.43	0.33	0.30	0.36	0.33	0.20	0.14	0.18	0.21	0.40	0.12	0.21	0.63
MgO	14.92	15.06	15.31	15.37	14.42	14.16	14.83	15.14	15.16	15.12	13.77	14.90	14.27	17.08	13.97	13.36
CaO	22.41	22.87	21.40	21.84	21.87	22.39	22.14	23.11	22.66	22.99	22.62	23.72	21.85	23.31	24.21	21.91
Na_2O	0.38	0.38	0.40	0.38	0.39	0.40	0.40	0.70	0.28	0.25	0.34	0.26	0.38	0.14	0.27	0.39
TOTAL	99.19	99.68	98.81	98.53	98.41	98.44	99.22	99.81	98.86	98.91	98.59	99.64	98.22	98.07	99.01	97.82
FeO_T	6.63	6.58	7.11	7.12	6.91	7.10	7.16	5.68	6.05	6.30	7.15	5.60	7.76	3.72	6.95	8.68
MG #	86.97	90.43	84.37	90.34	85.77	90.55	86.12	94.22	88.26	91.91	87.83	91.84	82.97	96.05	80.21	83.90

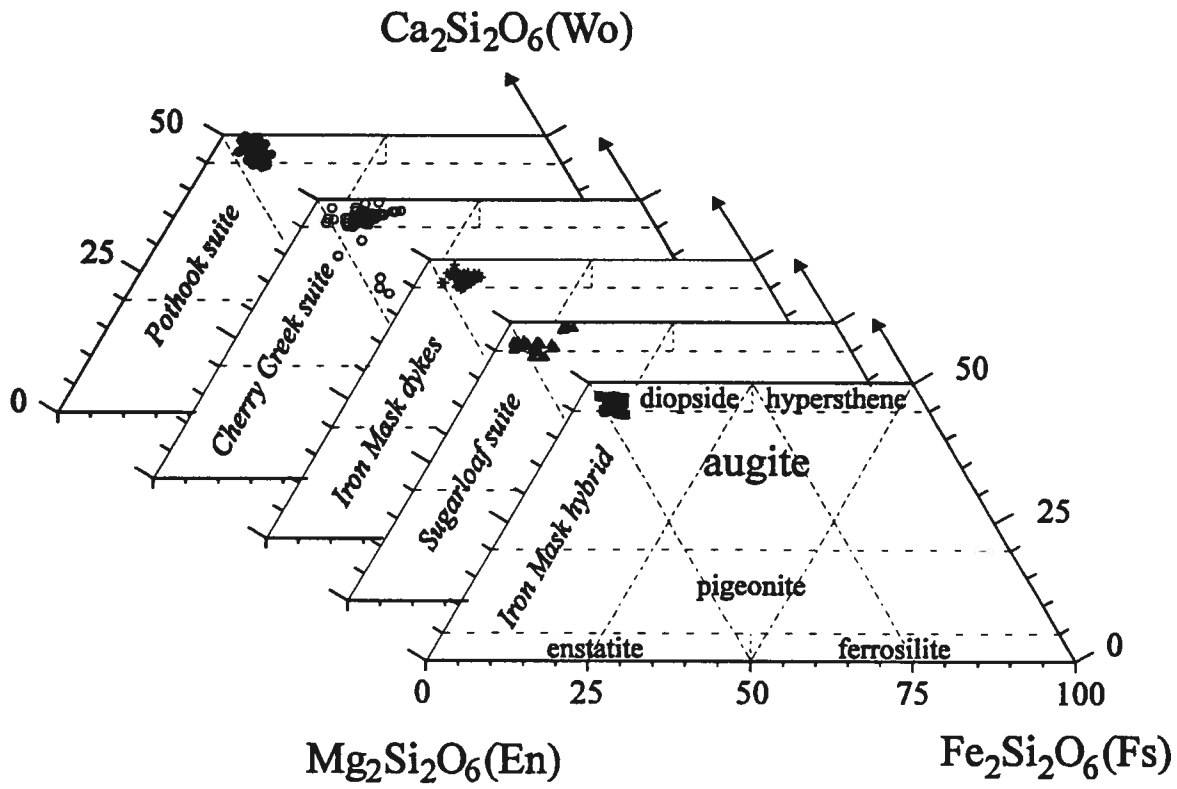

Figure 2.4. Pyroxene quadrilateral showing clinopyroxene compositions for intrusive rocks from the Iron Mask batholith.

Clinopyroxene compositions were obtained for two Sugarloaf rocks. MG#'s range from 80.2 to 96.0 and zoning in the grains averages 6.2 MG units (n=6). The stronger zoning in the clinopyroxene may be due to the hypabyssal nature of these rocks. Al^{IV} contents of the clinopyroxene from Sugarloaf rocks are slightly greater than the majority of those from the other two intrusive phases (Figure 2.5a) although 11 out of 33 grains exhibited tetrahedral site vacancy. Sugarloaf clinopyroxene contains less Fe_T and greater Cr_2O_3 (≤0.56 wt%) than does clinopyroxene from Pothook or Cherry Creek rocks.

Clinopyroxene from the Iron Mask hybrid unit have MG#'s which range from 85.8 to 94.2 and zoning averages 2.7 MG units (n=23). Iron Mask hybrid clinopyroxene (both matrix and xenoliths) contains significantly greater Al^{IV} than clinopyroxene from uncontaminated Pothook rocks and the transitional zone (Figure 2.5b). Average Al_2O_3 content of hybrid clinopyroxene is 3.1 wt% and only 4 out of 82 samples have tetrahedral site vacancy. TiO_2 concentrations averaging 0.54 wt% are also

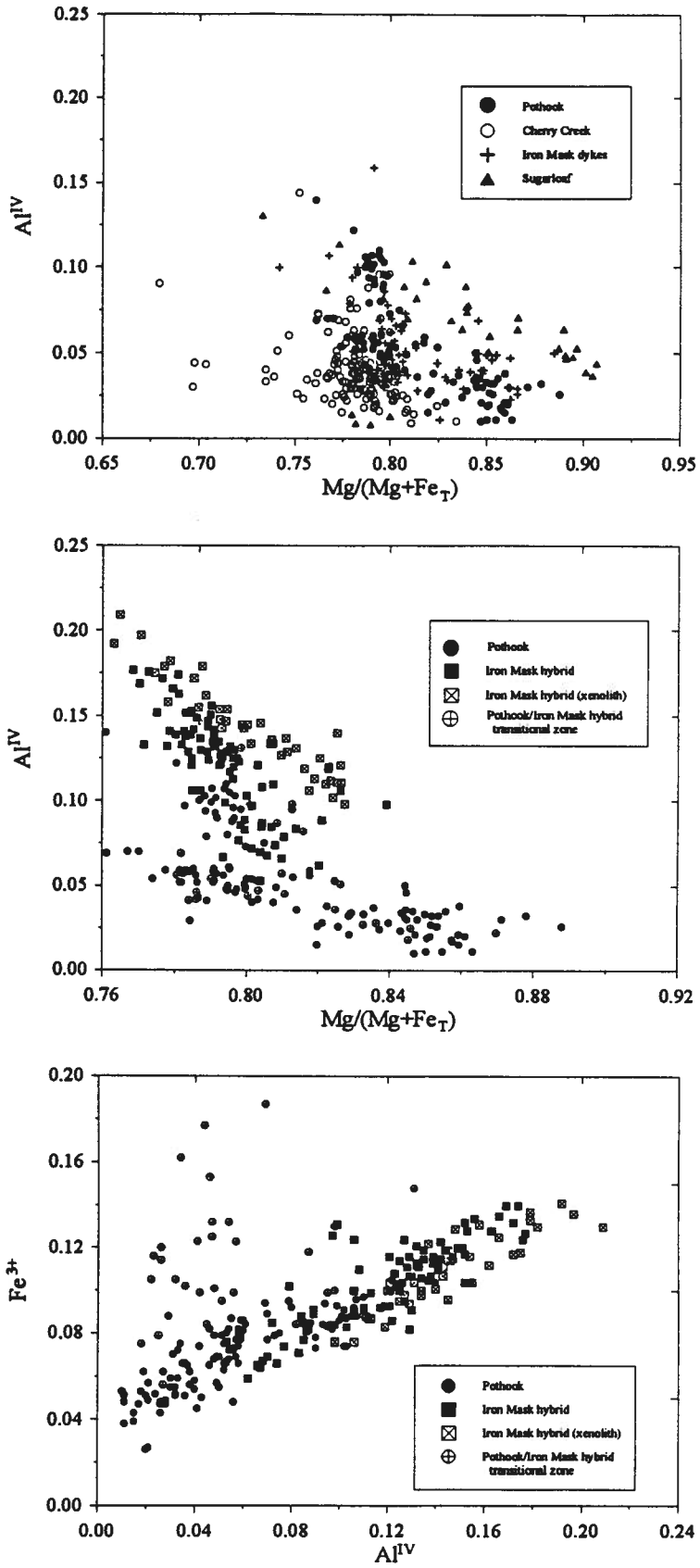

Figure 2.5. Clinopyroxene compositions from the Iron Mask batholith plotted as a, b) $Mg/(Mg+Fe_T)$ *vs* Al^{IV} and c) Al^{IV} *vs* calculated Fe^{3+}.

significantly greater than values of 0.24 wt% for Pothook diorite, 0.19 wt% for Cherry Creek rocks and 0.20 wt% for Sugarloaf diorite. Compositions of clinopyroxene from xenoliths in the Iron Mask hybrid contain significant Al^{IV} and all were found to contain sufficient Al to complete site occupancy in the tetrahedral site. Grains from the transitional zone are similar in Al^{IV} content to uncontaminated Pothook.

Clinopyroxene from the Iron Mask batholith contain significant calculated Fe^{3+} (Figure 2.5c), which ranges from 0.026 to 0.187 cation units in the Pothook and Iron Mask hybrid phases and 0.019 to 0.154 cation units in the Cherry Creek and Sugarloaf units (not shown). These high Fe^{3+} contents of clinopyroxene from the Iron Mask batholith supports LeBas (1962) who argued that alkaline magmas tend to crystallize at higher oxygen fugacities than calc-alkaline magmas. Additionally, island arc suites are characterized by high Fe^{3+} contents in clinopyroxenes implying systematically higher oxygen fugacities than other tectonic environments (Barsdell, 1988). Analyses of clinopyroxene collected from the transitional zone between the Pothook and Iron Mask hybrid unit contain consistently greater Fe^{3+} than clinopyroxene from uncontaminated Pothook rocks (Figure 2.5c).

Green-coloured clinopyroxene in the Iron Mask batholith contain systematically greater amounts of Al than colourless grains. Light-green clinopyroxene from the Pothook and Cherry Creek rocks, in general, contain sufficient aluminum to fill the vacancies in the tetrahedral site. The possibility of clinopyroxene derived from disaggregated xenoliths of Nicola Group rocks occurring in Iron Mask rocks appears to be quite high. However, the absence of strongly reacted rims or resorption features in the clinopyroxene from the Iron Mask units precludes significant xenocrystic contribution.

Some of the variation in clinopyroxene chemistry is inferred to be a consequence of assimilation processes. Iron Mask hybrid clinopyroxenes contain more Al than the intrusive rocks in the Iron Mask batholith suggesting that selective incorporation of felsic material from the xenoliths of Nicola Group rocks may increase the Al available for clinopyroxene crystallization. Also, the enrichment in Fe^{3+} in the Iron Mask hybrid unit and, more significantly, rocks from the transitional zone compared to most of the

other rock types rocks may record more highly oxidizing conditions during this assimilation/hybridization process.

2.5 GEOCHEMISTRY

2.5.1 Major and Trace Elements

Whole rock major and trace element composition of intrusive units and the Iron Mask hybrid unit are given in Table 2.2. For more detailed analyses and analytical methods, see appendix E, F and G. Chemically, the Iron Mask batholith is alkaline to mildly subalkaline (Figure 2.6a). Trace element compositions place the rocks of the Iron Mask batholith within the volcanic arc granitoid field on tectonic discrimination diagrams (Figure 2.6b).

Compositions of Pothook and Cherry Creek rocks show strong negative correlations between SiO_2 and CaO, MgO and FeO(T). Sugarloaf rocks have intermediate SiO_2 and do not follow this trend; they are relatively enriched in MgO and depleted in CaO for a given SiO_2. Iron Mask intrusive rocks have consistent Al_2O_3 (14.9 to 19.4 wt%) over the entire range of SiO_2. Widespread K-feldspar metasomatism of Pothook and Cherry Creek rocks and abundant titanite in some samples from the Cherry Creek make it difficult to evaluate inter-suite variation in TiO_2 and K_2O. However, Sugarloaf rocks are highly enriched in K_2O and marginally depleted in TiO_2 (and Na_2O) compared other Iron Mask intrusive rock compositions.

Chemical analyses of rocks from the Iron Mask hybrid unit show significant variation in only a few of the major elements. Samples IM-173 and IM-306 represent the matrix of Type I and Type II hybrid. Two analyses are Type III matrix (IM-120; IM-256) and two analyses are recrystallized (pyroxenite) xenoliths. One xenolithic sample (IM-121) is part of a 0.2m diameter fragment found just inside the margin of the batholith whereas the other (IM-268) is from a 250m clast near the Ajax pits.

Table 2.2. Whole rock chemical analyses of rocks in the Iron Mask batholith.

	IM-251 PH	IM-119 PH	IM-257 PH	IM-265 PH	IM-124 PH	IM-242 PH-TZ	IM-237 CC	IM-171 CC	IM-303 CC	IM-27G CC	IM-253 CC	IM-11 CC	IM-254 DIKE	IM-208 DIKE	IM-226 DIKE
SiO_2	44.8	45.7	49.5	50.2	50.4	46.7	50.3	52.6	54.4	55.2	56.5	61.0	55.3	46.4	50.9
TiO_2	1.030	0.820	0.752	0.832	0.702	0.910	0.749	0.919	0.693	0.654	0.656	0.404	0.629	0.796	0.887
Al_2O_3	17.50	16.20	19.10	16.70	18.50	17.10	19.40	17.90	18.70	18.30	18.30	17.70	18.40	20.20	19.00
Fe_2O_3	7.07	8.25	5.04	6.77	5.06	6.84	4.48	3.75	3.23	3.34	3.39	2.01	3.73	5.82	5.11
FeO	5.07	4.55	3.50	2.69	2.82	3.20	3.28	3.45	3.53	2.70	2.37	2.13	2.40	4.03	3.40
MnO	0.19	0.15	0.19	0.21	0.08	0.16	0.15	0.17	0.14	0.12	0.17	0.09	0.18	0.18	0.20
MgO	5.73	5.03	4.36	4.12	3.55	5.97	3.51	3.87	2.84	2.45	2.18	1.47	2.52	4.35	3.67
CaO	12.50	11.70	10.40	7.19	8.80	12.00	9.08	8.02	7.36	6.57	6.19	5.13	6.57	10.90	8.44
Na_2O	2.28	2.53	3.60	3.65	5.10	2.48	4.64	3.86	4.32	4.83	5.05	4.80	4.74	3.23	4.53
K_2O	1.03	1.44	1.50	3.10	0.89	1.76	1.03	2.27	2.50	1.97	3.31	3.04	2.70	0.93	1.41
P_2O_5	0.60	0.44	0.32	0.39	0.37	0.15	0.36	0.33	0.35	0.37	0.30	0.18	0.29	0.65	0.39
H_2O+	1.9	1.5	1.3	1.6	1.9	2.1	1.2	1.6	1.0	1.4	0.9	1.0	1.4	1.4	1.2
CO_2	0.03	0.20	0.06	0.05	0.19	0.39	0.01	0.04	0.32	0.05	0.07	0.06	0.02	0.03	0.08
SUM	99.73	98.50	99.62	97.50	98.36	99.76	98.19	98.78	99.39	97.95	99.38	99.02	98.88	98.92	99.22
LOI	1.80	1.70	1.40	2.00	2.30	2.45	1.25	1.65	1.45	1.70	1.00	1.45	1.45	1.45	1.50
D.I.	22.81	27.14	36.21	46.27	45.48	27.70	43.01	44.66	49.89	56.05	60.30	73.65	55.42	30.53	43.60
T_{Zr} (°C)	519.12	534.61	560.53	628.43	598.44	541.39	584.80	625.45	634.33	639.98	657.26	670.98	651.25	550.54	590.01
Trace Elements															
Ba[1]	643	523	1182	1420	389	435	722	990	1250	1130	1340	1700	1355	1220	1600
Rb[1]	19	32	30	52	17	45	20	40	43	33	54	37	47	21	29
Sr[1]	1080	787	985	674	689	652	840	798	756	679	731	597	647	1330	961
Nb[1]	6	5	4	5	5	6	7	4	8	7	8	5	6	6	5
Zr[1]	27	40	33	79	53	41	37	65	62	59	86	72	79	24	41
Y[2]	--	16.85	--	20.80	--	--	--	--	20.60	19.94	--	15.47		--	--
Ni[1]	10	19	3	7	27	18	5	7	b.d.	9	b.d.	6	2	3	b.d.
Cr[4]	33	b.d.	44	25	54	27	40	28	24	b.d.	20	22	23	26	25
V[2]	--	421.23	--	289.60	--	--	--	--	206.62	177.40	--	119.81	--	--	--
Sc	30.7[3]	25.94[2]	23.7[3]	25.30[2]	16.5[3]	--	16.7[3]	20.6[3]	13.24[2]	10.43[2]	9.2[3]	5.81[2]	8.8[3]	16.8[3]	18.5[3]
Hf[2]	--	1.09	--	1.32	--	--	--	--	0.97	0.82	--	1.26	--	--	--
Ga[1]	29	28	30	29	28	28	29	29	29	29	30	30	28	29	30
Zn[1]	83	57	42	77	36	51	48	69	43	42	55	35	62	65	59
Cs[2]	--	0.51	--	0.48	--	--	--	--	0.80	0.39	--	0.42	--	--	--
Ta[2]	--	0.48	--	0.31	--	--	--	--	0.57	0.75	--	1.19	--	--	--

[1] XRF Pressed Pellet [2] Inductively Coupled Plasma Mass Spectrometry [3] Neutron Activation [4] XRF Fused Pellet

D.I. = qz + or + ab + ne + lc (normative mole%) TZ = Pothook/Hybrid Transitional Zone

Table 2.2. (continued)

	IM-308 DIKE	IM-173 HY-I	IM-306 HY-II	IM-120 HY-III	IM-256 HY-III	IM-121 HY-XE	IM-268 HY-XE	IM-267 SL	IM-271 SL	IM-296 SL	IM-274 SL	IM-272 SL	IM-266 SL	IM-295 SL	IM-249 SL
SiO_2	49.5	41.8	43.7	41.9	42.0	45.4	40.5	48.1	48.7	50.0	50.5	51.8	52.3	52.5	54.5
TiO_2	0.878	0.954	1.020	1.010	0.844	0.706	1.150	0.820	0.693	0.635	0.829	0.491	0.588	0.678	0.668
Al_2O_3	18.90	20.70	16.40	17.60	17.80	3.90	5.48	16.70	17.70	17.70	14.90	18.40	17.80	18.6	17.40
Fe_2O_3	3.85	11.50	7.38	8.26	7.41	8.47	13.81	5.01	4.89	4.48	4.99	3.84	3.61	4.42	3.82
FeO	3.00	--	4.70	4.98	5.30	5.88	7.64	4.94	4.10	5.87	4.50	3.89	3.24	3.76	4.40
MnO	0.13	0.13	0.21	0.18	0.24	0.15	0.18	0.14	0.29	0.06	0.16	0.08	0.15	0.13	0.14
MgO	4.43	6.49	6.54	6.69	7.22	13.40	11.20	6.13	4.82	4.39	6.18	3.59	2.79	3.03	3.96
CaO	13.60	15.40	13.20	15.30	14.90	20.00	16.70	7.39	9.01	6.11	8.81	6.78	7.02	6.69	5.68
Na_2O	3.56	1.22	1.91	1.04	1.03	0.20	0.35	2.70	2.54	3.93	3.61	3.68	3.70	4.02	5.73
K_2O	0.37	0.60	0.97	0.49	0.33	0.02	0.57	3.39	3.58	2.66	1.83	3.64	3.38	3.50	1.09
P_2O_5	0.46	0.08	0.36	0.42	0.15	0.02	0.04	0.27	0.25	0.27	0.29	0.25	0.37	0.25	0.28
H_2O+	1.1	1.3	1.3	1.6	1.8	0.6	1.0	2.2	2.3	2.2	1.6	1.4	1.9	1.4	1.8
CO_2	0.02	0.01	0.17	0.03	0.02	0.02	0.11	0.19	0.36	0.14	0.65	0.28	2.24	0.03	0.17
SUM	99.79	100.18	97.86	99.51	99.04	98.76	98.73	97.98	99.23	98.44	98.85	98.12	99.09	99.01	99.64
LOI	1.35	1.10	1.35	1.55	1.60	0.40	0.55	1.95	2.70	2.20	2.25	1.75	4.25	1.48	1.75
D.I.	30.17	31.53	19.50	10.37	9.50	1.57	2.40	38.67	38.55	45.62	37.43	49.58	50.72	51.52	52.34
T_{Zr} (°C)	574.38	518.05	511.47	464.60	490.75	103.10	206.29	601.24	584.12	638.87	582.03	619.31	640.25	642.11	635.46
Trace Elements															
Ba[1]	263	333	442	251	315	88	254	2210	1670	899	589	1460	1390	1694	724
Rb[1]	17	10	23	16	9	5	22	64	53	53	26	64	29	64	27
Sr[1]	1180	1145	814	1060	988	84	136	487	562	704	544	537	742	563	587
Nb[1]	7	4	4	4	4	6	6	4	5	5	5	4	8	6	6
Zr[1]	69	28	39	14	25	23	28	51	50	65	72	50	72	71	64
Y[2]	14.74	--	--	14.14	--	6.90	--	--	--	--	--	10.74	16.96	18.22	--
Ni[1]	7	8	12	12	8	46	54	40	16	14	27	10	6	4	16
Cr[4]	b.d.	14	23	b.d.	22	182	52	99	37	55	133	29	26	13	49
V[2]	259.38	--	--	481.36	--	382.35	--	--	--	--	--	194.01	216.15	220.37	--
Sc	25.49[2]	39.3[3]	42.9[3]	48.06[2]	37.4[3]	121.80[2]	98.8[3]	40.3[3]	26.4[3]	21.4[3]	35.9[3]	15.42[2]	15.09[2]	16.94[2]	20.6[3]
Hf[2]	0.87	--	--	0.63	--	0.55	--	--	--	--	--	1.30	1.96	1.73	--
Ga[1]	28	28	29	30	29	23	25	24	27	25	26	29	30	28	27
Zn[1]	124	66	69	69	124	54	76	53	91	34	50	39	60	44	74
Cs[2]	1.42	--	--	1.02	--	0.02	--	--	--	--	--	0.72	0.10	0.32	--
Ta[2]	0.54	--	--	0.37	--	0.32	--	--	--	--	--	0.31	0.46	0.40	--

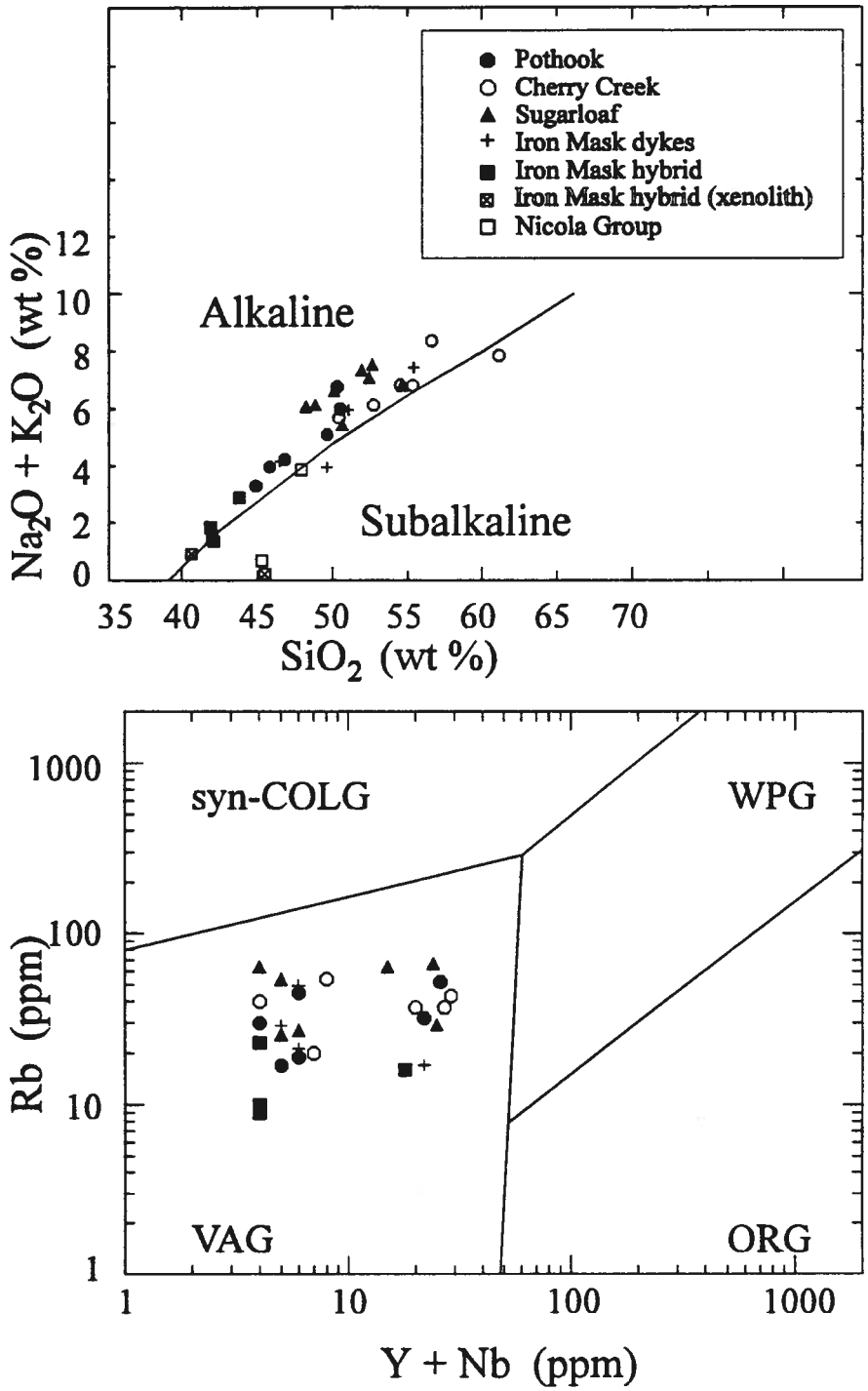

Figure 2.6. Iron Mask hybrid and Nicola Group rocks plotted as a) SiO_2 *vs* $Na_2O + K_2O$ (Irvine and Barager, 1971) b) Rb *vs* Y+Nb (Pearce et al., 1984).

Rocks from the Iron Mask hybrid unit are more basic (40.5 to 43.7 wt% SiO_2), depleted in alkalis and enriched in TiO_2 and CaO compared to the intrusive rocks in the batholith. They are highly variable in Al_2O_3, MnO and P_2O_5. The two xenolith analyses are similar in major element concentrations to a sample from a pyroxene-phyric andesitic flow of the Nicola Group near the western margin of the batholith (IM-185).

Based on measured FeO and Fe_2O_3, the dominant normative mineralogy of Pothook rocks and the Iron Mask dykes include olivine ± nepheline. One Pothook sample (IM-119) is hypersthene normative and one dyke (IM-254) contains quartz in the norm. Cherry Creek rocks are mainly quartz normative with only one sample (IM-237) containing calculated olivine and nepheline. Most rocks from the Sugarloaf unit are olivine + hypersthene normative, however, one sample (IM-266) is quartz and corundum normative and IM-271 contains nepheline in the norm. Iron Mask hybrid unit are either hypersthene or nepheline normative. Because samples collected from the Iron Mask batholith are generally weathered, the measured Fe_2O_3 may not reflect magmatic conditions. Therefore, normative calculations were also performed with $Fe_2O_3 = 0.15\ Fe_T$ for comparison. Under these conditions quartz normative rocks are limited to three samples and nepheline dominates. Leucite appears in some samples of the Iron Mask hybrid unit.

Trace element abundances for rocks in the Iron Mask batholith (Table 2.2) show significant overlap in all units; only a few differences are observed. Sugarloaf rocks are slightly enriched in Cr and Ni and depleted in Sr with respect to Pothook and Cherry Creek samples. The compositions of Type II and Type III Iron Mask hybrid are relatively depleted in Ba and Rb compared to the intrusive phases.

2.5.2 Zircon Saturation Index

Rocks from the Iron Mask batholith contain very little Zr (14 to 86 ppm) and almost no modal zircon (Mortensen and Ghosh, in review), suggesting that zircon crystallization is relatively late or absent.

The saturation potential of zircon can be modeled as a function of bulk rock chemistry using the empirical model of Watson and Harrison (1983, 1984) which predicts the hypothetical zircon saturation temperature for a specific zircon concentration and rock composition. The equation is:

$$D_{Zr}^{zir\,/\,liq} = \{-3.8 - [0.85(M-1)]\} + 12900/T$$

where M is the cation ratio (Na + K + 2Ca)/(Si • Al) and T the absolute temperature. High T_{Zr} implies that the rock may crystallize zircon as an early igneous phase while low T_{Zr} suggests that the rock will probably not saturate with respect to zircon before reaching the magmatic solidus. The calculated zircon saturation temperatures (T_{Zr}) for rocks of the Iron Mask batholith range from 464°C to 670°C (Table 2.2).

Figure 10 plots calculated zircon saturation temperatures against the Differentiation Index (D.I.) for rocks in the Iron Mask batholith (xenoliths in the Iron Mask hybrid are excluded). D.I. is the sum of normative quartz, albite, orthoclase, nepheline, leucite and kalsitite (Thornton and Tuttle, 1960). It is an estimate of the relative differentiation of the rocks; more highly evolved rocks will have a higher D.I. Differentiation Index for the rocks from the Iron Mask batholith ranges from 9.50 to 73.65, with the Iron Mask hybrid showing the least evolved signatures and Cherry Creek the most evolved.

Rocks of the Iron Mask batholith show a regular trend of increasing D.I. with increasing T_{Zr}, consistent with the rocks representing an alkaline series of magmas which did not saturate with respect zircon (Figure 2.7). If zircon were to saturate, the calculated T_{Zr} would remain constant or decrease due to loss of Zr from the melt. Also shown on Figure 2.7 are surfaces representing the experimental magmatic solidus for water-saturated melts at 1 and 3Kb (Russell, et al., in preparation). Rock compositions and Zr concentrations of Iron Mask hybrid rocks suggest that zircon is well below saturation throughout crystallization. Pothook rocks exhibit the most variation in D.I. and a range of T_{Zr} from 519°C to 628°C. These data suggest that zircon would not saturate in Pothook magma (*cf*, curve for shallow-level solidus).

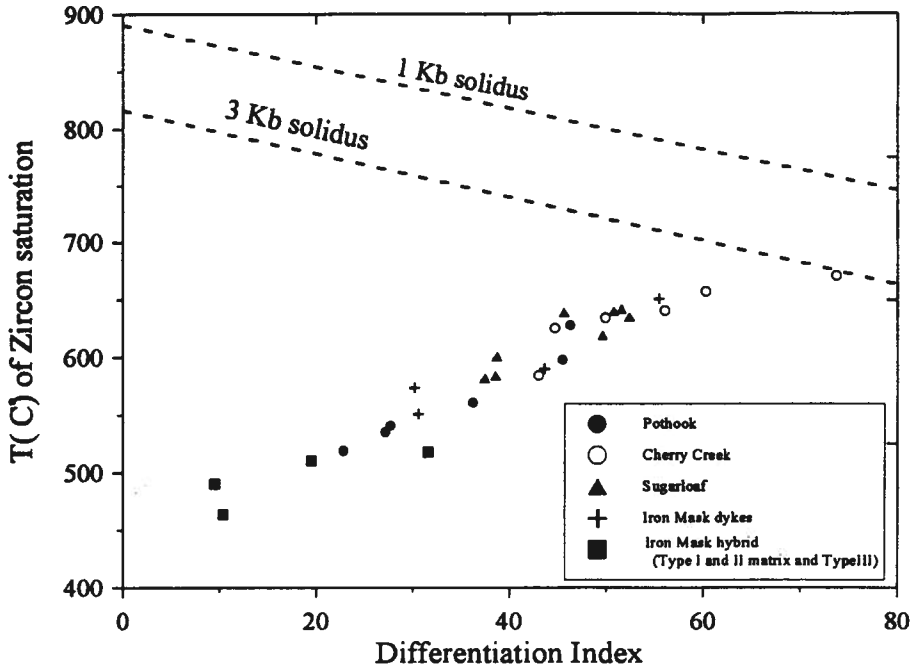

Figure 2.7. Calculated zircon saturation temperatures for all Iron Mask rocks are plotted against D.I. (Σ normative qz+ab+or+ne+lc). Most evolved rocks have the highest D.I. and the highest T_{Zr} indicating the greatest potential for zircon saturation (see text).

Sugarloaf rocks are slightly more differentiated than the Pothook but T_{Zr} (582°C to 642°C) is still sufficiently low to inhibit crystallization of zircon in the early stages. Rocks of the Cherry Creek have the highest D.I. and the highest T_{Zr} (585°C to 671°C). These rocks represent the best candidates in the Iron Mask batholith for containing early magmatic zircon. The trend of the Cherry Creek rock compositions flattens at the most evolved sample, suggesting that zircon may have saturated.

Results of this modeling imply that for mafic alkaline magmas which contain low Zr, such as the Iron Mask rocks, zircon crystallization is restricted to the last stages. To date, the only successful U-Pb dates from Iron Mask rocks are from the Cherry Creek (205 ± 4 Ma) and from a coarse grained Type III Iron Mask hybrid sample (204.6 ± 2.6 Ma). The Iron Mask hybrid zircons show strong inheritance (Mortensen and Ghosh, in review), indicating that their presence was not fully due to magmatic crystallization. A reliable date has not been obtained for the Pothook phase and zircon has not been recovered from any rocks belonging to the Sugarloaf (J. Mortensen, personal communication).

2.5.3 Rare Earth Elements

The REE profiles for all three intrusive rock units are similar in relative element abundance and shape (Figure 2.8a). The patterns are slightly LREE enriched and flatten considerably toward the HREE's. $(La/Lu)_{CN}$ ratios are 3.42, 3.54 and 3.29 for the Pothook, Cherry Creek and Sugarloaf phases respectively; no Eu anomaly is apparent. The overlaps in enrichment and pattern suggest that these rocks are not related through simple crystal fractionation. A single dyke shows a small negative europium anomaly consistent with minor plagioclase fractionation. One sample of Sugarloaf shows slightly lower REE abundances.

Profiles of the Iron Mask hybrid unit are decidedly different (Figure 2.8b). Patterns for Type III Iron Mask hybrid and the xenolith are similarly depleted in both the LREE's and the HREE's and relatively enriched in the MREE's. The profile of the xenolith has lower total REE abundances than the hybrid rock. The similarity of the REE profile for a clinopyroxene-phyric andesitic flow (IM-185) from the Nicola Group near the batholith contact is consistent with this unit being the source of xenoliths in the hybrid unit. The Nicola Group rock falls between the xenolith and the Type III Iron Mask hybrid sample which, under an assimilation-driven scenario, would represent a mixture of assimilated xenolithic material and original magma. These relationships suggest that the hybridization process involved melting and assimilation of REE bearing phases in Nicola Group rocks. These three rock compositions may represent a 'mixing line' between the Nicola Group and the Pothook diorite and record the hybridization process which formed the Iron Mask hybrid unit.

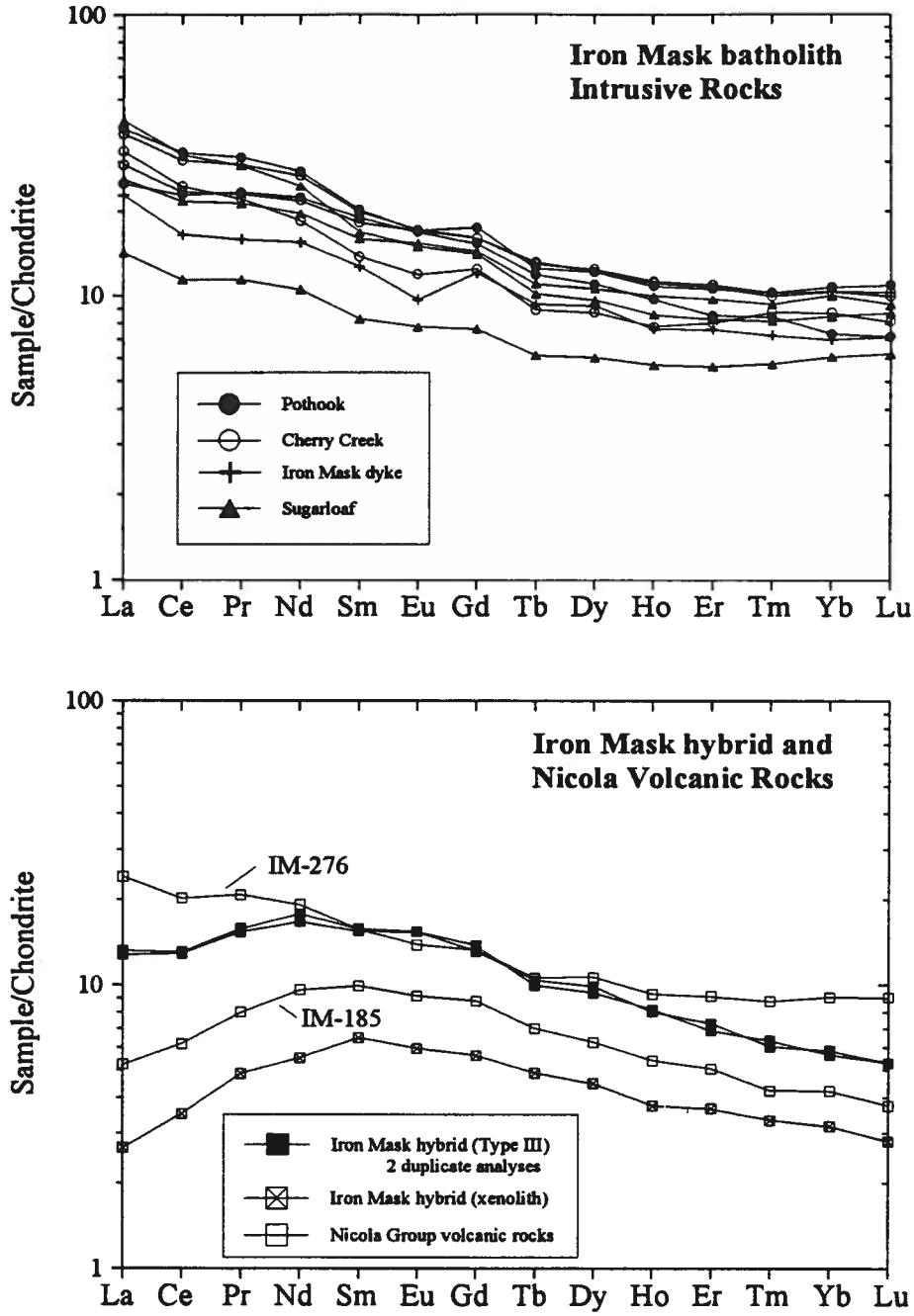

Figure 2.8. Normalized rare earth element plots of a) magmatic rocks of the Iron Mask batholith and b) Iron Mask hybrid and Nicola Group rocks. Normalizing data of Boynton (1984).

2.6 DISCUSSION

2.6.1 Magmatic Lineage's

Table 2.3 presents a synopsis of characteristics for the rock units in the Iron Mask batholith. The textural and mineralogical similarities and local gradational nature of the Pothook and Cherry Creek units suggest that these rocks may be derived from the same parental magma. This is supported by the continuous linear trends observed in most of the major elements when plotted against SiO_2. The Cherry Creek and Pothook suites differ, however, in: 1) plagioclase composition, 2) morphology and abundance of magnetite, 3) abundance of apatite, 4) morphology of biotite, 5) abundance of opaque inclusions in clinopyroxene and, 5) presence of primary quartz, amphibole and K-feldspar. Many of these differences could result from magmatic differentiation under changing physical conditions.

Sugarloaf rocks differ from the Pothook and Cherry Creek in occurrence, mineralogy, texture and chemistry. The Sugarloaf diorite is intrusive into other Iron Mask rock units and exhibits localized, structurally controlled emplacement along the western margin of the batholith and in surrounding Nicola Group rocks. Amphibole is abundant and, in company with plagioclase, is commonly found as aligned phenocrysts in a very fine-grained groundmass suggesting a hypabyssal environment of emplacement. The clinopyroxene in Sugarloaf rocks is less abundant and chemically and optically distinct from clinopyroxene in the Pothook and Cherry Creek units. Sugarloaf rocks do not fall on the linear chemical trend seen for most of the major elements defined by samples from the Cherry Creek and Pothook units. Finally, the alteration style of Sugarloaf diorite is dominated by albitic alteration as opposed to the K-feldspar and epidote assemblage of the other intrusive phases. Consequently, these rocks are considered to be a separate and younger magmatic event than the other intrusive rocks of Iron Mask batholith.

The process of testing genetic linkages concerning the intrusive phases of the Iron Mask batholith was undertaken using Pearce Element Ratio diagrams (Pearce, 1968; Russell and Nicholls,

Table 2.3. Distinguishing features of the Iron Mask rock units.

	Pothook suite	Cherry Creek suite	Sugarloaf suite	Iron Mask hybrid unit
Distinctive field and petrographic features	-weak to strong foliation -late poikilitic biotite -magnetite veining -abundant early apatite -clinopyroxene as primary mafic mineral -abundant opaques in clinopyroxene -An_{43}-An_{52}	-tabular, interlocking or sub-trachytic feldspar -weakly to strongly zoned plagioclase -clinopyroxene, hornblende or biotite as primary mafic phase -sparce primary quartz -An_{32}-An_{45}	-hornblende phenocrysts -sparce clinopyroxene; no biotite -trachytic texture in both . hornblende and feldspar -An_{32}-An_{38}	-abundant partially digested heterolithic xenoliths -extreme textural and mineralogical variability -abundant coarse magnetite -pyroxene as dominant mafic mineral -An_{60}
Intrusive relationships	-gradational and intrusive contacts with the Cherry Creek unit -transitional zone (50-250m) between the Pothhook and Iron Mask hybrid	-gradational to and brecciates the Pothook unit -matrix of intrusive breccia with Iron Mask hybrid and Nicola Group clasts -late stage dykes	-intrudes all other units -dykes and small stocks along the western margin of the batholith -found as small dykes in Nicola Group volcanic rocks	-gradational contact with Pothook suite and Nicola volcanic rocks -gradational contacts between the three recognized types -hybrid clasts incorporated into one phase of the Cherry Creek
Chemical features	-monzodiorite to monzonite	-gabbro to diorite	-diorite -relatively enriched in Cr -clinopyroxene shows relative enrichment in Cr	-REE signatures show same pattern as Nicola Group rocks -clinopyroxene shows relative enrichment in Al
Mineralization/ Alteration	-hosts lode magnetite-apatite deposits -intense K-feldpar overprint at contacts with the Cherry Creek	-intense K-felspar alteration along contacts with Pothook diorite -hosts mineralization at the Crescent pit -local secondary titanite	-hosts mineralization at the Ajax property -albitization is dominant alteration	-local K-feldspar alteration

1988; Nicholls and Russell, 1991). Diagrams (*cf*, Figure 12) are designed by: i) choosing an appropriate conserved element for the denominator and ii) choosing a set of numerator elements for the x and y-axes that will model the effects of the target mineral assemblage (Stanley and Russell, 1989; Nicholls and Gordon, 1994). The low calculated zircon saturation temperature (T_{Zr}) of rocks from the Iron Mask batholith suggests that Zr was retained in the melt phase throughout much of the crystallization history. Therefore, Zr is a conserved element in these rocks and was chosen as the denominator element.

On Figure 2.9, the chosen axes model the fractionation of feldspar, clinopyroxene, biotite, apatite, titanite and the edenite component of amphibole as a slope of 1. Magnetite and quartz fractionation have no effect on the diagram and common hornblende causes displacements less than one (0.79). Error ellipses on each data point are shown for 1s analytical error as determined through duplicate analyses on sample IM-295.

Compositional variations within the Pothook unit are shown in Figure 2.9a. The model line was constructed through averaging lines representing a slope of one through each data point and is shown with 1s confidence limits. Fractionation of the observed mineral assemblage in the Pothook rocks (plagioclase, clinopyroxene, biotite, K-feldspar, apatite and titanite) accounts for the variation among three of the samples. Three compositions do not fall on the line and are inconsistent with the model. Two of the samples (IM-242 and IM-124) are from or near the transitional zone with the Iron Mask hybrid and the other, sample IM-251, was collected very close to the contact with Cherry Creek. The inconsistency of these samples may reflect magmas which are not related to the other Pothook samples through fractionation of the observed mineral assemblage or hybridization, contamination or alteration of Pothook magma.

Cherry Creek compositions are shown on the same diagram in Figure 2.9b. The dashed line is the model fractionation trend fitted to the Pothook rocks (Figure 2.9a) and the heavy solid line represents a Cherry Creek model line drawn through IM-303, a sample from the central part of the batholith. Cherry

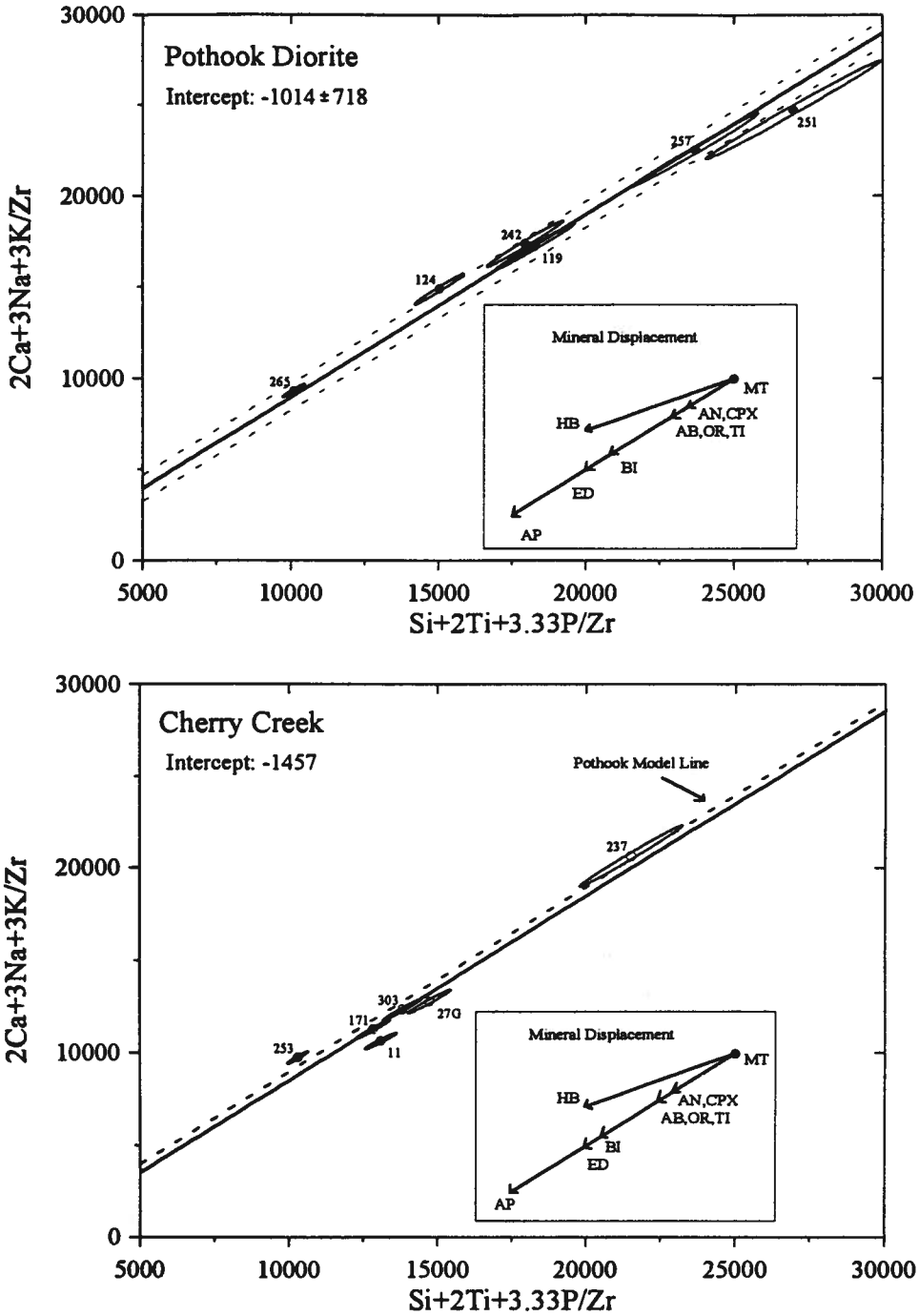

Figure 2.9. Pearce Element Ratio diagram of Si+2Ti+3.33P/Zr *vs* 2Ca+3K+3Na/Zr used to test for fractionation of the observed mineral assemblage in Iron Mask rocks for a) Pothook diorite and b) Cherry Creek monzodiorite to monzonite.

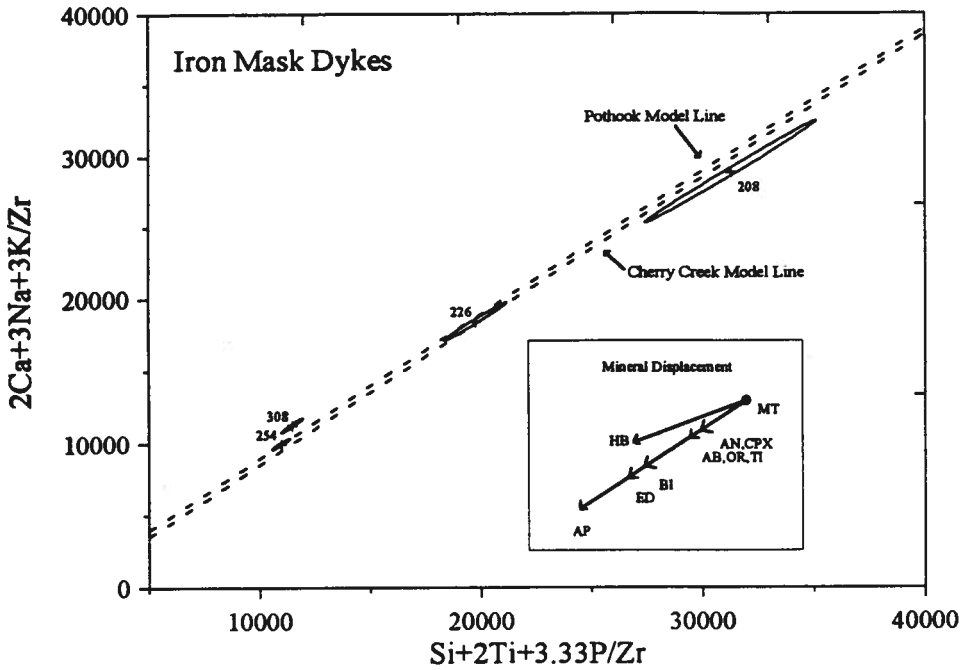

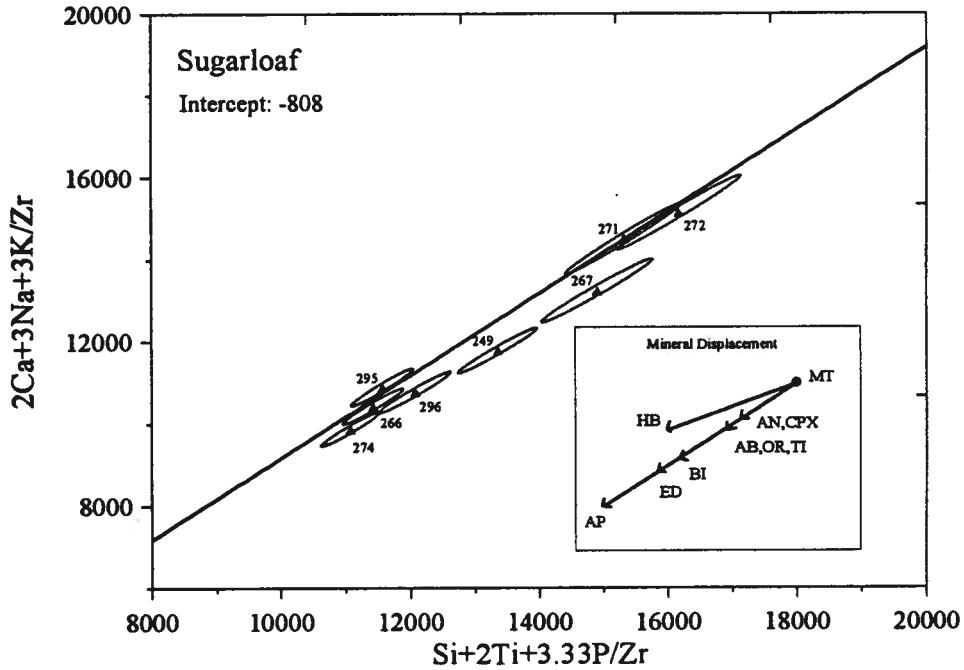

Figure 2.9 (continued). Pearce Element Ratio diagram of Si+2Ti+3.33P/Zr vs 2Ca+3K+3Na/Zr used to test for fractionation of the observed mineral assemblage in Iron Mask rocks for c) Iron Mask dykes and d) Sugarloaf diorite.

Creek rocks, as a group, neither fit the Pothook fractionation trend nor fall on a single trend of their own. Samples IM-237 and IM-253 lie very close to the Pothook model line, suggesting that they may be genetically related to the Pothook through fractionation. Samples IM-303 and IM-171 define their own model line, suggesting that these two samples may be derived from a single magma. Other samples, however, appear to be inconsistent with fractionation of the modal mineral assemblage. These results imply that the Cherry Creek samples are not all cogenetic or that they are not related through fractionation of the observed mineral assemblage. In addition, not all of the Cherry Creek rocks may be derived from fractionation of Pothook magma. Alternatively, the rocks may be related through alteration processes or, more likely, they represent a series of separate magmas.

Compositions of dykes in the Iron Mask batholith are shown in comparison to the Pothook and Cherry Creek trends in Figure 2.9c. The dykes are both mineralogically and chemically diverse and the data is insufficient to apply genetic interpretations. However, all of the dykes fall within a 'compositional envelope' defined by ranges in rock compositions of the Pothook and Cherry Creek units (similar element ratios). It is therefore probable that the dykes are a part of the Iron Mask magmatic system, although genetic affinity to either Pothook or Cherry Creek remains to be demonstrated.

For Sugarloaf rocks, the model line is drawn through a sample from the type locality of this unit on Sugarloaf Hill (Figure 2.9d). These rocks span a narrower range of element ratio values than the other intrusive units and the dykes, although the model intercept is similar. Some of these amphibole-phyric rocks may be related through fractionation of the model mineral assemblage. Other samples are clearly non-cogenetic, and may represent a different magma series.

Modeling the intrusive rocks in the Iron Mask batholith suggests that these alkaline rocks are not related through simple magmatic fractionation. It is possible that variable amounts of magmatic contamination through interaction with crustal rocks accounts for some of the chemical diversity observed

in these rocks. The overlap in composition of the intrusive phases and the diverse dykes in the Iron Mask batholith suggests that the intrusive history is quite complex.

2.6.2 Petrogenesis and Volatile Budget of the Iron Mask hybrid

The Iron Mask hybrid unit has been previously interpreted as a separate magmatic unit, distinct from the Pothook, Cherry Creek and Sugarloaf phases (Preto, 1967; Northcote, 1977). However, we document a transitional zone between the Pothook diorite and Type II Iron Mask hybrid unit. Recognition of the transitional zone was instrumental in new interpretations of the 'hybridization' process and the timing and nature of the relationship between the Pothook suite and the Iron Mask hybrid unit.

Uncontaminated Pothook diorite can be traced through a gradational interface with hybridized rocks and is clear evidence of interaction between Pothook magma and Nicola Group country rocks. Clasts derived from the Nicola Group are rounded, recrystallized and partially digested suggesting that chemical and mass transfer must have occurred between these two end-members. Indeed, some exposures freeze this process in place, with pieces of recrystallized xenoliths being physically disaggregated and the crystals being incorporated into the magmatic phase (Plate 2.4). Partial incorporation of xenolithic material is defined as selective assimilation as opposed to total fusion and bulk assimilation. One implication of the process of selective assimilation is that the two end-members (Pothook magma and Nicola Group xenoliths) both contribute to the chemical composition of the hybridized rocks.

The 'mixing line' between the two endmembers would not be linear. First, the xenolith variety and abundance is not uniform between outcrops. Second, it is evident that not all of the xenolithic material is incorporated into the Pothook diorite, but that the process is selective and incorporates mainly constituents which are the most mobile under magmatic conditions. Third it is likely that different parts of the 'hybridization system' were operating under different physical and chemical conditions. For example,

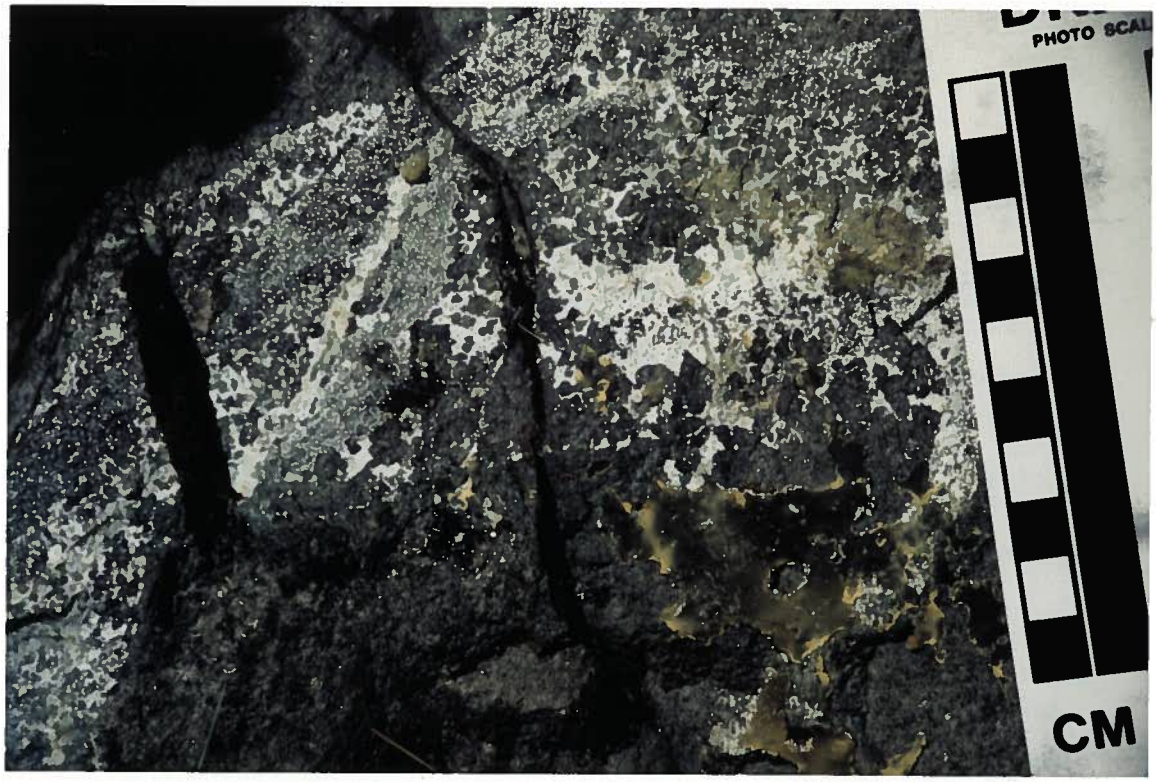

Plate 2.5. The incomplete nature of the assimilation of Nicola group rocks by the Pothook magma. The magma is actively disaggregating the clast at the contact and incorporating the pieces.

variation in depth, temperature and magma accessibility and the type and amount of xenolithic material available. These different conditions are manifested by the occurrence of both xenolithic (Types I and II) and non-xenolithic (Type III) varieties of Iron Mask hybrid and by the compositional heterogeneity of the recognized types. Type III Iron Mask hybrid probably represents the effects of more complete fusion and assimilation of Nicola Group rocks. Therefore, these rocks provide the most likely candidates for evaluating relative chemical contributions of the two endmembers. Major and trace element chemistry do not appear to define a linear mixing line, although data from the different units in the Nicola Group are sparse. Rare earth element patterns of Nicola Group and Iron Mask hybrid rocks, however, may elucidate one component of the assimilation and hybridization process. The very similar, but more enriched pattern of a Type III Iron Mask hybrid rock compared to lava from the Nicola Group suggest that chemical and physical mixing of Pothook magma and Nicola Group rocks which produce a "hybrid" rock unit is a valid hypothesis.

One possible consequence of recrystallization and partial assimilation of Nicola Group rocks in a Pothook magma is a change in the volatile budget of the system. A number of variables may influence the volatile content of a system being affected by magmatic assimilation. These are: 1) the original water content of the magma (X^o), 2) the water incorporated into the crystallizing assemblage (X_s), 3) the original water content of the assimilated material ($X_{a,o}$), 4) the final water content of the residual xenoliths ($X_{a,f}$), 5) the ratio of crystallization to assimilation (α), and 6) the amount of material that is added to the system through partial fusion of the assimilant (r). These parameters may be used in the equation:

$$x_r = \frac{[x^o - x_s F + (x_{a,o} - x_{a,f}) \bullet \alpha F}{[1 - F + r\alpha F]}$$

to model the volatile production induced by selective assimilation. The variable F is the fraction of original magma crystallized and ranges from 0 to 1 where 1 represents complete crystallization. A schematic representation of the selective assimilation process and the components described above is shown in Figure 2.10.

Table 2.4 shows the values of the variables used in modeling the volatile budget in the Iron Mask batholith. These parameters, which affect the amount of material and volatile change in the system, are estimated from field and petrographic observations and chemical analyses. Textural relationships in the Pothook diorite between plagioclase and clinopyroxene in addition to the absence of primary amphibole suggests a water-undersaturated initial melt composition (X^o) (Eggler, 1972; Naney, 1983). The amount of water in the Nicola group volcanic rocks before and after recrystallization (X_a and X_f respectively) are derived from chemical analyses of these rock types. The water in the crystallizing assemblage (X_s) is estimated from the modal mineralogy of Pothook and Cherry Creek rocks and the amount of material incorporated into the Pothook magma (r) is estimated from field observation.

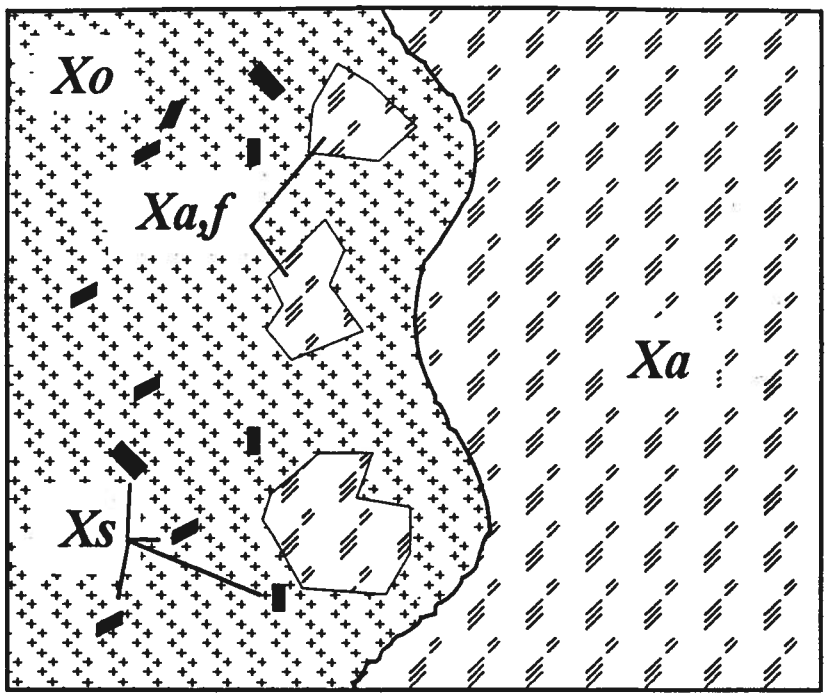

Figure 2.10. Schematic representation of the components involved in modeling volatile changes during assimilation processes.

Table 2.4. Variables used in Modeling Volatile Production.

Model	X^o	X_s	X_a	X_f	α	r
Crystallization	0.085	0 - 0.08	-	-	-	-
Bulk Assimilation and Crystallization	0.085	0.02	0.075	-	0.2-5	-
Selective Assimilation and Crystallization	0.085	0.02	0.075	0.02		0.15
Selective Assimilation (Dehydration)	0.085	0.02	0.075	0.02		0.075

Figure 2.11 shows the results of selective assimilation, as F (fraction of magma crystallized) *vs* the water content (mole%) of the system, of Nicola Group rocks into the Pothook diorite constructed from values in Table 2.4. Model lines are shown for a several assimilation to crystallization ratios (α). Also shown is the model line for crystallization of Pothook diorite with no assimilation and a crystallizing assemblage with 0.2 mole% average water content (X_s) as well as a model line calculated with $r = 0.5$, which represents more complete assimilation. In addition, the 2Kb and 4Kb saturation surfaces are represented. When a model line crosses a saturation surface at a given confining pressure, a volatile phase may separate from the magma.

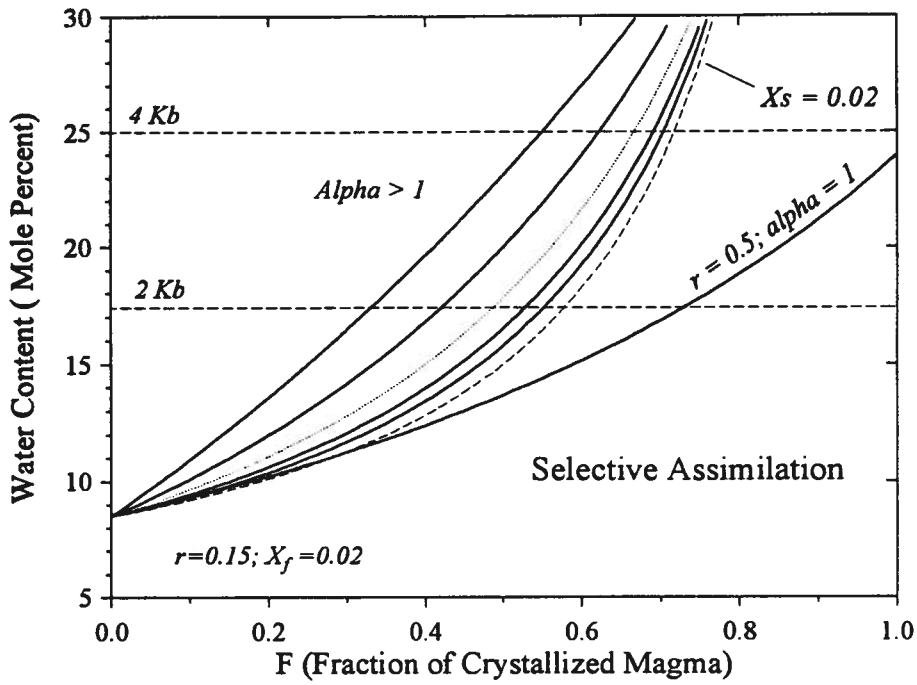

Figure 2.11. Model for Pothook diorite selectively assimilating rocks from the Nicola Group. Model lines derived from the values in Table 2.4 shown with 2 and 4Kb saturation surfaces. α values are 0.25, 0.5, 1, 2 and 4.

Figure 2.11 suggests that, for all values of α, selective assimilation of Nicola Group rocks by Pothook magma may potentially raise the volatile content of the magma, thus promoting exsolution of a volatile phase earlier in the crystallization history. For example, with no assimilation at a confining pressure of 2Kb, the Pothook system may saturate with water at 58% crystallization while during selective assimilation with $r = 0.15$ and $\alpha = 1$ it may saturate at only 44% crystallization. The greater the ratio of crystallization to assimilation, the greater the volatile enrichment. Most significantly, it is shown that the value of r (material added to the system) has a very large effect on the volatile budget. When a large amount of material is added to the magmatic system ($r = 0.5$), the process serves to inhibit volatile production.

Figure 2.12 illustrates the extreme end of selective assimilation-the initial thermal dehydration of the country rocks during magmatism. This model assumes that no material is added to the magmatic system except for the volatiles in the assimilant. As expected, this process serves to enhance the volatile

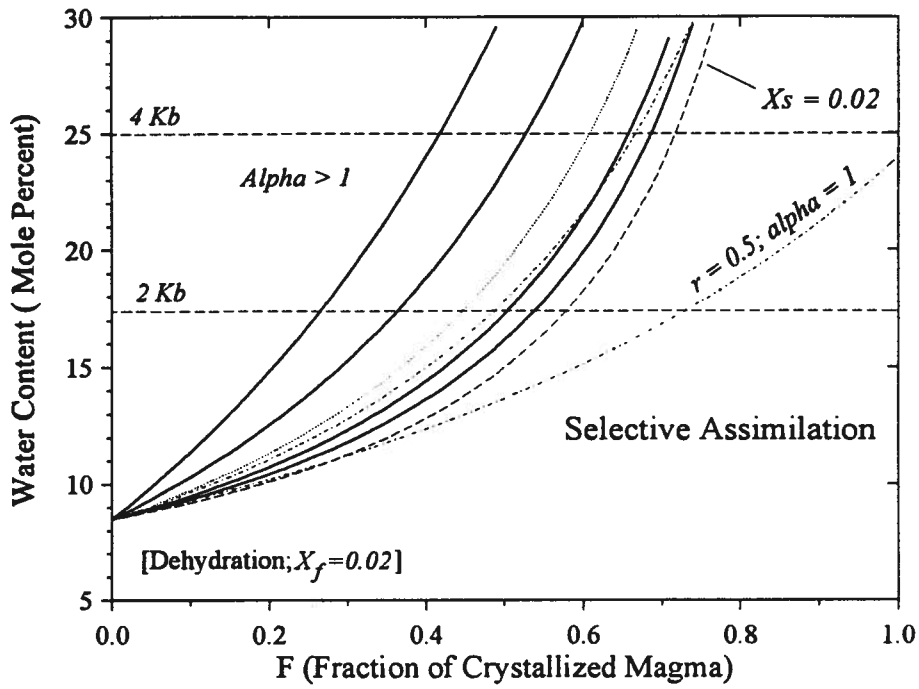

Figure 2.12. Dehydration of Nicola Group rocks and the effect on the volatile budget of the Pothook diorite. Reference curves from Figure 2.11.

potential to an even greater degree (reference curve for $\alpha = 1$ from Figure 15). With $\alpha = 1$, volatile exsolution may occur at 42% crystallization at 2 Kb confining pressure. The dehydration assimilation model may be especially applicable to the margins of the magmatic system.

Results of modeling selective assimilation in the Iron Mask batholith indicate that the recrystallization of hydrous material (Greenschist Nicola Volcanic rocks) to a more anhydrous assemblage (the 'pyroxenite' xenoliths of the Iron Mask hybrid unit) has the potential for raising the volatile content of a magma (Pothook). The most influential parameter in this process is the amount of material incorporated into the melt phase. If a large amount of material is added (*e.g.*, bulk assimilation), the dilution effects of the additional material offset the total volatiles in the system. If, instead, selective dehydration reactions

are considered, it is seen that the volatile content of the magmatic phase is increased dramatically. The water content of a magma is of interest because it effects the density and viscosity of the magma, convection in the magma chamber and the possibility of exsolving a volatile phase. Higher volatile contents promote earlier volatile exsolution and thus can enhance the opportunities for establishing a magmatic-hydrothermal system. This has implications on the ability of the system to produce an ore deposit through the transport of metals in an aqueous phase.

3.0 KAMLOOPS LAKE PICRITIC BASALTS

3.1 INTRODUCTION

Picritic basalt is exposed in the Intermontane Belt of south-central British Columbia near Kamloops Lake (Figure 3.1). These volcanic rocks are olivine ± clinopyroxene porphyritic volcanic breccias, flows and sills. The Kamloops Lake picrites contain extremely high MgO, anomalously low Al_2O_3 and low TiO_2. They have low abundances of all rare earth elements and are enriched in chromium and nickel. Incompatible element abundances and mineral compositions suggest that the Kamloops Lake rocks represent ultramafic magmatism in an island arc setting. Origin and tectonic affinity of the Kamloops Lake picritic basalts is investigated through comparisons to other suites of mafic and ultramafic rocks (i.e., komatiite suites, oceanic suites, island arc suites).

This paper presents petrographic and chemical data on the Kamloops Lake picrites and discusses evidence for these ultramafic rocks representing high-MgO primary liquids. Differentiation of these ultramafic lavas is shown to be satisfactorily modeled by olivine fractionation or accumulation. Primary melt compositions for the Kamloops Lake suite and selected ultramafic suites are estimated from thermodynamic calculations which model equilibrium between the observed olivine composition and a residual melt. The calculations also elucidate the oxidation state of the ultramafic melts as a function of Fe^{3+}/Fe^{2+}.

3.2 REGIONAL GEOLOGY

The exact stratigraphic position of the Kamloops Lake ultramafic volcanic rocks is not certain. The picritic basalts occur as small, poorly exposed, disconnected bodies in the area of Kamloops Lake in the Intermontane Belt of the Canadian Cordillera (Figure 3.1). They are found in the Quesnellia terrane which is interpreted to be part of a late Triassic volcanic arc which was accreted onto the western margin

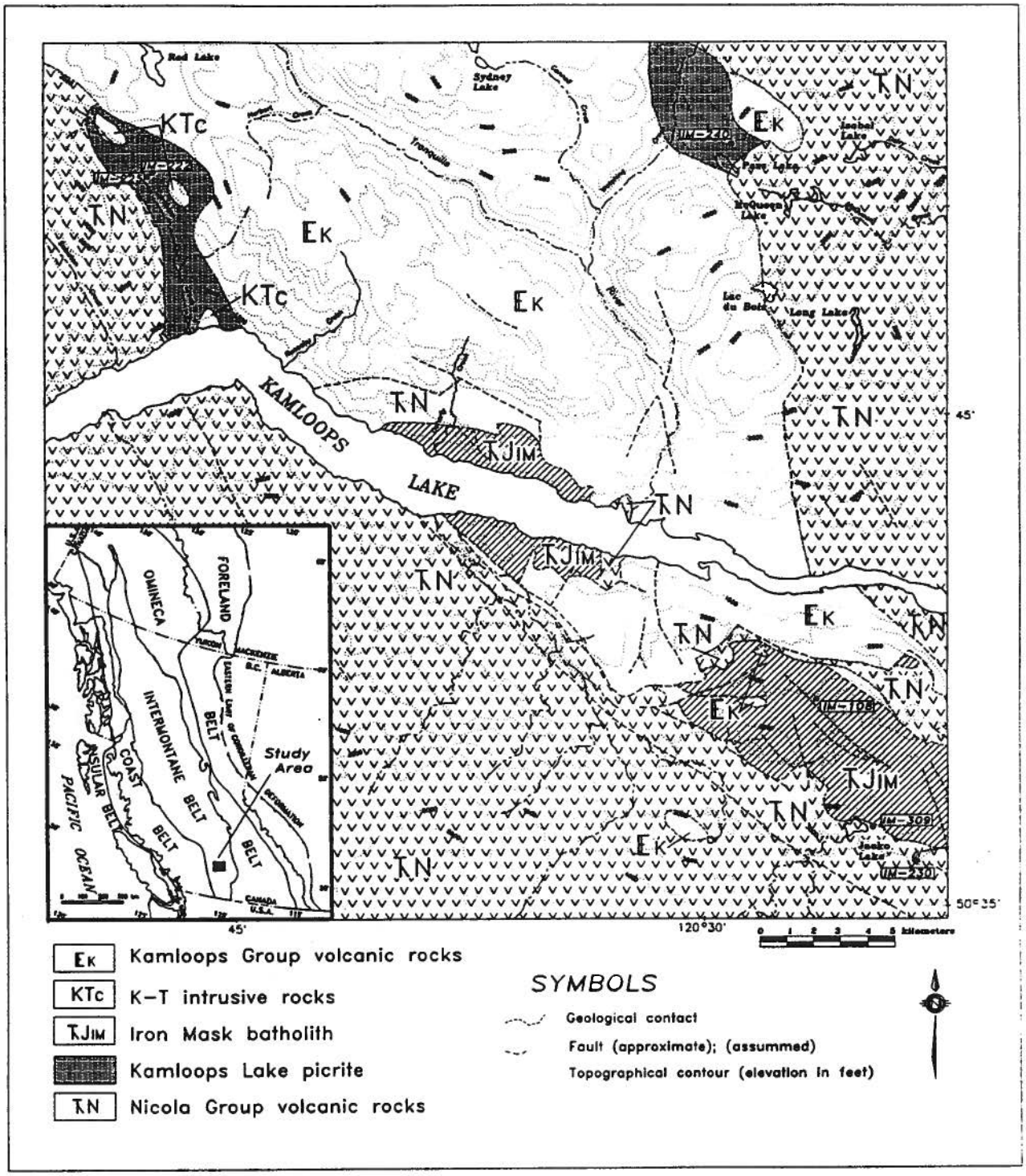

Figure 3.1. Simplified geology of the Kamloops Lake area. Nicola Group volcanic and sedimentary rocks underlie most of the region. Picrite occurrences are shown in the stippled pattern.

of North America in the Late Triassic (Monger et al., 1982; Monger, 1989a). Nicola Group is the most voluminous rock unit in the study area comprising a sequence of alkalic volcanic, volcaniclastic and minor sedimentary rocks (Schau, 1970; Preto, 1979; Mortimer, 1987). In the vicinity of Kamloops Lake, the Nicola Group consists of abundant green and red augite porphyry flows and related breccias, bedded and massive tuffaceous siltstones, and miner cherty sediments. The rocks are regionally metamorphosed to greenschist facies and are, in general, broadly folded, weakly foliated and cut by prominent northwest trending structures.

Intruding and overlying the Nicola Group are a variety of younger intrusive and volcanic rocks. The Iron Mask batholith, a northwesterly trending Early Jurassic composite alkaline intrusive complex, is exposed in the southeast part of the study area (Preto, 1967; Northcote, 1977; Kwong, 1987). Intrusion of the Iron Mask batholith is concentrated along deep-seated northwest-trending structures and the batholith contains numerous xenoliths of serpentinized picritic basalt. Eocene Kamloops Group volcanic rocks consist of abundant alkali basalt flows and miner intercalated sediments. They overlie much of the study area as small erosional remnants and more extensive downdropped blocks (Ewing, 1981a, 1981b, 1982).

Kamloops Lake ultramafic volcanic rocks crop out at four known localities (Figure 3.1): near Carabine Creek on the north side of Kamloops Lake (Cockfield, 1948), north of Pass Lake near Watching Creek (Cockfield, 1948), on an isolated knoll near Jacko Lake one kilometer from the southwest margin of the Iron Mask batholith (Mathews 1941) and as screens, rafts and xenoliths within the Iron Mask batholith (Kwong, 1987).

Picrite outcrops near Carabine Creek are distinctly olivine porphyritic and have sparse vesicles up to 0.2cm in size. The basalt contains sparse rounded knots of olivine and clinopyroxene which range in size from 1 to 10cm. These knots are recognized on weathered surfaces but are indistinguishable on fresh surfaces as they are identical in mineralogy and texture to the surrounding material. The picrite at Carabine Creek is intruded by small granitic stocks belonging to the Copper Creek plutonic suite which is

thought to be post-Early Cretaceous (Cockfield, 1948). Picritic basalt at Watching Creek is massive; the outcrops are typically dense, black and structureless. The rocks contain volumetrically more olivine (up to 50%) than observed at the other localities and are weakly porphyritic. The exposures of picritic basalt near Jacko Lake have a subtle layering defined by the relative abundance of olivine and clinopyroxene knots which range up to 20cm across. These rounded knots comprise up to 50 volume% of the outcrops near Jacko Lake and impart a unique pockmarked weathering texture. In contrast to these three locations of remarkably well preserved picritic basalt, exposures in the Iron Mask batholith comprise serpentinized rafts and septa. Olivine is commonly the only primary mineral preserved, although relict clinopyroxene is found. Serpentine replaces original minerals, commonly preserving original volcanic textures.

3.3 PETROGRAPHY

Picritic basalts in the Kamloops Lake area are olivine and clinopyroxene porphyritic. The groundmass comprises 20 to 50% of the rock and most of it is altered to serpentine and/or talc. The picrite basalts may be subdivided texturally into cumulate and volcanic rocks. The Watching Creek locality typifies the cumulate phase; subhedral partially serpentinized olivine phenocrysts with abundant intercumulus clinopyroxene phenocrysts occur in a fine-grained groundmass (Plate 3.1). Fresh rocks from the other localities have distinctive volcanic textures; subhedral olivine phenocrysts up to 3mm in size are set in a matrix of euhedral clinopyroxene microphenocrysts (Plate 3.2). Picritic basalt at Carabine Creek is amydaloidal, vesicles (≤0.2cm) are filled with secondary fibrous thomsonite, a calcium-rich variety of zeolite.

3.3.1 Olivine

Subhedral to euhedral olivine phenocrysts range in size from 0.5 to 3.5mm. The grains show no resorption features and secondary alteration is confined to rims and along fractures. Olivine phenocrysts

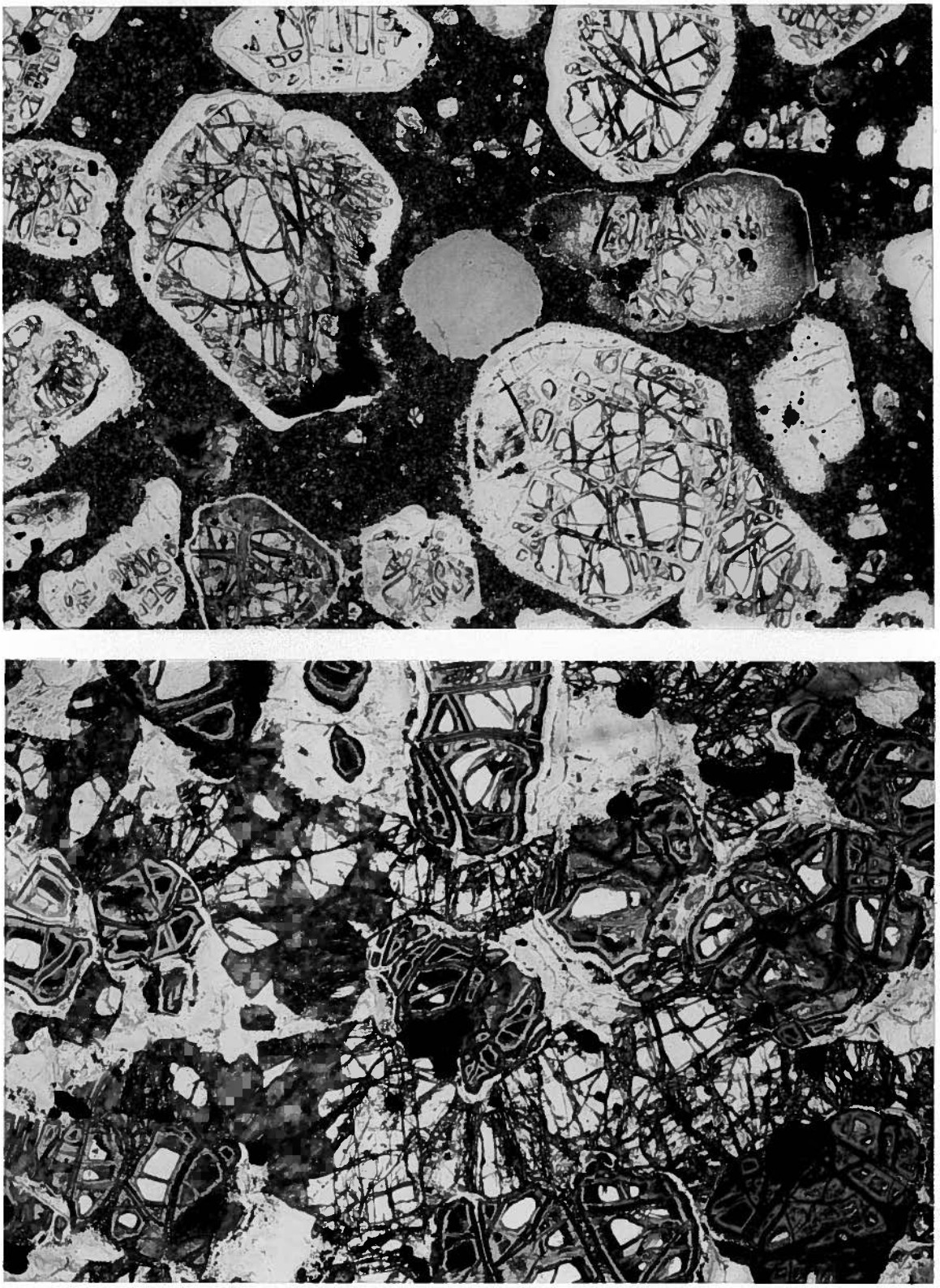

Plate 3.1. Photomicrograph of a) picrite from Carabine Creek showing olivine phenocrysts in a matrix of euhedral clinopyroxene, and b) cumulate rock from Watching Creek with intercumulus pyroxene. FOV=5mm.

abundances in the Kamloops Lake picrites range from 20 to 30% at Carabine Creek, Jacko Lake and Iron Mask and 35 to 50% at Watching Creek. Anhedral inclusions of Cr-spinel within olivine grains are common in most samples. In highly serpentinized samples, phenocrysts are rimmed by anhedral, fine grained opaque material representing secondary spinel produced through the breakdown of olivine.

3.3.2 Clinopyroxene

Clinopyroxene in the Kamloops Lake suite occurs as subhedral to euhedral phenocrysts (Watching Creek) and microphenocrysts (Carabine Creek, Jacko Lake, Iron Mask). Pyroxene shows weak yellow pleochroism and microphenocrysts in the non-cumulate rocks are compositionally zoned. Clinopyroxene varies in size and abundance from 0.5 to 2.5mm and 20 to 25% at Watching Creek to 0.05 to 0.25mm and 30 to 45% at Carabine Creek and Jacko Lake. Inclusions of subhedral to anhedral Cr-spinel in clinopyroxene from all three unserpentinized localities are abundant. Pigeonite has been reported at the Jacko Lake locality by Mathews (1941), but none was found during this study.

3.3.3 Cr-spinel

Cr-spinel in the Kamloops Lake picrites is found in various sizes and morphologies throughout the crystallization sequence. It occurs as inclusions in olivine and clinopyroxene, as subhedral to anhedral microphenocrysts up to 0.3mm and is scattered throughout the groundmass in subhedral to anhedral crystals ranging from 0.005 to 0.15mm. A large proportion of spinel in the Iron Mask batholith are thought to represent an alteration product through the breakdown of olivine and clinopyroxene to serpentine, talc and tremolite during hydrothermal alteration induced by the Iron Mask intrusive suite. The majority of spinels from these samples are not primary and are not included in following discussions of mineral compositions.

3.4 MINERAL CHEMISTRY

3.4.1 Analytical Methods

Chemical compositions of olivine, clinopyroxene and spinel were determined using a Cameca SX-50 electron microprobe at The University of British Columbia. Olivine and clinopyroxene compositions were measured using a focused beam at operating conditions of 15 kV and 20 nA for 30 seconds. Background counts were collected for 10 seconds. Standards for olivine include forsterite (Si, Mg), diopside (Ca), grossular (Al), fayalite (Fe), spessartine (Mn), nickel-olivine (Ni), chromite (Cr) and rutile (Ti). Pyroxene standards are: diopside (Si, Mg, Ca), aegerine (Fe, Na), grossular (Al), pyromangite (Mn), rutile (Ti), chromite (Cr) and nickel-olivine (Ni). Spinel analyses were obtained with operating conditions of 20 kV and 30 nA. Standards for spinel analyses include: fayalite (Fe), forsterite (Mg), chromite (Cr), pyromangite (Mn), grossular (Al), rutile (Ti), nickel-olivine (Ni), diopside (Si, Ca) and sphalerite (Zn).

3.4.2 Olivine

Representative olivine compositions from each of the Kamloops Lake picrite localities are given in Table 3.1. Structural formulae were calculated on the basis of 4 oxygen atoms per unit cell. Olivine phenocryst compositions range from $Fo_{92.9}$ to $Fo_{89.5}$, reflecting the highly magnesian character of the magma. Olivine is unzoned in the Watching Creek locality and slightly zoned (up to 1 mole% Fo from core to rim) at the Carabine Creek, Jacko Lake, and Iron Mask localities. Lack of distinct zoning patterns in olivine phenocrysts, especially from the cumulate locality, may indicate chemical equilibration of the mineral at high temperature (Van Kooten and Buseck, 1978).

Forsterite component in olivine is not correlated with rock texture; cumulate rocks and non-cumulate rocks show considerable overlap. Simkin and Smith (1970) suggest that Mn concentration in

Table 3.1. Representative electron microprobe analyses of olivine from the Kamloops Lake picritic basalts.

	Carabine Creek				Watching Creek				Jacko Lake				Iron Mask			
Sample	IM-224	IM-224	IM-225	IM-225	IM-240	IM-240	IM-241	IM-241	IM-230	IM-230	IM-99	IM-99	KR-07	KR-07	KR-07	KR-07
Position	c	r	i	r	c	r	c	r	r	c	r	i	c	r	i	r
SiO_2	41.24	41.16	40.83	40.39	39.95	39.66	40.03	40.04	40.80	40.91	40.60	40.74	40.92	40.80	40.79	40.91
Al_2O_3	0.04	b.d.	0.04	0.05	0.05	0.02	b.d.	0.04	0.04	b.d.	0.05	0.03	0.04	0.02	0.05	0.05
Cr_2O_3	0.08	b.d.	b.d.	b.d.	b.d.	b.d.	b.d.	b.d.	b.d.	b.d.	b.d.	b.d.	0.11	b.d.	b.d.	0.08
FeO	6.96	7.66	9.03	8.88	10.07	10.10	10.33	10.07	7.63	7.66	8.84	8.98	7.73	8.92	7.81	7.69
MnO	0.12	0.17	0.18	0.13	0.24	0.22	0.18	0.24	0.11	0.08	0.19	0.17	0.08	0.17	0.13	0.10
MgO	51.25	50.94	49.39	49.19	48.67	48.43	48.82	48.91	50.40	50.22	50.31	49.96	51.37	50.07	51.26	51.71
CaO	0.05	0.06	0.38	0.42	0.28	0.28	0.26	0.25	0.08	0.07	0.29	0.23	0.09	0.18	0.09	0.11
NiO	0.43	0.33	0.22	0.32	0.30	0.31	0.28	0.33	0.41	0.39	0.32	0.34	0.42	0.31	0.28	0.39
TOTAL	100.17	100.32	100.07	99.38	99.56	99.02	99.90	99.88	99.47	99.33	100.60	100.45	100.76	100.47	100.41	101.04
Cation calculation based on 4 oxygens																
Si	0.997	0.997	0.998	0.995	0.988	0.987	0.988	0.987	0.997	1.001	0.988	0.992	0.988	0.993	0.989	0.986
Al	0.001	0.000	0.001	0.001	0.001	0.001	0.000	0.001	0.001	0.000	0.001	0.001	0.001	0.001	0.001	0.001
Cr	0.002	0.000	0.000	0.000	0.000	0.000	0.000	0.000	0.000	0.000	0.000	0.000	0.002	0.000	0.000	0.002
Fe^{2+}	0.141	0.155	0.185	0.183	0.208	0.210	0.213	0.208	0.156	0.157	0.180	0.183	0.156	0.182	0.158	0.155
Mn	0.002	0.003	0.004	0.003	0.005	0.005	0.004	0.005	0.002	0.002	0.004	0.004	0.002	0.004	0.003	0.002
Mg	1.848	1.840	1.800	1.806	1.795	1.797	1.796	1.798	1.836	1.831	1.825	1.815	1.850	1.817	1.852	1.857
Ca	0.001	0.002	0.010	0.011	0.007	0.007	0.007	0.007	0.002	0.002	0.008	0.006	0.002	0.005	0.002	0.003
Ni	0.008	0.006	0.004	0.006	0.006	0.006	0.006	0.007	0.008	0.008	0.006	0.007	0.008	0.006	0.005	0.008
FO%	92.4	91.9	90	90.2	89.7	89.9	89.8	89.9	91.8	91.5	91.2	90.7	92.5	90.8	92.6	92.9

Sample numbers refer to whole-rock analyses in Table 2.4. c=core, i=interior, r=rim

olivine is inversely correlated with forsterite content. This feature is not observed in olivine from the Kamloops Lake picritic basalts. MnO contents in olivine from the cumulate rocks of Watching Creek range from 0.18 to 0.27 wt%, slightly greater that the 0.08 to 0.21 wt% in grains from non-cumulate localities whereas forsterite content is indistinguishable. CaO concentration in olivine phenocrysts averages 0.25 wt% which for basaltic rocks would suggest an extrusive or hypabyssal crystallization environment (Simkin and Smith, 1970).

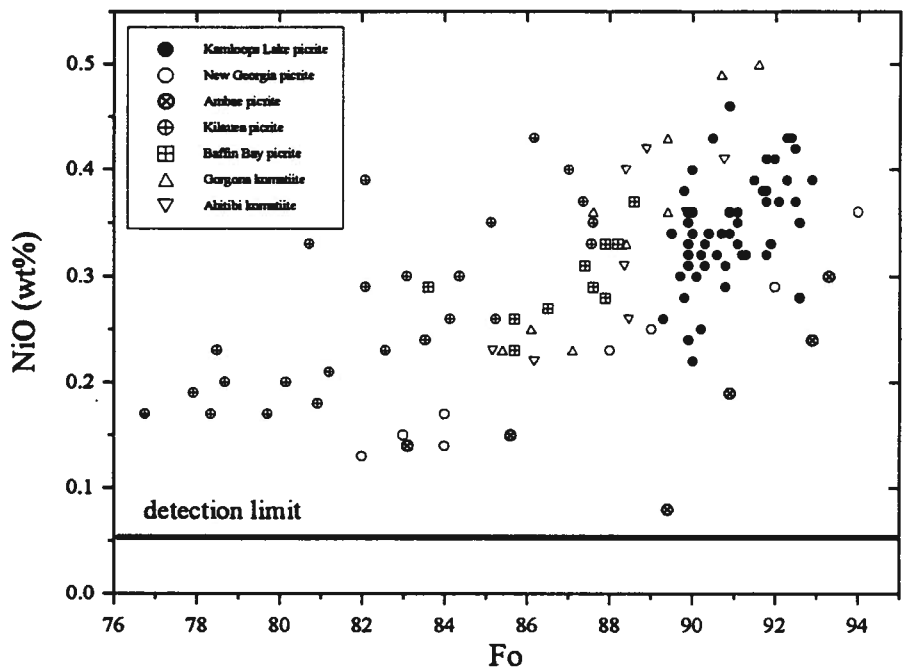

Figure 3.2. Plot of forsterite contents *vs* nickel concentrations in the Kamloops Lake picritic basalts and other ultramafic suites. Sources of data: New Georgia (Ramsay et al., 1984), Baffin Bay (Francis, 1985), Kilauea (Nicholls and Stout, 1988), Ambae (Eggins, 1993), Gorgona (Echeverria, 1980) and Abitibi (Barnes et al., 1980).

The NiO concentrations in the olivine phenocrysts from the Kamloops Lake suite ranges from 0.22 to 0.43 wt% (Figure 3.2) and shows no correlation with forsterite content. These nickel concentrations, as well as the forsterite component, are consistent with mantle-derived olivine (Sato, 1977). Comparison of forsterite content versus NiO concentrations in other ultramafic rocks shown in Fig. 4 reveals that olivine from most suites (Gorgona Island, Echeverria, 1980; Kilauea, Nicholls and Stout, 1988; New Georgia, Ramsay et al., 1984; Ambae (Aoba), Eggins, 1990), in contrast to Kamloops Lake,

exhibit a well defined trend of increasing NiO with increasing forsterite content. The NiO content of the olivines from Gorgona and Kilauea are slightly greater for a similar forsterite composition, while olivines from New Georgia and Ambae are, in general, marginally depleted with respect to NiO in comparison to the Kamloops Lake suite.

3.4.3 Clinopyroxene

Analyses of representative clinopyroxene phenocrysts and microphenocrysts from the Kamloops Lake picritic basalts are given in Table 3.2. Structural formulae was calculated on the basis of 6 oxygens per unit cell. Clinopyroxenes are diopsidic with a slightly sub-calcic signature (Figure 3.3). There is no significant differences in clinopyroxene composition between or within the four localities. Clinopyroxene grains from Watching Creek exhibit normal zoning of core to rim 5 mole% Mg, while the non-cumulate rocks are more strongly zoned with core to rim normal zoning up to 16 mole%. MG# [100•Mg/(Mg + Fe^{2+})] for clinopyroxene ranges from 87.1 to 99.7 and calculated Fe_2O_3 contents range from 1.44 to 6.66 wt%.

Cr_2O_3 content in clinopyroxene ranges from below detection to 1.32 wt% with an average of 0.66 wt%. No systematic differences in Cr contents of clinopyroxene are observed between the cumulate and non-cumulate rocks. The moderate Al_2O_3 content of clinopyroxene grains (1.63 to 4.70 wt%) is anomalous compared to the very low whole-rock Al_2O_3 contents, but Al_2O_3, TiO_2 (0.12 to 0.43 wt%) and Na_2O (0.17 to 0.33 wt%) contents of the Kamloops Lake picritic basalts are comparable to island arc picritic suites such as Grenada (Arculus, 1978), New Georgia (Ramsay et al., 1984) and Ambae (Eggins, 1990). Clinopyroxene in komatiites from Gorgona Island (Echeverria 1980) and the Abitibi Greenstone Belt (Barnes et al., 1983) contain more Al_2O_3.

Table 3.2. Representative electron microprobe analyses of clinopyroxene from the Kamloops Lake picritic basalts.

	Carabine Creek				Watching Creek				Jacko Lake				Iron Mask			
Sample	IM-224	IM-224	IM-225	IM-225	IM-240	IM-240	IM-241	IM-241	IM-230	IM-230	IM-99	IM-99	KR-07	KR-07	KR-07	KR-07
Position	Mp-c	Mp-i	Mp-c	Mp-i	Ph-c	Ph-r	Ph-c	Ph-i	Mp	Mp	Mp-c	Mp-i	Mp-c	Mp-i	Mp-i	Mp-i
SiO_2	51.80	50.84	52.01	52.95	51.17	51.15	51.72	49.32	51.07	51.14	51.24	51.98	50.84	52.57	51.52	51.67
TiO_2	0.16	0.25	0.18	0.15	0.20	0.28	0.15	0.41	0.25	0.25	0.19	0.17	0.20	0.14	0.19	0.17
Al_2O_3	2.54	3.26	2.46	1.62	2.97	3.01	2.22	4.32	2.96	2.89	2.79	2.21	3.32	1.94	2.73	2.41
Cr_2O_3	0.94	0.62	0.92	0.85	0.69	0.51	0.77	0.43	0.26	0.26	0.83	0.78	0.98	0.80	0.87	0.80
FeT	4.65	5.39	4.23	3.50	4.98	5.01	4.27	6.02	5.32	5.87	4.71	4.26	4.75	3.93	4.32	4.22
MnO	0.09	0.12	0.06	0.09	0.07	0.07	b.d.	0.12	b.d.	0.14	0.10	0.12	0.08	0.07	0.08	0.08
MgO	16.80	16.05	16.79	17.34	16.55	16.51	17.20	15.64	16.51	16.38	16.74	17.40	16.82	17.98	17.32	17.69
CaO	22.26	22.38	22.52	22.44	22.53	22.40	22.63	22.72	22.17	21.99	22.48	22.35	21.94	21.88	22.34	22.10
Na_2O	0.26	0.28	0.25	0.23	0.29	0.29	0.28	0.27	0.24	0.31	0.28	0.28	0.24	0.22	0.22	0.22
TOTAL	99.50	99.26	99.42	99.17	99.45	99.23	99.24	99.25	98.78	99.23	99.36	99.55	99.17	99.60	99.59	99.36
Cation calculation based on 6 oxygens																
Si	1.901	1.875	1.909	1.944	1.879	1.882	1.897	1.820	1.888	1.885	1.882	1.900	1.870	1.918	1.883	1.890
Ti^{4+}	0.004	0.007	0.005	0.004	0.006	0.008	0.004	0.011	0.007	0.007	0.005	0.005	0.006	0.004	0.005	0.005
Al^{IV}	0.099	0.125	0.091	0.056	0.121	0.118	0.096	0.180	0.112	0.115	0.121	0.095	0.130	0.082	0.117	0.104
Al^{VI}	0.011	0.017	0.015	0.014	0.007	0.012	0.000	0.008	0.017	0.011	0.003	0.000	0.014	0.001	0.001	0.000
Cr^{3+}	0.027	0.018	0.027	0.025	0.020	0.015	0.022	0.013	0.008	0.008	0.024	0.023	0.028	0.023	0.025	0.023
Fe^{3+}	0.070	0.096	0.056	0.025	0.103	0.095	0.098	0.154	0.091	0.105	0.100	0.091	0.093	0.066	0.095	0.098
Fe^{2+}	0.072	0.070	0.073	0.082	0.050	0.059	0.033	0.031	0.074	0.076	0.044	0.039	0.053	0.054	0.037	0.031
Mn	0.003	0.004	0.002	0.003	0.002	0.002	0.000	0.004	0.000	0.004	0.003	0.004	0.002	0.002	0.002	0.002
Mg	0.919	0.882	0.919	0.949	0.906	0.906	0.941	0.861	0.910	0.900	0.917	0.948	0.922	0.978	0.944	0.965
Ca	0.875	0.884	0.886	0.882	0.886	0.883	0.889	0.898	0.878	0.868	0.885	0.875	0.865	0.855	0.875	0.866
Na	0.018	0.020	0.018	0.016	0.021	0.021	0.020	0.019	0.017	0.022	0.020	0.020	0.017	0.016	0.016	0.016
Ni	0.000	0.002	0.000	0.000	0.000	0.000	0.000	0.000	0.000	0.000	0.000	0.000	0.000	0.002	0.000	0.000
MG#	92.73	92.65	92.64	92.05	94.77	93.89	96.61	96.52	92.48	92.21	95.42	96.05	94.56	94.77	96.23	96.89

MG# = 100•Mg/(Mg+Fe^{2+}). Sample numbers refer to whole-rock analyses in Table 2.4. Ph=phenocryst, Mp=microphenocryst, c=core, i=interior, r=rim

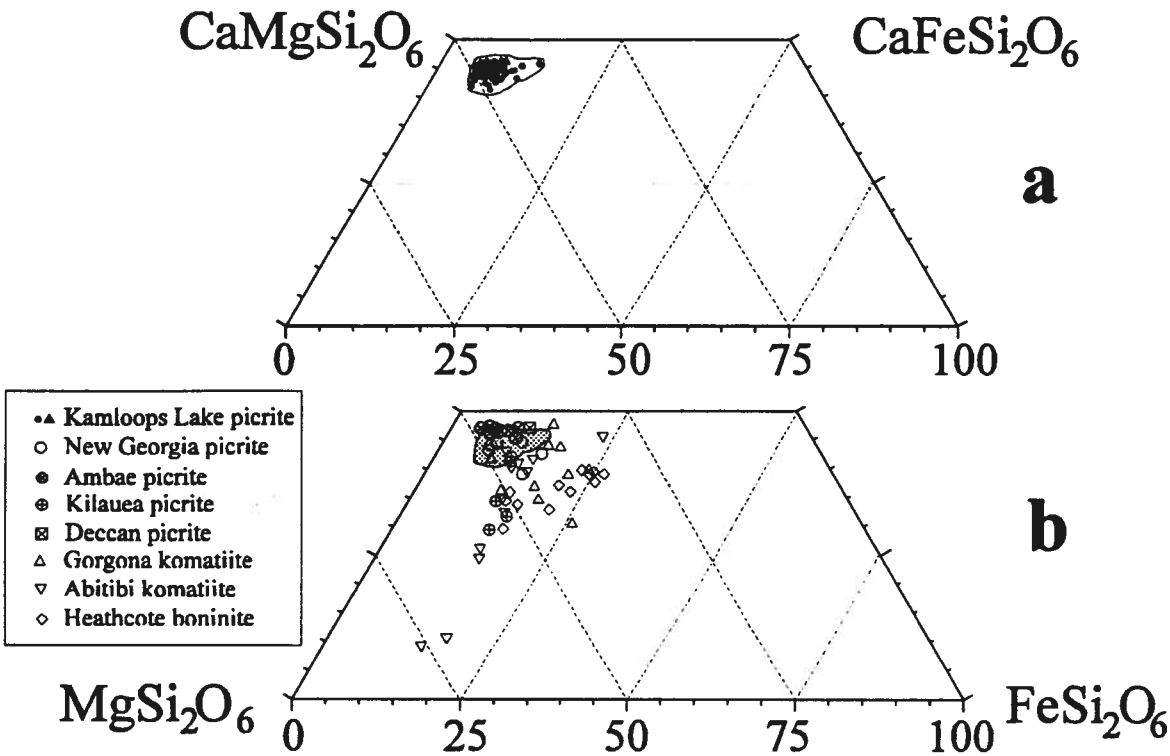

Figure 3.3. Plot of clinopyroxene compositions from **a)** the Kamloops Lake picritic basalts, and **b)** selected ultramafic suites. Sources of data: New Georgia (Ramsay et al., 1984), Kilauea (Nicholls and Stout, 1988), Deccan (Krishnamurthy and Cox, 1977), Ambae (Eggins, 1993), Gorgona (Echeverria, 1980), Abitibi (Barnes et al., 1980) and Heathcote (Crawford and Cameron, 1985).

3.4.4 Cr-spinel

Cr-spinel from the Kamloops Lake picritic basalts exhibit a range of compositions; representative analyses are given in Table 3.3. Structural formulae was calculated on the basis of 32 oxygens. Systematic zoning in Cr-spinel grains is not observed. Spinels have consistently low Al_2O_3 content (average 8.39 wt%) and variable Cr and Fe^{3+} (Figure 3.4). The continuous spectrum of spinel compositions fall in two groups representing cumulate rocks from Watching Creek which are enriched in Fe and non-cumulate rocks from the Carabine Creek and Jacko Lake which lie on the Cr-rich side of the spectrum. TiO_2 concentration of Cr-spinel from cumulate samples (0.70 to 3.87 wt%) is greater than that from non-cumulate samples (0.14 5 to 0.76 wt%). Spinel from cumulate rocks contain 0.35 to 0.46 wt% NiO compared to 0.11 to 0.39 wt% in non-cumulate rocks.

Table 3.3. Representative electron microprobe analyses of spinel from the Kamloops Lake picritic basalts.

	Carabine Creek				Watching Creek				Jacko Lake					
Sample	IM-224	IM-224	IM-225	IM-225	IM-240	IM-240	IM-240	IM-240	IM-230	IM-230	IM-230	IM-230	IM-99	IM-99
Position	Gm	In-ol	In-px-c	In-ol-c	Ph-r	Ph-c	In-px-i	In-px-i	Ph-c	Ph-i	Gm	Gm	In-px-i	Inc-px
SiO_2	0.15	0.06	0.06	0.03	0.04	0.06	0.07	0.04	0.03	0.05	0.56	0.92	0.06	0.74
TiO_2	0.60	0.40	0.58	0.58	1.43	1.16	1.22	1.03	0.48	0.56	0.40	0.72	0.55	0.51
Al_2O_3	8.83	7.17	8.53	8.30	12.08	9.25	8.62	8.63	8.10	8.56	7.16	9.02	7.63	6.94
Cr_2O_3	28.70	49.46	30.60	27.92	10.82	13.65	16.04	15.81	33.75	30.50	32.93	22.45	26.09	27.10
Fe_2O_3	16.00	14.56	15.06	15.57	20.32	19.02	18.62	18.41	14.43	14.95	18.73	19.52	14.88	15.20
FeO	33.22	14.63	32.36	35.32	45.45	46.67	45.31	45.77	30.89	33.91	30.56	37.08	38.34	36.08
MnO	0.43	0.10	0.16	0.21	0.26	0.20	0.23	0.22	0.15	0.17	0.23	0.24	0.20	0.16
MgO	10.83	11.74	11.54	11.21	8.83	9.31	9.58	9.52	12.10	12.03	9.60	9.53	11.50	11.64
CaO	0.09	0.03	0.13	b.d.	0.03	b.d.	0.02	0.02	b.d.	b.d.	0.04	0.08	0.17	0.14
NiO	0.25	0.17	0.28	0.30	0.40	0.39	0.39	0.41	0.29	0.28	0.24	0.31	0.31	0.34
ZnO	0.09	0.10	b.d.	b.d.	b.d.	b.d.	0.09	0.08	0.08	b.d.	0.07	b.d.	b.d.	b.d.
TOTAL	99.19	98.43	99.30	99.44	99.66	99.71	100.19	99.94	100.29	101.01	100.52	99.86	99.73	98.85
					Cation calculation based on 32 oxygens									
Si	0.040	0.016	0.016	0.008	0.011	0.016	0.019	0.011	0.008	0.013	0.151	0.249	0.016	0.201
Ti^{4+}	0.122	0.081	0.117	0.118	0.291	0.238	0.249	0.211	0.096	0.111	0.081	0.146	0.111	0.104
Al	2.808	2.280	2.699	2.636	3.846	2.972	2.759	2.770	2.535	2.661	2.281	2.873	2.421	2.218
Cr^{3+}	6.123	10.553	6.496	5.950	2.311	2.943	3.444	3.405	7.086	6.361	7.038	4.797	5.555	5.810
Fe^{3+}	6.745	2.971	6.539	7.163	9.240	9.576	9.260	9.381	6.172	6.730	6.216	7.540	7.769	7.362
Fe^{2+}	3.610	3.287	3.380	3.509	4.590	4.338	4.228	4.194	3.203	3.297	4.234	4.410	3.350	3.448
Mn^{2+}	0.098	0.023	0.036	0.048	0.059	0.046	0.053	0.051	0.034	0.038	0.053	0.055	0.046	0.037
Mg	4.357	4.723	4.619	4.504	3.556	3.785	3.879	3.866	4.790	4.731	3.869	3.840	4.617	4.706
Ca	0.026	0.009	0.037	0.000	0.009	0.000	0.006	0.006	0.000	0.000	0.012	0.023	0.049	0.041
Ni	0.054	0.037	0.060	0.065	0.087	0.086	0.085	0.090	0.062	0.059	0.052	0.067	0.067	0.074
Zn	0.018	0.020	0.000	0.000	0.000	0.000	0.018	0.016	0.016	0.000	0.014	0.000	0.000	0.000
CR#	68.56	82.23	70.65	69.30	37.53	49.75	55.52	55.14	73.65	70.51	75.52	62.54	69.65	72.37
MG#	54.69	58.96	57.74	56.21	43.65	46.60	47.85	47.97	59.93	58.93	47.75	46.55	57.95	57.71

CR# = 100•Cr/(Cr+Al); MG# = 100•Mg/(Mg+Fe^{2+}). Sample numbers refer to whole-rock analyses in Table 2.4. Ph=phenocryst, Gm=groundmass, In=inclusion (host mineral indicated; ol=olivine; px=clinopyroxene), c=core, i=interior, r=rim

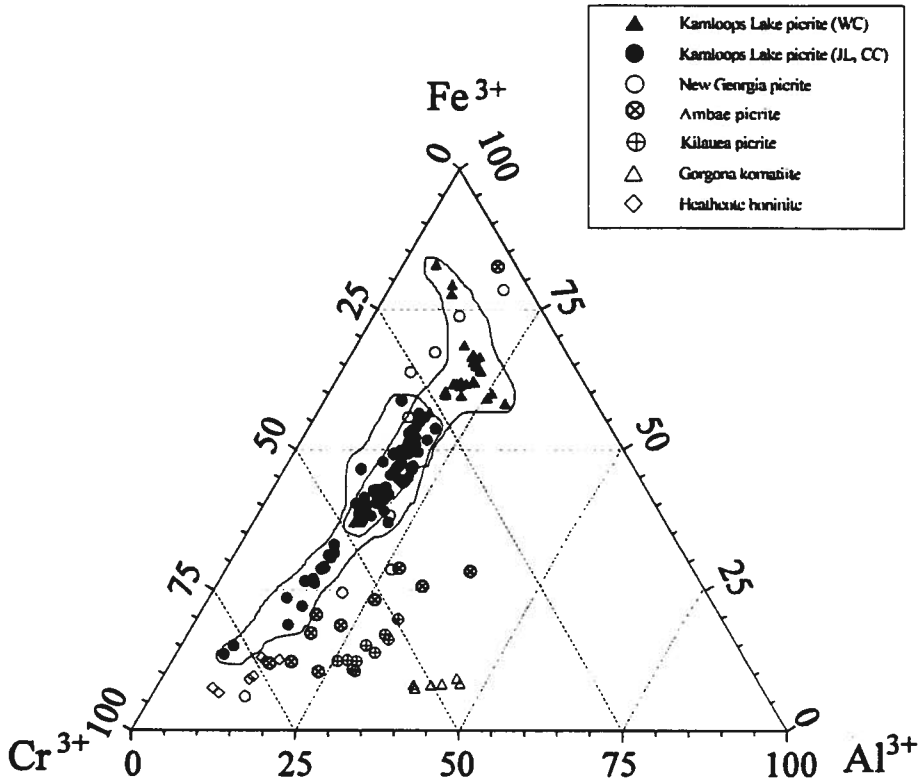

Figure 3.4. Ternary plot of the proportions of the cations Cr^{3+}, Al^{3+}, and Fe^{3+} in the spinels of the Kamloops Lake picrites. Fields are indicated for localities with volcanic textures (solid circles) and cumulate rocks (solid triangles). Other data from: New Georgia (Ramsay et al., 1984), Kilauea (Nicholls and Stout, 1988), Ambae (Eggins, 1993), Gorgona (Echeverria, 1980) and Heathcote (Crawford and Cameron, 1985).

Compositions of spinel from other ultramafic suites (Figure 3.4) are similar to the Kamloops Lake rocks but most suites show slightly higher Al contents. Spinels from komatiites on Gorgona Island (Echeverria, 1980) show the greatest Al concentrations (21.6 to 25.7 wt% Al_2O_3). Spinel from the Kamloops Lake suite are further distinguished from those found in komatiites by their relative depletion in ZnO and MnO (Plaksenko and Smol'kin, 1990).

Cr-spinel compositions from Kamloops Lake picritic rocks and other selected suites are plotted on diagrams of $100 \bullet Mg/(Mg + Fe^{2+})$ *vs* $100 \bullet Cr/(Cr + Al)$ and $100 \bullet Mg/(Mg + Fe^{3+})$ *vs* $100 \bullet Fe^{3+}/(Cr + Al + Fe^{3+})$ (Figure 3.5). A weak positive correlation exists between $Cr/(Cr + Al)$ and $Mg/(Mg + Fe^{2+})$ in spinels from the Kamloops Lake suite; a similar trend is seen in spinels from picritic lavas associated with

island arc magmatism (Ramsay et al., 1984; Eggins, 1993). Spinels from the Kamloops Lake picritic basalts are highly oxidized (Figure 3.5b); $100 \cdot Fe^{3+}/(Fe^{3+} + Cr + Al)$ ratios range from 13.7 to 82.9. Picritic rocks from New Georgia (Ramsay et al., 1984) and Ambae (Eggins, 1990) have similar ratios and Ramsay et al. (1984) and Utter (1978) report that highly oxidized spinels are restricted to island arc lavas.

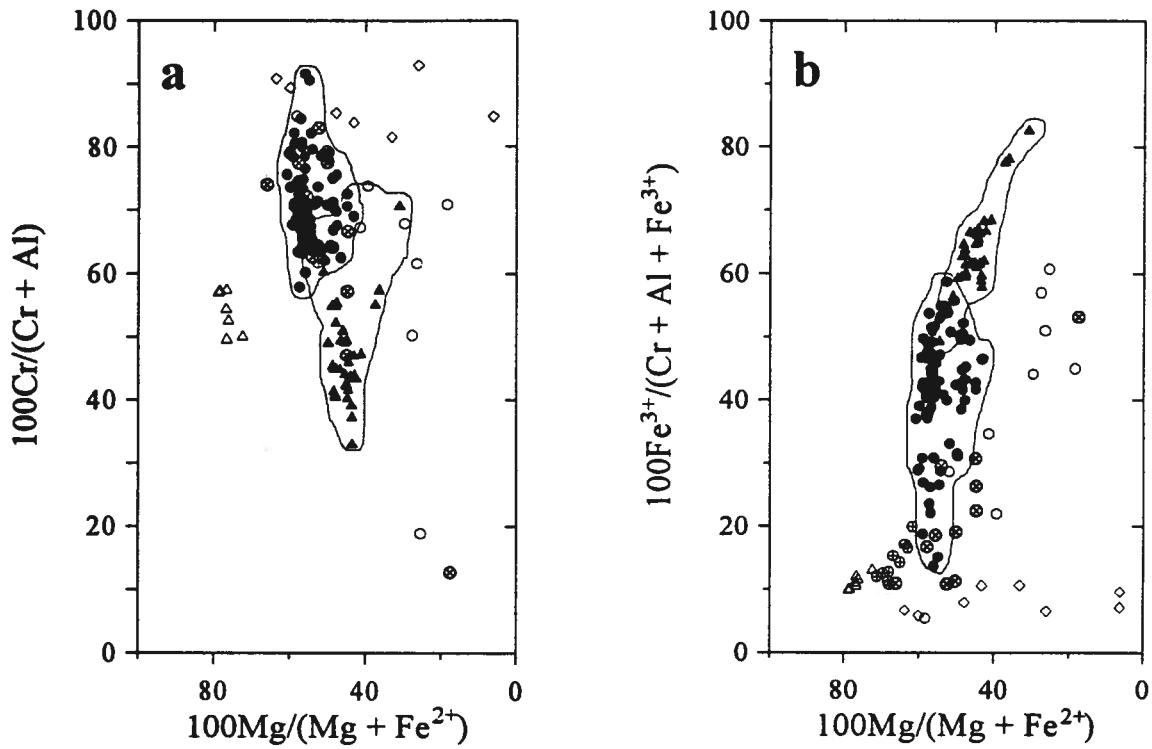

Figure 3.5. Spinel compositions for the Kamloops Lake picritic basalts shown as a) $100 \cdot Mg/Mg + Fe^{2+}$ *vs* $100 \cdot Cr/(Cr + Al)$, and b) $100 \cdot Mg/(Mg + Fe^{2+})$ *vs* $100 \cdot Fe^{3+}/(Fe^{3+} + Cr + Al)$. Other data from: New Georgia (Ramsay et al., 1984), Kilauea (Nicholls and Stout, 1988), Ambae (Eggins, 1993), Gorgona (Echeverria, 1980) and Heathcote (Crawford and Cameron, 1985). Symbols as in Figure 3.4.

Cr/(Cr + Al) ratios in spinels from the Kamloops Lake picritic basalts also suggest an island arc tectonic affinity (Dick and Bullen, 1984). Cr/(Cr + Al) ratio in Cr-spinel has been used as an indication of the volume of mantle melt needed to produce lavas of picritic composition, and this ratio, which averages 49 for cumulate rocks and 71 for non cumulate rocks, indicates significant melting of the mantle source (Dick and Bullen, 1984).

3.5 WHOLE-ROCK GEOCHEMISTRY

3.5.1 Major Element Variation

Whole rock chemical compositions for the Kamloops Lake ultramafic rocks are given in Table 3.4; two from Carabine Creek, one from Watching Creek, and one from Jacko Lake. See Appendix E and G for analytical techniques. Two serpentinites from the Iron Mask batholith, one of which was analyzed 6 times, are also given. These ultramafic rocks have exceptionally low Al_2O_3 contents (2.17 to 6.84 wt%), low SiO_2 (38.4 to 43.2 wt%), and very high MgO (24.3 to 33.65 wt%). TiO_2 and CaO contents in the Kamloops Lake picrites, which range from 0.166 to 0.386 wt% and 3.20 to 6.03 wt% respectively, are very low, possibly reflecting the very high MgO. Kamloops Lake rocks are highly enriched with respect to Ni (920 to 1420 ppm) and Cr (1670 to 3040 ppm).

MgO *vs* SiO_2 concentration of the Kamloops Lake picritic basalts and selected mafic and ultramafic suites are given in Figure 3.6a. Kamloops Lake picritic basalt contains the lowest SiO_2 and, with the exception of komatiites from the Abitibi Greenstone Belt, the highest MgO. The suites presented, except for Abitibi komatiites, boninitic suites and Vanuatu island arc basalts, exhibit a linear trend of increasing MgO with decreasing SiO_2. The Kamloops Lake picrites are at the MgO-rich end of this trend. Abitibi komatiites show a consistent SiO_2 concentration over a range of MgO as do boninitic rocks, which also contain greater SiO_2. Vanuatu arc basalts, while having similar SiO_2 contents for a given MgO content as most of the other suites, are more restricted in MgO concentration and therefore exhibit a cluster of points with consistent SiO_2 concentrations.

The Kamloops Lake picritic rocks show extreme depletion with respect to Al_2O_3 compared to all other suites of rocks except the Abitibi komatiites (Figure 3.6b). Well-defined trends of decreasing Al_2O_3 with increasing MgO are seen in most of the suites investigated, however, the position of the trend in chemical space is variable. Island arc picrites (New Georgia, Ambae) as well as a hot-spot picritic suite

Table 3.4. Whole rock analyses of Kamloops Lake picritic basalts.

	IM-225 CC	IM-222 CC	IM-241 WC	IM-230 JL	IM-108* IM	IM-309 IM	1 σ
SiO_2	40.40	38.70	38.40	41.30	39.33	43.20	0.197
TiO_2	0.230	0.193	0.166	0.240	0.21	0.386	0.005
Al_2O_3	3.80	3.08	2.17	3.94	2.74	6.84	0.056
Fe_2O_3	5.32	6.42	10.30	4.48	11.00	5.01	0.063
FeO	3.97	2.64	--	4.72	--	4.40	-
MnO	0.17	0.17	0.18	0.17	0.20	0.14	0.004
MgO	31.40	32.80	32.60	32.30	33.65	24.30	0.217
CaO	4.72	3.20	5.32	4.91	3.53	6.03	0.109
Na_2O	0.09	0.02	0.08	0.18	0.15	0.30	0.012
K_2O	0.95	0.22	0.15	1.50	0.57	2.21	0.012
P_2O_5	0.11	0.10	0.05	0.10	0.06	0.13	0.005
H_2O^+	7.80	11.10	9.20	4.70	7.38	4.80	
CO_2	0.08	0.08	0.36	0.04	0.08	0.03	
SUM	99.04	98.72	98.97	98.58	98.90	97.78	
LOI	8.45	11.80	9.75	4.80	7.10	5.00	
			Trace Elements				
Ba[1]	213	147	226	521	129	354	
Rb[2]	31.11	16[1]	3.83	26.03	16.30	54[1]	
Sr[2]	216.44	122[1]	41.00	112.92	14.00	201[1]	
Nb[2]	0.59	6[1]	0.13	0.37	0.31	3[1]	
Zr[2]	11.80	21[1]	4.35	10.85	10.55	33[1]	
Y[2]	4.34	b.d.[1]	2.57	4.03	3.90	b.d.[1]	
Ni[1]	1350	1380	1420	1410	1254	920	
Cr[4]	2580	3040	2790	2990	2902	1670	
V[2]	110.91	--	61.90	103.12	74.95	--	
Sc[2]	18.27	14.9[3]	21.41	17.41	20.73	23.6[3]	
Th[2]	0.23	b.d.[1]	0.10	0.27	0.28	b.d.[1]	
U[2]	0.30	b.d.[1]	0.06	0.09	0.20	b.d.[1]	
Pb[2]	1.50	b.d.[1]	0.99	1.65	0.31	b.d.[1]	
Hf[2]	0.51	b.d.[3]	0.16	0.44	0.39	0.6[3]	
Cl[1]	128	109	293	125	396	125	
Co[1]	80	85	87	85	92	66	
Cu[1]	25	15	20	30	25	17	
F[1]	75	110	20	90	45	192	
Ga[1]	16	16	16	16	17	19	
S[1]	b.d.	b.d.	1120	b.d.	1662	b.d.	
Sn[1]	10	10	7	12	4	10	
Ti[1]	1210	981	746	1160	1210	1780	
Zn[1]	58	60	61	60	50	58	
Li[2]	6.57	--	7.70	6.62	4.69	--	
Be[2]	0.65	--	0.01	0.82	0.81	--	
Mo[2]	0.11	b.d.[1]	0.47	0.25	3.40	b.d.[1]	
Cs[2]	0.63	1[3]	0.24	1.43	0.80	2[3]	
Ta[2]	0.37	--	0.08	0.17	0.15	--	
Tl[2]	0.23	--	-0.08	0.09	0.09	--	
Bi[2]	0.07	--	-0.06	0.17	0.10	--	

* Average of six analyses

[1] XRF Pressed Pellet [2] Inductively Coupled Plasma Mass Spectrometry

[3] Neutron Activation [4] XRF Fused Pellet

CC=Carabine Creek, WC=Watching Creek,

JL=Jacko Lake, IM=Iron Mask

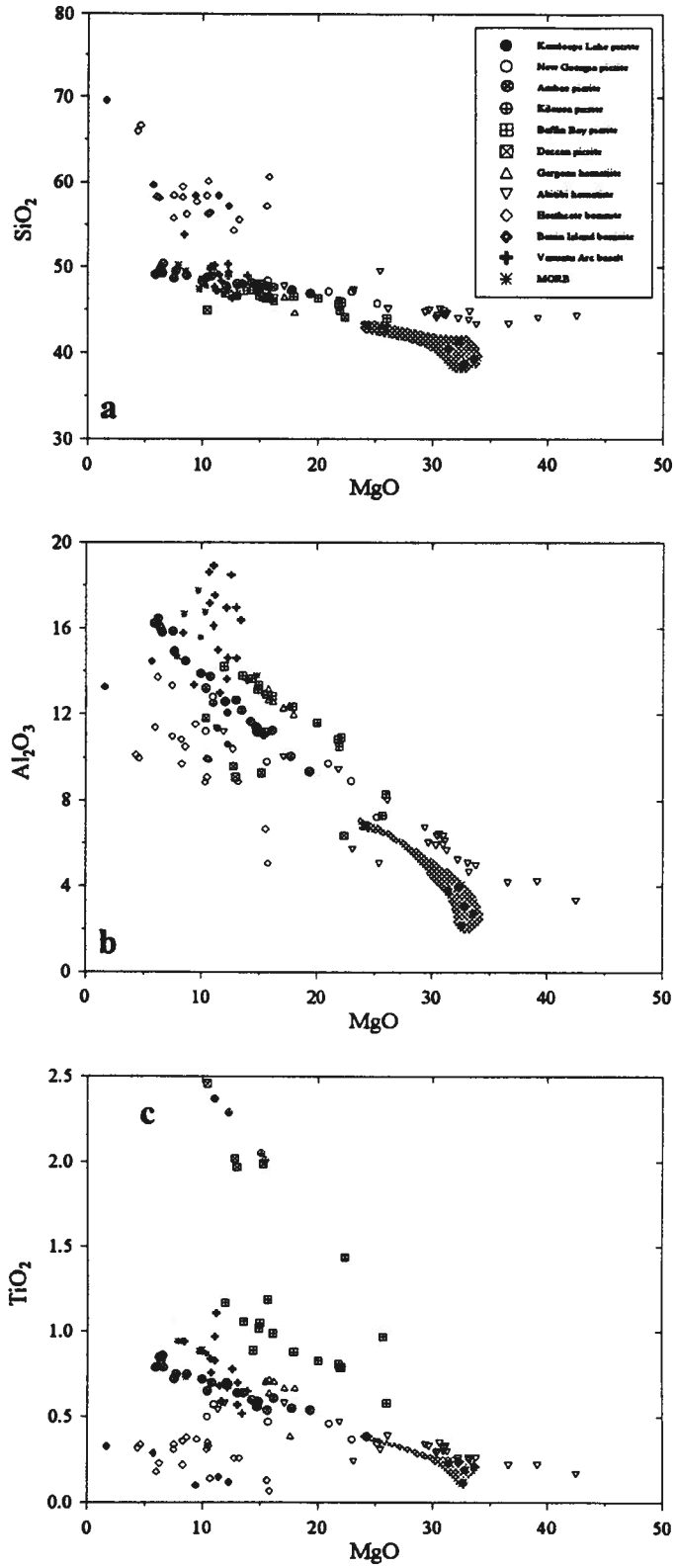

Figure 3.6. Chemical compositions of Kamloops Lake picritic basalts (shaded) and other suites of mafic rocks: a) MgO *vs* SiO_2, b) MgO *vs* Al_2O_3 and c) MgO *vs* TiO_2. Sources of data: New Georgia (Ramsay et al., 1984), Baffin Bay (Francis, 1985), Kilauea picrite (Nicholls and Stout, 1988), Ambae (Eggins, 1993), Deccan (Krishnamurthy and Cox, 1977), Gorgona (Echeverria, 1980), Abitibi (Barnes et al., 1983), Heathcote (Crawford and Cameron, 1985), Bonin Island (Hickey and Frey, 1982), Vanuatu (Dupuy et al., 1982) and MORB (Sun et al., 1979).

(Kilauea) define a trend with Kamloops Lake compositions at the extreme. The other picritic suites (Deccan, Baffin Bay) and the komatiitic suites (Gorgona, Abitibi) have trends of similar slopes but in a different chemical space. Boninitic suites and Vanuatu arc basalts show a large variation in Al_2O_3 over a small range of MgO concentrations.

Depletion of Al_2O_3 in the Kamloops Lake rocks may reflect initial low aluminum in the source region, the presence of a residual aluminous phase (such as garnet or spinel) after partial melting (Bence et al., 1980), or plagioclase fractionation. However, the trend seen in Figure 3.6b of increasing Al_2O_3 with decreasing MgO suggests that evolution of the Kamloops Lake suite did not involve plagioclase fractionation (Perfit, 1980).

MgO *vs* TiO_2 concentrations is given in Figure 3.6c. Ti has been used as a discriminator element in the study of komatiites and boninites (Sun and Nesbitt ,1978; Crawford and Cameron, 1985). The Kamloops Lake picritic basalts are depleted in TiO_2 in comparison to the other mafic and ultramafic suites with the exception of the Abitibi komatiites and the boninitic suites. On this diagram, it appears that each suite defines a trend of different slope. Picritic rocks from Deccan and Kilauea are enriched in TiO_2 which falls off sharply with increasing MgO. Baffin Bay picrites have a slightly shallower slope, yet still a significant amount of TiO_2. Arc picrites from New Georgia and Ambae define a slope which includes the Kamloops Lake suite.

3.5.2 Rare Earth Elements

Rare earth element patterns for the Kamloops Lake picrite suite are shown in Figure 3.7 and element concentrations in Table 3.5. See Appendix G for details of rock preparation. REE abundances in the Kamloops Lake suite are very low; all normalized (Boynton, 1984) values are less than 4 and the patterns are quite flat. The Jacko Lake, Carabine Creek and Iron Mask occurrences have similar profiles

which show slight enrichment of the LREE's (La/Sm averaging 1.1) relative to HREE (Nd/Lu averaging 1.4). The serpentinite from the Iron

Table 3.5. REE concentrations the Kamloops Lake picritic basalts.

	IM-225 CC	IM-225 CC	IM-225* CC	IM-222 CC	IM-241 WC	IM-230 JL	IM-108 IM	IM-309 IM
La	0.99	0.99	0.99	0.9[1]	0.44	1.15	0.77	2.7[1]
Ce	2.39	2.32	2.36	b.d.[1]	1.06	2.62	1.94	7[1]
Pr	0.34	0.35	0.34	--	0.20	0.41	0.31	--
Nd	1.78	1.87	1.82	b.d.[1]	1.02	2.18	1.69	b.d.[1]
Sm	0.53	0.60	0.56	0.4[1]	0.37	0.56	0.48	0.9[1]
Eu	0.17	0.21	0.19	0.2[1]	0.13	0.20	0.15	0.2[1]
Gd	0.72	0.75	0.74	--	0.42	0.75	0.64	--
Tb	0.11	0.11	0.11	b.d.[1]	0.07	0.10	0.11	b.d.[1]
Dy	0.82	0.78	0.80	--	0.49	0.78	0.78	--
Ho	0.15	0.17	0.16	--	0.11	0.16	0.15	--
Er	0.51	0.46	0.48	--	0.29	0.49	0.39	--
Tm	0.07	0.07	0.07	--	0.04	0.07	0.06	--
Yb	0.54	0.42	0.48	0.3[1]	0.30	0.49	0.40	0.7[1]
Lu	0.08	0.07	0.08	b.d.[1]	0.04	0.07	0.07	0.11[1]

* Average of two analyses
Analyses by Inductively Coupled Plasma Mass Spectrometry
except where noted
[1] Neutron Activation

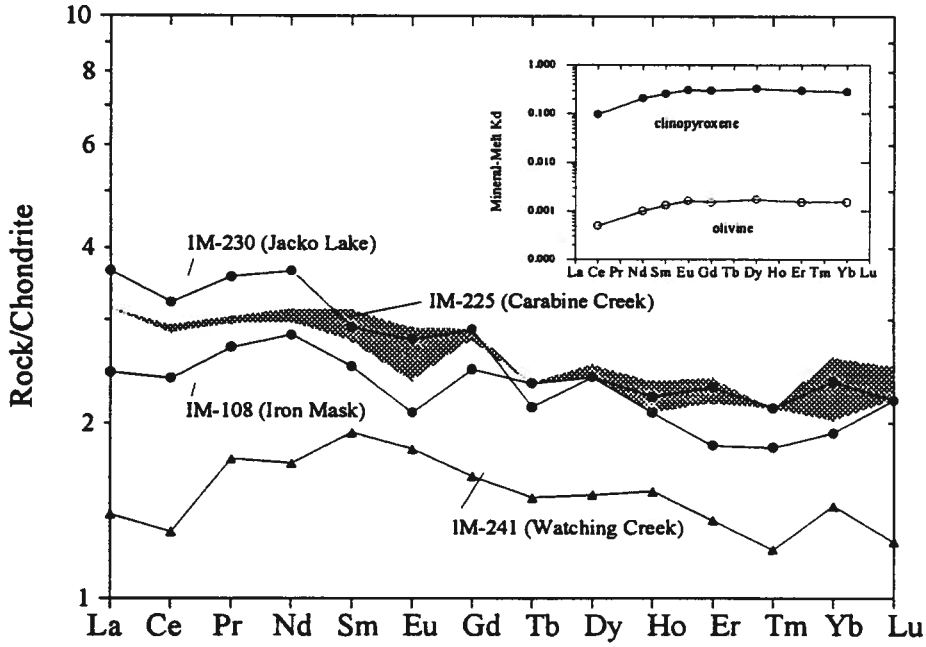

Figure 3.7. Chondrite normalized REE Patterns of the Kamloops Lake picritic basalts. Duplicate analyses of sample IM-225 is shown in the shaded region. Chondrite data of Boynton (1984).

Mask diverges slightly; it has a slight depletion in the HREE Er. This divergence may be an expression of REE mobility during serpentinization processes. The cumulate sample from Watching Creek contains significantly lower abundances of the REE's than the volcanic samples and exhibits a slightly different pattern. The $(La/Yb)_{CH}$ of the Watching Creek sample is 0.97 compared to 1.27(IM), 1.36(CC) and 1.53(JL). A consistent feature of REE patterns from the Kamloops Lake picritic basalts is a slight depletion in Ce with respect to La; a feature typical of island arc suites (Dupuy et at., 1982). The samples do not show a significant depletion or enrichment in Eu with respect to Sm and Gd outside of analytical error (see shaded area in Figure 3.7), indicating that plagioclase fractionation was not involved in the evolution of these ultramafic lavas.

Also shown in Figure 3.7 are crystal/liquid REE partition coefficients for olivine and clinopyroxene (Hanson, 1980). The depleted, flat REE profiles of the Kamloops Lake lavas are consistent with olivine control. In addition, the Watching Creek cumulate locality has significantly lower normalized values for all elements, consistent with the greater modal olivine observed in the rock.

Figure 3.8 shows REE profiles from other mafic-ultramafic suites. Patterns from island arc suites (Figure, 3.8a) are enriched in LREE's, with the Ambae picritic suite (Eggins, 1993) showing the greatest enrichment. All of the chosen island suites show depletion in Ce with respect to La. although this feature is not as pronounced as in the Kamloops Lake suite. Absolute REE abundances for New Georgia (Ramsay et al., 1984), Ambae (Eggins, 1993) and Vanuatu basalts (Dupuy et al., 1982) are significantly greater than in Kamloops Lake rocks. Both the greater REE concentrations and the LREE enriched patterns of these suites may be manifestations of the relative role of the minerals in the magmatic system. Olivine and clinopyroxene partition coefficients (Figure 3.7) indicate that olivine coupled with clinopyroxene could produce a slightly LREE enriched pattern, as is seen in these systems.

Data from komatiitic rocks of Gorgona Island (Echeverria, 1980) and the Abitibi Greenstone Belt (Barnes et al., 1983) along with normal MORB (Sun et al., 1979) are shown in Figure 3.8b. The patterns

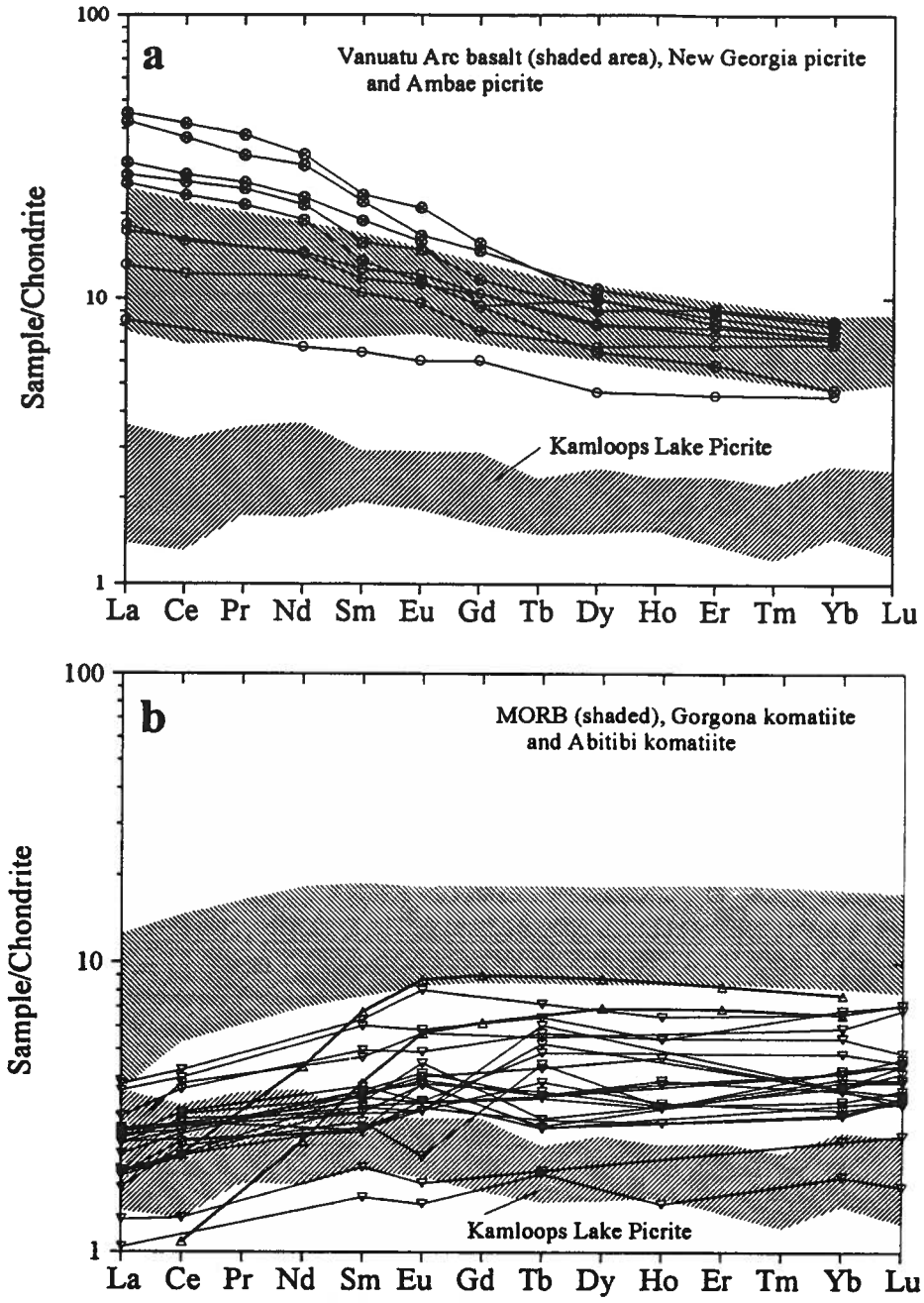

Figure 3.8. Chondrite normalized REE patterns for selected ultramafic suites; a) island arc suites, and b) komatiite suites and MORB. Data from: New Georgia (Ramsay et al., 1984), Ambae (Eggins, 1993), Gorgona (Echeverria, 1980), Abitibi (Barnes et al., 1983), Vanuatu (Dupuy et al., 1982) and MORB (Sun et al., 1979). Symbols as in Figure 3.6.

for these rocks are distinctly different than both the Kamloops Lake suite and the island arc suites. These suites show LREE depleted patterns and are relatively lower in absolute abundances than the island arc

rocks. These patterns reflect the different origin and evolution of these suites compared to island arc suites.

The overall flat REE pattern of the Kamloops Picrites indicates substantial melting in the source region (Dick and Bullen, 1984; Hanson, 1980). Experiments have shown that magmas produced from small amounts of mantle melting exhibit LREE enriched patterns, whereas larger amounts of melt (≈20 % or greater) produce magmas with flat REE patterns (Hanson, 1989). In addition, because garnet concentrates the HREE's, the lack of HREE enrichment may indicates a mantle source region that is garnet-poor or had a garnet-enriched residuum.

3.5.3 Incompatible Elements

A spidergram for incompatible elements in the Kamloops Lake picritic basalts normalized to primitive mantle (Taylor and McLennan, 1985) is shown in Figure 3.9 along with MORB compositions (Sun et al., 1979; Taylor, 1980) for comparison. Incompatible element abundances are a function of both the source components and fractionation processes. The patterns, therefore, indicate tectonic affinity for the suite.

The Kamloops Lake picritic basalts are depleted, with respect to MORB compositions, in REE's, Ti, Zr, Y and Hf. Intra-suite variation in Ti, Zr, Y and Nb has been shown to correspond to fractional crystallization of olivine and clinopyroxene ± magnetite (Perfit et al., 1980). Kamloops Lake ultramafic rocks are highly enriched in Rb Ba, K and to a lesser degree in Sr with respect to MORB. One serpentinite from the Iron Mask batholith is aberantly low in Sr, a feature which is considered to represent the alteration process and not the original magmatic Sr content. The depletions and enrichments of the specified elements are indicative of an island-arc affinity (Perfit et al., 1980).

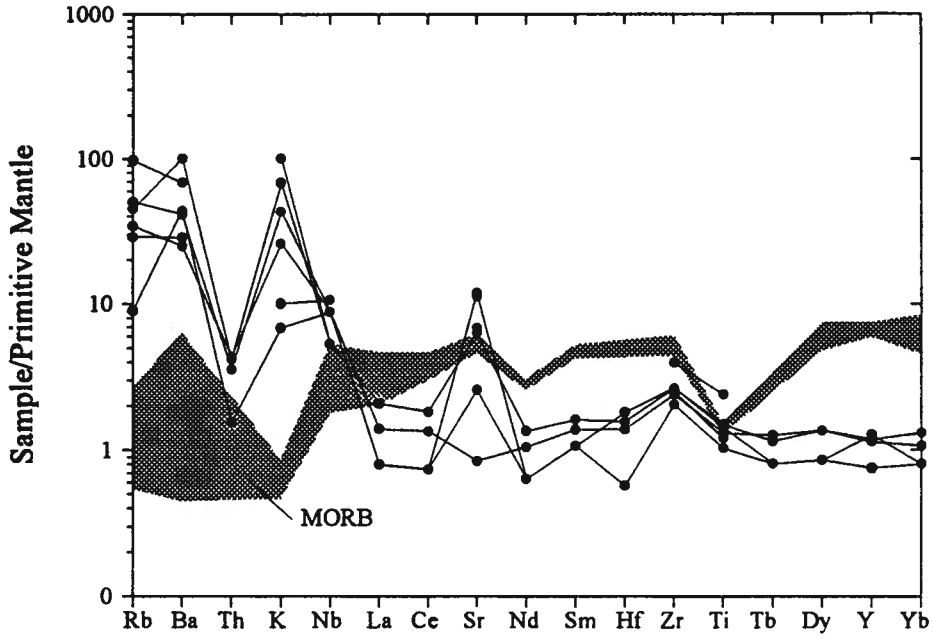

Figure 3.9. A spidergram of incompatible element concentrations in the Kamloops Lake picritic basalt with Normal MORB (Sun et al., 1979) shown for comparison. Normalization data from Taylor and McLennan (1985) and Boynton (1984).

Figure 3.10 presents incompatible element diagrams constructed from available data for selected suites of mafic-ultramafic rocks from a variety of tectonic environments overlain on the pattern produced by the Kamloops Lake suite. Incompatible element data from modern island arc settings exhibit similar patterns to the Kamloops Lake suite, with enrichment in K and Sr and depletion of Nb compared to normal MORB (Figure 3.10a). Absolute abundances for most of the incompatible elements in these suites are, in general, slightly greater than the Kamloops Lake picrites and the intra-suite variation is less pronounced. Ambae picritic rocks are similar to the Kamloops lake suite in the relative enrichment in Ba compared to Rb, while New Georgia picrites exhibit the opposite correlation. Both suites of picritic rocks are more depleted in Nb and enriched in Ti than the Kamloops Lake suite. However, the overall patterns of these modern arc systems correspond very well with the observed ratios in the Kamloops Lake suite, confirming an island arc tectonic affinity.

Komatiites from the Abitibi greenstone belt show extreme depletion with respect to K and Sr, but otherwise produce a relatively flat signature (Figure 3.10b). Plaksenko and Smol'kin (1990) distinguish

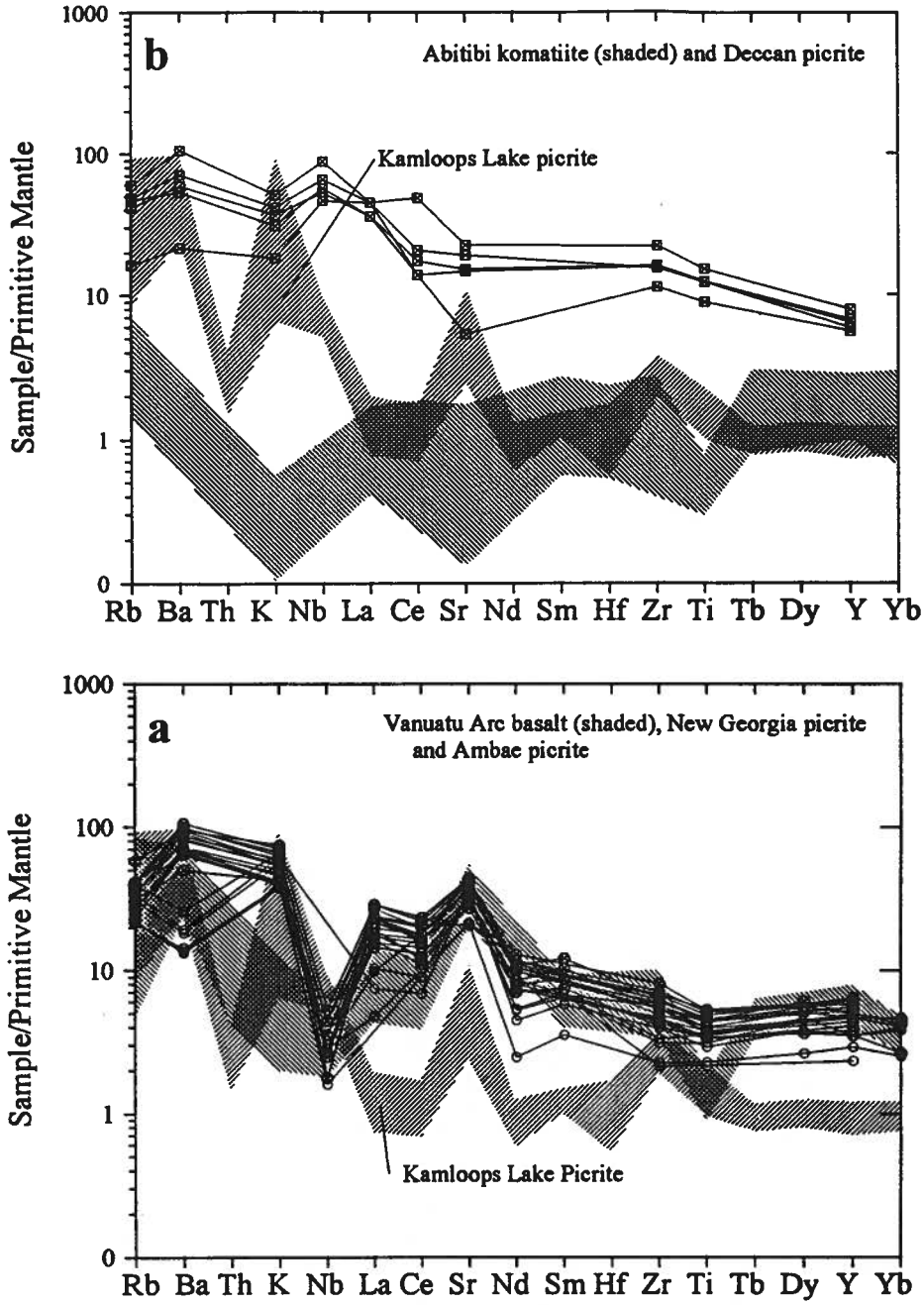

Figure 3.10. Spidergrams of incompatible element concentrations for **a)** island arc rock suites, and **b)** suites with other tectonic affinities. Data from: New Georgia (Ramsay et al., 1984), Ambae (Eggins, 1993), Deccan (Krishnamurthy and Cox, 1977), Abitibi (Barnes et al., 1983) and Vanuatu (Dupuy et al., 1982).

komatiites by depletion of Sr, Ba, Ni and Cr relative to picritic rocks. Data from picritic basalts from the Deccan flood basalt province (Krishnamurthy and Cox, 1977) exhibit a relatively flat, uniform pattern, with only slight relative enrichment in Nb and REE's.

3.6 MAGMATIC DIFFERENTIATION

The process of simultaneously evaluating magmatic relationships and the nature of the magmatic differentiation controlling the composition of the picritic basalts was undertaken using Pearce Element Ratio diagrams (Pearce, 1968; Russell and Nicholls, 1988; Nicholls and Russell, 1991). Diagrams (*cf*, Figure 3.11) were designed by: i) choosing an appropriate conserved element for the denominator and ii) choosing a set of numerator elements for the x and y-axes that will model the effects of the target mineral assemblage (Stanley and Russell, 1989; Nicholls and Gordon,. 1994). The target mineral assemblage for the Kamloops Lake picritic basalts are the phenocryst and microphenocryst phases- olivine and clinopyroxene. Ti was chosen as the denominator element for diagrams concerning the Kamloops Lake suite because of low analytical error and the absence of a major Ti-bearing phase in the phenocryst assemblage of the picritic basalts.

The main concept behind this method is that rocks that are related to each other through fractionation or accumulation of a given mineral or mineral assemblage will define a line with predictable slope. For example, Figure 3.11 shows the diagram designed to test whether olivine sorting can explain the compositional variation in the Kamloops Lake picrites. The axes are chosen so that the accumulation or loss of olivine would cause cogenetic rock compositions to lie along a line with unit slope. If the picrite occurrences can be related through the fractionation of olivine, then each point should plot along this reference line.

One sample from Carabine Creek (IM-225) was chosen as the reference composition and the model line is forced through this data point. It is one of the least altered picrite samples and has a well-preserved, pronounced volcanic character. If the rock compositions fall the model line, then the hypothesis of a cogenetic suite can not be rejected. If the compositions do not fall on the model line defined by the axes, then the rocks may either be non-cogenetic or may be related through fractionation or accumulation

of minerals not accounted for on the diagram. Error ellipses are obtained from 6 duplicate analyses and represent 1s error.

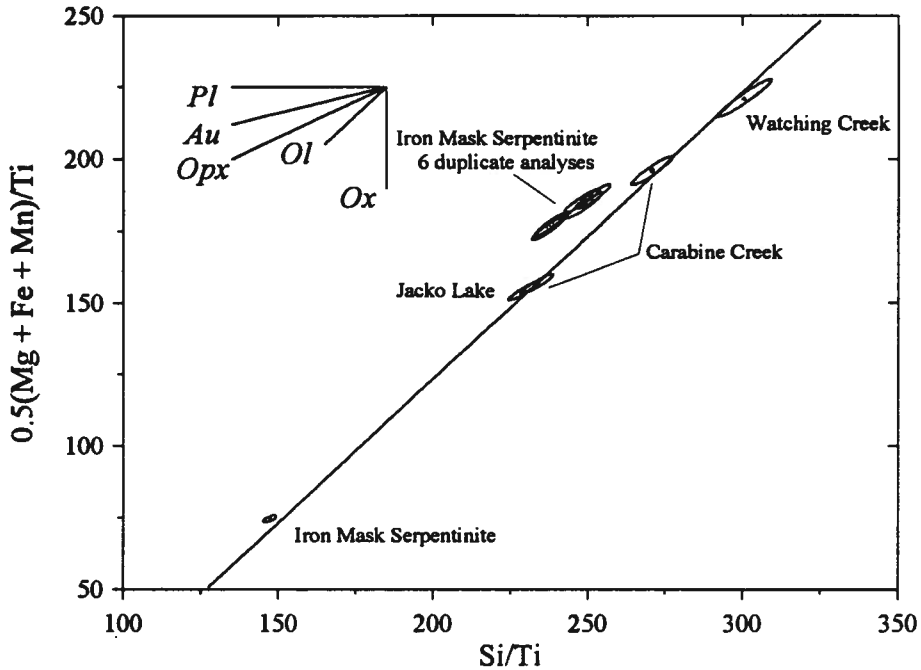

Figure 3.11. Diagram designed to test the hypothesis that olivine crystallization or accumulation may account for the chemical variation in the Kamloops Lake picritic suite. See text for discussion.

Figure 3.11 shows that the three relatively unserpentinized picrite localities can be related through fractionation or accumulation of olivine. The model line drawn through IM-225 intersects the other Carabine Creek sample as well as samples from Watching Creek and Jacko Lake within analytical error. Two serpentinite samples from the Iron Mask batholith do not fall on the model line and fail the test for comagmatism with the other localities. Furthermore, the serpentinites do not define a simple trend with unit slope indicating that they are not related to each other through fractionation or accumulation of olivine. It is likely that the process of serpentinization has caused addition or removal of one of the elements used in the diagram (Si, Ti, Mg or Fe) (Viljoen and Viljoen, 1969; Blais and Auvray, 1990). If this is the case, comagmatism cannot be discounted.

Selected mafic-ultramafic rock suites have been plotted on the same olivine "sorting" diagram (Figure 3.12). Boninitic rocks are not shown because orthopyroxene is the dominant fractionating phase (Jenner, 1981). Model fractionation trends (e.g., slope = 1.0) were projected from the most magnesian sample in each suite. The trend of Kamloops Lake picritic rocks, shown as a heavy line, lies at greater element ratio values than most of the other suites in this chemical space due to the low concentration of the denominator element (Ti) in the Kamloops Lake suite. Only two suites exhibit overlap with the Kamloops Lake picrites-Abitibi komatiites and New Georgia picrites.

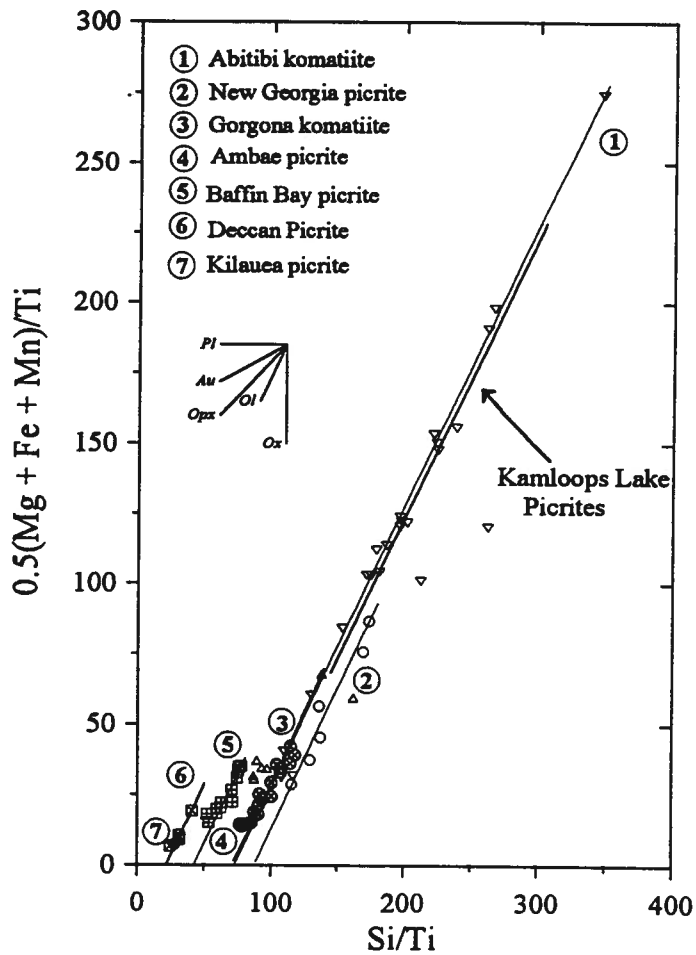

Figure 3.12. Selected suites of ultramafic rocks plotted on an element ratio diagram designed to test whether fractionation of olivine can explain chemical variation observed within the suite. Data from: New Georgia (Ramsay et al., 1984), Baffin Bay (Francis, 1985), Kilauea picrite (Nicholls and Stout, 1988), Ambae (Eggins, 1993), Deccan (Krishnamurthy and Cox, 1977), Gorgona (Echeverria, 1980) and Abitibi (Barnes et al., 1983).

Data from all of the selected suites show scatter around their model trend (Figure 3.12); some suites (Baffin Bay and New Georgia) show excellent fit of the data points. The total intra-suite chemical variation seen in several groups of ultramafic rocks is much less than seen in the Kamloops Lake suite (e.g. Si/Ti = 145-300). Abitibi komatiites are the only suite showing a similar scale of variation. Olivine fractionation consistently explains at least some of the crystallization-fractionation processes functioning in these suites of ultramafic volcanic rocks. There are at least two explanations for large amounts of scatter seen in the Gorgona komatiites and Abitibi komatiites. Another phase, possible pyroxene or plagioclase, may have been involved in fractionation processes or the individual suites may comprise more than one magma batch.

The intercept of the model lines on element ratio diagrams are a measure of processes in the source region. Thus the intercepts on Figure 3.12 **for those systems where fractionation processes are controlled by olivine**, are a function of the source region for the suites (Cui and Russell, in review). Picritic suites from Kilauea and Deccan have very almost identical intercepts (-20.7 and -21.4 respectively), whereas picrites from Baffin Bay intercept slightly more negatively (-41.9). Model lines for the picritic island arc suites of New Georgia and Ambae intercept at -86.8 and -72.1 respectively and the Kamloops Lake picritic suite intercepts at a similar value (-76.7). The similarity in the intercepts for the olivine controlled fractionation of island arc suites suggests that the processes operating at the source region are similar to each other yet can be shown to be distinguishable from other tectonic settings. This is logical, since it is believed that source regions for arc systems involve a unique blend of material and processes (Perfit et al., 1980; Dupuy et al., 1982; Eggins, 1990).

3.7 SATURATION TEMPERATURE, OLIVINE COMPOSITION AND FO2

Picritic magmas have been interpreted to represent either primary mantle-derived liquids (O'Hara, 1982) or to be strictly products of olivine accumulation (Hart and Davis, 1979). Thus, it is relevant to document the existence of primary liquids and to investigate their differentiation and

evolution. Differentiates of the Kamloops Lake picritic basalts are not exposed, and testing the accumulation-differentiation theory was undertaken by calculating olivine saturation temperatures, the coexisting oxygen fugacity and the amount of olivine crystallization for the suites examined in this study. The investigation of the physical and chemical state of primary liquids will provide clues to the environment of formation and differentiation processes of mantle-derived arc liquids.

3.7.1 Method

Bulk rock compositions were forced to equilibrate with the most forsteritic coexisting olivine composition at a variety of Fe^{3+}/Fe^{2+} ratios. This process produced values for temperature and oxygen fugacity of the melt, the amount (moles per 100 moles) of olivine which would have been crystallized out of the melt to that point and the composition of the residual liquid. The calculated values define a path in T-lnfO_2 space which is unique for each rock. By superimposing buffering curves onto the rock paths, reasonable limits may be set on the actual value of these variables.

Considerations which are unable to be accounted for include: the range of olivine compositions found in each rock (an average value was used) and/or compositional modification in a cumulate pile (Van Kooten and Buseck, 1978) . In addition, the serpentinites from the Iron Mask batholith have been excluded from model calculations because of the likelihood of major element addition or loss during serpentinization (Viljoen and Viljoen, 1969; Blais and Auvray, 1990). The method is proposed to give reasonable limits on the conditions of oxygen fugacity, temperature and primary melt composition for unaltered rock compositions.

3.7.2 Results

Figure 3.13 presents calculated results for T-lnfO_2 paths for a variety of rock suites. Common buffer curves are shown for reference. Each path represents one bulk rock composition with its coexisting

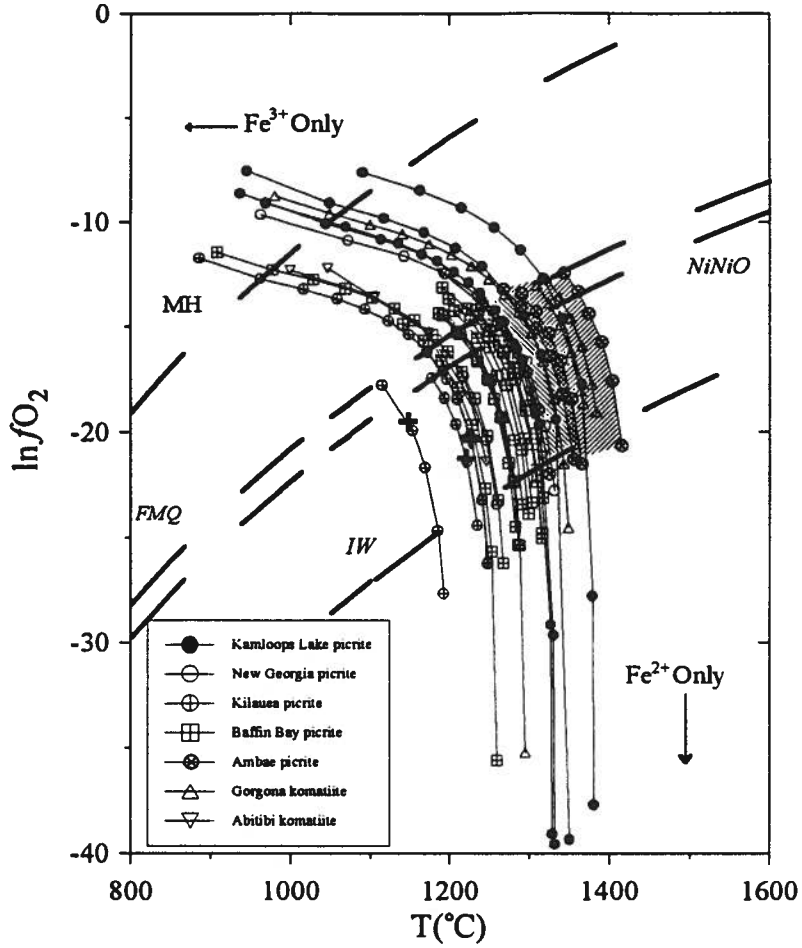

Figure 3.13. Temperature *vs* $\ln fO_2$ diagram of the Kamloops Lake picrites and other selected mafic-ultramafic suites. Bold crosses represent measured FeO contents of picrites from Kilauea. Data from: New Georgia (Ramsay et al., 1984), Baffin Bay (Francis, 1985), Kilauea picrite (Nicholls and Stout, 1988), Ambae (Eggins, 1993), Gorgona (Echeverria, 1980) and Abitibi (Barnes et al., 1983).

olivine composition and over a range of Fe^{3+}/Fe^{2+}. For picritic rocks from Kilauea (Nicholls and Stout, 1988), the measured Fe^{3+}/Fe^{2+} ratio is shown for the samples as a bold cross. The rock compositions with the longest paths represent calculations with mole% Fe^{3+} from approximately 0.01 to 1.4 ($Fe^{3+}/Fe^{2+} \approx$ 0.004 to 0.5). A lack of data from the Ambae suite prevented this one to one correlation between rock composition and olivine composition. The two shaded areas represent two rock compositions from the Ambae suite calculated with two end-member olivine compositions each (the actual olivine composition in each of the rocks is assumed to lie between the two forsterite values chosen).

Picritic lavas from Kamloops Lake and modern island arcs as well as komatiites from Gorgona Island produce T-lnfO_2 paths showing consistently greater oxygen fugacity for a given temperature than the selected ultramafic suites from many other tectonic environments (Figure 3.13). Compositions from picritic rocks from Baffin Bay and Kilauea and komatiitic lavas of the Abitibi Belt indicate relatively more reduced environments of crystallization. In particular, the Kilauea picritic rocks give significantly lower oxygen fugacities.

Figure 3.14 presents observed olivine compositions plotted against the calculated amount of olivine crystallization (moles per 100 moles) for a single rock composition over a range of Fe^{3+}/Fe^{2+}. Points shown on the diagram are the values from Figure 3.13 which span from near the IW buffer curve to slightly greater than the FMQ buffer curve. This range of oxygen fugacity is assumed to include a reasonable estimate of mantle conditions (Ballhaus et al., 1990) and therefore the true oxidation conditions for each suite should be represented on the diagram. The Kamloops Lake suite are, with the exception of the Abitibi komatiite suite, the most cumulate compositions represented. In order to crate a liquid that could equilibrate with the observed olivine compositions, 65 to 80% of olivine must be removed. Most of the other ultramafic suites require significantly less olivine accumulation and Gorgona Island komatiites show the least cumulate component. These results suggest that the Kamloops Lake rocks represent cumulate portions of a magma chamber although the phase chemistry reflects original magmatic (crystallization) conditions.

Calculated primary melt compositions and the attendant magmatic conditions for the Kamloops Lake picritic basalts are given in Table 3.6. Calculated compositions are shown for Fe^{3+}/Fe_T values of 0.1 and 0.15 showing that as Fe^{3+}/Fe^{2+} increases, the oxygen fugacity rises, the temperature lowers and the required parental melt composition becomes less magnesian.

Table 3.6. Calculated residual liquid compositions for the Kamloops Lake picrites.

	Carabine Creek				Watching Creek		Jacko Lake	
	IM-225		IM-222		IM-241		IM-230	
Fe^{3+}/Fe_T	0.1	0.15	0.1	0.15	0.1	0.15	0.1	0.15
FO (observed)	90.2	90.2	90.6	90.6	89.1	89.1	90.2	90.2
$\ln fO_2$	-14.47	-12.91	-13.19	-11.57	-15.03	-13.50	-15.20	-13.58
T (°C)	1293	1264	1325	1295	1271	1241	1275	1243
mole% ol	66	68	72	73	75	76	67	69
SiO_2	50.81	51.78	51.76	52.91	49.12	49.96	50.48	51.43
TiO_2	0.49	0.51	0.50	0.53	0.45	0.47	0.51	0.53
Al_2O_3	6.30	6.61	6.27	6.62	4.57	4.78	6.52	6.83
Fe_2O_3	0.85	1.25	0.91	1.36	0.88	1.29	0.79	1.18
FeO	6.58	5.89	7.08	6.36	6.73	6.00	6.15	5.45
MnO	0.41	0.43	0.50	0.52	0.54	0.57	0.40	0.42
MgO	18.25	16.42	20.45	18.47	16.65	14.92	17.10	15.23
CaO	14.23	14.93	11.84	12.50	20.36	21.30	14.76	15.48
Na_2O	0.25	0.26	0.07	0.07	0.28	0.29	0.49	0.51
K_2O	1.71	1.79	0.48	0.51	0.34	0.36	2.68	2.81
P_2O_5	0.13	0.14	0.15	0.15	0.08	0.08	0.12	0.12
MG#	0.83	0.83	0.84	0.84	0.82	0.82	0.83	0.83

MG# = $Mg/(Mg + Fe^{2+})$

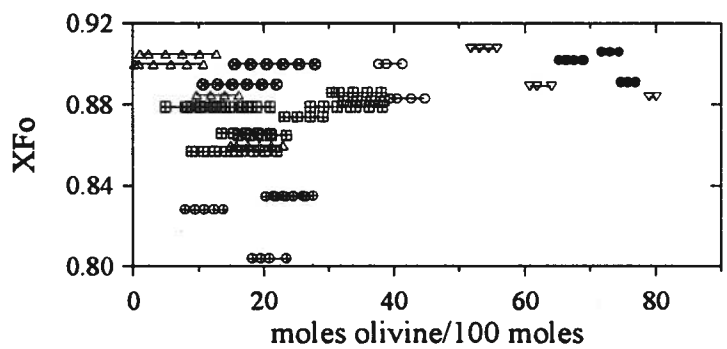

Figure 3.14. Forsterite content *vs* calculated olivine accumulation in the Kamloops Lake picritic basalts and selected ultramafic suites.

The calculated values of olivine 'accumulation' are plotted against the MgO content of the calculated residual liquid (Figure 3.15). The points represent model solutions which span the IW and FMQ oxygen buffers. Although the Kamloops Lake suite represents more olivine crystallization, the residual liquids are well within reasonable limits. MgO contents in residual liquids range from 16.65 to 20.45 wt% at an Fe^{3+}/Fe_T ratio of 0.1 and 14.92 to 18.47 wt% at a ratio of 0.15. These values correspond to values obtained for most of the other suites. The Ambae picrites and the Gorgona komatiites may represent liquids with slightly greater MgO contents; up to 23 wt% for Ambae and 25 wt% for Gorgona.

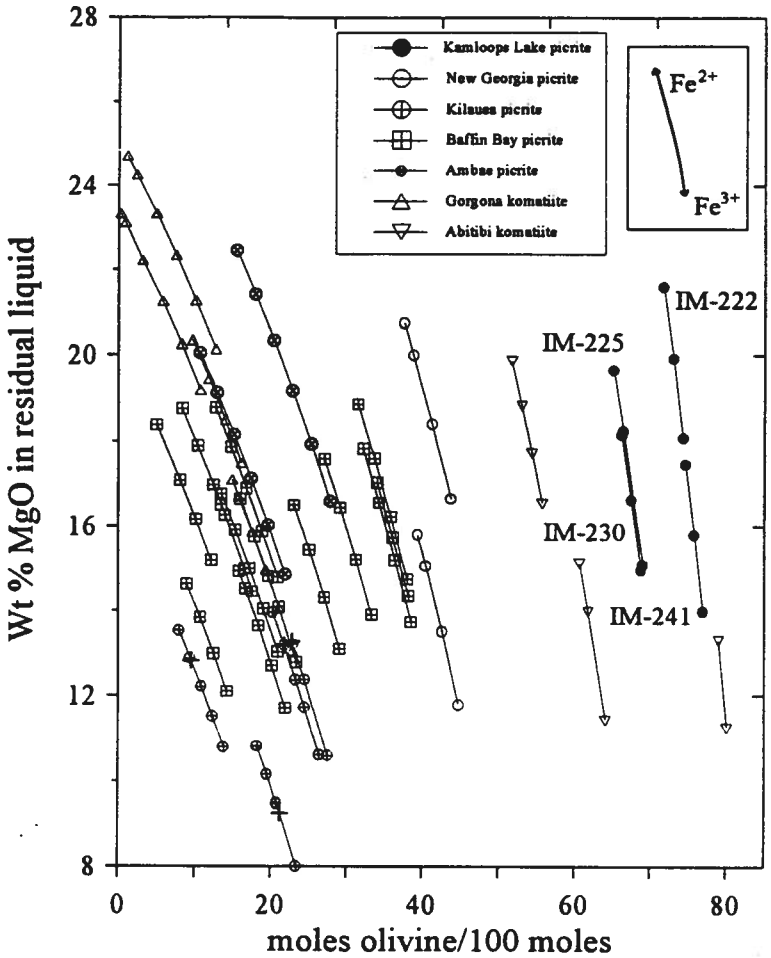

Figure 3.15. MgO contents of calculated residual liquids vs olivine accumulation in the Kamloops Lake picritic basalts and selected ultramafic suites.

3.8 DISCUSSION

The Kamloops Lake picritic basalts represent an episode of ultramafic volcanism attending the latter stages of Late Triassic Nicola volcanism. They lie stratigraphically above Nicola Group volcanic rocks and beneath Eocene Kamloops Group volcanic rocks. Based on relict mineralogy, textures and chemistry, the serpentinite bodies within the Iron Mask batholith are stratigraphically equivalent to the picrite occurrences found at Jacko Lake on the southern margin of the batholith, near Carabine Creek and Watching Creek. These relationships constrain the age of the ultramafic volcanic rocks to be Latest Triassic or Earliest Jurassic.

The Kamloops Lake picritic basalts are highly enriched in MgO (24 to 34 wt%), and depleted in SiO_2 (38 to 43 wt%) and Al_2O_3 (2.5 to 6.3 wt%) compared to other mafic and ultramafic suites. Cr and Ni concentrations are 1670 to 3040 and 920 to 1420 ppm respectively. Kamloops Lake rocks are olivine ± clinopyroxene porphyritic. Olivine composition range from $Fo_{89.5}$ to $Fo_{92.9}$. Clinopyroxene has MG#'s ranging from 87.1 to 99.7 and calculated Fe^{3+} (cation units) from 0.025 to 0.186, indicative of crystallization under high fO_2 (Barsdell, 1988). Cr-spinel compositions in the Kamloops Lake lavas are also highly oxidized and Cr/(Cr + Al) and Mg/(Mg + Fe^{2+}) are positively correlated. These mineral compositions suggest crystallization from an island arc-derived primary magma under oxidizing conditions.

REE signatures for the Kamloops Lake picritic basalts reflect an island arc tectonic affinity. Profiles for the Kamloops Lake picritic basalts are flat and abundances are very low, features which indicate olivine control on the REE concentrations. Estimates of volume of mantle melt needed to produce magmas with REE characteristics similar to the Kamloops Lake suite are ≈20% or greater (Hanson. 1980). The depletion in TiO_2 seen in the Kamloops Lake picritic basalts also supports these values of mantle melt (Sun et al., 1979).

The Kamloops Lake picritic basalts represent material derived from the upper mantle in an island arc tectonic environment. The magma shows no appreciable contamination. The extreme depletion in Al_2O_3 of the Kamloops Lake rocks appears to be a manifestation of an Al-poor source. Pearce Element ratio modeling indicates that the unaltered occurrences of the Kamloops Lake picritic basalt suite are related through fractionation or accumulation of olivine.

Calculation of T-lnfO_2 paths, primary melt compositions and olivine crystallization indicate that the Kamloops Lake ultramafic suite contains a significant cumulate component. Estimates of the amount of olivine crystallized from the magma range from 65 to 79 moles per 100 moles. The calculated rock

paths indicate that, along with modern island arc ultramafic suites, the Kamloops Lake basalts are characterized by crystallization in a highly oxidized environment. This conclusion is supported by Ballhaus et al. (1990) who argues that island arcs are characterized by higher oxygen fugacities that other tectonic environments. Calculated residual liquids range from 16.6 to 20.5 wt% MgO at $Fe^{3+}/Fe_T = 0.1$ and 14.9 to 18.5 wt% MgO at $Fe^{3+}/Fe_T = 0.15$, consistent with primary liquids from other localities and tectonic environments.

4.0 SUMMARY

4.1 IRON MASK BATHOLITH

Table 2.3 presents a summary of characteristics for the rock units of the Iron Mask batholith. The textural, mineralogical, and chemical similarities and local gradational contacts of the Pothook and Cherry Creek units suggest that these intrusive events are closely related. Many of the differences observed (see Table 2.3) could result from magmatic differentiation under changing physical conditions. Modeling fractionation of the observed mineral assemblage with Pearce Element Ratios, however, fails to relate these two units. Indeed, compositions assigned to the same unit, in general, fail to be related to other samples assigned to the same phase.

Rocks of the Sugarloaf unit are distinctive from the other intrusive units in occurrence, mineralogy, texture and chemistry. Compositions from this unit are not related to each other or the Pothook or Cherry Creek units through fractionation of the observed mineral assemblage. The distinct mineralogy, hypabyssal texture and structurally controlled mode of emplacement suggest that these rocks are a separate shallower-level and younger intrusive event.

Hybridization of Pothook magma is documented in a narrow (50 to 250m wide) zone which shows the gradual transition from typical Pothook rocks into an intrusion breccia and finally into Type II Iron Mask hybrid unit. Recognition of this zone was instrumental in evaluating the processes and consequences which formed the hybrid unit. The physical interaction with and selective assimilation of Nicola Group rocks by a Pothook magma formed the Iron Mask hybrid unit as a brittle carapace around the Iron Mask batholith. The present day map patterns, which show areal dominance of the Iron Mask hybrid unit, suggests that the current erosional level is near the top of the Iron Mask system.

The chemical mixing of Pothook magma and Nicola Group rocks is demonstrated by REE patterns. Profiles from a pyroxene-phyric Nicola lava flow, a xenolith within the Iron Mask hybrid and a Type III hybrid rock all are very similar. Relative REE abundances are depleted in the xenolith and enriched in the Type III compared to the Nicola lava. This implies that REE-bearing phases in the Nicola Group are melted and assimilated into Pothook magma.

One consequence of assimilation of water-rich greenschist facies Nicola Group rocks is the potential for volatile change in the Iron Mask system. The amount of assimilant incorporated into the magma is the most crucial factor determining whether assimilation will tend to increase or decrease volatile concentration in the melt. The more complete the assimilation process, the greater potential for dilution effects and lowering the total volatile content of the melt. Modeling dehydration and assimilation processes in the Iron Mask batholith using values for the required variables estimated from field and petrographic observations and chemical analyses indicate that selective assimilation of Nicola Group rocks will tend to raise the volatile content in Pothook magma. This, in turn, increases the possibility of exsolving a volatile phase which may be important in forming ore deposits.

Both the existence of the Iron Mask hybrid unit and the difficulty in satisfactorily modeling fractionation processes in the intrusive units suggest that magmatic contamination with crustal rocks is important in the Iron Mask batholith. The overlap in composition of the intrusive phases and the diverse dykes found in the Iron Mask batholith suggests that the magmatic history of the Iron Mask batholith is very complex. Magmatic history of the Iron Mask batholith is initiated by intrusion of Pothook diorite magma and interaction of Pothook magma with the surrounding Nicola Group rocks. The result of this assimilation and contamination process is the formation of the Iron Mask hybrid unit. Closely following, and perhaps partially coeval with hybridization, the Cherry Creek phases are intruded. Finally, Sugarloaf diorite is intruded along pre-existing structures in the Iron Mask batholith and surrounding Nicola Group rocks.

4.2 KAMLOOPS LAKE PICRITIC BASALTS

The Kamloops Lake picritic basalts represent ultramafic volcanism at the latter stages of the Nicola Arc. The serpentinite of the Iron Mask batholith is correlated through texture, mineralogy and chemistry with localities of relatively unaltered picritic rocks in the Kamloops Lake area. Olivine ($Fo_{89.5}$ to $Fo_{92.9}$) and rock compositions indicate that these are mantle-derived magmas which show no appreciable contamination.

Whole rock and mineral chemistry of the Kamloops Lake ultramafic rocks indicate an island arc tectonic affinity. These compositions are depleted, with respect to MORB compositions, in REE's, Ti, Zr, Y and Hf and enriched in Rb, Ba, K and Sr. The oxidized nature of clinopyroxene and Cr-spinel are unique to island arc environments. REE profiles of the Kamloops Lake picritic basalts are flat and abundances are very low indicating olivine control on the pattern. Fresh picrite localities are shown to be related through fractionation or accumulation of olivine. Serpentinites from he Iron Mask batholith are not conclusively cogenetic with these localities, however, the alteration process may have changed the major element chemistry.

Calculation of T-lnfO_2 paths, primary melt compositions and olivine crystallization indicate that the Kamloops Lake picritic basalts are largely cumulate. Estimates of the amount of olivine crystallized range from 65 to 79 mole%. The crystallization paths indicate that the Kamloops Lake rocks formed in an oxidized environment. Calculated residual liquids rang from 16.6 to 20.5 wt% MgO at $Fe^{3+}/Fe_T = 0.1$ and 14.9 to 18.5 wt% MgO at $Fe^{3+}/Fe_T = 0.15$. These values are consistent with primary liquids and other tectonic environments.

REFERENCES

Arculus, R.J. (1978): Mineralogy and petrology of Grenada, Lesser Antilles Island Arc, *Contributions to Mineralogy and Petrology*, vol. 65, pp. 413-424.

Ballhaus, C., Berry, R.F. and Green, D.H. (1990): Oxygen fugacity controls in the Earth's upper mantle, *Nature*, vol. 348, pp. 437-440.

Barnes, S.J., Gorton, M.P. and Naldrett, A.J. (1983): A comparative study of olivine and clinopyroxene spinifex flows from Alexo, Abitibi Greenstone Belt, Ontario, Canada, *Contributions to Mineralogy and Petrology*, vol. 83, pp. 293-308.

Barsdell, M. (1988): Petrology and petrogenesis of clinopyroxene-rich tholeiitic lavas, Merelava Volcano, Vanuatu, *Journal of Petrology*, vol. 29, pp. 927-964.

Bartch, R.D. (1993): Volcanic stratigraphy and lithochemistry of the Lower Jurassic Hazelton Group, host to the Eskay Creek precious and base metal volcanogenic deposit, unpublished M.Sc. thesis, *The University of British Columbia*, 178 p.

Barton, M. and van Bergen, M.J. (1981): Green clinopyroxenes and associated phases in a potassium-rich lava from the Leucite Hills, Wyoming, *Contributions to Mineralogy and Petrology*, vol. 77, pp. 101-114.

Beccaluva, L. and Serri, G. (1988): Boninitic and low-Ti subduction-related lavas from intraoceanic arc-backarc systems and low-Ti ophiolites: a reappraisal of their petrogenesis and original tectonic setting, *Tectonophysics*, vol. 146, pp. 291-315.

Bedard, J H.J., Francis D.M. and Ludden, J. (1988): Petrology and pyroxene chemistry of Monteregian dykes: the origin of concentric zoning and green cores in clinopyroxenes from alkali basalts and lamprophyres, *Canadian Journal of Earth Sciences*, vol. 25, pp. 2041-2058.

Bence, A.E., Grove, T.L. and Papike, J.J. (1980): Basalts as probes of planetary interiors: Constraints on the chemistry and mineralogy of their source regions, *Precambrian Research*, vol. 10, pp. 249-279.

Blais, S. and Auvray, B. (1990): Serpentinization in the Archean komatiitic rocks of the Kuhmo Greenstone Belt, eastern Finland, *Canadian Mineralogist*, vol. 28, pp. 55-66.

Boynton, W.V. (1984): Cosmochemistry of the rare earth elements: meteorite studies, *in* Henderson, P. editor, Rare Earth Geochemistry, Elsevier, Amsterdam, pp. 63-114.

Brooks, C.K. and Printzlau, I. (1978): Magma mixing in mafic alkaline volcanic rocks: the evidence from relict phenocryst phases and other inclusions, *Journal of Volcanology and Geothermal Research*, vol. 4, pp. 315-331.

Cann, R.M. (1979): Geochemistry of magnetite and the genesis of magnetite-apatite lodes in the Iron Mask batholith, B.C., unpublished. M.Sc. thesis, *The University of British Columbia*, 196 p.

Carr, J.M. (1956): (Copper) Deposits associated with the eastern part of the Iron Mask batholith near Kamloops, *Minister of Mines., B.C.*, annual report, 1956, pp. 47-69.

Carr, J.M. and Reed, A.J. (1976): Afton: A supergene copper deposit, *in* Sutherland Brown, A., editor, Porphyry Deposits of the Canadian Cordillera, *Canadian Institute of Mining and Metallurgy*, Special Volume 15, pp. 376-387.

Cockfield, W.E. (1948): Geology and mineral deposits of Nicola Map Area, British Columbia, *Geological Survey of Canada*, Memoir 249.

Crawford, A.J. and Cameron, W.E. (1985): Petrology and geochemistry of Cambrian boninites and low-Ti andesites from Heathcote, Victoria, *Contributions to Mineralogy and Petrology*, vol. 91, pp. 93-104.

Cui, Y. and Russell, J.K. (in review): Magmatic origins of calc-alkaline intrusions from the Coast Plutonic Complex, southwestern British Columbia, *Canadian Journal of Earth Sciences*.

Cundari, A. and Salviulo, G. (1989): Ti solubility in diopsidic pyroxene from a suite of New South Wales leucitites (Australia), *Lithos*, vol. 22, pp. 191-198.

Dick, H.J.B. and Bullen, T. (1984): Chromium spinel as a petrogenetic indicator in abyssal and alpine-type peridotites and spatially associated lavas, *Contributions to Mineralogy and Petrology*, vol. 86, pp. 54-76.

Dupey C., Dostal, J., Marcelot, G., Bougault, H., Joron, J.L. and Treuil, M. (1982): Geochemistry of basalts from central and southern New Hebrides arc: implication for their source rock composition, *Earth and Planetary Science Letters*, vol. 60, pp. 207-225.

Echeverria, L.M. (1980): Tertiary or Mesozoic Komatiites from Gorgona Island, Colombia: field relations and geochemistry, *Contributions to Mineralogy and Petrology*, vol. 73, pp. 253-266.

Eggins, S.M. (1993): Origin and differentiation of picritic arc magmas, Ambae (Aoba), Vanuatu, *Contributions to Mineralogy and Petrology*, vol. 114, pp. 79-100.

Eggler, D.H. (1972): Water-saturated and undersaturated melting relations in a Paricutin andesite and estimate of water content in the natural magma, *Contributions to Mineralogy and Petrology*, vol. 34, pp. 261-271.

Ewing T.E. (1981a) Regional stratigraphy and structural setting of the Kamloops Group, south-central British Columbia, *Canadian Journal of Earth Sciences*, vol. 18, pp. 1464-1477.

Ewing T.E. (1981b) Petrology and geochemistry of the Kamloops Group volcanics, British Columbia. *Canadian Journal of Earth Sciences*, vol. 18, pp. 1478-1491.

Ewing, T.E. (1982): Geology of the Kamloops Group near Kamloops, Preliminary Map No. 48 and accompanying notes, *B.C. Ministry of Energy, Mines and Petroleum Resources*, 19 p.

Francis, D (1985): The Baffin Bay lavas and the value of picrites as analogues of primary magmas, *Contributions to Mineralogy and Petrology*, vol. 89, pp. 144-154.

Govindaraju, K. (1984): 1984 compilation of working values and sample description for 170 International Reference samples of mainly silicate rocks and minerals, *Geostandards Newsletter*, vol. 8, Special Issue, July, 1984.

Hart, S.R. and Davis, K.E. (1979): Nickel partitioning between olivine and silicate melt, *Earth and Planetary Science Letters*, vol. 40, pp. 203-219.

Hickey, R.L. and Frey, F.A. (1982): Geochemical characteristics of boninite series volcanics: implications for their source, *Geochemica et Cosmochimica Acta*, vol. 46, pp. 2099-2115.

Hanson, G.N. (1980): Rare Earth Elements in petrogenetic studies of igneous systems, *Annual Review Earth and Planetary Science*, vol. 8, pp. 371-406.

Hanson, G.N. (1989): An approach to trace element modeling using a simple igneous system as an example, *in* Lipin, B.R. and McKay, G.A., eds., Geochemistry and Mineralogy of the Rare Earth Elements, *Mineralogical Society of America, Reviews in Mineralogy*, vol. 21, pp. 1-22.

Hill, R. and Roeder, P. (1974): The crystallization of spinel from basaltic liquid as a function of oxygen fugacity, *Journal of Geology*, vol. 82, pp. 709-729.

Hoiles, H.H.K. (1978): Nature and genesis of the Afton copper deposit, Kamloops, British Columbia, unpublished M.Sc. thesis, *The University of Alberta.*

Irvine T.N. and Baragar, W.R.A. (1971): A guide to the chemical classification of the common volcanic rocks, *Canadian Journal of Earth Sciences*, vol. 8, pp. 523-548.

Jenner, G.A. (1981): Geochemistry of high-Mg andesites from Cape Vogel, Papua New Guinea, *Chemical Geology*, vol. 33, pp. 307-332.

Jenner, G.A., Longerich, H.P., Jackson, S.E. and Fryer, B.J. (1990): ICP-MS: a powerful tool for high-precision trace-element analyses in earth sciences: evidence from analysis of selected USGS reference samples, *Chemical Geology*, vol. 83, pp. 133-148.

Krishnamurthy, P. and Cox, K.G. (1977): Picrite basalts and related lavas from the Deccan Traps of western India, *Contributions to Mineralogy and Petrology*, vol. 62, pp. 53-75.

Kwong, Y.T.J. (1987): Evolution of the Iron Mask batholith and its associated copper mineralization., *B.C. Ministry of Energy, Mines and Petroleum Resources*, Bulletin 77, 55 p.

Lang, J.R. (1994): Geology of the Crescent alkalic porphyry copper-gold deposit, Afton Mining Camp, British Columbia (92I/9), *in* Grant, B. and Newell, J. M., editors, Geological Fieldwork 1993, *B.C. Ministry of Energy, Mines and Petroleum Resources*, Paper 1994-1, pp. 285-296.

Lang, J.R. and Stanley, C.R. (in review): Contrasting styles of alkalic porphyry copper-gold deposits in the northern Iron Mask batholith, Kamloops, British Columbia, *in* Schroeter, T., editor, Porphyry Deposits of the Northwestern Cordillera of North America, CIM Special Volume 46.

LeBas, M.J. (1962): The role of aluminum in igneous clinopyroxenes with relation to their parentage, *American Journal of Science*, vol. 260, pp. 267-288.

Mathews, H.M. (1941): Geology of the Ironmask batholith, unpublished M.Sc. thesis, *The University of British Columbia*, 42 p.

Mehnert, K.R. (1971): Migmatites and the Origin of Granitic Rocks, Elsevier Publishing Company, 405 p.

Monger, J.W.H., Price, R.A. and Tempelman-Kluit, D.J. (1982): Tectonic accretion and the origin of two major metamorphic and plutonic welts in the Canadian Cordillera, *Geology*, vol. 10, pp. 70-75.

Monger, J.W.H. (1989a): Overview of Cordilleran Geology, *in* Ricketts, B. D., editor, Western Canada Sedimentary Basin: A Case History, *Canadian Society of Petroleum Geologists*, Institute of Sedimentary and Petroleum Geology, pp. 9-32.

Monger, J.W.H. (1989b): Geology of the Hope and Ashcroft Map Areas, British Columbia, *Geological Survey of Canada*, Maps 41-1989 and 42-1989.

Morimoto, N. (1989): Nomenclature of Pyroxenes, *The Canadian Mineralogist*, vol. 27, pp. 143-156.

Mortensen, J.K. and Ghosh, D. (in review): Geochronology, *in* Schroeter, T., editor, Porphyry Deposits of the Northwestern Cordillera of North America, CIM Special Volume 46.

Mortimer, N. (1987): The Nicola Group: Late Triassic and Early Jurassic subduction-related volcanism in British Columbia, *Canadian Journal of Earth Sciences*, vol. 24, pp. 2521-2536.

Naney, M.T. (1983): Phase equilibria of rock-forming ferromagnesian silicates in granitic systems, *American Journal of Science*, vol. 283, pp. 993-1033.

Nicholls, J. and Gordon, T.M. (1994): Procedures for the calculation of axial ratios on Pearce Element-Ratio diagrams, Canadian Mineralogist, vol.

Nicholls, J. and Russell, J.K. (1991): Major-element chemical discrimination of magma-batches in lavas from Kilauea Volcano, Hawaii, 1954 - 1971 eruptions, *Canadian Mineralogist*, vol. 29, pp. 981-993.

Nicholls, J. and Stout, M.Z. (1988): Picritic melts in Kilauea--Evidence from the 1967-1968 Halemaumau and Hiiaka eruptions, *Journal of Petrology*, vol. 29, pp. 1031-1057.

Northcote, K.E. (1974): Geology of the northwest half of the Iron Mask batholith, *in* Geological Fieldwork, 1974, Paper 1975-1, *B.C. Ministry of Energy, Mines and Petroleum Resources*, pp. 22-26.

Northcote, K.E. (1976): Geology of the southeast half of the Iron Mask batholith, *in* Geological Fieldwork, 1976, Paper 1977-1, *B.C. Ministry of Energy, Mines and Petroleum Resources*, pp. 41-46.

Northcote, K.E. (1977): Iron Mask batholith, Preliminary Map 26 and accompanying notes, *B.C. Ministry of Energy, Mines and Petroleum Resources*, 8 p.

Pearce, T.H. (1968): A contribution to the theory of variation diagrams; *Contributions to Mineralogy and Petrology*, vol. 19, pp. 142-157.

Pearce, J.A., Harris, N.B.W. and Tindle, A.G. (1984): Trace element discrimination diagrams for the tectonic interpretation of granitic rocks, *Journal of Petrology*, vol. 25, pp. 956-983.

Perfit, M.R., Gust, D.A., Bence, A.E., Arculus, R.J. and Taylor, S.R. (1980): Chemical characteristics of Island-Arc basalts: implication for mantle sources, *Chemical Geology*, vol. 30, pp. 227-256.

Plaksenko, A.N. and Smol'kin, V.F. (1990): Typomorphism of accessory chromium spinels in highly magnesian volcanics, *International Geology Review*, pp. 244-259.

Preto, V.A. (1967): Geology of the eastern part of the Iron Mask batholith, *Minister of Mines, B.C.*, Annual Report, 1967, pp. 137-147.

Preto, V.A. (1977): The Nicola Group: Mesozoic volcanism related to rifting in southern British Columbia, *in* Baragar, W.R.A., Coleman, L.C. and Hall, J.M., editors, Volcanic Regimes in Canada, *The Geological Association of Canada*, Special Paper No. 16, pp. 39-57.

Preto, V.A. (1979): Geology of the Nicola Group between Merritt and Princeton, *B.C. Ministry of Energy, Mines and Petroleum Resources*, Bulletin 69, 90 p.

Ramsay, W.R.H., Crawford, A.J. and Foden, J.D. (1984): Field setting, mineralogy, chemistry, and genesis of arc picrites, New Georgia, Solomon Islands, Contributions to Mineralogy and Petrology, vol. 88, pp. 386-402.

Ross, K.V., Dawson, K.M., Godwin, C.I., and Bond, L. (1993): Lithologies and alteration of the Ajax East zone, an alkalic copper gold porphyry deposit, Kamloops, B.C., *in* Current Research Part A, *Geological Survey of Canada*, Paper 93-1A, pp. 87-95.

Ross, K.V. and others (in review): Geology, alteration and mineralization in the Ajax East and Ajax West deposits, southern Iron Mask batholith, Kamloops, British Columbia, *in* Schroeter, T., editor, Porphyry Deposits of the Northwest Cordillera of North America, CIM Special Volume 46.

Russell, J.K. and Snyder, L.D. (1993a): Volatile production possibilities during magmatic assimilation, *in* Volcanoes and Ore Deposits, MDRU Short Course #14 Notes.

Russell, J.K. and Snyder, L.D. (1993b): Volatile production attending magmatic assimilation processes, *in* Ancient Volcanism and Modern Analogues, IAVCEI General Assembly, Canberra, Australia, p. 94.

Russell, J.K. and Nicholls, J. (1988): Analysis of petrologic hypotheses with Pearce Element Ratios, *Contributions to Mineralogy and Petrology*, vol. 99, pp. 25-35.

Sato, H. (1977): Nickel content of basaltic magmas: identification of Primary magmas and a measure of the degree of olivine fractionation, *Lithos*, vol. 10, pp. 113-120.

Schau, M. (1970): Stratigraphy and structure of the type area of the Upper Triassic Nicola Group in south-central British Columbia, *The Geological Association of Canada*, Special Paper No. 6, pp. 123-135.

Scott, P.W. (1976): Crystallization trends of pyroxenes from the alkaline volcanic rocks of Tenerife, Canary Islands, *Mineralogical Magazine*, vol. 40, pp. 805-816.

Simkin, T. and Smith, J.V. (1970): Minor-element distribution in olivine, *Journal of Geology*, vol. 78, pp. 304-325.

Snyder, L.D. and Russell, J.K. (1993): Field constraints on diverse igneous processes in the Iron Mask batholith (92I/9, 10), *in* Grant, B. and Newell, J. M., editors, Geological Fieldwork, 1992, *B.C. Ministry of Energy, Mines and Petroleum Resources*, Paper 1993-1, pp. 281-286.

Snyder, L.D. and Russell, J.K. (1994): Petrology and stratigraphic setting of the Kamloops Lake picritic basalts, Quesnellia Terrane, south-central B.C. (92I/9, 15 and 16), *in* Grant, B. and Newell J. M., editors, Geological Fieldwork 1993, *B.C. Ministry of Energy, Mines and Petroleum Resources*, Paper 1994-1, pp. 297-311.

Stanley, C.R. (1994): Geology of the Pothook alkalic copper-gold porphyry deposit, Afton Mining Camp, British Columbia (92I/9, 10), *in* Grant, B. and Newell, J. M., editors, Geological Fieldwork 1993, *B.C. Ministry of Energy, Mines and Petroleum Resources*, Paper 1994-1, pp. 275-284.

Stanley, C.R., Lang, J.R. and Snyder, L.D. (1994): Geology and mineralization in the northern part of the Iron Mask batholith, British Columbia (92I/9, 10), *in* Grant, B. and Newell, J. M., editors, Geological Fieldwork, 1993, *B.C. Ministry of Energy, Mines and Petroleum Resources*, Paper 1994-1, pp. 269-274.

Stanley, C.R. and Russell, J.K. (1989): Petrologic hypothesis testing with Pearce Element Ratio diagrams; derivation of diagram axes, *Contributions to Mineralogy and Petrology*, vol. 103, pp. 78-89.

Sun, S-S. and Nesbitt, R.W. (1978): Petrogenesis of Archean ultrabasic and basic volcanics: evidence from Rare Earth Elements, *Contributions to Mineralogy and Petrology*, vol. 65, pp. 301-325.

Sun, S-S., Nesbitt, R.W. and Sharaskin A.Y. (1979): Geochemical characteristics of mid-ocean ridge basalts, *Earth and Planetary Science Letters*, vol. 44, pp. 119-138.

Taylor, S.R. (1980): Refractory and moderately volatile element abundances in the earth, moon and meteorites, *Proceedings of the Eleventh Lunar Planetary Science Conference*, pp. 333-348.

Taylor, S.R. and McLennan, S.M. (1985): The Continental Crust: Its composition and evolution, *Blackwell, Oxford*, 312 p.

Thornton C.P. and Tuttle, O.F. (1960): Chemistry of igneous rocks--Pt 1, Differentiation Index, *American Journal of Earth Science*, vol. 258, pp. 664-684.

Utter, T. (1978): The origin of detrital chromites in the Klerksdorp Goldfield, Witwatersrand, South Africa, *N Jb Miner Abh*, vol. 133, pp. 191-209.

Van Kooten, G.K. and Buseck, P.R. (1978): Interpretation of olivine zoning: Study of a Maar from the San Francisco volcanic field, Arizona, *Geological Society of America Bulletin*, vol. 89, pp. 744-754.

Viljoen, R.P. and Viljoen, M.J. (1969): The effects of metamorphism and serpentinization of the volcanic and associated rocks of the Barberton region, *Geological Society of South Africa*, Special Publication 2, pp. 29-53.

Watson, E.B. and Harrison, T.M. (1983): Zircon saturation revisited: Temperature and composition effects in a variety of crustal magma types, *Earth and Planetary Science Letters*, vol. 64, pp. 295-304.

Watson, E.B. and Harrison, T.M. (1984): Accessory minerals and the geochemical evolution of crustal magmatic systems: a summary and prospectus of experimental approaches, *Physics of the Earth and Planetary Interiors*, vol. 35, pp. 19-30.

Wilkenson, J.F.G. and Hensel, H.D. (1988): The petrology of some picrites from Mauna Loa and Kilauea volcanoes, Hawaii, *Contributions to Mineralogy and Petrology*, vol. 98, pp. 326-345.

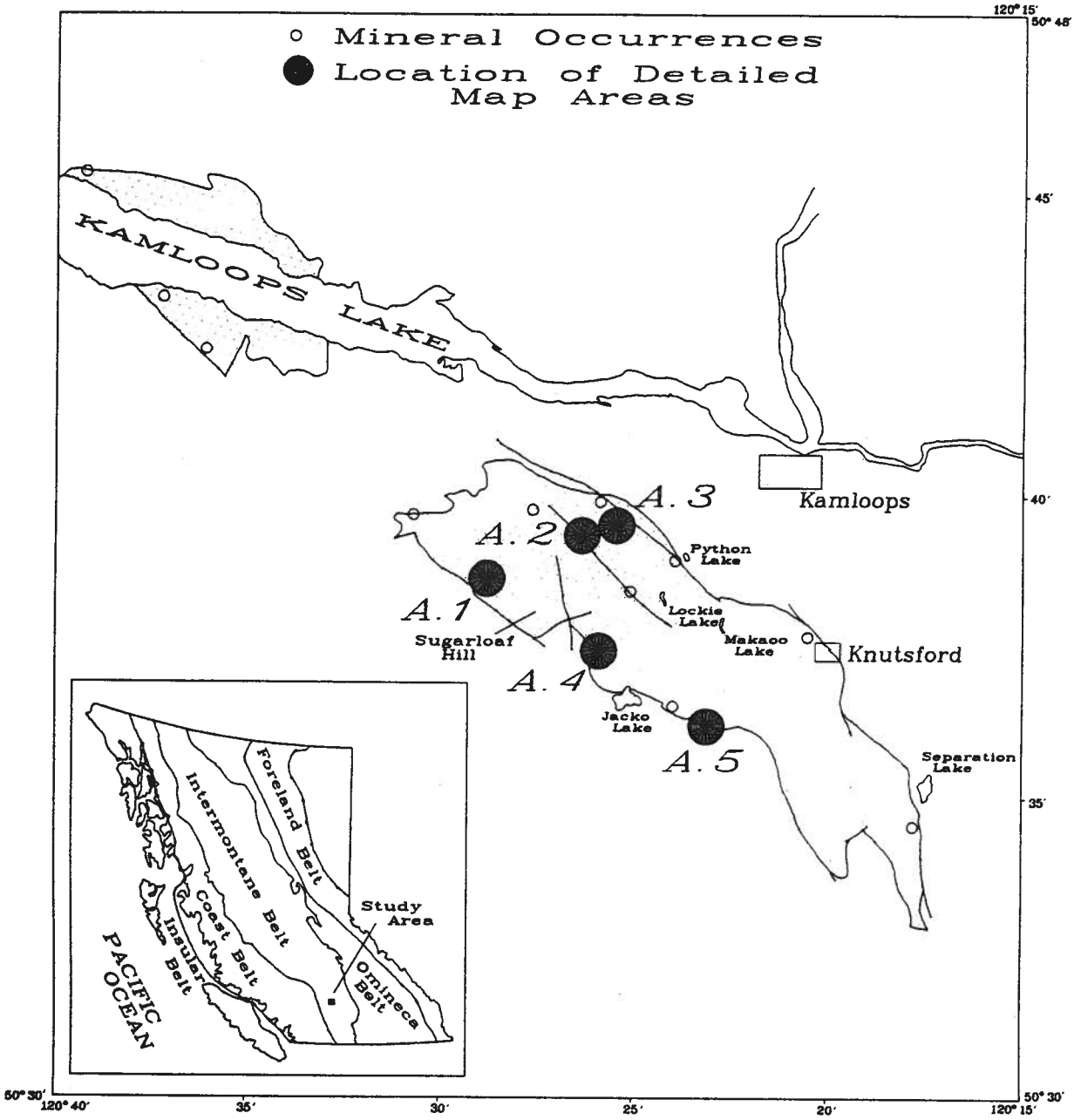

Figure A.1. Location of figures A.2-A.5. These five areas elucidate the relationships among the rock units in the Iron Mask batholith.

Legend for Appendix A. Figures A.2-A.6.

- Kamloops Group volcanic rocks
- Iron Mask dykes
- Sugarloaf diorite
- Cherry Creek Breccia
- Cherry Creek monzodiorite to monzonite
- Iron Mask hybrid unit
- Pothook diorite/Iron Mask hybrid transition zone
- Pothook diorite
- Picritic basalt
- Nicola Group volcanic rocks

Map Symbols

- geologic contact
- 3000 — topographic contour (elevation indicated)
- stream
- 42 — foliation (indicating dip)
- 22 — mineral lineation (indicating plunge)
- IM-100 — sample location
- outcrop

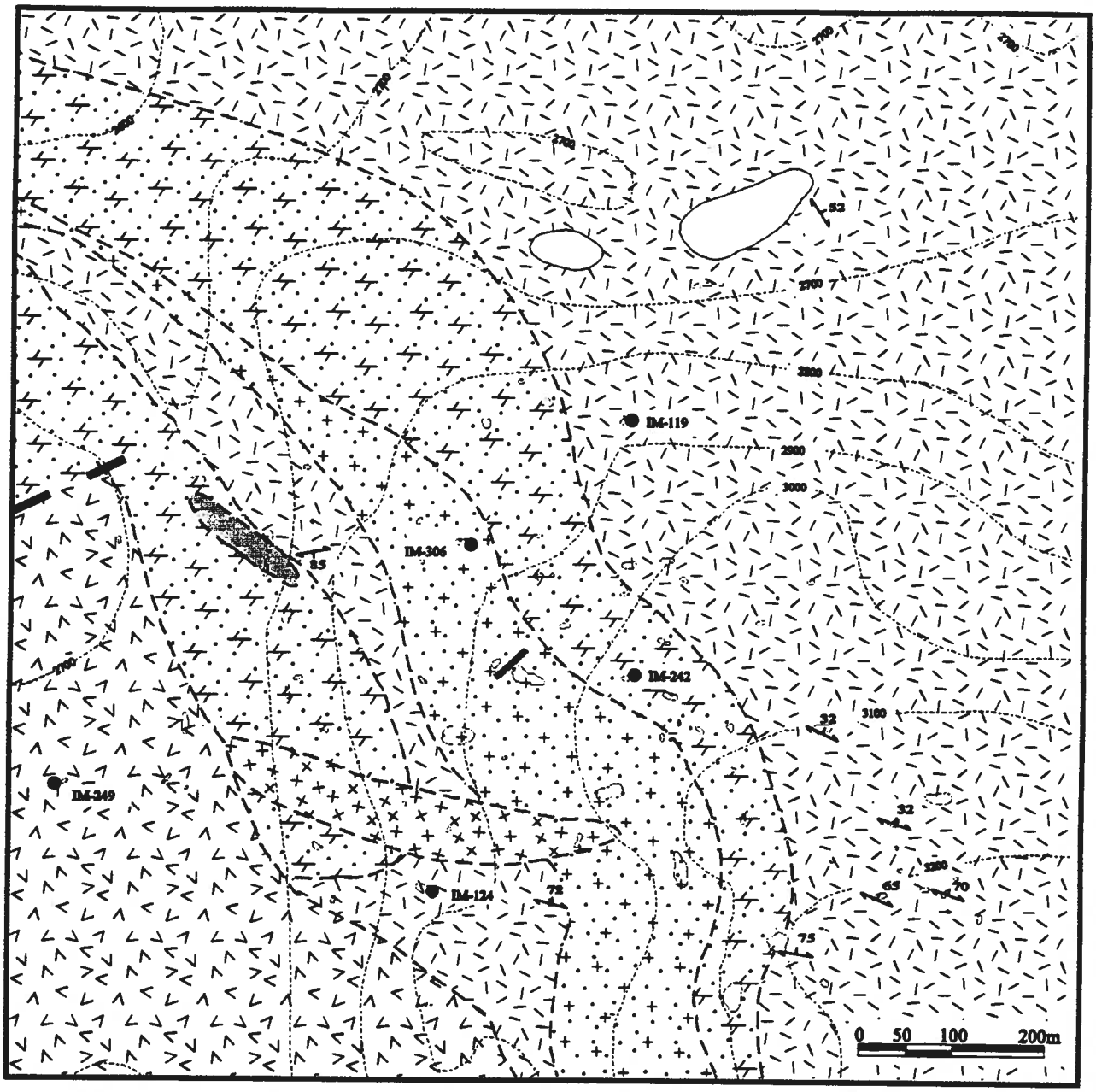

Figure A.2. Map of the Pothook/hybrid transitional zone on the west side of Sugarloaf Hill. The rocks in this area are intruded by a dyke assigned to the Cherry Creek phase.

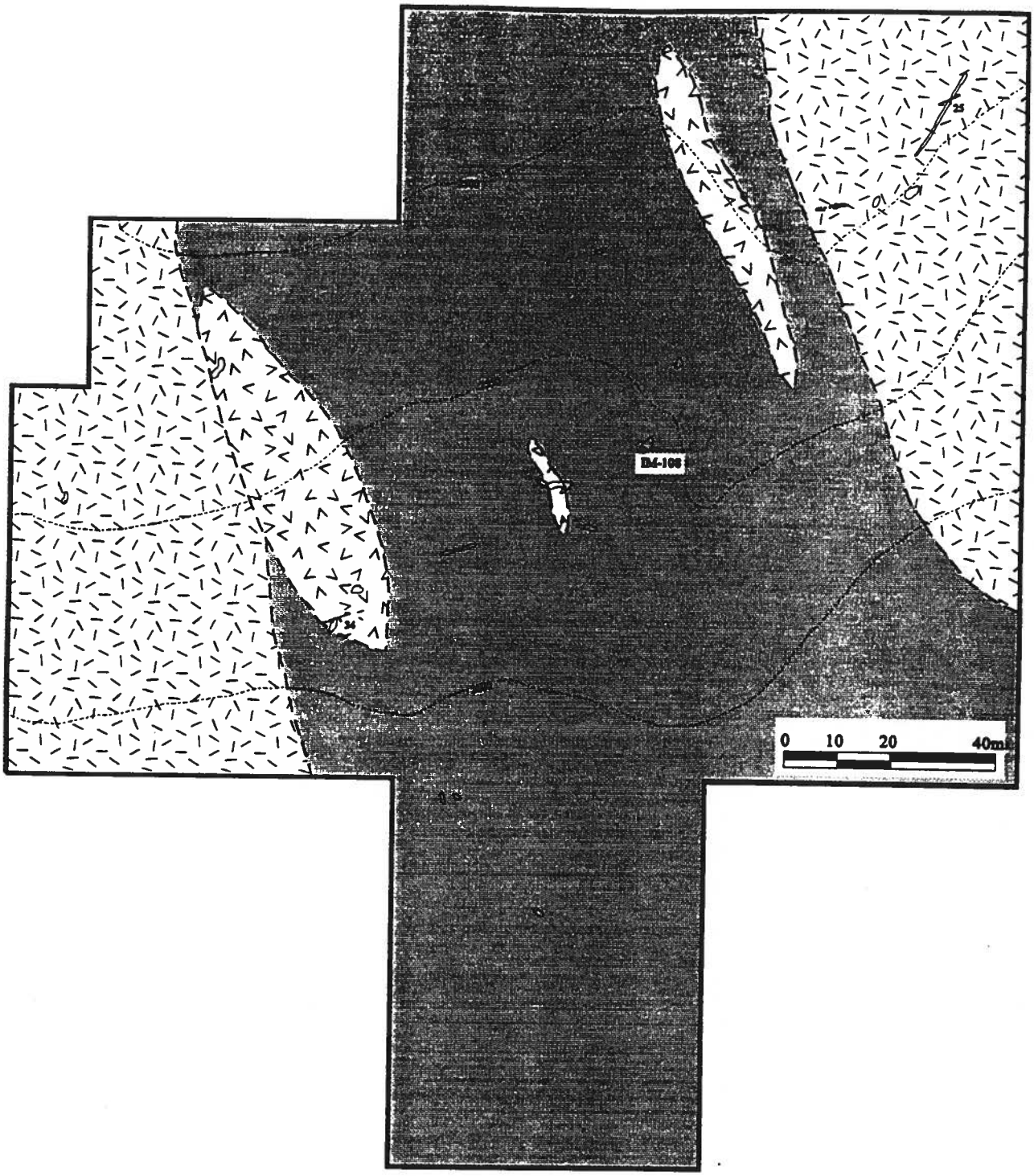

Figure A.3. A large block of serpentinized picrite is found in the Pothook unit. The serpentinite has subsequently been intruded by rocks of the Sugarloaf diorite.

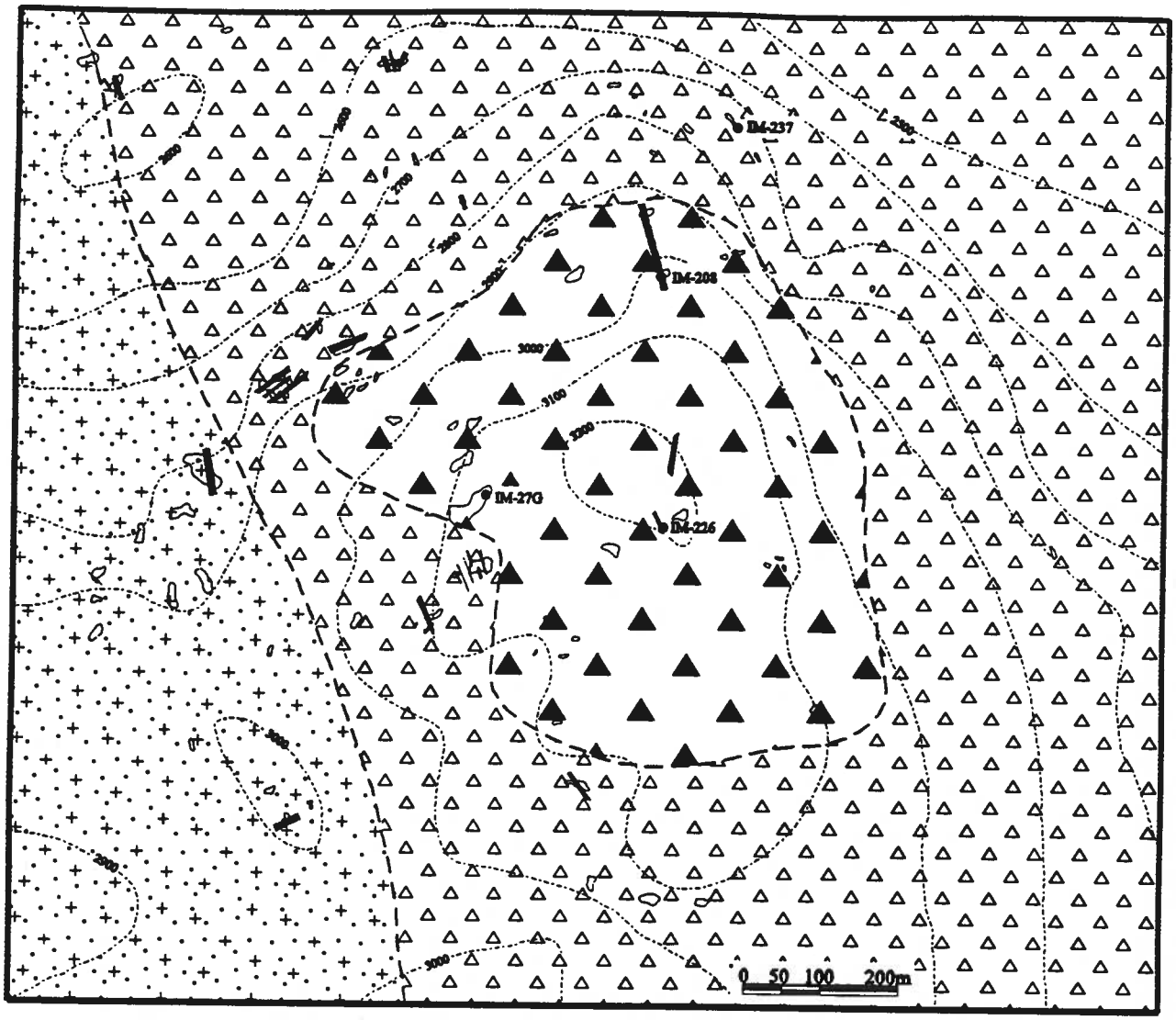

Figure A.4. This map represents exposures of monzonite breccia in the northeast part of the batholith. The breccia is subdivided on the nature of the clast/matrix boundary. Solid triangles represent sharp interfaces and angular clasts of Iron Mask hybrid and Nicola Group rocks. The open triangles are areas of rounder clasts and more diffuse clast/matrix interfaces. The area is cut by numerous biotite monzonite dykes interpreted to belong to the Cherry Creek unit.

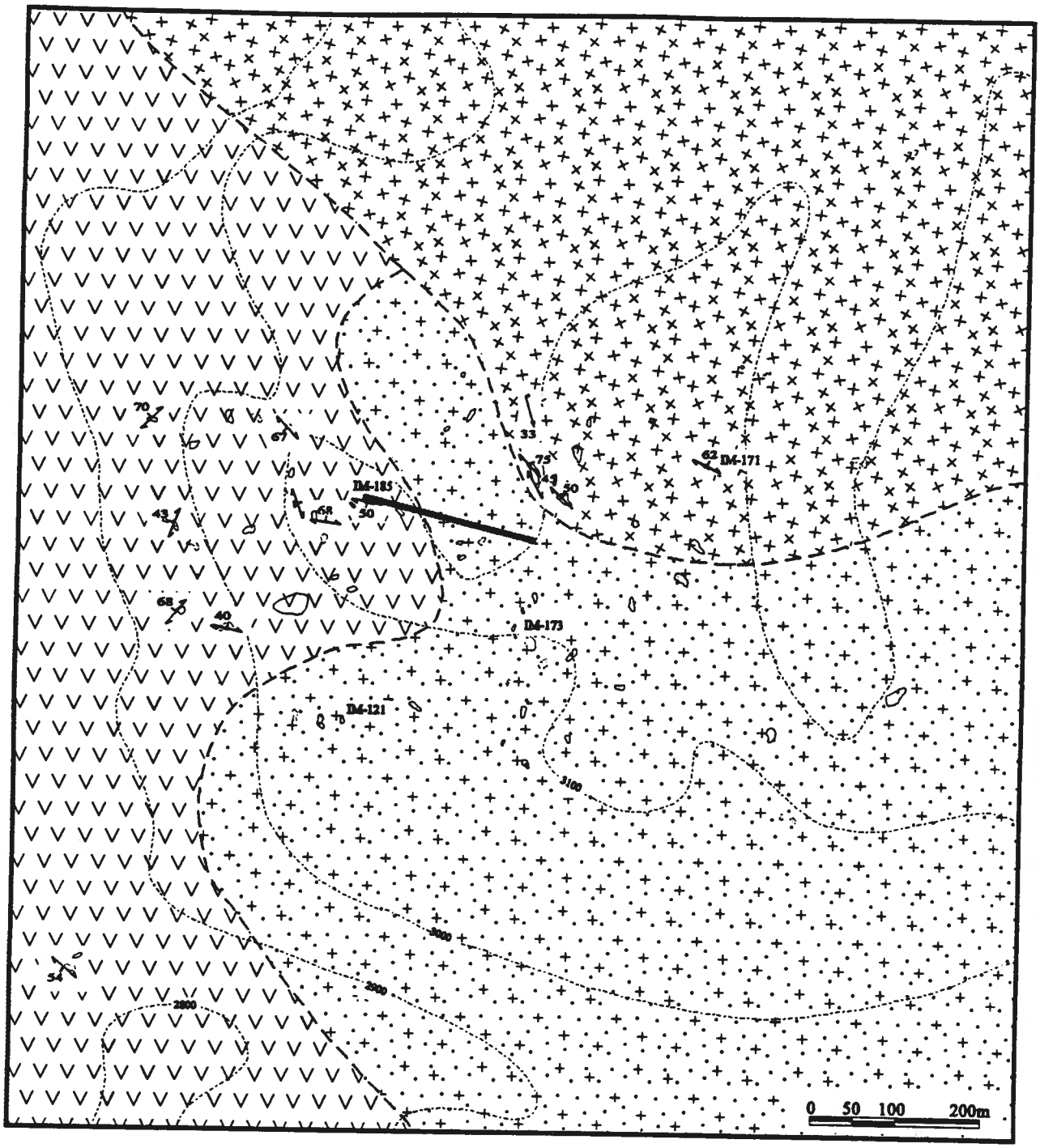

Figure A.5. In this area, Iron Mask rocks intrude Nicola Group rocks. Abundant recrystallized clasts of clinopyroxene-phyric flows are found in Type I and Type III Iron Mask hybrid. A late quartz vein (black line) crosscuts both of these rock units. Cherry Creek rocks are also found in the area.

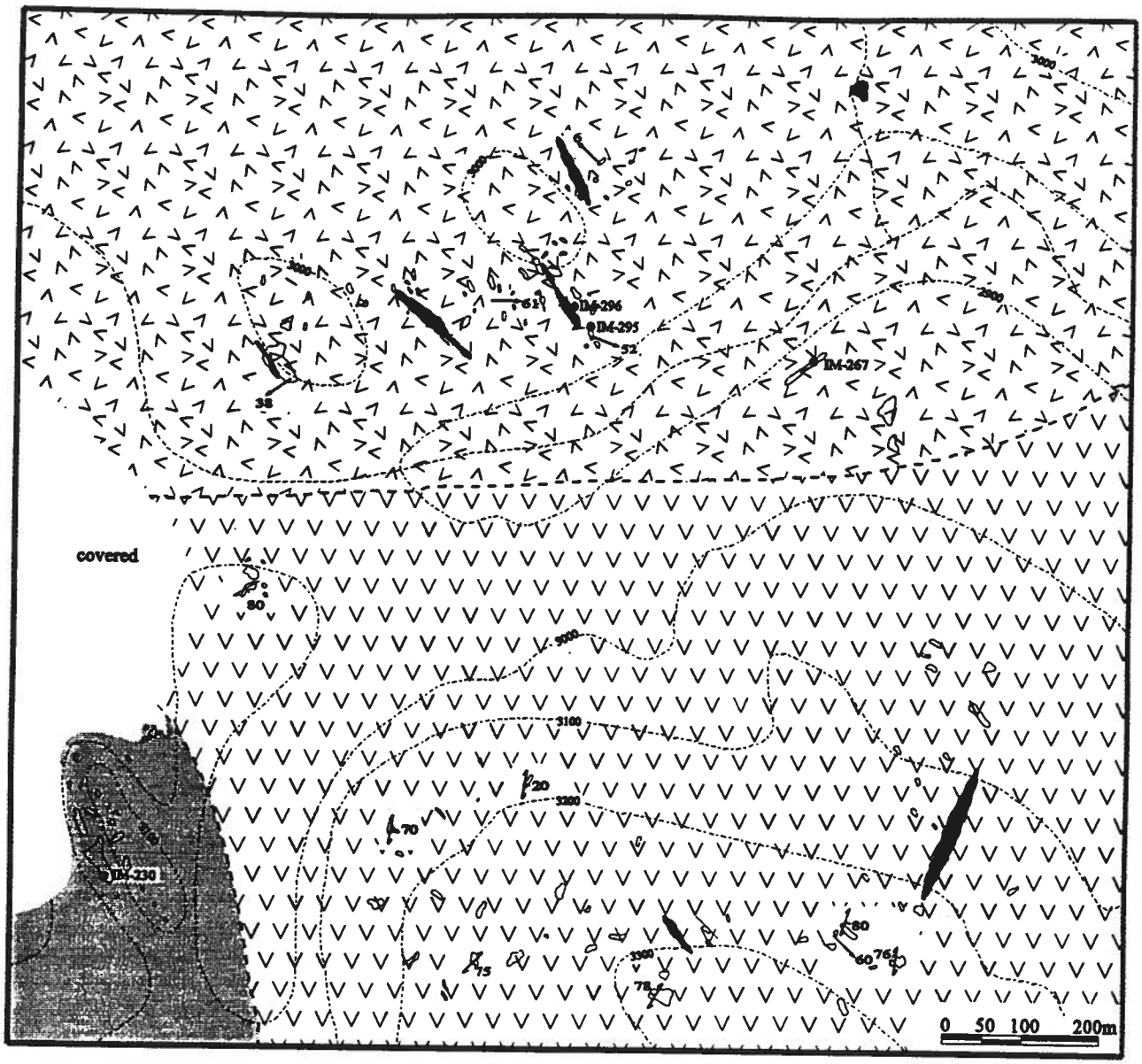

Figure A.6. This area shows the occurrence of well-preserved picritic basalt just outside of the batholith near Jacko Lake. Hornblende-phyric Sugarloaf rocks are at the margin of the batholith in this area. Sugarloaf, Nicola and picrite are all intruded by dark grey, fine-grained dykes belonging to the Sugarloaf unit.

APPENDIX B. Petrographic description of geochemical samples from the Iron Mask batholith.

Sample: IM-119
Unit: Pothook Location: Sugarloaf Hill

Mineral	Volume%	Description
plagioclase	50	up to 2mm subhedral; sericitized, An_{51}
k-feldspar	trace	interstitial
pyroxene	25	0.5 to 1.5mm subhedral; slight green pleochroism; opaque inclusions; associated with magnetite
biotite	12	0.5 to 1mm subhedral to anhedral; poikilitic with plagioclase and clinopyroxene; intergrown with clinopyroxene and epidote
magnetite	12	0.2 to 0.5mm euhedral to subhedral; inclusions in and associated with clinopyroxene
acc and alt		titanite, apatite

Rock Name: coarse-grained biotite-pyroxene diorite

Sample: IM-124
Unit: Pothook Location: Sugarloaf Hill

Mineral	Volume%	Description
plagioclase	55	0.5mm subhedral; equant; sericitized
k-feldspar	3	anhedral interstitial
pyroxene	30	0.3 to 0.7mm euhedral to subhedral; colourless, non-pleochroic
biotite	5	corroded; poikilitic
magnetite	7	0.4mm euhedral to subhedral, associated with pyroxene
chlorite	5	alteration of biotite, clinopyroxene
acc and alt		apatite, titanite, epidote

Rock Name: medium-grained pyroxene diorite

Sample: IM-242
Unit: Pothook/hybrid transitional zone Location: Sugarloaf Hill

MATRIX:

Mineral	Volume%	Description
plagioclase	65	0.5 to 0.2mm subhedral to anhedral; sericitized
pyroxene	25	0.5 to 3mm subhedral crystals
biotite	trace	small, some intergrown with clinopyroxene
magnetite	7	0.5mm euhedral to subhedral; associated with ferromagnesians
acc and alt		epidote, titanite

Rock Name: medium grained pyroxene diorite

CLAST:

Mineral	Volume%	Description
plagioclase	40	0.5 to 1mm sericitized; An_{38}
pyroxene	30	0.5mm subhedral poikilitic with plagioclase
amphibole	8	replacing clinopyroxene
biotite	5	up to 1mm; corroded
magnetite	15	0.05 to 0.3 subhedral to anhedral
acc and alt		apatite

Sample: IM-251
Unit: Pothook Location: Sugarloaf Hill

Mineral	Volume%	Description
plagioclase	45	0.5 to 1mm subhedral, slight normal zoning, very sericitized
k-feldspar	trace	interstitial
pyroxene	25	0.5 to 1mm subhedral, weakly chloritized, ass. with magnetite
biotite	8	0.5 to 1mm subhedral to anhedral, intergrown with epidote and pyroxene; poikilitic
magnetite	8	0.5mm subhedral to anhedral
acc and alt		apatite, chlorite

Rock Name: medium grained biotite-pyroxene diorite

Sample: IM-257
Unit: Pothook Location: Lockie Lake

Mineral	Volume%	Description
plagioclase	55	0.5mm euhedral to subhedral laths; weak normal zoning, slightly sericitized, An_{43}
k-feldspar	3	0.2mm subhedral
pyroxene	17	0.2 to 0.5mm euhedral to subhedral; colourless; non-pleochroic; few opaque inclusions
biotite	15	0.3 to 1mm subhedral to anhedral; poikilitic with plagioclase and pyroxene; brown-yellow pleochroism; no intergrowths
magnetite	7	0.1 to 0.4mm subhedral to anhedral; closely associated with and rimming clinopyroxene
acc and alt		apatite, zircon, chlorite

Rock Name: medium-grained biotite-pyroxene diorite

Sample: IM-265
Unit: Pothook Location: Golf Course

Mineral	Volume%	Description
plagioclase	50	0.5mm subhedral laths; sericitized
k-spar	10	0.5mm subhedral
pyroxene	20	0.3 to 0.7mm subhedral
biotite	5	0.5mm anhedral; poikilitic; very corroded; intergrown with epidote
magnetite	10	0.2 to 0.3mm euhedral-subhedral; disseminated; few inclusions in pyroxene
acc and alt		epidote, apatite, chlorite (5%), hematite, titanite

Comment: Epidote veining with chlorite envelope

Rock Name: medium-grained pyroxene monzodiorite

Sample: IM-11
Unit: Cherry Creek Location: Nelson Lake

Mineral	Volume%	Description
plagioclase	65	0.5-1mm euhedral to subhedral; moderately trachytic; zoned; An_{37} to An_{42}
k-feldspar	10	up to 0.5mm anhedral; interstitial
pyroxene	5	two populations: a) 2% 1mm subhedral; corroded; abundant opaque inclusions and; b) 3% 0.2mm euhedral to subhedral; light green to brown pleochroism; not corroded
amphibole	12	0.1 to 0.5mm euhedral anhedral; not altered
quartz	3	
magnetite	5	0.2mm subhedral; disseminated; minor inclusions in clinopyroxene
acc and alt		titanite (2%), apatite and epidote

Rock Name: medium-grained monzodiorite

Sample: IM-27G
Unit: Cherry Creek Location: Breccia zone

Mineral	Volume%	Description
plagioclase	55	up to 1mm subhedral; slightly trachytic; sericitized, An_{35}
k-feldspar	10	two populations: a) 3% large anhedral poikilitic grains and; b) 7% 0.1mm anhedral; interstitial
pyroxene	10	0.5mm subhedral; non-pleochroic
amphibole	trace	
biotite	8	0.4mm subhedral; some intergrown with clinopyroxene
magnetite	10	
acc and alt		epidote (3%), titanite, zircon

Rock Name: fine-grained biotite monzodiorite

Sample: IM-171
Unit: Cherry Creek Location: Lac Le Jeune Road

Mineral	Volume%	Description
plagioclase	50	0.5mm subhedral; slightly zoned; up to 80% sericitized; An_{42}
k-feldspar	10	0.1 to 0.2mm anhedral interstitial; and up to 1.5mm anhedral, poikilitic grains
pyroxene	20	0.4 to 0.5mm euhedral to subhedral; light green pleochroism; small euhedral opaque inclusions; exsolution
biotite	5	0.3mm anhedral; poikilitic; corroded
magnetite	10	0.2mm subhedral to anhedral, associated with clinopyroxene
acc and alt		apatite (ass. with pyroxene) , zircon, epidote, chlorite

Rock Name: medium grained monzonite

Sample: IM-237
Unit: Cherry Creek Location: Breccia zone

Mineral	Volume%	Description
plagioclase	45	0.1 to 0.5mm subhedral; trachytic; locally sericitized; normally zoned; An_{40}
k-spar	5	0.1mm anhedral
pyroxene	25	0.3mm subhedral grains; aligned; colourless; opaque inclusions
biotite	20	0.3mm anhedral; aligned; slightly poikilitic; minor chloritic alteration
magnetite	5	0.1mm subhedral to anhedral; disseminated; associated with ferromagnesians
acc and alt		epidote, titanite

Comments: linear zones of alteration

Rock Name: fin-grained biotite monzodiorite

Sample: IM-253
Unit: Cherry Creek Location: Makaoo Lake

Mineral	Volume%	Description
plagioclase	50	0.5mm subhedral; sub-trachytic; sericitized; An_{43}
k-feldspar	15	0.2 to 1mm anhedral; somewhat altered
pyroxene	15	0.5mm subhedral; light green pleochroism; opaque inclusions
biotite	7	two populations: a)5% 0.3 to 0.5mm subhedral; fresh and, b) 2% 0.2 to 0.3mm subhedral; intergrown with epidote, chlorite; corroded
magnetite	8	0.1 to 0.3mm subhedral to anhedral; associated with clinopyroxene
quartz	3	0.1 to 0.2mm anhedral
acc and alt		apatite

Rock Name: medium-grained monzonite

Sample: IM-303
Unit: Cherry Creek Location: south

Mineral	Volume%	Description
plagioclase	50	0.5 to 1mm euhedral to subhedral; sub-trachytic; mildly sericitized, An_{40}
k-feldspar	8	0.5mm subhedral
pyroxene	10	0.3mm subhedral; colourless; corroded
biotite	15	0.5mm subhedral; slightly poikilitic
chlorite	5	0.2mm anhedral
magnetite	7	0.1-0.5mm subhedral to anhedral; disseminated; also as inclusions in ferromagnesians
acc and alt		quartz (2%)

Rock Name: medium-grained biotite monzodiorite

Sample: IM-208
Unit: Iron Mask dyke Location: Cherry Creek Breccia zone

Mineral	Volume%	Description
plagioclase	45	0.1 to 0.6mm subhedral; sub-trachytic; unzoned; An_{38}
k-feldspar	5	0.2 to 0.4mm subhedral to anhedral
biotite	15	0.5mm subhedral, some chlorite alteration
pyroxene	20	0.2mm anhedral; disseminated; very light green colour; subhedral to anhedral opaque inclusions
magnetite	10	0.05 to 0.2 subhedral; disseminated
acc and alt		epidote, chlorite (7%)

Rock Name: fine-grained biotite monzodiorite

Sample: IM-226
Unit: Iron Mask dyke Location: Cherry Creek Breccia zone

Mineral	Volume%	Description
plagioclase	25	0.5mm subhedral; trachytic; strongly zoned, An_{37}
k-spar	15	0.5mm subhedral to anhedral
pyroxene	520	0.2mm subhedral; colourless to very light green
biotite	20	0.3 to 0.5mm subhedral; aligned; yellow to dark brown pleochroism; some grains slightly poikilitic
chlorite	5	0.2mm subhedral to anhedral
magnetite	510	0.1 to 0.3mm anhedral; disseminated
acc and alt		epidote

Rock Name: fine-grained biotite monzonite

Sample: IM-254
Unit: Iron Mask dyke Location: Makaoo Lake

Mineral	Volume%	Description
plagioclase	55	0.3 to 0.5mm subhedral; sub-trachytic; sericitized
k-feldspar	8	0.2mm anhedral
pyroxene	20	0.05 to 0.2mm subhedral; colourless(few larger 0.5mm grains)
biotite	2	0.3mm anhedral; intergrown with epidote; corroded
quartz	trace	
magnetite	7	0.1 to 0.2mm euhedral to subhedral
acc and alt		epidote (7%), titanite, chlorite, zircon

Rock Name: fine-grained monzodiorite

Sample: IM-308
Unit: Iron Mask dyke Location: north of Ajax East

Mineral	Volume%	Description
plagioclase	55	mainly 0.2mm subhedral; equant; altered cored and zoned overgrowths; few 1mm grains; An_{42} (large grain)
k-feldspar	2	interstitial
pyroxene	30	0.05 to 0.4mm subhedral; colourless; non-pleochroic; opaque inclusions
biotite	trace	0.1mm anhedral; light brown
magnetite	10	0.05-0.4mm subhedral to anhedral; disseminated and as inclusions in clinopyroxene
acc and alt		apatite

Rock Name: fine-grained pyroxene diorite

Sample: IM-249
Unit: Sugarloaf Location: west Sugarloaf Hill

Mineral	Volume%	Description
plagioclase	50	0.5mm subhedral; sericitized; mildly trachytic
k-feldspar	trace	interstitial
amphibole	30	up to 3mm subhedral; slightly chloritized
magnetite	15	0.3mm disseminated
acc and alt		chlorite, titanite, epidote

Rock Name: porphyritic amphibole diorite

Sample: IM-266
Unit: Sugarloaf Location: Jacko Lake

Mineral	Volume%	Description
plagioclase	40	0.2 to 0.7mm subhedral to euhedral; elongate; sericitized; thin zoned rims
k-feldspar	5	0.2mm anhedral
amphibole	20	0.5 to 1.5mm brownish, intergrown with pyroxene
magnetite	7	0.05 to 0.2mm subhedral to euhedral
chlorite	10	replacing amphibole
acc and alt		epidote (10%), titanite, apatite, calcite, quartz

Rock Name: fine-grained amphibole diorite

Sample: IM-267
Unit: Sugarloaf Location: Goose Lake Road

Mineral	Volume%	Description
plagioclase	25	0.2mm subhedral; sericitized; few large grains with epidote cores, An_{32}
k-feldspar	8	anhedral interstitial
amphibole	60	0.5 to 1.5mm subhedral; elongate; light green colour; brown and green pleochroism; altered along cleavage planes to chlorite
magnetite	5	0.1 to 0.3mm euhedral to subhedral
acc and alt		apatite (up to 0.3mm), titanite, epidote (5%)

Comment: contains amphibolite clast consisting of felted amphibole and minor pyroxene and quartz

Rock Name: porphyritic amphibole diorite

Sample: IM-271
Unit: Sugarloaf Location: Sugarloaf Hill

Mineral	Volume%	Description
plagioclase	45	0.5 to 1mm subhedral; sericitized
pyroxene	25	0.5 to 3mm subhedral; colourless; corroded
biotite	5	0.5 to 1mm anhedral; corroded; alteration of pyroxene(?)
amphibole	10	0.5-1mm subhedral chloritized
magnetite	7	up to 0.5mm subhedral to anhedral disseminated
acc and alt		chlorite (5%), apatite

Rock Name: medium-grained porphyritic pyroxene-hornblende diorite

Sample: IM-272
Unit: Sugarloaf Location: Sugarloaf Hill

Mineral	Volume%	Description
plagioclase	50	0.5-1mm euhedral to subhedral; sericitized; trachytic
k-feldspar	5	interstitial
pyroxene	5	0.5mm anhedral; very corroded
amphibole	10	up to 1.5mm subhedral; altered to chlorite
magnetite	7	up to 0.5mm anhedral disseminated
acc and alt		chlorite (20%), epidote, apatite

Rock Name: medium-grained porphyritic amphibole diorite

Sample: IM-274
Unit: Sugarloaf Location: Edith Lake

Mineral	Volume%	Description
plagioclase	30	0.2 to 0.5 subhedral to anhedral; moderately sericitized, An_{32}
k-feldspar	trace	anhedral; interstitial
pyroxene	10	0.4 to 1mm euhedral to subhedral; phenocrysts and aggregates; colourless
amphibole	35	0.5 to 2mm euhedral to subhedral, greenish pleochroism; zoning apparent in some grains
magnetite	5	0.05 to 0.2mm euhedral to subhedral
epidote	15	granular, secondary
acc and alt		titanite, apatite, chlorite, quartz

Rock Name: porphyritic amphibole-pyroxene diorite

Sample: IM-295
Unit: Sugarloaf Location: Ajax

Mineral	Volume%	Description
plagioclase	40	0.5 to 1mm subhedral, sericitized
k-feldspar	10	interstitial
amphibole	25	0.5 to 3mm subhedral, chloritized; opaque inclusions
magnetite	7	0.1 to 0.5mm anhedral-subhedral; disseminated; also as inclusions in ferromagnesians
acc and alt		apatite, titanite, epidote, hematite, chlorite (15%)

Rock Name: porphyritic amphibole diorite

Sample: IM-296
Unit: Sugarloaf dyke Location: Ajax

Mineral	Volume%	Description
plagioclase	5	1mm subhedral; sericitized
k-feldspar	trace	
pyroxene	trace	up to 1mm subhedral; corroded
amphibole	12	up to 3mm subhedral; slightly chloritized; opaque inclusions
magnetite	7	very fine disseminated
acc and alt		chlorite (5%)
groundmass	70	

Rock Name: amphibole diorite

Sample: IM-173
Unit: Iron Mask hybrid Type I matrix Location: Lac Le Jeune Road

Mineral	Volume%	Description
plagioclase	40	0.5 to 1mm subhedral; An_{61}
amphibole	30	0.5 to 2mm subhedral to anhedral; sometimes poikilitic
pyroxene	25	0.5 to 2mm euhedral to subhedral; poikilitic; very light green
magnetite	5	large, anhedral grains associated with ferromagnesians and surrounded by fine-grained alteration mineral
k-spar	trace	
acc and alt		

Comment: relative absence of opaque inclusions in ferromagnesians

Rock Name: coarse grained pyroxene diorite

Sample: IM-306
Unit: Iron Mask hybrid Type II matrix Location: Sugarloaf Hill

Mineral	Volume%	Description
plagioclase	35	0.1 to 0.5mm subhedral laths; partially sericitized, An_{60}
biotite	5	0.5 to 0.7mm anhedral; associated with amphibole; intergrown with epidote
pyroxene	30	0.05 to 0.5mm euhedral to subhedral; very light green colour; non-pleochroic; opaque inclusions; aggregates with interstitial opaques
amphibole	10	0.5 to 1mm subhedral to anhedral; associated with biotite; poikilitic with plagioclase, opaque, pyroxene; green colour and pleochroism
magnetite	15	0.05 to 0.4mm anhedral; associated with pyroxene and inclusions in ferromagnesians
acc and alt		apatite, k-spar

Rock Name: medium-grained pyroxene diorite

Sample: IM-120
Unit: Iron Mask hybrid Location: Python
Type III

Mineral	Volume%	Description
plagioclase	45	up to 2mm subhedral; equant; unzoned; An_{60}
biotite	Trace	0.2mm anhedral; interstitial associated with opaques
amphibole	4	alteration rims on clinopyroxene
pyroxene	40	0.5 to 1mm subhedral to anhedral; light green; numerous mafic inclusions; aggregates with matrix of opaque material
magnetite	10	0.1 to 0.5 anhedral; interstitial
acc and alt		apatite

Rock Name: coarse-grained pyroxene diorite

Sample: IM-256
Unit: Iron Mask hybrid Location: Makaoo Lake
Type III

Mineral	Volume%	Description
plagioclase	40	0.5 to 1.5mm euhedral to subhedral; trachytic; An_{58}
biotite	2	"patchy" overgrowths on pyroxene
amphibole	trace	
pyroxene	40	subhedral to anhedral; light green pleochroism; some poikilitic; inclusions of euhedral to subhedral opaques; some spinel exsolution
magnetite	10	0.2mm subhedral to anhedral; associated with clinopyroxene
k-spar	2	0.3mm anhedral
chlorite	3	0.3mm subhedral to anhedral; associated with alteration veining
acc and alt		apatite, epidote

Rock Name: pyroxene diorite

Sample: IM-121
Unit: Iron Mask hybrid Location: Lac Le Jeune Road
Xenolith

Mineral	Volume%	Description
amphibole	5	"patchy" alteration from clinopyroxene
pyroxene	80	3mm subhedral; equant; numerous spinel crosses; recrystallized
magnetite	15	0.5 to 1.5mm subhedral to euhedral; inclusions and interstitial
acc and alt		

Rock Name: pyroxenite

Sample: IM-268
Unit: Iron Mask hybrid Xenolith Location: Ajax area

Mineral	Volume%	Description
plagioclase	trace	sericitized
biotite	5	2mm anhedral; poikilitic with clinopyroxene
amphibole	7	1 to 2mm anhedral; green to brown; opaque inclusions
pyroxene	63	0.2 to 1mm euhedral to subhedral; opaque inclusions
magnetite	25	0.2 to 0.5mm anhedral to subhedral interstitial
acc and alt		

Rock Name: pyroxenite

Appendix C. Table C.1 Electron Microprobe analyses for clinopyroxene from the Pothook unit.

Sample	IM-251	IM-251	IM-251	IM-251	IM-251	IM-251	IM-251	IM-251	IM-251	IM-251	IM-251	IM-251	IM-251	IM-251	IM-251	IM-251
Grain	1	1	1	1	1	1	1	2	2	2	2	2	3	3	3	3
Position	r	i	c	i	r	i	r	r	i	c	i	r	r	c	i	r
SiO_2	50.27	50.70	49.92	50.96	50.78	50.38	50.91	50.51	50.56	49.34	50.44	50.79	51.36	50.40	50.68	50.50
TiO_2	0.57	0.46	0.64	0.46	0.48	0.54	0.46	0.59	0.50	0.57	0.52	0.43	0.36	0.52	0.48	0.47
Al_2O_3	2.64	2.60	2.98	2.40	2.40	2.71	2.48	2.82	2.57	3.88	2.83	2.41	2.18	2.69	2.60	2.73
Cr_2O_3	b.d.	b.d.	b.d.	b.d.	b.d.	b.d.	b.d.	b.d.	b.d.	b.d.	b.d.	b.d.	b.d.	b.d.	b.d.	b.d.
Fe_2O_3	3.44	3.24	3.70	2.97	3.29	3.12	2.99	2.62	3.05	3.67	2.63	2.94	3.02	3.26	3.12	3.08
FeO	3.82	4.05	3.92	4.31	4.15	3.99	4.20	4.66	4.43	4.47	4.59	4.20	4.29	4.23	4.37	4.05
MnO	0.49	0.45	0.38	0.39	0.46	0.44	0.45	0.46	0.36	0.36	0.36	0.46	0.41	0.44	0.41	0.34
MgO	14.95	14.84	14.45	14.89	15.06	14.76	15.08	14.64	14.83	13.87	14.75	15.23	15.40	14.82	14.89	14.99
CaO	21.80	22.02	22.08	22.04	21.83	21.91	21.84	21.84	21.74	21.92	21.78	21.67	21.81	21.75	21.80	21.79
Na_2O	0.38	0.41	0.42	0.41	0.38	0.42	0.39	0.38	0.40	0.41	0.36	0.34	0.36	0.39	0.39	0.39
TOTAL	98.36	98.77	98.49	98.83	98.83	98.27	98.80	98.52	98.44	98.49	98.26	98.47	99.19	98.50	98.74	98.34
FeO_T	6.92	6.97	7.25	6.98	7.11	6.8	6.89	7.02	7.17	7.77	6.96	6.85	7.01	7.16	7.18	6.82
Cation calculation based on 6 oxygens and Fe^{2+}/Fe^{3+} adjusted to 4 cations																
Si	1.890	1.898	1.878	1.907	1.901	1.895	1.904	1.897	1.900	1.860	1.898	1.905	1.912	1.894	1.899	1.897
Al^{IV}	0.110	0.102	0.122	0.093	0.099	0.105	0.096	0.103	0.100	0.140	0.102	0.095	0.088	0.106	0.101	0.103
Total	2.000	2.000	2.000	2.000	2.000	2.000	2.000	2.000	2.000	2.000	2.000	2.000	2.000	2.000	2.000	2.000
Ti^{4+}	0.016	0.013	0.018	0.013	0.014	0.015	0.013	0.017	0.014	0.016	0.015	0.012	0.010	0.015	0.014	0.013
Al^{VI}	0.007	0.013	0.010	0.013	0.007	0.015	0.013	0.022	0.014	0.032	0.023	0.012	0.008	0.013	0.014	0.018
Cr^{3+}	0.000	0.000	0.000	0.000	0.000	0.000	0.000	0.000	0.000	0.000	0.000	0.000	0.000	0.000	0.000	0.000
Fe^{3+}	0.097	0.091	0.105	0.084	0.093	0.088	0.084	0.074	0.086	0.104	0.074	0.083	0.085	0.092	0.088	0.087
Fe^{2+}	0.120	0.127	0.123	0.135	0.130	0.125	0.131	0.146	0.139	0.141	0.144	0.132	0.134	0.133	0.137	0.127
Mn	0.016	0.014	0.012	0.012	0.015	0.014	0.014	0.015	0.011	0.011	0.011	0.015	0.013	0.014	0.013	0.011
Mg	0.838	0.828	0.811	0.831	0.840	0.828	0.841	0.820	0.831	0.780	0.828	0.852	0.855	0.830	0.832	0.839
Ca	0.878	0.883	0.890	0.884	0.875	0.883	0.875	0.879	0.875	0.885	0.878	0.871	0.870	0.876	0.875	0.877
Na	0.028	0.03	0.031	0.03	0.028	0.031	0.028	0.028	0.029	0.03	0.026	0.025	0.026	0.028	0.028	0.028
MG #	87.47	86.70	86.83	86.02	86.60	86.88	86.52	84.89	85.67	84.69	85.19	86.59	86.45	86.19	85.86	86.85

MG# = 100•Mg/(Mg + Fe^{2+}) c = core; r = rim; i = interior

Appendix C. Table C.1 (continued)

Sample	IM-251	IM-251	IM-251	IM-251	IM-251	IM-119	IM-119	IM-119	IM-119	IM-119	IM-119	IM-119	IM-119	IM-119	IM-119	IM-119
Grain	4	4	5	5	5	1	1	1	1	2	2	3	3	3	3	3
Position	i	i	i	c	r	i	i	c	r	r	i	r	i	c	i	r
SiO_2	51.13	51.18	50.73	50.48	50.60	51.34	51.02	51.72	52.66	51.98	51.46	51.05	51.66	53.22	53.40	53.05
TiO_2	0.48	0.40	0.52	0.55	0.53	0.37	0.38	0.39	0.18	0.30	0.30	0.39	0.39	0.15	0.14	0.19
Al_2O_3	2.29	2.52	2.49	2.70	2.74	1.87	1.85	1.66	0.90	1.19	1.42	2.52	1.89	0.78	0.82	0.80
Cr_2O_3	b.d.	b.d.	0.07	b.d.	b.d.	b.d.	b.d.	b.d.	b.d.	b.d.	b.d.	b.d.	b.d.	b.d.	b.d.	b.d.
Fe_2O_3	2.79	2.59	2.90	3.41	3.14	2.82	2.78	1.68	0.93	2.39	2.42	3.33	3.28	2.11	1.99	2.39
FeO	4.43	4.67	4.73	3.99	4.12	3.80	4.00	4.35	3.87	3.73	4.63	3.83	3.77	3.01	3.26	2.86
MnO	0.50	0.43	0.56	0.47	0.42	0.31	0.34	0.32	0.26	0.43	0.43	0.34	0.38	0.27	0.34	0.28
MgO	15.19	14.96	14.82	14.90	14.99	14.68	14.55	14.81	15.15	15.52	14.51	14.36	14.61	15.64	15.36	15.51
CaO	21.76	21.90	21.50	21.68	21.88	22.90	22.43	22.73	23.19	22.39	22.35	22.79	23.10	23.67	23.83	23.72
Na_2O	0.37	0.38	0.41	0.45	0.37	0.46	0.51	0.44	0.50	0.42	0.49	0.53	0.51	0.50	0.54	0.53
TOTAL	98.94	99.03	98.73	98.63	98.79	98.55	97.86	98.1	97.64	98.35	98.01	99.14	99.59	99.35	99.68	99.33
FeO_T	6.94	7.00	7.34	7.06	6.95	6.34	6.50	5.86	4.71	5.88	6.81	6.83	6.72	4.91	5.05	5.01
Cation calculation based on 6 oxygens and Fe^{2+}/Fe^{3+} adjusted to 4 cations																
Si	1.910	1.910	1.903	1.893	1.893	1.925	1.927	1.944	1.980	1.946	1.943	1.906	1.920	1.967	1.970	1.963
Al^{IV}	0.090	0.090	0.097	0.107	0.107	0.075	0.073	0.056	0.020	0.053	0.057	0.094	0.080	0.033	0.030	0.035
Total	2.000	2.000	2.000	2.000	2.000	2.000	2.000	2.000	2.000	1.999	2.000	2.000	2.000	2.000	2.000	1.998
Ti^{4+}	0.013	0.011	0.015	0.016	0.015	0.010	0.011	0.011	0.005	0.008	0.009	0.011	0.011	0.004	0.004	0.005
Al^{VI}	0.011	0.021	0.013	0.012	0.014	0.008	0.009	0.018	0.020	0.000	0.006	0.017	0.003	0.001	0.006	0.000
Cr^{3+}	0.000	0.000	0.002	0.000	0.000	0.000	0.000	0.000	0.000	0.000	0.000	0.000	0.000	0.000	0.000	0.000
Fe^{3+}	0.078	0.073	0.082	0.096	0.088	0.080	0.079	0.048	0.026	0.067	0.069	0.094	0.092	0.059	0.055	0.066
Fe^{2+}	0.138	0.146	0.148	0.125	0.129	0.119	0.126	0.137	0.122	0.117	0.146	0.120	0.117	0.093	0.100	0.089
Mn	0.016	0.014	0.018	0.015	0.013	0.010	0.011	0.010	0.008	0.014	0.014	0.011	0.012	0.008	0.011	0.009
Mg	0.846	0.833	0.829	0.833	0.836	0.821	0.819	0.830	0.849	0.866	0.817	0.799	0.810	0.862	0.845	0.856
Ca	0.871	0.876	0.864	0.871	0.877	0.92	0.908	0.915	0.934	0.898	0.904	0.911	0.92	0.937	0.942	0.94
Na	0.027	0.028	0.030	0.033	0.027	0.033	0.037	0.032	0.036	0.030	0.036	0.038	0.037	0.036	0.039	0.038
MG #	85.98	85.09	84.85	86.95	86.63	87.34	86.67	85.83	87.44	88.10	84.84	86.94	87.38	90.26	89.42	90.58

Appendix C. Table C.1 (continued)

Sample	IM-119	IM-119	IM-119	IM-119	IM-119	IM-119	IM-119	IM-119	IM-119	IM-119	IM-257	IM-257	IM-257	IM-257	IM-257	IM-257
Grain	4	4	4	5	5	5	5	6	6	6	1	1	2	2	2	2
Position	r	c	i	r	c	i	r	i	c	r	r	i	r	i	i	r
SiO_2	52.63	51.52	51.11	52.66	51.72	52.93	52.54	53.15	52.89	52.56	51.98	52.97	52.52	51.44	52.33	52.99
TiO_2	0.23	0.33	0.40	0.22	0.31	0.11	0.19	0.13	0.23	0.20	0.20	0.02	b.d.	0.22	0.05	b.d.
Al_2O_3	0.80	1.24	1.80	1.00	1.31	0.61	0.89	0.88	1.12	1.31	1.22	0.24	0.33	1.35	0.63	0.23
Cr_2O_3	b.d.	b.d.	b.d.	b.d.	b.d.	b.d.	0.06	b.d.	b.d.	b.d.	b.d.	b.d.	b.d.	b.d.	b.d.	b.d.
Fe_2O_3	2.34	3.06	3.35	1.82	2.00	0.96	1.82	1.76	2.33	1.97	1.59	1.34	1.53	2.85	1.67	1.89
FeO	2.56	3.36	3.79	3.38	4.46	3.61	3.06	3.57	2.93	3.37	5.49	3.24	4.46	4.51	4.41	3.46
MnO	0.33	0.38	0.41	0.30	0.44	0.24	0.32	0.34	0.30	0.40	0.56	0.42	0.42	0.58	0.53	0.58
MgO	15.62	15.00	14.27	15.35	14.86	15.33	15.38	15.18	15.43	15.71	14.51	15.87	14.90	14.53	15.23	16.05
CaO	23.65	22.92	22.88	23.25	22.31	24.23	23.20	23.56	23.75	23.19	22.28	23.81	23.74	22.55	22.95	23.16
Na_2O	0.46	0.45	0.55	0.51	0.47	0.26	0.54	0.55	0.50	0.34	0.41	0.20	0.21	0.40	0.25	0.23
TOTAL	98.62	98.26	98.56	98.49	97.88	98.28	98.00	99.12	99.48	99.05	98.24	98.11	98.11	98.43	98.05	98.59
FeO_T	4.67	6.11	6.80	5.02	6.26	4.47	4.70	5.15	5.03	5.14	6.92	4.45	5.84	7.07	5.91	5.16
Cation calculation based on 6 oxygens and Fe^{2+}/Fe^{3+} adjusted to 4 cations																
Si	1.959	1.936	1.921	1.964	1.951	1.979	1.968	1.972	1.954	1.950	1.959	1.982	1.978	1.938	1.970	1.976
Al^{IV}	0.035	0.055	0.079	0.036	0.049	0.021	0.032	0.028	0.046	0.050	0.041	0.011	0.015	0.060	0.028	0.010
Total	1.994	1.991	2.000	2.000	2.000	2.000	2.000	2.000	2.000	2.000	2.000	1.993	1.993	1.998	1.998	1.986
Ti^{4+}	0.006	0.009	0.011	0.006	0.009	0.003	0.005	0.004	0.006	0.006	0.006	0.001	0.000	0.006	0.001	0.000
Al^{VI}	0.000	0.000	0.001	0.008	0.009	0.006	0.007	0.010	0.003	0.007	0.013	0.000	0.000	0.000	0.000	0.000
Cr^{3+}	0.000	0.000	0.000	0.000	0.000	0.000	0.002	0.000	0.000	0.000	0.000	0.000	0.000	0.000	0.000	0.000
Fe^{3+}	0.066	0.087	0.095	0.051	0.057	0.027	0.051	0.049	0.065	0.055	0.045	0.038	0.043	0.081	0.047	0.053
Fe^{2+}	0.080	0.106	0.119	0.106	0.141	0.113	0.096	0.111	0.091	0.105	0.173	0.102	0.141	0.142	0.139	0.108
Mn	0.010	0.012	0.013	0.009	0.014	0.008	0.010	0.011	0.009	0.013	0.018	0.013	0.013	0.019	0.017	0.018
Mg	0.867	0.840	0.800	0.854	0.836	0.855	0.859	0.840	0.850	0.869	0.815	0.885	0.837	0.816	0.855	0.892
Ca	0.943	0.923	0.921	0.929	0.901	0.971	0.931	0.937	0.940	0.922	0.900	0.955	0.958	0.910	0.926	0.925
Na	0.033	0.033	0.040	0.037	0.034	0.019	0.039	0.040	0.036	0.024	0.030	0.015	0.015	0.029	0.018	0.017
MG #	91.55	88.79	87.05	88.96	85.57	88.33	89.95	88.33	90.33	89.22	82.49	89.67	85.58	85.18	86.02	89.20

Appendix C. Table C.1 (continued)

Sample	IM-257	IM-257	IM-257	IM-257	IM-257	IM-257	IM-257	IM-257	IM-257	IM-257	IM-257	IM-257	IM-257	IM-257	IM-257	IM-257
Grain	3	3	3	3	3	3	4	4	4	5	5	5	6	6	7	7
Position	i	i	c	r	r	i	r	c	r	i	i	r	r	c	r	c
SiO_2	52.47	52.14	52.24	51.72	51.44	51.30	52.28	51.76	51.37	51.13	51.82	52.90	51.93	51.72	51.74	52.58
TiO_2	b.d.	0.10	0.07	0.17	0.20	0.17	0.14	0.17	0.15	0.14	0.15	0.05	0.18	0.17	0.25	0.14
Al_2O_3	0.60	1.09	0.65	1.17	1.31	1.07	0.86	1.22	1.18	1.08	1.12	0.25	1.32	0.94	1.38	1.01
Cr_2O_3	b.d.	b.d.	b.d.	b.d.	b.d.	b.d.	b.d.	b.d.	0.06	b.d.	b.d.	b.d.	b.d.	b.d.	b.d.	0.07
Fe_2O_3	1.52	2.42	3.11	2.66	2.89	2.76	1.99	2.90	2.81	3.54	2.42	1.82	2.55	2.61	2.98	1.92
FeO	4.51	4.68	4.51	4.62	4.37	4.34	4.14	4.11	4.02	3.59	4.73	3.35	4.60	4.10	4.15	5.00
MnO	0.57	0.72	0.86	0.64	0.60	0.62	0.54	0.71	0.63	0.64	0.62	0.51	0.60	0.60	0.62	0.78
MgO	15.01	15.16	14.92	14.89	14.83	14.82	15.43	15.11	14.96	15.22	15.06	15.95	14.89	14.72	14.90	15.28
CaO	23.24	22.07	22.17	22.03	22.14	21.94	22.56	22.11	22.18	22.13	21.95	23.61	22.39	22.71	22.40	21.97
Na_2O	0.25	0.38	0.47	0.43	0.42	0.44	0.34	0.43	0.4	0.34	0.39	0.17	0.4	0.43	0.45	0.4
TOTAL	98.17	98.76	99.00	98.33	98.20	97.46	98.28	98.52	97.76	97.81	98.26	98.61	98.86	98.00	98.87	99.15
FeO_T	5.88	6.86	7.31	7.01	6.97	6.82	5.93	6.72	6.55	6.78	6.91	4.99	6.89	6.45	6.83	6.73
Cation calculation based on 6 oxygens and Fe^{2+}/Fe^{3+} adjusted to 4 cations																
Si	1.974	1.952	1.957	1.947	1.939	1.948	1.961	1.942	1.943	1.934	1.950	1.973	1.944	1.953	1.936	1.960
Al^{IV}	0.026	0.048	0.029	0.052	0.058	0.048	0.038	0.054	0.053	0.048	0.050	0.011	0.056	0.042	0.061	0.040
Total	2.000	2.000	1.986	1.999	1.997	1.996	1.999	1.996	1.996	1.982	2.000	1.984	2.000	1.995	1.997	2.000
Ti^{4+}	0.000	0.003	0.002	0.005	0.006	0.005	0.004	0.005	0.004	0.004	0.004	0.001	0.005	0.005	0.007	0.004
Al^{VI}	0.001	0.000	0.000	0.000	0.000	0.000	0.000	0.000	0.000	0.000	0.000	0.000	0.002	0.000	0.000	0.004
Cr^{3+}	0.000	0.000	0.000	0.000	0.000	0.000	0.000	0.000	0.002	0.000	0.000	0.000	0.000	0.000	0.000	0.002
Fe^{3+}	0.043	0.068	0.088	0.075	0.082	0.079	0.056	0.082	0.080	0.101	0.069	0.051	0.072	0.074	0.084	0.054
Fe^{2+}	0.142	0.147	0.141	0.146	0.138	0.138	0.130	0.129	0.127	0.114	0.149	0.105	0.144	0.129	0.130	0.156
Mn	0.018	0.023	0.027	0.020	0.019	0.020	0.017	0.023	0.020	0.020	0.020	0.016	0.019	0.019	0.020	0.025
Mg	0.842	0.846	0.833	0.836	0.834	0.839	0.863	0.845	0.844	0.858	0.845	0.887	0.831	0.829	0.831	0.849
Ca	0.937	0.885	0.890	0.888	0.894	0.892	0.907	0.889	0.899	0.897	0.885	0.944	0.898	0.919	0.898	0.877
Na	0.018	0.028	0.034	0.031	0.031	0.032	0.025	0.031	0.029	0.025	0.028	0.012	0.029	0.031	0.033	0.029
MG #	85.57	85.20	85.52	85.13	85.80	85.88	86.91	86.76	86.92	88.27	85.01	89.42	85.23	86.53	86.47	84.48

Appendix C. Table C.1 (continued)

Sample	IM-257	IM-257	IM-257	IM-257	IM-257	IM-257	IM-257	IM-265	IM-265	IM-265	IM-265	IM-265	IM-265	IM-265	IM-265	IM-265
Grain	7	8	8	8	9	9	9	1	1	1	1	1	1	2	2	2
Position	r	r	c	i	r	c	i	i	c	r	r	i	i	r	i	c
SiO_2	51.81	52.75	52.06	51.96	51.73	52.07	53.37	52.38	52.12	51.58	52.07	52.33	51.59	51.88	51.95	51.93
TiO_2	0.26	0.05	0.14	0.16	0.21	0.20	0.05	0.31	0.24	0.34	0.22	0.18	0.32	0.24	0.20	0.20
Al_2O_3	1.52	0.47	1.15	1.11	1.37	0.92	0.26	1.36	1.32	1.68	1.35	1.24	1.60	1.35	1.32	1.36
Cr_2O_3	b.d.	b.d.	b.d.	b.d.	b.d.	b.d.	b.d.	b.d.	b.d.	b.d.	b.d.	b.d.	b.d.	b.d.	b.d.	b.d.
Fe_2O_3	2.34	2.02	2.80	2.45	3.04	2.06	1.71	2.77	2.34	2.72	2.77	2.56	3.18	3.06	2.85	2.73
FeO	4.86	3.76	4.30	4.55	4.14	4.62	3.35	3.73	4.89	5.33	4.86	4.35	5.10	4.88	4.86	4.91
MnO	0.65	0.35	0.68	0.57	0.62	0.60	0.41	0.60	0.59	0.60	0.70	0.62	0.64	0.71	0.59	0.63
MgO	14.74	15.15	15.24	15.16	14.98	15.18	16.20	15.62	14.91	14.67	14.74	15.07	14.67	14.96	14.90	14.90
CaO	22.16	23.99	22.17	22.09	22.41	22.01	23.60	22.46	22.22	21.84	22.30	22.66	21.84	21.95	22.11	21.87
Na_2O	0.44	0.28	0.40	0.40	0.41	0.43	0.22	0.43	0.44	0.42	0.45	0.41	0.46	0.41	0.43	0.47
TOTAL	98.78	98.82	98.94	98.45	98.91	98.09	99.17	99.66	99.07	99.18	99.46	99.42	99.40	99.44	99.21	99.00
FeO_T	6.97	5.58	6.82	6.75	6.88	6.47	4.89	6.22	7.00	7.78	7.35	6.65	7.96	7.63	7.42	7.37
Cation calculation based on 6 oxygens and Fe^{2+}/Fe^{3+} adjusted to 4 cations																
Si	1.942	1.970	1.945	1.950	1.936	1.960	1.977	1.938	1.947	1.930	1.941	1.946	1.927	1.935	1.940	1.943
Al^{IV}	0.058	0.021	0.051	0.049	0.060	0.040	0.011	0.059	0.053	0.070	0.059	0.054	0.070	0.059	0.058	0.057
Total	2.000	1.991	1.996	1.999	1.996	2.000	1.988	1.997	2.000	2.000	2.000	2.000	1.997	1.994	1.998	2.000
Ti^{4+}	0.007	0.001	0.004	0.005	0.006	0.006	0.001	0.009	0.007	0.010	0.006	0.005	0.009	0.007	0.006	0.006
Al^{VI}	0.009	0.000	0.000	0.000	0.000	0.001	0.000	0.000	0.005	0.004	0.000	0.000	0.000	0.000	0.000	0.003
Cr^{3+}	0.000	0.000	0.000	0.000	0.000	0.000	0.000	0.000	0.000	0.000	0.000	0.000	0.000	0.000	0.000	0.000
Fe^{3+}	0.066	0.057	0.079	0.069	0.086	0.058	0.048	0.077	0.066	0.077	0.078	0.072	0.089	0.086	0.080	0.077
Fe^{2+}	0.152	0.117	0.134	0.143	0.129	0.145	0.104	0.115	0.153	0.167	0.151	0.135	0.159	0.152	0.152	0.154
Mn	0.021	0.011	0.022	0.018	0.020	0.019	0.013	0.019	0.019	0.019	0.022	0.020	0.020	0.022	0.019	0.020
Mg	0.824	0.843	0.849	0.848	0.836	0.852	0.895	0.862	0.830	0.818	0.819	0.836	0.817	0.832	0.830	0.831
Ca	0.890	0.960	0.888	0.888	0.898	0.888	0.936	0.890	0.889	0.876	0.891	0.903	0.874	0.877	0.885	0.877
Na	0.032	0.020	0.029	0.029	0.030	0.031	0.016	0.031	0.032	0.030	0.033	0.030	0.033	0.030	0.031	0.034
MG #	84.43	87.81	86.37	85.57	86.63	85.46	89.59	88.23	84.44	83.05	84.43	86.10	83.71	84.55	84.52	84.37

Appendix C. Table C.1 (continued)

Sample	IM-265	IM-265	IM-265	IM-265	IM-265	IM-265	IM-265	IM-265	IM-265	IM-265	IM-265	IM-124	IM-124	IM-124	IM-124	IM-124
Grain	2	2	3	3	3	3	3	4	4	4	4	1	1	1	2	2
Position	i	r	r	i	i	c	r	r	i	i	r	i	c	r	r	i
SiO_2	51.24	52.21	51.96	52.00	51.92	51.93	51.69	52.20	51.87	53.33	51.80	53.15	52.79	53.59	52.92	53.46
TiO_2	0.28	0.23	0.19	0.19	0.21	0.24	0.17	0.18	0.19	0.19	0.19	0.15	0.20	0.12	0.14	0.09
Al_2O_3	1.56	1.36	1.29	1.36	1.35	1.36	1.36	1.23	1.44	0.69	1.35	0.62	0.84	0.35	0.78	0.48
Cr_2O_3	b.d.	b.d.	0.08	b.d.	b.d.	b.d.	0.06	b.d.	b.d.	b.d.	b.d.	b.d.	b.d.	b.d.	b.d.	b.d.
Fe_2O_3	3.31	2.43	2.33	2.34	2.86	2.64	2.87	1.79	2.24	2.14	2.58	2.23	2.34	1.41	2.70	1.77
FeO	5.21	5.53	5.32	5.19	4.76	4.92	4.57	5.68	5.17	2.44	4.88	2.87	3.31	3.29	2.70	3.40
MnO	0.68	0.59	0.65	0.64	0.66	0.62	0.49	0.70	0.63	0.49	0.65	0.29	0.45	0.27	0.29	0.37
MgO	14.68	14.80	14.95	14.67	14.85	14.86	15.16	15.04	14.79	16.55	14.84	15.71	15.43	15.57	15.52	15.52
CaO	21.35	21.91	21.56	22.06	22.14	22.03	21.75	21.44	21.80	23.46	21.98	23.82	23.22	24.71	23.74	24.07
Na_2O	0.46	0.45	0.45	0.46	0.44	0.45	0.44	0.42	0.46	0.32	0.43	0.44	0.50	0.27	0.51	0.38
TOTAL	98.77	99.51	98.78	98.91	99.19	99.05	98.56	98.68	98.59	99.61	98.7	99.28	99.08	99.58	99.3	99.54
FeO_T	8.19	7.72	7.42	7.30	7.33	7.30	7.15	7.29	7.19	4.37	7.20	4.88	5.42	4.56	5.13	4.99
Cation calculation based on 6 oxygens and Fe^{2+}/Fe^{3+} adjusted to 4 cations																
Si	1.927	1.946	1.948	1.948	1.940	1.942	1.939	1.957	1.948	1.961	1.944	1.967	1.961	1.979	1.959	1.976
Al^{IV}	0.069	0.054	0.052	0.052	0.059	0.058	0.060	0.043	0.052	0.030	0.056	0.027	0.037	0.015	0.034	0.021
Total	1.996	2.000	2.000	2.000	1.999	2.000	1.999	2.000	2.000	1.991	2.000	1.994	1.998	1.994	1.993	1.997
Ti^{4+}	0.008	0.006	0.005	0.005	0.006	0.007	0.005	0.005	0.005	0.005	0.005	0.004	0.006	0.003	0.004	0.003
Al^{VI}	0.000	0.006	0.005	0.008	0.000	0.002	0.000	0.011	0.012	0.000	0.004	0.000	0.000	0.000	0.000	0.000
Cr^{3+}	0.000	0.000	0.002	0.000	0.000	0.000	0.002	0.000	0.000	0.000	0.000	0.000	0.000	0.000	0.000	0.000
Fe^{3+}	0.094	0.068	0.066	0.066	0.080	0.074	0.081	0.050	0.063	0.059	0.073	0.062	0.065	0.039	0.075	0.049
Fe^{2+}	0.164	0.172	0.167	0.163	0.149	0.154	0.143	0.178	0.162	0.075	0.153	0.089	0.103	0.101	0.084	0.105
Mn	0.022	0.019	0.021	0.020	0.021	0.020	0.016	0.022	0.020	0.015	0.021	0.009	0.014	0.008	0.009	0.012
Mg	0.823	0.822	0.836	0.819	0.827	0.829	0.848	0.841	0.828	0.907	0.830	0.867	0.855	0.857	0.857	0.855
Ca	0.86	0.875	0.866	0.885	0.886	0.883	0.874	0.861	0.877	0.924	0.884	0.944	0.924	0.978	0.942	0.953
Na	0.034	0.033	0.033	0.033	0.032	0.033	0.032	0.031	0.033	0.023	0.031	0.032	0.036	0.019	0.037	0.027
MG #	83.38	82.70	83.35	83.40	84.73	84.33	85.57	82.53	83.64	92.36	84.44	90.69	89.25	89.46	91.07	89.06

Appendix C. Table C.1 (continued)

Sample	IM-124	IM-124	IM-124	IM-124	IM-124	IM-124	IM-124	IM-124	IM-124	IM-124	IM-124	IM-124	IM-124	IM-124	IM-124	IM-242
Grain	2	2	3	3	3	4	4	4	5	5	5	5	6	6	6	1
Position	c	i	i	c	r	i	c	r	r	c	i	i	r	c	i	r
SiO_2	53.54	52.92	53.32	52.36	53.18	53.21	53.08	53.12	52.87	52.74	53.50	53.27	53.68	53.57	52.85	52.30
TiO_2	0.00	0.17	0.12	0.26	0.18	0.04	0.06	0.20	0.15	0.18	b.d.	b.d.	0.08	0.05	0.22	0.27
Al_2O_3	0.60	0.70	0.62	1.05	0.75	0.74	0.54	0.69	0.76	0.87	0.46	0.44	0.41	0.39	0.83	1.02
Cr_2O_3	b.d.	b.d.	b.d.	b.d.	b.d.	b.d.	b.d.	b.d.	b.d.	b.d.	b.d.	b.d.	b.d.	b.d.	b.d.	b.d.
Fe_2O_3	1.72	2.50	1.70	2.94	1.96	1.88	1.86	2.12	2.58	2.23	1.84	2.24	1.90	1.69	2.34	2.99
FeO	2.11	2.88	3.26	4.18	3.08	2.22	3.60	3.11	3.12	2.58	2.92	2.91	2.96	3.14	4.00	3.70
MnO	0.00	0.35	0.28	0.32	0.33	0.10	0.26	0.35	0.31	0.35	0.33	0.35	0.29	0.33	0.25	0.50
MgO	16.30	15.62	15.62	14.99	15.66	15.82	15.22	15.69	15.26	15.68	15.88	15.68	15.80	15.76	15.03	15.38
CaO	24.59	23.47	23.86	22.50	23.60	24.77	23.86	23.62	23.83	23.50	24.02	23.90	24.29	24.12	23.25	22.68
Na_2O	0.30	0.50	0.42	0.61	0.48	0.31	0.43	0.44	0.48	0.49	0.36	0.41	0.38	0.36	0.56	0.46
TOTAL	99.16	99.11	99.20	99.21	99.22	99.09	98.91	99.34	99.36	98.62	99.31	99.20	99.79	99.41	99.33	99.30
FeO_T	3.66	5.13	4.79	6.83	4.84	3.91	5.27	5.02	5.44	4.59	4.58	4.93	4.67	4.66	6.11	6.39
Cation calculation based on 6 oxygens and Fe^{2+}/Fe^{3+} adjusted to 4 cations																
Si	1.973	1.963	1.974	1.950	1.968	1.967	1.976	1.965	1.960	1.962	1.977	1.974	1.976	1.979	1.963	1.945
Al^{IV}	0.026	0.031	0.026	0.046	0.032	0.032	0.024	0.030	0.033	0.038	0.020	0.019	0.018	0.017	0.036	0.045
Total	1.999	1.994	2.000	1.996	2.000	1.999	2.000	1.995	1.993	2.000	1.997	1.993	1.994	1.996	1.999	1.990
Ti^{4+}	0.000	0.005	0.003	0.007	0.005	0.001	0.002	0.006	0.004	0.005	0.000	0.000	0.002	0.001	0.006	0.008
Al^{VI}	0.000	0.000	0.001	0.000	0.001	0.000	0.000	0.000	0.000	0.000	0.000	0.000	0.000	0.000	0.000	0.000
Cr^{3+}	0.000	0.000	0.000	0.000	0.000	0.000	0.000	0.000	0.000	0.000	0.000	0.000	0.000	0.000	0.000	0.000
Fe^{3+}	0.048	0.070	0.047	0.082	0.055	0.052	0.052	0.059	0.072	0.062	0.051	0.062	0.053	0.047	0.066	0.084
Fe^{2+}	0.065	0.089	0.101	0.130	0.095	0.069	0.112	0.096	0.097	0.080	0.090	0.090	0.091	0.097	0.124	0.115
Mn	0.000	0.011	0.009	0.010	0.010	0.003	0.008	0.011	0.010	0.011	0.010	0.011	0.009	0.010	0.008	0.016
Mg	0.896	0.864	0.862	0.832	0.864	0.872	0.845	0.865	0.843	0.87	0.875	0.866	0.867	0.868	0.832	0.853
Ca	0.971	0.933	0.946	0.898	0.936	0.981	0.951	0.936	0.947	0.937	0.951	0.949	0.958	0.955	0.925	0.903
Na	0.021	0.036	0.030	0.044	0.034	0.022	0.031	0.032	0.035	0.035	0.026	0.029	0.027	0.026	0.040	0.033
MG #	93.24	90.66	89.51	86.49	90.09	92.67	88.30	90.01	89.68	91.58	90.67	90.59	90.50	89.95	87.03	88.12

Appendix C. Table C.1 (continued)

Sample	IM-242	IM-242	IM-242	IM-242	IM-242	IM-242	IM-242	IM-242	IM-242	IM-242	IM-242	IM-242	IM-242	IM-242	IM-242	IM-242
Grain	1	1	2	2	2	3	3	3	4	4	4	4	4	5	5	6
Position	i	c	r	c	i	r	i	i	i	r	r	c	i	i	i	i
SiO_2	48.94	51.18	49.59	50.98	50.57	50.94	53.05	50.46	51.57	50.67	50.71	52.13	51.75	52.05	50.59	50.61
TiO_2	0.35	0.30	0.26	0.22	0.43	0.25	0.08	0.14	0.24	0.24	0.28	0.07	0.26	0.11	0.17	0.31
Al_2O_3	1.53	1.98	0.97	1.06	2.37	1.05	0.62	0.76	0.94	1.03	1.28	0.52	1.16	0.60	0.92	1.21
Cr_2O_3	b.d.	b.d.	b.d.	b.d.	b.d.	b.d.	b.d.	b.d.	b.d.	b.d.	b.d.	b.d.	b.d.	b.d.	b.d.	b.d.
Fe_2O_3	6.46	4.20	6.16	4.39	3.55	4.65	2.01	5.69	3.49	5.37	4.31	4.13	3.36	4.06	4.29	4.61
FeO	1.36	2.58	1.12	2.61	3.36	2.70	3.81	0.54	3.96	2.27	2.32	1.36	2.65	1.22	3.27	2.75
MnO	0.42	0.38	0.43	0.41	0.35	0.48	0.42	0.40	0.60	0.35	0.37	0.30	0.30	0.27	0.58	0.43
MgO	14.45	15.13	14.98	15.04	14.78	14.94	15.63	15.38	14.67	14.67	14.88	15.32	15.20	15.88	14.48	14.60
CaO	22.57	22.79	22.77	22.88	22.40	22.52	22.99	23.42	22.65	22.93	22.97	23.69	23.46	23.87	22.43	22.58
Na_2O	0.52	0.51	0.46	0.44	0.46	0.54	0.43	0.46	0.47	0.58	0.49	0.67	0.44	0.43	0.49	0.58
TOTAL	96.60	99.05	96.74	98.03	98.27	98.07	99.04	97.25	98.59	98.11	97.61	98.19	98.58	98.49	97.22	97.68
FeO_T	7.17	6.36	6.66	6.56	6.55	6.88	5.62	5.66	7.10	7.10	6.20	5.08	5.67	4.87	7.13	6.90
Cation calculation based on 6 oxygens and Fe^{2+}/Fe^{3+} adjusted to 4 cations																
Si	1.881	1.907	1.899	1.924	1.902	1.923	1.971	1.914	1.940	1.915	1.920	1.952	1.935	1.942	1.931	1.919
Al^{IV}	0.069	0.087	0.044	0.047	0.098	0.047	0.027	0.034	0.042	0.046	0.057	0.023	0.051	0.026	0.041	0.054
Total	1.950	1.994	1.943	1.971	2.000	1.970	1.998	1.948	1.982	1.961	1.977	1.975	1.986	1.968	1.972	1.973
Ti^{4+}	0.010	0.008	0.007	0.006	0.012	0.007	0.002	0.004	0.007	0.007	0.008	0.002	0.007	0.003	0.005	0.009
Al^{VI}	0.000	0.000	0.000	0.000	0.007	0.000	0.000	0.000	0.000	0.000	0.000	0.000	0.000	0.000	0.000	0.000
Cr^{3+}	0.000	0.000	0.000	0.000	0.000	0.000	0.000	0.000	0.000	0.000	0.000	0.000	0.000	0.000	0.000	0.000
Fe^{3+}	0.187	0.118	0.177	0.125	0.100	0.132	0.056	0.162	0.099	0.153	0.123	0.116	0.095	0.114	0.123	0.132
Fe^{2+}	0.044	0.081	0.036	0.082	0.106	0.085	0.118	0.017	0.125	0.072	0.074	0.043	0.083	0.038	0.104	0.087
Mn	0.014	0.012	0.014	0.013	0.011	0.015	0.013	0.013	0.019	0.011	0.012	0.01	0.01	0.009	0.019	0.014
Mg	0.828	0.841	0.855	0.846	0.829	0.841	0.866	0.870	0.823	0.827	0.840	0.855	0.848	0.883	0.824	0.825
Ca	0.929	0.910	0.934	0.925	0.902	0.911	0.915	0.952	0.913	0.928	0.932	0.951	0.940	0.954	0.917	0.917
Na	0.039	0.037	0.034	0.032	0.034	0.040	0.031	0.034	0.034	0.042	0.036	0.049	0.032	0.031	0.036	0.043
MG #	94.95	91.21	95.96	91.16	88.66	90.82	88.01	98.08	86.81	91.99	91.90	95.21	91.08	95.87	88.79	90.46

Appendix C. Table C.1 (continued)

Sample	IM-242	IM-242	IM-242	IM-242	IM-242	IM-242	IM-242	IM-242	IM-242	IM-242	IM-242	IM-242
Grain	6	6	7	7	7	8	8	9	9	10	10	10
Position	c	r	r	c	i	c	r	i	r	r	c	i
SiO_2	51.72	51.33	51.94	52.98	52.20	50.22	49.18	51.06	51.26	51.67	52.37	51.66
TiO_2	0.19	0.31	0.08	0.14	0.09	0.42	0.54	0.37	0.39	0.12	0.09	0.11
Al_2O_3	0.82	1.27	0.50	0.81	0.57	2.22	2.93	2.24	1.96	0.58	0.41	0.71
Cr_2O_3	b.d.	b.d.	b.d.	b.d.	b.d.	b.d.	b.d.	b.d.	b.d.	b.d.	0.05	b.d.
Fe_2O_3	3.59	3.48	3.73	1.76	2.80	4.59	5.21	3.53	3.00	4.25	2.67	3.69
FeO	2.55	4.07	0.95	3.77	2.61	2.19	2.04	3.18	3.46	1.97	2.72	2.29
MnO	0.41	0.43	0.24	0.28	0.42	0.34	0.26	0.34	0.38	0.42	0.31	0.34
MgO	15.32	14.38	16.14	15.31	15.82	15.41	14.97	15.46	15.25	15.42	15.64	15.27
CaO	23.14	22.49	23.94	23.26	22.98	22.29	22.16	22.27	22.44	23.42	23.39	23.32
Na_2O	0.46	0.59	0.34	0.51	0.40	0.41	0.42	0.39	0.41	0.44	0.40	0.47
TOTAL	98.20	98.35	97.86	98.82	97.89	98.09	97.71	98.84	98.55	98.29	98.05	97.86
FeO_T	5.78	7.2	4.31	5.35	5.13	6.32	6.73	6.36	6.16	5.79	5.12	5.61
Cation calculation based on 6 oxygens and Fe^{2+}/Fe^{3+} adjusted to 4 cations												
Si	1.942	1.935	1.946	1.972	1.960	1.889	1.860	1.905	1.918	1.939	1.964	1.946
Al^{IV}	0.036	0.056	0.022	0.028	0.025	0.098	0.131	0.095	0.082	0.026	0.018	0.032
Total	1.978	1.991	1.968	2.000	1.985	1.987	1.991	2.000	2.000	1.965	1.982	1.978
Ti^{4+}	0.005	0.009	0.002	0.004	0.003	0.012	0.015	0.010	0.011	0.003	0.003	0.003
Al^{VI}	0.000	0.000	0.000	0.008	0.000	0.000	0.000	0.003	0.004	0.000	0.000	0.000
Cr^{3+}	0.000	0.000	0.000	0.000	0.000	0.000	0.000	0.000	0.000	0.000	0.001	0.000
Fe^{3+}	0.102	0.099	0.105	0.049	0.079	0.130	0.148	0.099	0.084	0.120	0.075	0.105
Fe^{2+}	0.080	0.128	0.030	0.117	0.082	0.069	0.065	0.099	0.108	0.062	0.085	0.072
Mn	0.013	0.014	0.008	0.009	0.013	0.011	0.008	0.011	0.012	0.013	0.010	0.011
Mg	0.858	0.808	0.902	0.849	0.885	0.864	0.844	0.860	0.851	0.863	0.875	0.857
Ca	0.931	0.908	0.961	0.927	0.924	0.898	0.898	0.890	0.900	0.942	0.940	0.941
Na	0.033	0.043	0.025	0.037	0.029	0.03	0.031	0.028	0.03	0.032	0.029	0.034
MG #	91.47	86.32	96.78	87.89	91.52	92.60	92.85	89.68	88.74	93.30	91.15	92.25

Appendix C. Table C.2 Electron Microprobe analyses of clinopyroxene from the Cherry Creek unit.

Sample	IM-237	IM-237	IM-237	IM-237	IM-237	IM-237	IM-237	IM-237	IM-237	IM-237	IM-237	IM-237	IM-237	IM-237	IM-237	IM-237
Grain	1	1	1	2	2	3	4	4	4	5	5	5	6	6	6	6
Position	r	c	i	r	r	c	i	c	r	i	c	r	i	c	i	r
SiO_2	52.72	52.36	52.59	51.14	52.78	52.93	52.62	52.36	51.94	52.65	52.67	52.54	52.49	51.88	52.41	52.13
TiO_2	0.17	0.23	0.15	0.34	0.17	0.16	0.22	0.15	0.22	0.24	0.20	0.14	0.20	0.20	0.19	0.16
Al_2O_3	0.83	1.16	0.81	1.71	0.88	0.64	0.88	1.26	0.94	0.98	0.89	0.82	0.91	0.94	1.03	0.98
Cr_2O_3	b.d.	b.d.	b.d.	b.d.	b.d.	b.d.	b.d.	b.d.	b.d.	b.d.	b.d.	b.d.	b.d.	b.d.	b.d.	b.d.
Fe_2O_3	1.86	2.20	1.89	3.16	1.63	1.45	1.62	1.87	2.98	1.85	1.47	2.11	1.65	3.15	1.96	2.31
FeO	5.15	5.11	5.16	4.28	5.22	5.73	5.30	4.93	4.45	5.18	5.39	5.08	5.22	3.99	5.11	4.73
MnO	0.76	0.84	0.78	0.80	0.76	0.87	0.76	0.61	0.82	0.76	0.88	0.92	0.72	0.80	0.81	0.79
MgO	14.82	14.69	14.62	14.37	14.95	14.87	14.87	14.82	14.84	14.89	14.84	14.66	15.02	14.92	14.70	14.76
CaO	22.70	22.23	22.75	22.44	22.41	22.24	22.42	22.57	22.26	22.42	22.47	22.48	22.39	22.64	22.44	22.42
Na_2O	0.39	0.48	0.41	0.44	0.42	0.40	0.40	0.41	0.45	0.43	0.36	0.44	0.34	0.40	0.43	0.42
TOTAL	99.40	99.30	99.16	98.68	99.22	99.29	99.09	98.98	98.90	99.40	99.17	99.19	98.94	98.92	99.08	98.70
FeO_T	6.82	7.09	6.86	7.12	6.69	7.03	6.76	6.61	7.13	6.84	6.71	6.98	6.70	6.82	6.87	6.81
Cation calculation based on 6 oxygens and Fe^{2+}/Fe^{3+} adjusted to 4 cations																
Si	1.965	1.954	1.966	1.923	1.968	1.975	1.966	1.956	1.947	1.961	1.967	1.964	1.963	1.943	1.960	1.956
Al^{IV}	0.035	0.046	0.034	0.076	0.032	0.025	0.034	0.044	0.042	0.039	0.033	0.036	0.037	0.041	0.040	0.043
Total	2.000	2.000	2.000	1.999	2.000	2.000	2.000	2.000	1.989	2.000	2.000	2.000	2.000	1.984	2.000	1.999
Ti^{4+}	0.005	0.006	0.004	0.010	0.005	0.004	0.006	0.004	0.006	0.007	0.006	0.004	0.006	0.006	0.005	0.005
Al^{VI}	0.001	0.005	0.002	0.000	0.007	0.003	0.005	0.011	0.000	0.004	0.006	0.000	0.003	0.000	0.005	0.000
Cr^{3+}	0.000	0.000	0.000	0.000	0.000	0.000	0.000	0.000	0.000	0.000	0.000	0.000	0.000	0.000	0.000	0.000
Fe^{3+}	0.052	0.062	0.053	0.089	0.046	0.041	0.046	0.053	0.084	0.052	0.041	0.059	0.046	0.089	0.055	0.065
Fe^{2+}	0.160	0.159	0.161	0.135	0.163	0.179	0.166	0.154	0.139	0.161	0.168	0.159	0.163	0.125	0.160	0.148
Mn	0.024	0.027	0.025	0.025	0.024	0.027	0.024	0.019	0.026	0.024	0.028	0.029	0.023	0.025	0.026	0.025
Mg	0.823	0.817	0.815	0.806	0.831	0.827	0.828	0.826	0.829	0.827	0.826	0.817	0.837	0.833	0.819	0.826
Ca	0.906	0.889	0.911	0.904	0.895	0.889	0.897	0.903	0.894	0.895	0.899	0.900	0.897	0.909	0.899	0.901
Na	0.028	0.035	0.030	0.032	0.030	0.029	0.029	0.030	0.033	0.031	0.026	0.032	0.025	0.029	0.031	0.031
MG #	83.72	83.71	83.50	85.65	83.60	82.21	83.30	84.29	85.64	83.70	83.10	83.71	83.70	86.95	83.66	84.80

MG# = 100•Mg/(Mg + Fe^{2+}) c=core; r=rim; i=interior

Appendix C. Table C.2 (continued)

Sample	IM-237	IM-237	IM-237	IM-237	IM-237	IM-237	IM-237	IM-237	IM-237	IM-237	IM-237	IM-237	IM-237	IM-171	IM-171	IM-171
Grain	7	7	8	8	8	9	9	9	10	10	11	11	11	1	1	1
Position	c	c	r	r	i	r	c	i	i	c	i	c	r	r	i	c
SiO_2	52.58	52.72	52.94	52.20	52.62	52.22	53.08	52.21	50.76	51.76	52.49	53.04	52.49	52.74	52.97	52.26
TiO_2	0.23	0.23	0.20	0.20	0.20	0.17	0.20	0.20	0.39	0.25	0.18	0.20	0.20	0.12	0.11	0.17
Al_2O_3	0.95	0.99	0.89	1.02	0.94	0.89	0.81	0.89	2.33	1.49	0.84	0.92	1.03	0.55	0.53	0.88
Cr_2O_3	b.d.	b.d.	b.d.	b.d.	b.d.	b.d.	b.d.	b.d.	b.d.	b.d.	b.d.	b.d.	b.d.	b.d.	b.d.	b.d.
Fe_2O_3	1.57	1.91	1.31	2.28	2.02	2.52	0.98	2.45	2.82	2.58	1.91	1.40	1.71	1.15	1.77	2.08
FeO	5.26	5.39	5.56	4.81	4.84	4.45	5.67	4.53	4.28	4.24	4.94	5.77	5.39	5.52	5.06	5.76
MnO	0.82	0.83	0.75	0.83	0.75	0.79	0.79	0.75	0.59	0.62	0.82	0.81	0.76	0.77	0.81	0.62
MgO	14.89	14.78	14.92	14.85	14.96	14.89	14.99	14.97	14.27	14.76	14.85	14.90	14.68	14.89	15.01	14.21
CaO	22.31	22.48	22.51	22.44	22.68	22.62	22.43	22.60	22.53	22.73	22.57	22.49	22.48	22.65	23.02	22.61
Na_2O	0.41	0.41	0.38	0.38	0.39	0.40	0.38	0.37	0.41	0.40	0.39	0.36	0.40	0.29	0.29	0.43
TOTAL	99.02	99.74	99.46	99.01	99.40	98.95	99.33	98.97	98.38	98.83	98.99	99.89	99.14	98.68	99.57	99.02
FeO_T	6.67	7.11	6.74	6.86	6.66	6.72	6.55	6.73	6.82	6.56	6.66	7.03	6.93	6.55	6.65	7.63
Cation calculation based on 6 oxygens and Fe^{2+}/Fe^{3+} adjusted to 4 cations																
Si	1.965	1.960	1.970	1.953	1.959	1.954	1.976	1.953	1.912	1.938	1.963	1.967	1.962	1.978	1.971	1.962
Al^{IV}	0.035	0.040	0.030	0.045	0.041	0.039	0.024	0.039	0.088	0.062	0.037	0.033	0.038	0.022	0.023	0.038
Total	2.000	2.000	2.000	1.998	2.000	1.993	2.000	1.992	2.000	2.000	2.000	2.000	2.000	2.000	1.994	2.000
Ti^{4+}	0.006	0.006	0.006	0.006	0.006	0.005	0.006	0.006	0.011	0.007	0.005	0.006	0.006	0.003	0.003	0.005
Al^{VI}	0.007	0.003	0.009	0.000	0.000	0.000	0.012	0.000	0.015	0.004	0.000	0.007	0.007	0.002	0.000	0.001
Cr^{3+}	0.000	0.000	0.000	0.000	0.000	0.000	0.000	0.000	0.000	0.000	0.000	0.000	0.000	0.000	0.000	0.000
Fe^{3+}	0.044	0.053	0.037	0.064	0.057	0.071	0.028	0.069	0.080	0.073	0.054	0.039	0.048	0.033	0.049	0.059
Fe^{2+}	0.164	0.168	0.173	0.150	0.151	0.139	0.176	0.142	0.135	0.133	0.154	0.179	0.168	0.173	0.157	0.181
Mn	0.026	0.026	0.024	0.026	0.024	0.025	0.025	0.024	0.019	0.020	0.026	0.025	0.024	0.024	0.026	0.020
Mg	0.830	0.819	0.828	0.828	0.830	0.831	0.832	0.835	0.801	0.824	0.828	0.824	0.818	0.833	0.833	0.795
Ca	0.893	0.895	0.897	0.900	0.905	0.907	0.895	0.906	0.909	0.912	0.904	0.894	0.900	0.910	0.918	0.909
Na	0.030	0.030	0.027	0.028	0.028	0.029	0.027	0.027	0.030	0.029	0.028	0.026	0.029	0.021	0.021	0.031
MG #	83.50	82.98	82.72	84.66	84.61	85.67	82.54	85.47	85.58	86.10	84.32	82.15	82.96	82.80	84.14	81.45

Appendix C. Table C.2 (continued)

Sample	IM-171	IM-171	IM-171	IM-171	IM-171	IM-171	IM-171	IM-171	IM-171	IM-171	IM-171	IM-171	IM-171	IM-171	IM-171	IM-171
Grain	1	1	2	2	2	2	3	3	3	3	3	4	4	5	5	6
Position	i	r	i	c	i	r	i	i	c	i	r	i	c	i	i	i
SiO_2	52.51	52.56	51.66	51.65	51.65	51.68	51.00	52.00	52.07	52.89	52.38	52.40	52.57	51.68	52.14	52.87
TiO_2	0.26	0.12	0.30	0.25	0.22	0.28	0.14	0.21	0.10	0.09	0.18	0.13	0.16	0.28	0.17	0.08
Al_2O_3	0.92	0.64	1.39	1.16	1.14	1.26	1.36	0.79	0.50	0.38	0.81	0.66	0.60	1.26	0.82	0.41
Cr_2O_3	b.d.	b.d.	b.d.	b.d.	b.d.	b.d.	b.d.	b.d.	b.d.	b.d.	b.d.	b.d.	b.d.	b.d.	b.d.	b.d.
Fe_2O_3	1.60	1.52	2.19	2.65	2.02	2.96	2.92	2.55	2.54	1.59	2.38	2.24	2.27	2.72	2.89	1.49
FeO	5.98	5.02	4.99	4.84	5.33	4.88	6.23	5.37	5.11	4.88	5.05	5.35	5.00	4.97	5.08	5.64
MnO	0.67	0.62	0.57	0.56	0.62	0.57	0.68	0.70	0.78	0.77	0.58	0.62	0.73	0.65	0.64	0.77
MgO	14.23	14.60	14.70	14.50	14.47	14.72	14.70	14.18	14.45	15.02	14.67	14.39	14.75	14.48	14.14	14.82
CaO	22.74	23.25	22.32	22.64	22.41	22.45	20.28	22.86	22.57	22.91	22.78	22.89	22.79	22.47	23.15	22.68
Na_2O	0.41	0.33	0.37	0.38	0.33	0.35	0.44	0.38	0.39	0.34	0.40	0.40	0.39	0.40	0.42	0.31
TOTAL	99.32	98.66	98.49	98.63	98.19	99.15	97.75	99.04	98.51	98.87	99.23	99.08	99.26	98.91	99.45	99.07
FeO_T	7.42	6.39	6.96	7.22	7.15	7.54	8.86	7.66	7.40	6.31	7.19	7.37	7.04	7.42	7.68	6.98
Cation calculation based on 6 oxygens and Fe^{2+}/Fe^{3+} adjusted to 4 cations																
Si	1.964	1.973	1.943	1.943	1.951	1.935	1.940	1.954	1.964	1.979	1.958	1.964	1.964	1.940	1.951	1.979
Al^{IV}	0.036	0.027	0.057	0.051	0.049	0.056	0.060	0.035	0.022	0.017	0.036	0.029	0.026	0.056	0.036	0.018
Total	2.000	2.000	2.000	1.994	2.000	1.991	2.000	1.989	1.986	1.996	1.994	1.993	1.990	1.996	1.987	1.997
Ti^{4+}	0.007	0.003	0.008	0.007	0.006	0.008	0.004	0.006	0.003	0.003	0.005	0.004	0.004	0.008	0.005	0.002
Al^{VI}	0.005	0.001	0.005	0.000	0.002	0.000	0.001	0.000	0.000	0.000	0.000	0.000	0.000	0.000	0.000	0.000
Cr^{3+}	0.000	0.000	0.000	0.000	0.000	0.000	0.000	0.000	0.000	0.000	0.000	0.000	0.000	0.000	0.000	0.000
Fe^{3+}	0.045	0.043	0.062	0.075	0.057	0.083	0.084	0.072	0.072	0.045	0.067	0.063	0.064	0.077	0.081	0.042
Fe^{2+}	0.187	0.158	0.157	0.152	0.168	0.153	0.198	0.169	0.161	0.153	0.158	0.168	0.156	0.156	0.159	0.176
Mn	0.021	0.020	0.018	0.018	0.020	0.018	0.022	0.022	0.025	0.024	0.018	0.020	0.023	0.021	0.020	0.024
Mg	0.794	0.817	0.824	0.813	0.815	0.822	0.833	0.794	0.813	0.838	0.817	0.804	0.822	0.810	0.789	0.827
Ca	0.911	0.935	0.899	0.913	0.907	0.901	0.826	0.920	0.912	0.918	0.912	0.919	0.912	0.904	0.928	0.909
Na	0.030	0.024	0.027	0.028	0.024	0.025	0.032	0.028	0.029	0.025	0.029	0.029	0.028	0.029	0.030	0.022
MG #	80.94	83.79	84.00	84.25	82.91	84.31	80.80	82.45	83.47	84.56	83.79	82.72	84.05	83.85	83.23	82.45

Appendix C. Table C.2 (continued)

Sample	IM-171	IM-171	IM-171	IM-171	IM-171	IM-171	IM-171	IM-303	IM-303	IM-303	IM-303	IM-303	IM-303	IM-303	IM-303	IM-303
Grain	6	6	7	7	7	8	8	1	1	1	1	2	2	2	3	3
Position	r	r	r	i	r	i	c	r	i	c	r	r	c	r	i	i
SiO_2	51.70	51.80	52.02	52.10	52.67	52.78	52.58	51.56	52.74	52.94	52.10	52.31	53.25	53.39	52.91	52.83
TiO_2	0.23	0.20	0.13	0.18	0.16	0.10	0.14	0.16	0.18	0.05	0.17	b.d.	0.02	0.08	0.13	0.12
Al_2O_3	0.98	0.87	0.63	0.84	0.70	0.73	0.65	0.89	0.97	0.60	0.79	0.20	0.22	0.46	0.70	0.60
Cr_2O_3	b.d.	b.d.	b.d.	b.d.	b.d.	b.d.	b.d.	b.d.	b.d.	b.d.	b.d.	b.d.	b.d.	b.d.	b.d.	b.d.
Fe_2O_3	3.24	3.36	2.81	2.18	1.62	2.08	2.46	2.54	1.52	1.94	1.83	2.30	1.24	0.86	0.69	1.23
FeO	4.73	4.84	4.83	5.59	5.87	5.29	5.16	5.21	6.14	4.74	5.69	4.07	4.33	5.38	6.16	5.34
MnO	0.63	0.62	0.75	0.69	0.72	0.68	0.74	0.93	0.89	0.87	0.87	0.40	0.29	0.55	0.75	0.73
MgO	14.34	14.11	15.17	14.16	14.35	14.59	14.61	14.31	14.69	14.64	14.19	14.73	15.38	14.92	14.65	14.62
CaO	22.78	23.06	22.04	22.65	22.73	23.05	22.85	22.10	21.92	23.20	22.38	23.88	23.65	23.47	22.41	23.10
Na_2O	0.42	0.43	0.32	0.42	0.40	0.37	0.39	0.40	0.42	0.42	0.42	0.27	0.30	0.29	0.36	0.34
TOTAL	99.05	99.29	98.70	98.81	99.22	99.67	99.58	98.10	99.47	99.40	98.44	98.16	98.68	99.40	98.76	98.91
FeO_T	7.65	7.86	7.36	7.55	7.33	7.16	7.37	7.50	7.51	6.49	7.34	6.14	5.45	6.15	6.78	6.45
Cation calculation based on 6 oxygens and Fe^{2+}/Fe^{3+} adjusted to 4 cations																
Si	1.941	1.943	1.954	1.960	1.971	1.965	1.961	1.954	1.967	1.973	1.967	1.972	1.988	1.986	1.984	1.978
Al^{IV}	0.043	0.038	0.028	0.037	0.029	0.032	0.029	0.040	0.033	0.026	0.033	0.009	0.010	0.014	0.016	0.022
Total	1.984	1.981	1.982	1.997	2.000	1.997	1.990	1.994	2.000	1.999	2.000	1.981	1.998	2.000	2.000	2.000
Ti^{4+}	0.006	0.006	0.004	0.005	0.005	0.003	0.004	0.005	0.005	0.001	0.005	0.000	0.001	0.002	0.004	0.003
Al^{VI}	0.000	0.000	0.000	0.000	0.002	0.000	0.000	0.000	0.010	0.000	0.002	0.000	0.000	0.006	0.015	0.004
Cr^{3+}	0.000	0.000	0.000	0.000	0.000	0.000	0.000	0.000	0.000	0.000	0.000	0.000	0.000	0.000	0.000	0.000
Fe^{3+}	0.091	0.095	0.079	0.062	0.046	0.058	0.069	0.073	0.043	0.054	0.052	0.065	0.035	0.024	0.019	0.035
Fe^{2+}	0.148	0.152	0.152	0.176	0.184	0.165	0.161	0.165	0.192	0.148	0.180	0.128	0.135	0.167	0.193	0.167
Mn	0.020	0.020	0.024	0.022	0.023	0.021	0.023	0.030	0.028	0.027	0.028	0.013	0.009	0.017	0.024	0.023
Mg	0.803	0.789	0.850	0.794	0.801	0.810	0.812	0.808	0.817	0.813	0.799	0.828	0.856	0.827	0.819	0.816
Ca	0.916	0.927	0.887	0.913	0.912	0.919	0.913	0.897	0.876	0.926	0.905	0.965	0.946	0.935	0.900	0.927
Na	0.031	0.031	0.023	0.031	0.029	0.027	0.028	0.029	0.030	0.030	0.031	0.020	0.022	0.021	0.026	0.025
MG #	84.44	83.85	84.83	81.86	81.32	83.08	83.45	83.04	80.97	84.60	81.61	86.61	86.38	83.20	80.93	83.01

Appendix C. Table C.2 (continued)

Sample	IM-303	IM-303	IM-303	IM-303	IM-303	IM-303	IM-303	IM-303	IM-303	IM-27G	IM-27G	IM-27G	IM-27G	IM-27G	IM-27G	IM-27G
Grain	4	4	4	4	5	5	5	6	6	1	1	1	2	3	4	4
Position	r	c	r	i	r	c	i	i	i	r	c	r	c	Gm-c	c	i
SiO_2	51.34	50.88	49.34	52.18	51.23	51.55	51.84	52.72	52.72	52.56	52.50	52.53	52.32	52.34	52.66	51.96
TiO_2	0.19	0.47	0.44	0.17	0.14	0.27	0.23	0.11	0.06	0.20	0.15	0.15	0.18	0.20	0.00	0.18
Al_2O_3	0.99	2.38	2.15	1.08	0.59	1.18	1.04	0.58	0.43	0.77	0.75	0.78	0.85	0.84	0.35	0.96
Cr_2O_3	b.d.	b.d.	b.d.	b.d.	b.d.	b.d.	b.d.	b.d.	b.d.	b.d.	b.d.	b.d.	b.d.	b.d.	b.d.	b.d.
Fe_2O_3	3.32	3.14	5.21	2.15	3.13	2.89	2.33	1.83	1.64	1.67	1.39	1.13	2.37	1.74	1.50	2.75
FeO	4.30	4.16	2.04	5.11	4.24	4.68	5.50	5.71	4.34	5.79	5.61	5.94	5.13	5.66	4.80	4.67
MnO	0.89	0.41	0.45	0.74	0.93	0.85	1.04	0.78	0.77	1.05	0.91	0.86	0.84	0.83	0.42	0.92
MgO	14.92	15.10	15.05	14.85	14.28	14.77	14.36	14.28	15.30	14.48	14.58	14.46	14.53	14.40	14.50	14.52
CaO	21.88	21.85	22.12	22.09	22.58	21.90	21.92	22.92	22.87	22.06	22.30	22.28	22.44	22.17	24.20	22.34
Na_2O	0.38	0.39	0.38	0.42	0.40	0.43	0.43	0.40	0.31	0.46	0.40	0.40	0.46	0.48	0.20	0.48
TOTAL	98.21	98.78	97.18	98.79	97.52	98.52	98.69	99.33	98.44	99.04	98.59	98.53	99.12	98.66	98.63	98.78
FeO_T	7.29	6.99	6.73	7.04	7.06	7.28	7.60	7.36	5.82	7.29	6.86	6.96	7.26	7.23	6.15	7.14
Cation calculation based on 6 oxygens and Fe^{2+}/Fe^{3+} adjusted to 4 cations																
Si	1.939	1.904	1.878	1.956	1.952	1.941	1.953	1.972	1.977	1.970	1.974	1.977	1.959	1.968	1.978	1.952
Al^{IV}	0.044	0.096	0.096	0.044	0.026	0.052	0.046	0.026	0.019	0.030	0.026	0.023	0.038	0.032	0.015	0.042
Total	1.983	2.000	1.974	2.000	1.978	1.993	1.999	1.998	1.996	2.000	2.000	2.000	1.997	2.000	1.993	1.994
Ti^{4+}	0.005	0.013	0.013	0.005	0.004	0.008	0.007	0.003	0.002	0.006	0.004	0.004	0.005	0.006	0.000	0.005
Al^{VI}	0.000	0.009	0.000	0.004	0.000	0.000	0.000	0.000	0.000	0.004	0.007	0.012	0.000	0.005	0.000	0.000
Cr^{3+}	0.000	0.000	0.000	0.000	0.000	0.000	0.000	0.000	0.000	0.000	0.000	0.000	0.000	0.000	0.000	0.000
Fe^{3+}	0.094	0.088	0.149	0.061	0.090	0.082	0.066	0.052	0.046	0.047	0.039	0.032	0.067	0.049	0.042	0.078
Fe^{2+}	0.136	0.130	0.065	0.160	0.135	0.147	0.173	0.179	0.136	0.182	0.176	0.187	0.160	0.178	0.151	0.147
Mn	0.028	0.013	0.015	0.023	0.030	0.027	0.033	0.025	0.024	0.033	0.029	0.027	0.027	0.026	0.013	0.029
Mg	0.840	0.842	0.854	0.830	0.811	0.829	0.806	0.797	0.855	0.809	0.817	0.811	0.811	0.807	0.812	0.813
Ca	0.885	0.876	0.902	0.887	0.922	0.883	0.885	0.919	0.919	0.886	0.898	0.898	0.900	0.893	0.974	0.899
Na	0.028	0.028	0.028	0.031	0.030	0.031	0.031	0.029	0.023	0.033	0.029	0.029	0.033	0.035	0.015	0.035
MG #	86.07	86.63	92.93	83.84	85.73	84.94	82.33	81.66	86.28	81.63	82.28	81.26	83.52	81.93	84.32	84.69

Appendix C. Table C.2 (continued)

Sample	IM-27G	IM-27G	IM-27G	IM-27G	IM-27G	IM-27G	IM-27G	IM-27G	IM-27G	IM-27G	IM-27G	IM-27G	IM-27G	IM-253	IM-253	IM-253
Grain	5	5	5	6	6	6	7	7	8	8	8	8	8	1	1	1
Position	r	c	i	i	c	i	i	i	r	i	c	i	r	i	c	r
SiO_2	52.16	48.27	52.03	52.26	51.72	52.17	52.43	52.27	50.98	52.25	52.39	52.24	51.61	51.64	51.46	51.76
TiO_2	0.34	0.41	0.22	0.16	0.26	0.20	0.20	0.22	0.34	0.15	0.21	0.17	0.26	0.30	0.26	0.30
Al_2O_3	1.74	3.47	0.88	0.86	1.32	0.87	0.83	0.80	2.10	0.84	0.85	0.97	1.63	1.41	1.07	1.02
Cr_2O_3	b.d.	b.d.	b.d.	b.d.	b.d.	b.d.	b.d.	b.d.	b.d.	b.d.	b.d.	b.d.	b.d.	b.d.	b.d.	b.d.
Fe_2O_3	1.09	4.70	2.22	2.41	2.88	2.44	1.65	2.20	2.81	1.89	2.05	1.94	2.56	2.41	2.89	2.50
FeO	6.18	4.66	5.12	4.97	4.73	5.06	5.97	5.19	4.71	5.19	5.34	5.08	4.69	5.00	4.77	4.81
MnO	0.82	0.89	0.85	0.92	0.69	0.97	1.09	0.96	0.64	0.79	0.89	0.58	0.87	0.80	0.92	0.89
MgO	14.34	15.15	14.39	14.51	14.81	14.47	14.51	14.44	14.33	14.50	14.56	14.73	14.40	13.87	14.01	14.14
CaO	21.93	18.50	22.32	22.49	22.12	22.42	21.91	22.11	22.17	22.35	22.28	22.36	22.33	22.54	22.34	22.46
Na_2O	0.44	0.40	0.48	0.45	0.42	0.44	0.41	0.54	0.43	0.47	0.46	0.45	0.46	0.57	0.54	0.54
TOTAL	99.04	96.45	98.51	99.03	98.95	99.04	99.00	98.73	98.51	98.43	99.03	98.52	98.81	98.54	98.26	98.42
FeO_T	7.16	8.89	7.12	7.14	7.32	7.26	7.45	7.17	7.24	6.89	7.18	6.83	6.99	7.17	7.37	7.06
Cation calculation based on 6 oxygens and Fe^{2+}/Fe^{3+} adjusted to 4 cations																
Si	1.952	1.856	1.960	1.959	1.938	1.956	1.967	1.964	1.919	1.967	1.963	1.962	1.937	1.946	1.947	1.953
Al^{IV}	0.048	0.144	0.039	0.038	0.058	0.038	0.033	0.035	0.081	0.033	0.037	0.038	0.063	0.054	0.048	0.045
Total	2.000	2.000	1.999	1.997	1.996	1.994	2.000	1.999	2.000	2.000	2.000	2.000	2.000	2.000	1.995	1.998
Ti^{4+}	0.010	0.012	0.006	0.005	0.007	0.006	0.006	0.006	0.010	0.004	0.006	0.005	0.007	0.009	0.007	0.009
Al^{VI}	0.029	0.013	0.000	0.000	0.000	0.000	0.004	0.000	0.012	0.004	0.001	0.005	0.009	0.009	0.000	0.000
Cr^{3+}	0.000	0.000	0.000	0.000	0.000	0.000	0.000	0.000	0.000	0.000	0.000	0.000	0.000	0.000	0.000	0.000
Fe^{3+}	0.031	0.136	0.063	0.068	0.081	0.069	0.047	0.062	0.080	0.054	0.058	0.055	0.072	0.068	0.082	0.071
Fe^{2+}	0.193	0.150	0.161	0.156	0.148	0.159	0.187	0.163	0.148	0.163	0.167	0.159	0.147	0.158	0.151	0.152
Mn	0.026	0.029	0.027	0.029	0.022	0.031	0.035	0.031	0.020	0.025	0.028	0.018	0.028	0.026	0.029	0.028
Mg	0.800	0.868	0.808	0.811	0.827	0.809	0.812	0.809	0.804	0.814	0.813	0.825	0.806	0.779	0.790	0.795
Ca	0.879	0.762	0.901	0.903	0.888	0.901	0.881	0.890	0.894	0.901	0.894	0.900	0.898	0.910	0.906	0.908
Na	0.032	0.030	0.035	0.033	0.031	0.032	0.030	0.039	0.031	0.034	0.033	0.033	0.033	0.042	0.040	0.039
MG #	80.56	85.27	83.38	83.87	84.82	83.57	81.28	83.23	84.45	83.32	82.96	83.84	84.58	83.14	83.95	83.95

Appendix C. Table C.2 (continued)

Sample	IM-253	IM-253	IM-253	IM-253	IM-253	IM-253	IM-253	IM-253	IM-253	IM-253	IM-253	IM-253	IM-253	IM-253	IM-253	IM-253
Grain	2	2	2	3	3	3	3	4	4	4	5	5	5	5	6	6
Position	r	i	r	r	i	c	r	i	r	r	i	c	i	r	i	r
SiO_2	51.91	52.65	51.18	51.07	51.55	51.56	52.01	52.31	51.64	51.44	51.31	51.04	50.79	51.88	50.87	52.18
TiO_2	0.26	0.09	0.29	0.30	0.28	0.27	0.14	0.18	0.25	0.31	0.38	0.36	0.37	0.22	0.36	0.10
Al_2O_3	1.06	0.53	1.39	1.63	1.14	1.00	0.53	0.72	1.01	1.52	1.59	1.66	1.71	0.95	1.41	0.44
Cr_2O_3	b.d.	b.d.	b.d.	b.d.	b.d.	b.d.	b.d.	b.d.	b.d.	b.d.	b.d.	b.d.	b.d.	b.d.	b.d.	b.d.
Fe_2O_3	2.14	1.47	3.29	3.67	3.24	3.34	2.36	2.38	2.93	2.48	3.40	3.20	4.18	2.44	3.67	1.86
FeO	5.20	5.58	4.52	4.52	4.56	4.40	4.86	5.12	4.65	4.94	3.78	4.76	3.53	4.93	3.85	5.14
MnO	0.86	0.90	0.78	0.69	0.89	0.88	1.06	1.05	0.94	0.73	0.67	0.73	0.70	0.90	0.89	1.06
MgO	14.17	14.72	13.88	14.06	14.19	14.16	14.78	14.38	14.20	14.26	14.89	13.72	14.40	14.13	14.36	14.65
CaO	22.32	22.38	22.48	22.42	22.49	22.55	22.06	22.48	22.32	22.14	22.07	22.58	22.50	22.54	22.19	22.26
Na_2O	0.52	0.36	0.57	0.51	0.51	0.54	0.39	0.46	0.54	0.51	0.53	0.54	0.51	0.51	0.52	0.36
TOTAL	98.44	98.68	98.38	98.87	98.85	98.70	98.19	99.08	98.48	98.33	98.62	98.59	98.69	98.50	98.12	98.05
FeO_T	7.13	6.90	7.48	7.82	7.48	7.41	6.98	7.26	7.29	7.17	6.84	7.64	7.29	7.13	7.15	6.81
Cation calculation based on 6 oxygens and Fe^{2+}/Fe^{3+} adjusted to 4 cations																
Si	1.957	1.978	1.935	1.922	1.939	1.942	1.965	1.962	1.948	1.940	1.925	1.927	1.911	1.956	1.925	1.974
Al^{IV}	0.043	0.022	0.062	0.072	0.051	0.044	0.024	0.032	0.045	0.060	0.070	0.073	0.076	0.042	0.063	0.020
Total	2.000	2.000	1.997	1.994	1.990	1.986	1.989	1.994	1.993	2.000	1.995	2.000	1.987	1.998	1.988	1.994
Ti^{4+}	0.007	0.003	0.008	0.008	0.008	0.008	0.004	0.005	0.007	0.009	0.011	0.010	0.010	0.006	0.010	0.003
Al^{VI}	0.004	0.001	0.000	0.000	0.000	0.000	0.000	0.000	0.000	0.008	0.000	0.001	0.000	0.000	0.000	0.000
Cr^{3+}	0.000	0.000	0.000	0.000	0.000	0.000	0.000	0.000	0.000	0.000	0.000	0.000	0.000	0.000	0.000	0.000
Fe^{3+}	0.061	0.041	0.094	0.104	0.092	0.095	0.067	0.067	0.083	0.070	0.096	0.091	0.118	0.069	0.105	0.053
Fe^{2+}	0.164	0.175	0.143	0.142	0.143	0.139	0.154	0.160	0.147	0.156	0.119	0.150	0.111	0.155	0.122	0.163
Mn	0.027	0.029	0.025	0.022	0.028	0.028	0.034	0.033	0.030	0.023	0.021	0.023	0.022	0.029	0.029	0.034
Mg	0.797	0.824	0.782	0.789	0.796	0.795	0.832	0.804	0.799	0.802	0.833	0.772	0.808	0.794	0.810	0.826
Ca	0.902	0.901	0.910	0.904	0.906	0.910	0.893	0.903	0.902	0.895	0.887	0.913	0.907	0.911	0.900	0.902
Na	0.038	0.026	0.042	0.037	0.037	0.039	0.029	0.033	0.039	0.037	0.039	0.040	0.037	0.037	0.038	0.026
MG #	82.93	82.48	84.54	84.75	84.77	85.12	84.38	83.40	84.46	83.72	87.50	83.73	87.92	83.67	86.91	83.52

Appendix C. Table C.2 (continued)

Sample	IM-253	IM-253	IM-253	IM-253	IM-253	IM-253	IM-11	IM-11	IM-11	IM-11	IM-11	IM-11	IM-11	IM-11	IM-11	IM-11
Grain	7	7	7	8	8	8	1	1	1	2	2	3	4	4	5	5
Position	i	r	i	r	c	r	r	i	i	i	i	c	i	r	r	c
SiO_2	51.52	50.98	52.80	51.74	52.23	50.95	52.12	52.50	51.29	51.78	52.36	49.88	51.95	51.09	51.58	51.95
TiO_2	0.34	0.37	0.14	0.11	0.16	0.33	0.10	0.13	0.18	0.18	0.15	0.36	0.13	0.23	0.21	0.15
Al_2O_3	1.75	1.66	0.49	0.70	0.57	1.52	0.52	0.58	1.32	1.09	0.64	2.23	0.83	1.21	1.00	0.74
Cr_2O_3	b.d.	b.d.	b.d.	b.d.	b.d.	b.d.	b.d.	b.d.	b.d.	b.d.	b.d.	b.d.	b.d.	b.d.	b.d.	b.d.
Fe_2O_3	1.29	2.76	1.20	2.67	1.93	3.41	2.01	1.43	1.91	1.77	1.67	3.06	1.97	2.87	2.26	1.48
FeO	5.74	4.84	5.89	4.80	4.77	4.15	5.74	6.13	7.69	6.65	5.86	7.24	5.87	5.59	6.37	6.63
MnO	0.80	0.65	1.10	0.80	0.98	0.71	1.36	1.13	1.04	1.18	1.20	0.98	0.95	0.86	1.12	1.14
MgO	13.98	13.96	14.90	14.38	15.24	14.05	13.81	13.92	12.18	13.08	13.94	11.89	13.64	13.08	13.01	13.48
CaO	21.33	22.31	21.90	22.34	21.92	22.51	22.31	22.34	22.41	22.24	22.35	22.38	22.45	22.24	22.33	22.19
Na_2O	0.68	0.51	0.36	0.46	0.35	0.54	0.46	0.48	0.51	0.53	0.48	0.41	0.51	0.66	0.56	0.44
TOTAL	97.43	98.04	98.78	98.00	98.15	98.17	98.43	98.64	98.53	98.50	98.65	98.43	98.30	97.83	98.44	98.20
FeO_T	6.90	7.32	6.97	7.20	6.51	7.22	7.55	7.42	9.41	8.24	7.36	9.99	7.64	8.17	8.40	7.96
Cation calculation based on 6 oxygens and Fe^{2+}/Fe^{3+} adjusted to 4 cations																
Si	1.957	1.931	1.981	1.960	1.968	1.928	1.973	1.980	1.956	1.964	1.975	1.910	1.968	1.949	1.960	1.974
Al^{IV}	0.043	0.069	0.019	0.031	0.025	0.068	0.023	0.020	0.044	0.036	0.025	0.090	0.032	0.051	0.040	0.026
Total	2.000	2.000	2.000	1.991	1.993	1.996	1.996	2.000	2.000	2.000	2.000	2.000	2.000	2.000	2.000	2.000
Ti^{4+}	0.010	0.011	0.004	0.003	0.005	0.009	0.003	0.004	0.005	0.005	0.004	0.010	0.004	0.007	0.006	0.004
Al^{VI}	0.035	0.005	0.003	0.000	0.000	0.000	0.000	0.006	0.015	0.013	0.003	0.011	0.005	0.003	0.005	0.007
Cr^{3+}	0.000	0.000	0.000	0.000	0.000	0.000	0.000	0.000	0.000	0.000	0.000	0.000	0.000	0.000	0.000	0.000
Fe^{3+}	0.037	0.079	0.034	0.076	0.055	0.097	0.057	0.041	0.055	0.050	0.047	0.088	0.056	0.082	0.064	0.042
Fe^{2+}	0.182	0.153	0.185	0.152	0.150	0.131	0.182	0.193	0.245	0.211	0.185	0.232	0.186	0.178	0.202	0.211
Mn	0.026	0.021	0.035	0.026	0.031	0.023	0.044	0.036	0.034	0.038	0.038	0.032	0.030	0.028	0.036	0.037
Mg	0.792	0.789	0.833	0.812	0.856	0.792	0.780	0.783	0.693	0.740	0.784	0.679	0.770	0.744	0.737	0.764
Ca	0.868	0.906	0.880	0.907	0.885	0.912	0.905	0.903	0.916	0.904	0.903	0.918	0.911	0.909	0.909	0.903
Na	0.050	0.037	0.026	0.034	0.026	0.040	0.034	0.035	0.038	0.039	0.035	0.030	0.037	0.049	0.041	0.032
MG #	81.31	83.76	81.83	84.23	85.09	85.81	81.08	80.23	73.88	77.81	80.91	74.53	80.54	80.69	78.49	78.36

Appendix C. Table C.2 (continued)

Sample	IM-11	IM-11	IM-11	IM-11	IM-11	IM-11	IM-11	IM-11	IM-11	IM-269	IM-269	IM-269	IM-269	IM-269	IM-269	IM-269
Grain	5	6	6	7	7	8	8	9	9	1	1	1	2	3	3	3
Position	i	i	r	r	i	i	i	i	r	r	c	i	r	r	c	i
SiO_2	51.52	52.76	52.33	52.38	52.28	52.24	51.87	51.76	51.20	52.09	51.91	50.17	49.96	52.59	52.68	52.27
TiO_2	0.16	0.13	0.07	0.17	0.13	0.13	0.21	0.13	0.20	0.22	0.20	0.13	0.18	0.19	0.14	0.19
Al_2O_3	0.89	0.47	0.44	0.60	0.57	0.80	0.99	0.97	1.36	0.80	0.89	0.82	0.85	0.92	0.83	0.98
Cr_2O_3	b.d.	b.d.	b.d.	b.d.	b.d.	b.d.	b.d.	b.d.	b.d.	b.d.	b.d.	b.d.	b.d.	b.d.	b.d.	b.d.
Fe_2O_3	1.74	1.43	1.29	1.73	1.76	1.98	1.70	1.47	1.81	2.36	2.45	4.93	5.33	1.41	1.83	2.30
FeO	6.81	5.70	6.05	6.34	5.66	5.22	6.32	8.14	7.58	4.83	4.80	2.52	1.96	5.74	5.02	5.00
MnO	1.32	1.18	1.36	1.22	1.16	0.65	1.16	1.14	1.06	0.91	0.82	0.84	0.79	0.89	0.69	0.83
MgO	13.05	14.37	13.93	13.59	14.07	14.73	13.68	12.20	12.27	14.70	14.57	14.69	14.73	14.47	14.57	14.66
CaO	22.04	22.28	22.15	22.22	22.26	22.38	21.86	22.50	22.21	22.19	22.32	22.39	22.43	22.19	22.97	22.14
Na_2O	0.46	0.47	0.44	0.55	0.48	0.39	0.51	0.47	0.53	0.46	0.45	0.41	0.47	0.48	0.44	0.51
TOTAL	97.99	98.79	98.06	98.80	98.37	98.52	98.30	98.78	98.22	98.56	98.41	96.90	96.70	98.88	99.17	98.88
FeO_T	8.38	6.99	7.21	7.90	7.24	7.00	7.85	9.46	9.21	6.95	7.00	6.96	6.76	7.01	6.67	7.07
Cation calculation based on 6 oxygens and Fe^{2+}/Fe^{3+} adjusted to 4 cations																
Si	1.967	1.982	1.985	1.977	1.976	1.964	1.966	1.970	1.957	1.959	1.956	1.921	1.916	1.971	1.968	1.959
Al^{IV}	0.033	0.018	0.015	0.023	0.024	0.035	0.034	0.030	0.043	0.035	0.040	0.037	0.038	0.029	0.032	0.041
Total	2.000	2.000	2.000	2.000	2.000	1.999	2.000	2.000	2.000	1.994	1.996	1.958	1.954	2.000	2.000	2.000
Ti^{4+}	0.005	0.004	0.002	0.005	0.004	0.004	0.006	0.004	0.006	0.006	0.006	0.004	0.005	0.005	0.004	0.005
Al^{VI}	0.007	0.003	0.005	0.004	0.001	0.000	0.010	0.014	0.018	0.000	0.000	0.000	0.000	0.012	0.005	0.002
Cr^{3+}	0.000	0.000	0.000	0.000	0.000	0.000	0.000	0.000	0.000	0.000	0.000	0.000	0.000	0.000	0.000	0.000
Fe^{3+}	0.050	0.040	0.037	0.049	0.050	0.056	0.049	0.042	0.052	0.067	0.070	0.142	0.154	0.040	0.051	0.065
Fe^{2+}	0.218	0.179	0.192	0.200	0.179	0.164	0.200	0.259	0.242	0.152	0.151	0.081	0.063	0.180	0.157	0.157
Mn	0.043	0.038	0.044	0.039	0.037	0.021	0.037	0.037	0.034	0.029	0.026	0.027	0.026	0.028	0.022	0.026
Mg	0.743	0.805	0.788	0.765	0.793	0.826	0.773	0.692	0.699	0.824	0.818	0.839	0.842	0.809	0.811	0.819
Ca	0.902	0.897	0.900	0.899	0.901	0.902	0.888	0.918	0.909	0.894	0.901	0.919	0.922	0.891	0.919	0.889
Na	0.034	0.034	0.032	0.040	0.035	0.028	0.037	0.035	0.039	0.034	0.033	0.030	0.035	0.035	0.032	0.037
MG #	77.32	81.81	80.41	79.27	81.58	83.43	79.45	72.77	74.28	84.43	84.42	91.20	93.04	81.80	83.78	83.91

Appendix C. Table C.2 (continued)

Sample	IM-269	IM-269	IM-269	IM-269	IM-269	IM-269	IM-269	IM-269	IM-269	IM-269	IM-269	IM-269	IM-269	IM-269	IM-269	IM-269
Grain	4	4	4	5	5	5	6	6	7	7	7	8	8	9	9	9
Position	r	c	i	r	c	i	i	i	c	r	i	r	c	r	c	i
SiO_2	52.22	52.18	52.08	52.14	52.32	52.72	52.42	52.90	53.02	52.82	52.73	52.48	52.69	52.94	52.64	52.60
TiO_2	0.18	0.17	0.11	0.16	0.11	0.23	0.16	0.12	0.14	0.20	0.19	0.22	0.15	0.16	0.22	0.13
Al_2O_3	0.93	0.90	1.02	0.84	0.59	0.94	0.82	0.53	0.74	0.91	0.80	0.94	0.71	0.72	0.81	0.65
Cr_2O_3	0.06	b.d.	b.d.	b.d.	b.d.	b.d.	b.d.	b.d.	b.d.	b.d.	b.d.	b.d.	b.d.	b.d.	b.d.	b.d.
Fe_2O_3	2.02	2.28	1.20	2.32	1.87	1.77	1.92	1.56	1.66	2.03	1.86	1.64	1.73	1.63	1.73	1.54
FeO	5.04	4.86	5.69	4.92	4.90	5.31	5.45	4.80	5.49	5.41	4.85	5.27	5.40	5.48	5.54	5.58
MnO	0.85	0.88	0.73	0.99	0.83	0.91	0.85	0.82	0.84	0.89	0.80	0.93	0.82	0.81	0.86	0.88
MgO	14.65	14.76	14.76	14.54	14.77	14.68	14.60	14.80	14.84	14.72	14.78	14.62	14.74	14.71	14.62	14.60
CaO	22.31	22.12	22.11	22.25	22.46	22.48	22.27	23.59	22.46	22.39	22.73	22.27	22.42	22.65	22.30	22.44
Na_2O	0.44	0.47	0.29	0.47	0.40	0.45	0.43	0.25	0.43	0.46	0.46	0.47	0.42	0.42	0.46	0.39
TOTAL	98.70	98.62	97.99	98.63	98.25	99.49	98.92	99.37	99.62	99.83	99.20	98.84	99.08	99.52	99.18	98.81
FeO_T	6.86	6.91	6.77	7.01	6.58	6.90	7.18	6.20	6.98	7.24	6.52	6.75	6.96	6.95	7.10	6.97
Cation calculation based on 6 oxygens and Fe^{2+}/Fe^{3+} adjusted to 4 cations																
Si	1.961	1.960	1.967	1.961	1.971	1.964	1.965	1.972	1.972	1.962	1.967	1.967	1.971	1.972	1.968	1.974
Al^{IV}	0.039	0.040	0.033	0.037	0.026	0.036	0.035	0.023	0.028	0.038	0.033	0.033	0.029	0.028	0.032	0.026
Total	2.000	2.000	2.000	1.998	1.997	2.000	2.000	1.995	2.000	2.000	2.000	2.000	2.000	2.000	2.000	2.000
Ti^{4+}	0.005	0.005	0.003	0.005	0.003	0.006	0.005	0.003	0.004	0.006	0.005	0.006	0.004	0.004	0.006	0.004
Al^{VI}	0.002	0.000	0.012	0.000	0.000	0.005	0.001	0.000	0.004	0.002	0.002	0.009	0.002	0.004	0.004	0.003
Cr^{3+}	0.002	0.000	0.000	0.000	0.000	0.000	0.000	0.000	0.000	0.000	0.000	0.000	0.000	0.000	0.000	0.000
Fe^{3+}	0.057	0.064	0.034	0.066	0.053	0.050	0.054	0.044	0.046	0.057	0.052	0.046	0.049	0.046	0.049	0.043
Fe^{2+}	0.158	0.153	0.180	0.155	0.154	0.165	0.171	0.150	0.171	0.168	0.151	0.165	0.169	0.171	0.173	0.175
Mn	0.027	0.028	0.023	0.032	0.026	0.029	0.027	0.026	0.026	0.028	0.025	0.030	0.026	0.026	0.027	0.028
Mg	0.820	0.827	0.831	0.815	0.830	0.815	0.816	0.822	0.823	0.815	0.822	0.817	0.822	0.817	0.815	0.817
Ca	0.897	0.890	0.895	0.896	0.907	0.897	0.895	0.942	0.895	0.891	0.909	0.894	0.898	0.904	0.893	0.902
Na	0.032	0.034	0.021	0.034	0.029	0.033	0.031	0.018	0.031	0.033	0.033	0.034	0.030	0.030	0.033	0.028
MG #	83.84	84.39	82.20	84.02	84.35	83.16	82.67	84.57	82.80	82.91	84.48	83.20	82.95	82.69	82.49	82.36

Appendix C. Table C.3 Electron Microprobe analyses of clinopyroxene from Iron Mask dykes.

Sample	IM-254	IM-254	IM-254	IM-254	IM-254	IM-254	IM-254	IM-254	IM-254	IM-254	IM-254	IM-254	IM-254	IM-254	IM-254	IM-254
Grain	1	1	1	2	2	3	3	4	4	4	4	5	6	6	6	7
Position	r	i	i	r	c	i	i	r	i	i	r	i	i	r	i	i
SiO_2	52.09	51.66	51.64	51.92	52.13	52.83	52.36	51.56	51.79	52.30	51.99	51.80	51.75	51.65	52.47	51.59
TiO_2	0.15	0.18	0.24	0.12	0.17	b.d.	0.21	0.21	0.15	0.16	0.16	0.16	0.17	0.18	0.23	0.17
Al_2O_3	0.79	0.99	0.96	0.68	0.82	0.24	0.86	0.88	0.84	0.84	0.83	0.89	0.90	0.78	0.63	0.92
Cr_2O_3	b.d.	b.d.	b.d.	b.d.	b.d.	b.d.	b.d.	b.d.	b.d.	b.d.	b.d.	b.d.	b.d.	b.d.	b.d.	b.d.
Fe_2O_3	1.92	2.40	2.65	2.93	2.23	2.05	2.26	2.91	2.40	2.60	2.84	3.10	3.29	2.76	2.61	3.72
FeO	5.45	4.72	4.46	4.22	4.85	3.94	4.69	3.96	4.62	4.33	3.97	3.85	4.08	4.62	4.05	3.93
MnO	0.91	0.92	0.94	0.82	0.92	0.98	0.95	0.92	0.88	1.02	0.89	0.94	0.76	0.92	0.87	0.92
MgO	14.44	15.10	15.31	15.09	15.05	15.43	15.26	15.23	14.98	15.40	15.46	15.16	15.15	14.95	15.69	15.21
CaO	22.38	21.61	21.49	22.29	22.08	23.44	22.17	21.91	22.02	22.04	22.05	22.27	22.28	21.96	22.25	22.04
Na_2O	0.36	0.37	0.38	0.37	0.35	0.16	0.34	0.38	0.36	0.36	0.36	0.38	0.36	0.35	0.34	0.36
TOTAL	98.49	97.95	98.07	98.44	98.60	99.07	99.10	97.96	98.04	99.05	98.55	98.55	98.74	98.17	99.14	98.86
FeO_T	7.18	6.88	6.84	6.86	6.86	5.78	6.72	6.58	6.78	6.67	6.53	6.64	7.04	7.1	6.4	7.28
Cation calculation based on 6 oxygens and Fe^{2+}/Fe^{3+} adjusted to 4 cations																
Si	1.964	1.952	1.948	1.953	1.958	1.971	1.955	1.947	1.956	1.953	1.950	1.945	1.942	1.951	1.955	1.935
Al^{IV}	0.035	0.044	0.043	0.030	0.036	0.011	0.038	0.039	0.037	0.037	0.037	0.039	0.040	0.035	0.028	0.041
Total	1.999	1.996	1.991	1.983	1.994	1.982	1.993	1.986	1.993	1.990	1.987	1.984	1.982	1.986	1.983	1.976
Ti^{4+}	0.004	0.005	0.007	0.003	0.005	0.000	0.006	0.006	0.004	0.004	0.005	0.005	0.005	0.005	0.006	0.005
Al^{VI}	0.000	0.000	0.000	0.000	0.000	0.000	0.000	0.000	0.000	0.000	0.000	0.000	0.000	0.000	0.000	0.000
Cr^{3+}	0.000	0.000	0.000	0.000	0.000	0.000	0.000	0.000	0.000	0.000	0.000	0.000	0.000	0.000	0.000	0.000
Fe^{3+}	0.054	0.068	0.075	0.083	0.063	0.058	0.063	0.083	0.068	0.073	0.080	0.088	0.093	0.078	0.073	0.105
Fe^{2+}	0.172	0.149	0.141	0.133	0.152	0.123	0.146	0.125	0.146	0.135	0.124	0.121	0.128	0.146	0.126	0.123
Mn	0.029	0.029	0.030	0.026	0.029	0.031	0.030	0.029	0.028	0.032	0.028	0.030	0.024	0.029	0.027	0.029
Mg	0.812	0.851	0.861	0.846	0.843	0.858	0.850	0.857	0.843	0.857	0.864	0.849	0.847	0.842	0.872	0.851
Ca	0.904	0.875	0.868	0.898	0.888	0.937	0.887	0.886	0.891	0.882	0.886	0.896	0.896	0.889	0.888	0.886
Na	0.026	0.027	0.028	0.027	0.025	0.012	0.025	0.028	0.026	0.026	0.026	0.028	0.026	0.026	0.025	0.026
MG #	82.52	85.10	85.93	86.41	84.72	87.46	85.34	87.27	85.24	86.39	87.45	87.53	86.87	85.22	87.37	87.37

$MG\# = 100 \cdot Mg/(Mg + Fe^{2+})$ c=core; r=rim; i=interior

Appendix C. Table C.3 (continued)

Sample	IM-254	IM-254	IM-254	IM-254	IM-254	IM-254	IM-254	IM-208	IM-208	IM-208	IM-208	IM-208	IM-208	IM-208	IM-208	IM-208
Grain	8	8	8	9	10	10	11	1	1	1	1	2	2	2	2	3
Position	r	c	i	c	c	r	i	r	i	r	i	r	i	c	r	r
SiO_2	52.70	52.45	52.40	52.34	52.50	52.26	52.29	52.69	50.98	51.32	51.51	52.23	51.96	52.17	52.58	51.75
TiO_2	0.15	0.17	0.15	0.21	0.14	0.20	0.18	0.21	0.36	0.36	0.34	0.17	0.21	0.24	0.22	0.21
Al_2O_3	0.80	0.79	0.80	0.80	0.86	0.83	0.78	1.54	2.48	2.52	2.07	1.32	1.35	1.58	1.62	1.56
Cr_2O_3	b.d.	b.d.	b.d.	b.d.	b.d.	b.d.	0.20	b.d.	b.d.	b.d.	b.d.	b.d.	b.d.	b.d.	b.d.	b.d.
Fe_2O_3	1.80	1.79	2.08	2.49	2.12	2.48	2.08	0.89	2.64	2.00	1.99	2.18	2.72	1.70	1.28	2.20
FeO	5.30	5.15	5.18	4.51	4.96	4.77	5.12	5.81	4.11	5.35	4.82	4.48	4.51	5.67	5.14	4.46
MnO	0.98	0.94	0.91	0.92	0.96	0.94	0.94	0.66	0.63	0.63	0.66	0.74	0.78	0.68	0.67	0.69
MgO	14.88	14.90	15.00	15.23	15.09	14.85	14.94	14.67	14.23	14.12	14.32	14.84	14.70	14.35	14.73	14.63
CaO	22.33	22.30	22.14	22.14	22.23	22.44	22.20	22.40	22.73	22.30	22.65	22.54	22.63	22.44	22.66	22.57
Na_2O	0.38	0.36	0.35	0.40	0.35	0.38	0.34	0.41	0.45	0.43	0.41	0.45	0.40	0.42	0.43	0.42
TOTAL	99.32	98.85	99.01	99.04	99.21	99.15	99.07	99.28	98.61	99.03	98.77	98.95	99.26	99.25	99.33	98.49
FeO_T	6.92	6.76	7.05	6.75	6.87	7.00	6.99	6.61	6.49	7.15	6.61	6.44	6.96	7.20	6.29	6.44
Cation calculation based on 6 oxygens and Fe^{2+}/Fe^{3+} adjusted to 4 cations																
Si	1.966	1.965	1.961	1.956	1.960	1.955	1.957	1.962	1.914	1.921	1.931	1.951	1.940	1.949	1.955	1.943
Al^{IV}	0.034	0.035	0.035	0.035	0.038	0.037	0.034	0.038	0.086	0.079	0.069	0.049	0.059	0.051	0.045	0.057
Total	2.000	2.000	1.996	1.991	1.998	1.992	1.991	2.000	2.000	2.000	2.000	2.000	1.999	2.000	2.000	2.000
Ti^{4+}	0.004	0.005	0.004	0.006	0.004	0.006	0.005	0.006	0.010	0.010	0.010	0.005	0.006	0.007	0.006	0.006
Al^{VI}	0.001	0.000	0.000	0.000	0.000	0.000	0.000	0.030	0.024	0.032	0.022	0.009	0.000	0.019	0.026	0.012
Cr^{3+}	0.000	0.000	0.000	0.000	0.000	0.000	0.006	0.000	0.000	0.000	0.000	0.000	0.000	0.000	0.000	0.000
Fe^{3+}	0.051	0.050	0.059	0.070	0.060	0.070	0.059	0.025	0.074	0.056	0.056	0.061	0.076	0.048	0.036	0.062
Fe^{2+}	0.165	0.161	0.162	0.141	0.155	0.149	0.160	0.181	0.129	0.168	0.151	0.140	0.141	0.177	0.160	0.140
Mn	0.031	0.030	0.029	0.029	0.030	0.030	0.030	0.021	0.020	0.020	0.021	0.023	0.025	0.022	0.021	0.022
Mg	0.828	0.832	0.837	0.848	0.840	0.828	0.834	0.815	0.796	0.788	0.800	0.827	0.818	0.799	0.817	0.819
Ca	0.893	0.895	0.888	0.886	0.889	0.899	0.89	0.894	0.914	0.895	0.91	0.902	0.905	0.898	0.903	0.908
Na	0.027	0.026	0.025	0.029	0.025	0.028	0.025	0.030	0.033	0.031	0.030	0.033	0.029	0.030	0.031	0.031
MG #	83.38	83.79	83.78	85.74	84.42	84.75	83.90	81.83	86.05	82.43	84.12	85.52	85.30	81.86	83.62	85.40

Appendix C. Table C.3 (continued)

Sample	IM-208	IM-208	IM-208	IM-208	IM-208	IM-208	IM-208	IM-208	IM-208	IM-208	IM-208	IM-208	IM-208	IM-208	IM-208	IM-208
Grain	3	3	4	4	5	5	6	6	7	7	7	8	9	10	11	11
Position	c	i	i	r	i	r	i	c	r	c	i	Gm	Gm	Gm	Gm	Gm
SiO_2	50.06	51.70	50.79	50.87	51.84	50.89	52.75	52.51	52.31	52.70	51.70	51.83	51.09	52.11	51.63	51.62
TiO_2	0.46	0.16	0.34	0.30	0.16	0.24	0.20	0.16	0.24	0.24	0.28	0.19	0.25	0.23	0.23	0.25
Al_2O_3	2.54	1.29	2.27	1.80	1.16	1.48	1.44	1.09	1.60	1.60	1.66	1.48	1.65	1.60	1.51	1.71
Cr_2O_3	b.d.	b.d.	b.d.	b.d.	b.d.	b.d.	b.d.	0.06	b.d.	b.d.	b.d.	b.d.	b.d.	b.d.	b.d.	b.d.
Fe_2O_3	3.21	2.57	3.54	3.13	3.17	3.59	1.25	1.38	1.84	1.31	2.46	2.78	3.46	2.84	2.73	2.88
FeO	4.04	4.27	3.95	3.70	3.57	3.06	5.31	5.37	4.44	5.34	4.50	4.08	3.17	3.89	3.92	3.90
MnO	0.68	0.78	0.69	0.74	0.78	0.73	0.74	0.74	0.74	0.65	0.71	0.76	0.73	0.68	0.66	0.70
MgO	13.99	14.82	14.20	14.50	15.17	14.76	14.68	14.71	14.92	14.79	14.63	14.82	14.85	14.74	14.88	14.62
CaO	22.36	22.45	22.69	22.51	22.57	22.82	22.58	22.46	22.72	22.64	22.49	22.54	22.73	23.22	22.68	22.92
Na_2O	0.43	0.38	0.44	0.43	0.40	0.38	0.46	0.40	0.41	0.41	0.43	0.44	0.40	0.42	0.39	0.42
TOTAL	97.77	98.42	98.91	97.98	98.82	97.95	99.41	98.88	99.22	99.68	98.86	98.92	98.33	99.73	98.63	99.02
FeO_T	6.93	6.58	7.14	6.52	6.42	6.29	6.43	6.61	6.10	6.52	6.71	6.58	6.28	6.45	6.38	6.49
Cation calculation based on 6 oxygens and Fe^{2+}/Fe^{3+} adjusted to 4 cations																
Si	1.900	1.944	1.906	1.922	1.939	1.923	1.962	1.965	1.947	1.954	1.936	1.938	1.922	1.934	1.935	1.930
Al^{IV}	0.100	0.056	0.094	0.078	0.051	0.066	0.038	0.035	0.053	0.046	0.064	0.062	0.073	0.066	0.065	0.070
Total	2.000	2.000	2.000	2.000	1.990	1.989	2.000	2.000	2.000	2.000	2.000	2.000	1.995	2.000	2.000	2.000
Ti^{4+}	0.013	0.005	0.010	0.009	0.005	0.007	0.006	0.005	0.007	0.007	0.008	0.005	0.007	0.006	0.006	0.007
Al^{VI}	0.014	0.001	0.006	0.002	0.000	0.000	0.025	0.013	0.017	0.024	0.009	0.003	0.000	0.004	0.002	0.005
Cr^{3+}	0.000	0.000	0.000	0.000	0.000	0.000	0.000	0.002	0.000	0.000	0.000	0.000	0.000	0.000	0.000	0.000
Fe^{3+}	0.092	0.073	0.100	0.089	0.089	0.102	0.035	0.039	0.052	0.037	0.069	0.078	0.098	0.079	0.077	0.081
Fe^{2+}	0.128	0.134	0.124	0.117	0.112	0.097	0.165	0.168	0.138	0.166	0.141	0.128	0.100	0.121	0.123	0.122
Mn	0.022	0.025	0.022	0.024	0.025	0.023	0.023	0.023	0.023	0.020	0.023	0.024	0.023	0.021	0.021	0.022
Mg	0.792	0.831	0.794	0.817	0.846	0.831	0.814	0.821	0.828	0.818	0.817	0.826	0.833	0.815	0.832	0.815
Ca	0.909	0.904	0.912	0.911	0.905	0.924	0.900	0.901	0.906	0.900	0.902	0.903	0.916	0.923	0.911	0.918
Na	0.032	0.028	0.032	0.032	0.029	0.028	0.033	0.029	0.030	0.029	0.031	0.032	0.029	0.030	0.028	0.030
MG #	86.09	86.11	86.49	87.47	88.31	89.55	83.15	83.01	85.71	83.13	85.28	86.58	89.28	87.07	87.12	86.98

Appendix C. Table C.3 (continued)

Sample	IM-208	IM-308	IM-308	IM-308	IM-308	IM-308	IM-308	IM-308	IM-308	IM-308	IM-308	IM-308	IM-308	IM-308	IM-308	IM-308
Grain	12	1	1	1	2	2	2	2	3	4	4	5	5	5	5	5
Position	Gm	r	i	i	r	c	i	r	i	i	i	r	i	r	c	i
SiO_2	51.99	51.51	53.08	52.54	52.29	53.10	52.53	52.46	52.77	52.42	52.36	51.66	50.34	52.05	52.78	52.10
TiO_2	0.29	0.18	0.18	0.20	0.14	0.14	0.19	0.21	0.15	0.23	0.20	0.34	0.43	0.22	0.17	0.23
Al_2O_3	1.72	1.51	0.68	0.92	0.82	0.67	0.92	0.81	0.91	1.26	0.94	1.57	2.55	1.14	1.14	1.08
Cr_2O_3	0.06	b.d.	b.d.	b.d.	b.d.	b.d.	b.d.	b.d.	b.d.	b.d.	b.d.	b.d.	0.06	b.d.	0.31	0.26
Fe_2O_3	2.16	2.74	1.91	2.25	1.48	1.30	2.01	2.38	2.54	2.01	1.77	2.61	3.89	3.06	1.76	2.28
FeO	4.43	4.15	2.90	3.46	4.29	3.28	3.42	3.57	2.83	3.09	3.38	2.63	4.12	2.34	2.39	2.66
MnO	0.73	0.46	0.43	0.40	0.44	0.46	0.44	0.35	0.33	0.34	0.31	0.27	0.48	0.40	0.18	0.20
MgO	14.78	15.40	16.20	15.65	15.38	16.08	15.55	15.50	15.98	15.52	15.64	15.25	14.15	15.70	17.20	16.57
CaO	22.71	22.11	23.50	23.04	22.86	23.30	23.05	23.35	23.45	23.46	23.20	24.20	22.22	23.40	22.89	22.62
Na_2O	0.4	0.3	0.29	0.38	0.27	0.3	0.41	0.32	0.34	0.38	0.33	0.22	0.5	0.38	0.16	0.25
TOTAL	99.27	98.36	99.17	98.84	97.97	98.63	98.52	98.95	99.30	98.71	98.13	98.75	98.74	98.69	98.98	98.25
FeO_T	6.37	6.62	4.62	5.48	5.62	4.45	5.23	5.71	5.12	4.90	4.97	4.98	7.62	5.09	3.97	4.71
Cation calculation based on 6 oxygens and Fe^{2+}/Fe^{3+} adjusted to 4 cations																
Si	1.937	1.933	1.964	1.956	1.966	1.974	1.961	1.954	1.952	1.951	1.960	1.927	1.893	1.939	1.947	1.943
Al^{IV}	0.063	0.067	0.030	0.040	0.034	0.026	0.039	0.036	0.040	0.049	0.040	0.069	0.107	0.050	0.050	0.047
Total	2.000	2.000	1.994	1.996	2.000	2.000	2.000	1.990	1.992	2.000	2.000	1.996	2.000	1.989	1.997	1.990
Ti^{4+}	0.008	0.005	0.005	0.006	0.004	0.004	0.005	0.006	0.004	0.006	0.006	0.010	0.012	0.006	0.005	0.006
Al^{VI}	0.013	0.000	0.000	0.000	0.002	0.003	0.001	0.000	0.000	0.006	0.001	0.000	0.006	0.000	0.000	0.000
Cr^{3+}	0.002	0.000	0.000	0.000	0.000	0.000	0.000	0.000	0.000	0.000	0.000	0.000	0.002	0.000	0.009	0.008
Fe^{3+}	0.060	0.077	0.053	0.063	0.042	0.036	0.056	0.067	0.071	0.056	0.050	0.073	0.110	0.086	0.049	0.064
Fe^{2+}	0.138	0.130	0.090	0.108	0.135	0.102	0.107	0.111	0.088	0.096	0.106	0.082	0.130	0.073	0.074	0.083
Mn	0.023	0.015	0.013	0.013	0.014	0.014	0.014	0.011	0.01	0.011	0.01	0.009	0.015	0.013	0.006	0.006
Mg	0.821	0.862	0.894	0.869	0.862	0.891	0.865	0.861	0.881	0.861	0.873	0.848	0.793	0.872	0.946	0.921
Ca	0.907	0.889	0.931	0.919	0.921	0.928	0.922	0.932	0.930	0.936	0.931	0.967	0.895	0.934	0.905	0.904
Na	0.029	0.022	0.021	0.027	0.020	0.022	0.030	0.023	0.024	0.027	0.024	0.016	0.036	0.027	0.011	0.018
MG #	85.61	86.90	90.85	88.95	86.46	89.73	88.99	88.58	90.92	89.97	89.17	91.18	85.92	92.28	92.75	91.73

Appendix C. Table C.3 (continued)

Sample	IM-308	IM-308	IM-308	IM-308	IM-308	IM-308	IM-308	IM-308	IM-308	IM-308	IM-308	IM-308	IM-308	IM-254	IM-254	IM-254
Grain	5	6	6	7	7	7	7	7	8	8	8	9	10	6	6	7
Position	i	i	r	r	r	i	r	r	r	i	c	Gm	Gm	r	i	i
SiO_2	49.85	52.74	51.80	53.05	51.82	52.72	48.95	52.15	52.35	52.76	52.45	53.10	52.56	51.65	52.47	51.59
TiO_2	0.35	0.10	0.20	0.10	0.25	0.08	0.68	0.18	0.20	0.20	0.16	0.10	0.23	0.18	0.23	0.17
Al_2O_3	2.50	0.68	0.75	0.52	1.26	0.65	4.17	1.00	1.12	0.86	0.86	0.67	1.06	0.78	0.63	0.92
Cr_2O_3	b.d.	b.d.	b.d.	b.d.	b.d.	b.d.	b.d.	b.d.	b.d.	b.d.	b.d.	b.d.	b.d.	b.d.	b.d.	b.d.
Fe_2O_3	3.49	1.96	2.90	1.65	2.53	2.06	4.09	2.36	2.11	1.44	2.62	1.63	2.13	2.76	2.61	3.72
FeO	5.09	2.79	3.88	3.12	4.66	3.59	3.12	3.76	2.88	3.69	2.78	3.01	2.93	4.62	4.05	3.93
MnO	0.37	0.23	0.62	0.49	0.76	0.43	0.27	0.52	0.32	0.43	0.34	0.25	0.33	0.92	0.87	0.92
MgO	13.26	15.88	14.86	16.17	15.26	15.82	14.45	15.58	15.80	15.90	15.99	16.24	15.77	14.95	15.69	15.21
CaO	22.49	23.96	22.58	23.28	21.61	22.98	22.35	22.57	23.49	22.91	23.25	23.43	23.45	21.96	22.25	22.04
Na_2O	0.44	0.25	0.48	0.28	0.41	0.32	0.30	0.34	0.29	0.32	0.32	0.30	0.36	0.35	0.34	0.36
TOTAL	97.84	98.59	98.07	98.66	98.56	98.65	98.38	98.46	98.56	98.51	98.77	98.73	98.82	98.17	99.14	98.86
FeO_T	8.23	4.55	6.49	4.6	6.94	5.44	6.8	5.88	4.78	4.99	5.14	4.48	4.85	7.1	6.4	7.28
Cation calculation based on 6 oxygens and Fe^{2+}/Fe^{3+} adjusted to 4 cations																
Si	1.900	1.963	1.954	1.972	1.944	1.966	1.841	1.952	1.950	1.967	1.951	1.970	1.953	1.951	1.955	1.935
Al^{IV}	0.100	0.030	0.033	0.023	0.056	0.029	0.159	0.044	0.049	0.033	0.038	0.029	0.046	0.035	0.028	0.041
Total	2.000	1.993	1.987	1.995	2.000	1.995	2.000	1.996	1.999	2.000	1.989	1.999	1.999	1.986	1.983	1.976
Ti^{4+}	0.010	0.003	0.006	0.003	0.007	0.002	0.019	0.005	0.006	0.006	0.004	0.003	0.006	0.005	0.006	0.005
Al^{VI}	0.012	0.000	0.000	0.000	0.000	0.000	0.026	0.000	0.000	0.005	0.000	0.000	0.000	0.000	0.000	0.000
Cr^{3+}	0.000	0.000	0.000	0.000	0.000	0.000	0.000	0.000	0.000	0.000	0.000	0.000	0.000	0.000	0.000	0.000
Fe^{3+}	0.100	0.055	0.082	0.046	0.071	0.058	0.116	0.067	0.059	0.040	0.073	0.046	0.060	0.078	0.073	0.105
Fe^{2+}	0.162	0.087	0.122	0.097	0.146	0.112	0.098	0.118	0.090	0.115	0.086	0.093	0.091	0.146	0.126	0.123
Mn	0.012	0.007	0.020	0.015	0.024	0.014	0.009	0.016	0.010	0.014	0.011	0.008	0.010	0.029	0.027	0.029
Mg	0.753	0.881	0.836	0.896	0.853	0.879	0.810	0.869	0.878	0.884	0.887	0.898	0.874	0.842	0.872	0.851
Ca	0.918	0.956	0.912	0.927	0.869	0.918	0.901	0.905	0.938	0.915	0.927	0.931	0.934	0.889	0.888	0.886
Na	0.033	0.018	0.035	0.02	0.03	0.023	0.022	0.025	0.021	0.023	0.023	0.022	0.026	0.026	0.025	0.026
MG #	82.30	91.01	87.27	90.23	85.39	88.70	89.21	88.04	90.70	88.49	91.16	90.62	90.57	85.22	87.37	87.37

Appendix C. Table C.4 Electron Microprobe analyses of clinopyroxene from the Sugarloaf unit.

Sample	IM-274	IM-274	IM-274	IM-274	IM-274	IM-274	IM-274	IM-274	IM-274	IM-274	IM-274	IM-274	IM-274	IM-274	IM-274	IM-274
Grain	1	1	1	1	1	1	1	1	1	2	2	2	2	2	2	2
Position	c	c	i	i	i	c	r	i	r	r	i	c	i	i	i	r
SiO_2	52.12	53.01	51.70	52.08	50.69	52.39	51.28	50.73	50.37	50.63	52.33	52.20	50.53	52.00	51.60	50.20
TiO_2	0.14	0.19	0.24	0.22	0.30	0.14	0.26	0.25	0.35	0.29	0.21	0.14	0.26	0.21	0.25	0.43
Al_2O_3	1.73	1.36	1.84	1.46	2.33	1.22	1.99	2.05	2.55	2.36	1.79	1.21	2.01	1.56	1.96	3.25
Cr_2O_3	0.23	0.23	0.14	0.28	0.15	0.49	b.d.	b.d.	0.07	b.d.	0.13	0.24	0.16	0.20	0.14	b.d.
Fe_2O_3	1.72	1.18	1.92	1.61	3.43	2.02	2.66	3.09	3.14	2.80	2.30	2.38	3.39	1.94	2.29	2.79
FeO	2.14	2.68	3.95	3.68	2.67	1.70	4.07	3.85	3.44	5.24	2.49	1.67	2.39	2.83	3.42	5.07
MnO	b.d.	0.10	0.13	0.13	0.13	b.d.	0.16	0.22	0.14	0.40	0.14	0.12	0.12	0.11	0.12	0.28
MgO	16.76	17.05	15.72	16.50	15.74	17.14	15.80	15.56	15.10	14.27	16.62	16.94	15.85	16.53	16.07	14.49
CaO	23.20	23.13	22.63	22.28	22.56	23.23	22.06	21.96	22.61	21.85	23.08	23.30	22.60	22.76	22.44	21.90
Na_2O	0.16	0.17	0.21	0.16	0.25	0.17	0.20	0.21	0.24	0.38	0.21	0.16	0.21	0.18	0.22	0.26
TOTAL	98.20	99.10	98.48	98.40	98.25	98.50	98.48	97.92	98.01	98.22	99.30	98.36	97.52	98.32	98.51	98.67
FeO_T	3.69	3.74	5.68	5.13	5.76	3.52	6.46	6.63	6.27	7.76	4.56	3.81	5.44	4.58	5.48	7.58
Cation calculation based on 6 oxygens and Fe^{2+}/Fe^{3+} adjusted to 4 cations																
Si	1.936	1.951	1.931	1.940	1.898	1.940	1.918	1.911	1.896	1.913	1.929	1.938	1.905	1.936	1.923	1.886
Al^{IV}	0.064	0.049	0.069	0.060	0.102	0.053	0.082	0.089	0.104	0.087	0.071	0.053	0.089	0.064	0.077	0.114
Total	2.000	2.000	2.000	2.000	2.000	1.993	2.000	2.000	2.000	2.000	2.000	1.991	1.994	2.000	2.000	2.000
Ti^{4+}	0.004	0.005	0.007	0.006	0.008	0.004	0.007	0.007	0.010	0.008	0.006	0.004	0.007	0.006	0.007	0.012
Al^{VI}	0.012	0.010	0.012	0.004	0.001	0.000	0.006	0.002	0.009	0.018	0.007	0.000	0.000	0.004	0.009	0.030
Cr^{3+}	0.007	0.007	0.004	0.008	0.004	0.014	0.000	0.000	0.002	0.000	0.004	0.007	0.005	0.006	0.004	0.000
Fe^{3+}	0.048	0.033	0.054	0.045	0.097	0.056	0.075	0.088	0.089	0.080	0.064	0.067	0.096	0.054	0.064	0.079
Fe^{2+}	0.067	0.082	0.123	0.115	0.084	0.053	0.127	0.121	0.108	0.165	0.077	0.052	0.075	0.088	0.107	0.159
Mn	0.000	0.003	0.004	0.004	0.004	0.000	0.005	0.007	0.004	0.013	0.004	0.004	0.004	0.003	0.004	0.009
Mg	0.928	0.936	0.875	0.917	0.879	0.946	0.881	0.874	0.848	0.804	0.913	0.938	0.891	0.917	0.893	0.811
Ca	0.923	0.912	0.906	0.889	0.905	0.922	0.884	0.886	0.912	0.884	0.911	0.927	0.913	0.908	0.896	0.881
Na	0.012	0.012	0.015	0.012	0.018	0.012	0.015	0.015	0.018	0.028	0.015	0.012	0.015	0.013	0.016	0.019
MG #	93.27	91.94	87.68	88.86	91.28	94.69	87.40	87.84	88.70	82.97	92.22	94.75	92.24	91.24	89.30	83.61

MG# = $100 \cdot Mg/(Mg + Fe^{2+})$ c=core; r=rim; i=interior

Appendix C. Table C.4 (continued)

Sample	IM-274	IM-274	IM-274	IM-274	IM-274	IM-274	IM-274	IM-274	IM-274	IM-274	IM-274	IM-272	IM-272	IM-272	IM-272	IM-272
Grain	2	3	3	3	3	3	4	4	4	4	5	1	1	2	2	2
Position	r	r	i	c	i	r	r	c	i	r	c	i	i	i	i	i
SiO_2	52.01	52.92	51.63	51.52	51.31	51.27	52.52	53.08	51.58	52.40	52.01	53.05	52.37	52.77	48.95	53.25
TiO_2	0.13	0.18	0.20	0.26	0.32	0.32	0.11	0.08	0.25	0.12	0.19	0.06	b.d.	b.d.	0.38	b.d.
Al_2O_3	1.08	1.52	1.74	2.03	2.41	2.12	0.84	0.89	1.81	1.09	1.54	0.20	0.31	0.17	3.00	0.32
Cr_2O_3	0.21	0.19	0.24	0.20	b.d.	b.d.	0.56	0.13	b.d.	0.44	0.08	b.d.	b.d.	b.d.	0.06	b.d.
Fe_2O_3	2.73	1.16	2.35	2.19	2.68	2.42	1.81	1.87	2.20	1.54	2.18	0.90	1.62	1.55	4.56	1.35
FeO	1.26	4.16	3.41	3.38	3.71	4.95	1.71	1.75	4.72	2.26	3.79	6.14	5.54	5.37	4.58	5.21
MnO	0.12	0.10	0.16	0.11	0.12	0.19	0.09	0.13	0.16	0.07	0.20	0.21	0.20	0.13	0.63	0.08
MgO	17.08	16.65	16.21	15.81	15.48	15.61	17.66	17.62	15.93	17.29	16.59	13.97	13.88	14.28	13.36	14.46
CaO	23.31	22.40	22.33	22.74	22.89	21.54	22.60	23.13	21.54	22.67	21.78	24.21	24.24	24.25	21.91	24.14
Na_2O	0.14	0.18	0.19	0.23	0.20	0.23	0.15	0.14	0.23	0.13	0.20	0.27	0.24	0.24	0.39	0.37
TOTAL	98.07	99.46	98.46	98.47	99.12	98.65	98.05	98.82	98.42	98.01	98.56	99.01	98.4	98.76	97.82	99.18
FeO_T	3.72	5.20	5.52	5.35	6.12	7.13	3.34	3.43	6.70	3.65	5.75	6.95	7.00	6.76	8.68	6.42
Cation calculation based on 6 oxygens and Fe^{2+}/Fe^{3+} adjusted to 4 cations																
Si	1.936	1.949	1.926	1.922	1.908	1.918	1.950	1.955	1.930	1.949	1.936	1.991	1.978	1.983	1.869	1.987
Al^{IV}	0.047	0.051	0.074	0.078	0.092	0.082	0.037	0.039	0.070	0.048	0.064	0.009	0.014	0.008	0.131	0.013
Total	1.983	2.000	2.000	2.000	2.000	2.000	1.987	1.994	2.000	1.997	2.000	2.000	1.992	1.991	2.000	2.000
Ti^{4+}	0.004	0.005	0.006	0.007	0.009	0.009	0.003	0.002	0.007	0.003	0.005	0.002	0.000	0.000	0.011	0.000
Al^{VI}	0.000	0.015	0.002	0.011	0.014	0.011	0.000	0.000	0.010	0.000	0.004	0.000	0.000	0.000	0.004	0.001
Cr^{3+}	0.006	0.006	0.007	0.006	0.000	0.000	0.016	0.004	0.000	0.013	0.002	0.000	0.000	0.000	0.002	0.000
Fe^{3+}	0.077	0.032	0.066	0.061	0.075	0.068	0.050	0.052	0.062	0.043	0.061	0.025	0.046	0.044	0.131	0.038
Fe^{2+}	0.039	0.128	0.106	0.106	0.115	0.155	0.053	0.054	0.148	0.070	0.118	0.193	0.175	0.169	0.146	0.163
Mn	0.004	0.003	0.005	0.003	0.004	0.006	0.003	0.004	0.005	0.002	0.006	0.007	0.006	0.004	0.020	0.003
Mg	0.948	0.914	0.902	0.880	0.858	0.871	0.978	0.968	0.889	0.959	0.921	0.782	0.782	0.800	0.761	0.804
Ca	0.930	0.884	0.893	0.909	0.912	0.863	0.899	0.913	0.864	0.903	0.869	0.973	0.981	0.976	0.896	0.965
Na	0.010	0.013	0.014	0.017	0.014	0.017	0.011	0.010	0.017	0.009	0.014	0.020	0.018	0.017	0.029	0.027
MG #	96.05	87.72	89.48	89.25	88.18	84.89	94.86	94.72	85.73	93.20	88.64	80.21	81.71	82.56	83.90	83.14

Appendix C. Table C.5 Electron Microprobe analyses of clinopyroxene from the Iron Mask hybrid unit.

Sample	IM-173	IM-173	IM-173	IM-173	IM-173	IM-173	IM-173	IM-173	IM-173	IM-173	IM-173	IM-173	IM-306	IM-306	IM-306	IM-306
Grain	1	1	1	1	2	2	2	3	3	3	3	3	1	1	1	2
Position	r	i	i	r	r	i	i	r	i	c	i	r	r	c	i	r
SiO_2	50.18	50.39	50.35	50.70	50.06	49.91	50.96	50.48	49.94	49.86	50.19	50.29	51.72	51.87	50.96	51.71
TiO_2	0.50	0.46	0.49	0.42	0.49	0.51	0.44	0.47	0.54	0.54	0.42	0.47	0.32	0.24	0.38	0.30
Al_2O_3	3.59	3.34	3.39	2.97	3.51	3.68	2.84	3.32	3.76	3.76	3.41	3.55	1.72	1.20	2.24	1.80
Cr_2O_3	b.d.	b.d.	b.d.	b.d.	b.d.	b.d.	b.d.	b.d.	b.d.	b.d.	b.d.	b.d.	b.d.	b.d.	b.d.	b.d.
Fe_2O_3	3.37	3.70	3.84	4.15	4.10	4.13	2.95	3.65	3.74	3.99	4.25	3.97	2.30	2.71	2.91	2.39
FeO	3.76	3.50	3.35	2.85	3.12	3.37	3.98	3.59	3.55	3.62	3.09	3.63	4.43	4.27	4.00	4.52
MnO	0.30	0.28	0.27	0.28	0.32	0.29	0.31	0.32	0.27	0.27	0.26	0.33	0.42	0.49	0.37	0.42
MgO	14.58	14.74	14.73	15.06	14.55	14.46	14.92	14.47	14.35	14.23	14.64	14.50	15.50	15.42	15.27	15.50
CaO	22.38	22.69	22.74	22.87	22.82	22.54	22.41	22.91	22.69	22.80	23.09	22.65	21.83	22.02	21.75	21.70
Na_2O	0.38	0.34	0.36	0.38	0.37	0.40	0.38	0.38	0.38	0.36	0.30	0.38	0.37	0.39	0.40	0.38
TOTAL	99.04	99.44	99.52	99.68	99.34	99.29	99.19	99.59	99.22	99.43	99.65	99.77	98.61	98.61	98.28	98.72
FeO_T	6.79	6.83	6.81	6.58	6.81	7.09	6.63	6.87	6.92	7.21	6.91	7.2	6.50	6.71	6.62	6.67
Cation calculation based on 6 oxygens and Fe^{2+}/Fe^{3+} adjusted to 4 cations																
Si	1.873	1.874	1.871	1.879	1.865	1.861	1.897	1.876	1.863	1.859	1.865	1.867	1.934	1.942	1.913	1.932
Al^{IV}	0.127	0.126	0.129	0.121	0.135	0.139	0.103	0.124	0.137	0.141	0.135	0.133	0.066	0.053	0.087	0.068
Total	2.000	2.000	2.000	2.000	2.000	2.000	2.000	2.000	2.000	2.000	2.000	2.000	2.000	1.995	2.000	2.000
Ti^{4+}	0.014	0.013	0.014	0.012	0.014	0.014	0.012	0.013	0.015	0.015	0.012	0.013	0.009	0.007	0.011	0.008
Al^{VI}	0.031	0.020	0.019	0.009	0.019	0.023	0.022	0.021	0.028	0.024	0.014	0.022	0.010	0.000	0.012	0.011
Cr^{3+}	0.000	0.000	0.000	0.000	0.000	0.000	0.000	0.000	0.000	0.000	0.000	0.000	0.000	0.000	0.000	0.000
Fe^{3+}	0.095	0.104	0.107	0.116	0.115	0.116	0.083	0.102	0.105	0.112	0.119	0.111	0.065	0.076	0.082	0.067
Fe^{2+}	0.117	0.109	0.104	0.088	0.097	0.105	0.124	0.112	0.111	0.113	0.096	0.113	0.138	0.134	0.126	0.141
Mn	0.009	0.009	0.008	0.009	0.010	0.009	0.010	0.010	0.009	0.009	0.008	0.010	0.013	0.016	0.012	0.013
Mg	0.811	0.817	0.816	0.832	0.808	0.804	0.828	0.802	0.798	0.791	0.811	0.803	0.864	0.861	0.855	0.863
Ca	0.895	0.904	0.905	0.908	0.911	0.900	0.894	0.912	0.907	0.911	0.919	0.901	0.874	0.883	0.875	0.869
Na	0.028	0.025	0.026	0.027	0.027	0.029	0.027	0.027	0.027	0.026	0.022	0.027	0.027	0.028	0.029	0.028
MG #	87.39	88.23	88.70	90.43	89.28	88.45	86.97	87.75	87.79	87.50	89.42	87.66	86.23	86.53	87.16	85.96

MG# = 100•Mg/(Mg + Fe^{2+}) c=core; r=rim; i=interior

Appendix C. Table C.5 (continued)

Sample	IM-306	IM-306	IM-306	IM-306	IM-306	IM-306	IM-306	IM-306	IM-306	IM-306	IM-306	IM-306	IM-306	IM-306	IM-306	IM-306
Grain	2	3	3	4	4	4	4	5	5	5	6	6	7	7	7	8
Position	i	i	i	i	c	c	r	i	c	r	r	c	r	i	c	i
SiO_2	51.03	51.58	50.25	50.31	49.65	49.61	50.93	51.51	51.18	51.57	52.28	51.29	51.69	50.32	50.76	51.62
TiO_2	0.37	0.37	0.44	0.53	0.49	0.50	0.40	0.36	0.39	0.38	0.32	0.39	0.33	0.38	0.32	0.28
Al_2O_3	2.09	2.04	2.23	2.83	3.00	3.14	2.22	2.01	2.29	2.17	1.61	2.05	1.81	2.19	1.78	1.66
Cr_2O_3	b.d.	b.d.	b.d.	b.d.	b.d.	b.d.	b.d.	b.d.	b.d.	b.d.	b.d.	b.d.	b.d.	b.d.	b.d.	b.d.
Fe_2O_3	3.23	2.64	4.65	3.52	4.36	4.00	2.73	2.35	2.50	2.90	2.13	3.02	2.47	4.44	3.61	3.02
FeO	3.91	4.58	2.94	3.61	2.91	3.44	4.12	4.44	4.58	4.38	4.18	3.89	4.54	2.77	3.23	4.13
MnO	0.41	0.45	0.43	0.35	0.39	0.34	0.43	0.41	0.44	0.50	0.43	0.44	0.42	0.46	0.48	0.42
MgO	15.28	15.39	15.37	14.80	14.71	14.43	15.17	15.48	15.28	15.53	15.52	15.48	15.54	15.34	15.51	15.51
CaO	21.90	21.49	21.84	22.22	22.07	21.98	21.73	21.62	21.44	21.70	22.66	21.91	21.56	21.98	21.81	21.78
Na_2O	0.38	0.44	0.38	0.40	0.44	0.46	0.40	0.39	0.40	0.36	0.33	0.37	0.40	0.39	0.37	0.41
TOTAL	98.6	98.98	98.53	98.57	98.02	97.9	98.13	98.57	98.5	99.49	99.46	98.84	98.76	98.27	97.87	98.83
FeO_T	6.82	6.96	7.12	6.78	6.83	7.04	6.58	6.55	6.83	6.99	6.10	6.61	6.76	6.77	6.48	6.85
Cation calculation based on 6 oxygens and Fe^{2+}/Fe^{3+} adjusted to 4 cations																
Si	1.911	1.923	1.886	1.887	1.873	1.875	1.915	1.926	1.917	1.914	1.938	1.915	1.930	1.892	1.913	1.928
Al^{IV}	0.089	0.077	0.099	0.113	0.127	0.125	0.085	0.074	0.083	0.086	0.062	0.085	0.070	0.097	0.079	0.072
Total	2.000	2.000	1.985	2.000	2.000	2.000	2.000	2.000	2.000	2.000	2.000	2.000	2.000	1.989	1.992	2.000
Ti^{4+}	0.010	0.010	0.012	0.015	0.014	0.014	0.011	0.010	0.011	0.011	0.009	0.011	0.009	0.011	0.009	0.008
Al^{VI}	0.003	0.013	0.000	0.012	0.006	0.015	0.013	0.015	0.018	0.009	0.008	0.005	0.010	0.000	0.000	0.001
Cr^{3+}	0.000	0.000	0.000	0.000	0.000	0.000	0.000	0.000	0.000	0.000	0.000	0.000	0.000	0.000	0.000	0.000
Fe^{3+}	0.091	0.074	0.131	0.099	0.124	0.114	0.077	0.066	0.071	0.081	0.059	0.085	0.069	0.126	0.102	0.085
Fe^{2+}	0.123	0.143	0.092	0.113	0.092	0.109	0.130	0.139	0.143	0.136	0.129	0.121	0.142	0.087	0.102	0.129
Mn	0.013	0.014	0.014	0.011	0.012	0.011	0.014	0.013	0.014	0.016	0.013	0.014	0.013	0.015	0.015	0.013
Mg	0.853	0.856	0.860	0.828	0.827	0.813	0.850	0.863	0.853	0.859	0.858	0.861	0.865	0.860	0.872	0.864
Ca	0.879	0.859	0.878	0.893	0.892	0.89	0.875	0.866	0.861	0.863	0.9	0.876	0.863	0.885	0.881	0.871
Na	0.028	0.032	0.028	0.029	0.032	0.034	0.029	0.028	0.029	0.026	0.024	0.027	0.029	0.028	0.027	0.030
MG #	87.40	85.69	90.34	87.99	89.99	88.18	86.73	86.13	85.64	86.33	86.93	87.68	85.90	90.81	89.53	87.01

Appendix C. Table C.5 (continued)

Sample	IM-306	IM-120	IM-120	IM-120	IM-120	IM-120	IM-120	IM-120	IM-120	IM-120	IM-120	IM-120	IM-120	IM-120	IM-120	IM-120
Grain	8	1	1	2	1	1	3	3	3	3	3	4	4	4	4	5
Position	i	r	i	r	i	c	r	i	c	C(dup)	r	i	c	i	r	r
SiO_2	51.71	49.02	49.74	50.11	50.55	49.81	50.10	49.58	49.20	49.31	49.20	49.91	48.51	49.65	50.06	50.56
TiO_2	0.27	0.67	0.53	0.57	0.41	0.53	0.55	0.62	0.67	0.61	0.67	0.56	0.71	0.58	0.58	0.52
Al_2O_3	1.90	3.77	3.73	3.42	2.46	3.30	3.25	3.68	3.82	3.77	3.88	3.18	4.43	3.48	3.20	2.85
Cr_2O_3	b.d.	b.d.	b.d.	b.d.	b.d.	b.d.	b.d.	b.d.	b.d.	b.d.	b.d.	b.d.	b.d.	b.d.	b.d.	b.d.
Fe_2O_3	2.28	4.51	3.21	3.03	3.91	3.27	3.67	3.78	4.25	4.67	4.25	3.92	4.67	3.75	3.29	3.23
FeO	5.06	2.97	3.94	4.05	3.09	3.79	3.42	3.70	3.12	2.90	3.02	3.27	2.96	3.44	3.76	3.46
MnO	0.48	0.34	0.32	0.31	0.34	0.25	0.32	0.35	0.30	0.28	0.32	0.31	0.25	0.30	0.27	0.30
MgO	15.31	14.38	14.19	14.58	15.25	14.46	14.80	14.36	14.29	14.40	14.41	14.65	13.91	14.44	14.74	14.98
CaO	21.40	22.28	22.45	22.20	22.26	22.24	22.25	22.18	22.38	22.51	22.31	22.48	22.60	22.46	22.12	22.46
Na_2O	0.40	0.38	0.36	0.36	0.37	0.38	0.39	0.39	0.41	0.40	0.40	0.37	0.37	0.36	0.38	0.37
TOTAL	98.81	98.32	98.47	98.63	98.64	98.03	98.75	98.64	98.44	98.85	98.46	98.65	98.41	98.46	98.40	98.73
FeO_T	7.11	7.03	6.83	6.78	6.61	6.73	6.72	7.10	6.94	7.10	6.84	6.80	7.16	6.81	6.72	6.37
Cation calculation based on 6 oxygens and Fe^{2+}/Fe^{3+} adjusted to 4 cations																
Si	1.933	1.847	1.870	1.878	1.892	1.879	1.875	1.862	1.851	1.848	1.849	1.872	1.828	1.866	1.880	1.890
Al^{IV}	0.067	0.153	0.130	0.122	0.108	0.121	0.125	0.138	0.149	0.152	0.151	0.128	0.172	0.134	0.120	0.110
Total	2.000	2.000	2.000	2.000	2.000	2.000	2.000	2.000	2.000	2.000	2.000	2.000	2.000	2.000	2.000	2.000
Ti^{4+}	0.008	0.019	0.015	0.016	0.012	0.015	0.015	0.018	0.019	0.017	0.019	0.016	0.020	0.016	0.016	0.015
Al^{VI}	0.017	0.014	0.035	0.029	0.001	0.026	0.018	0.025	0.020	0.014	0.021	0.013	0.025	0.020	0.022	0.016
Cr^{3+}	0.000	0.000	0.000	0.000	0.000	0.000	0.000	0.000	0.000	0.000	0.000	0.000	0.000	0.000	0.000	0.000
Fe^{3+}	0.064	0.128	0.091	0.086	0.110	0.093	0.103	0.107	0.120	0.132	0.120	0.111	0.132	0.106	0.093	0.091
Fe^{2+}	0.158	0.094	0.124	0.127	0.097	0.120	0.107	0.116	0.098	0.091	0.095	0.103	0.093	0.108	0.118	0.108
Mn	0.015	0.011	0.010	0.010	0.011	0.008	0.010	0.011	0.010	0.009	0.010	0.010	0.008	0.010	0.009	0.009
Mg	0.853	0.808	0.795	0.815	0.851	0.813	0.826	0.804	0.801	0.805	0.808	0.819	0.782	0.809	0.825	0.835
Ca	0.857	0.899	0.904	0.892	0.893	0.899	0.892	0.892	0.902	0.904	0.898	0.903	0.913	0.905	0.890	0.900
Na	0.029	0.028	0.026	0.026	0.027	0.028	0.028	0.028	0.030	0.029	0.029	0.027	0.027	0.026	0.028	0.027
MG #	84.37	89.58	86.51	86.52	89.77	87.14	88.53	87.39	89.10	89.84	89.48	88.83	89.37	88.22	87.49	88.55

Appendix C. Table C.5 (continued)

Sample	IM-120	IM-120	IM-120	IM-120	IM-120	IM-120	IM-120	IM-120	IM-120	IM-256	IM-256	IM-256	IM-256	IM-256	IM-256	IM-256
Grain	5	5	6	6	6	6	6	7	7	1	1	1	1	1	1	1
Position	i	i	r	i	c	i	i	r	i	i	i	c	i	i	r	c
SiO_2	49.15	50.39	49.79	48.50	48.24	48.19	49.44	49.80	50.20	49.95	49.08	49.68	49.15	50.18	51.78	51.42
TiO_2	0.64	0.44	0.56	0.78	0.73	0.75	0.59	0.62	0.51	0.69	0.66	0.60	0.71	0.66	0.33	0.53
Al_2O_3	4.04	2.92	3.24	4.32	4.80	4.76	3.66	3.78	3.19	3.43	4.25	3.84	4.13	3.32	1.98	2.31
Cr_2O_3	b.d.	b.d.	b.d.	b.d.	b.d.	b.d.	b.d.	b.d.	b.d.	b.d.	b.d.	b.d.	b.d.	b.d.	b.d.	b.d.
Fe_2O_3	4.14	3.25	3.53	4.94	4.48	4.35	4.06	2.92	3.27	4.12	4.79	4.15	4.56	4.02	3.17	3.03
FeO	3.24	3.42	3.52	2.65	3.37	3.27	3.37	4.28	3.78	3.59	2.91	3.20	3.09	3.83	3.43	2.63
MnO	0.29	0.36	0.30	0.30	0.23	0.23	0.29	0.33	0.30	0.31	0.22	0.27	0.24	0.30	0.49	0.28
MgO	14.22	14.94	14.67	14.16	13.72	13.73	14.41	14.42	14.66	14.51	14.34	14.55	14.42	14.58	15.37	15.62
CaO	22.36	22.36	22.16	22.39	22.18	22.28	22.30	21.87	22.24	22.48	22.56	22.56	22.50	22.26	22.80	23.41
Na_2O	0.4	0.35	0.37	0.4	0.41	0.39	0.38	0.39	0.39	0.39	0.37	0.36	0.34	0.43	0.37	0.27
TOTAL	98.48	98.43	98.14	98.44	98.16	97.95	98.50	98.41	98.54	99.47	99.18	99.21	99.14	99.58	99.72	99.50
FeO_T	6.97	6.34	6.70	7.10	7.40	7.18	7.02	6.91	6.72	7.30	7.22	6.93	7.19	7.45	6.28	5.36
Cation calculation based on 6 oxygens and Fe^{2+}/Fe^{3+} adjusted to 4 cations																
Si	1.848	1.890	1.875	1.826	1.823	1.824	1.858	1.871	1.883	1.861	1.834	1.853	1.837	1.868	1.916	1.902
Al^{IV}	0.152	0.110	0.125	0.174	0.177	0.176	0.142	0.129	0.117	0.139	0.166	0.147	0.163	0.132	0.084	0.098
Total	2.000	2.000	2.000	2.000	2.000	2.000	2.000	2.000	2.000	2.000	2.000	2.000	2.000	2.000	2.000	2.000
Ti^{4+}	0.018	0.012	0.016	0.022	0.021	0.021	0.017	0.018	0.014	0.019	0.019	0.017	0.020	0.018	0.009	0.015
Al^{VI}	0.027	0.019	0.019	0.018	0.037	0.036	0.020	0.038	0.024	0.012	0.021	0.022	0.019	0.014	0.002	0.003
Cr^{3+}	0.000	0.000	0.000	0.000	0.000	0.000	0.000	0.000	0.000	0.000	0.000	0.000	0.000	0.000	0.000	0.000
Fe^{3+}	0.117	0.092	0.100	0.140	0.127	0.124	0.115	0.082	0.092	0.115	0.135	0.116	0.128	0.112	0.088	0.084
Fe^{2+}	0.102	0.107	0.111	0.083	0.106	0.104	0.106	0.134	0.119	0.112	0.091	0.100	0.097	0.119	0.106	0.081
Mn	0.009	0.011	0.010	0.010	0.007	0.007	0.009	0.011	0.010	0.010	0.007	0.009	0.008	0.009	0.015	0.009
Mg	0.797	0.835	0.824	0.795	0.773	0.775	0.808	0.808	0.820	0.806	0.799	0.809	0.803	0.809	0.848	0.861
Ca	0.901	0.898	0.894	0.903	0.898	0.904	0.898	0.880	0.894	0.898	0.903	0.902	0.901	0.888	0.904	0.928
Na	0.029	0.025	0.027	0.029	0.030	0.029	0.028	0.028	0.028	0.028	0.027	0.026	0.025	0.031	0.027	0.019
MG #	88.65	88.64	88.13	90.55	87.94	88.17	88.40	85.77	87.33	87.80	89.78	89.00	89.22	87.18	88.89	91.40

Appendix C. Table C.5 (continued)

Sample	IM-256	IM-256	IM-256	IM-256	IM-256	IM-256	IM-256	IM-256	IM-256	IM-256	IM-256	IM-256	IM-256	IM-256	IM-256	IM-256
Grain	1	2	2	2	2	3	3	3	4	4	5	5	5	5	5	6
Position	r	r	i	c	r	r	c	r	r	c	i	i	c	i	r	r
SiO_2	49.77	49.43	50.49	50.78	49.69	50.23	49.45	49.81	50.10	50.40	51.74	50.23	50.35	50.23	49.39	51.35
TiO_2	0.64	0.78	0.63	0.46	0.73	0.56	0.83	0.60	0.64	0.63	0.35	0.62	0.55	0.58	0.72	0.44
Al_2O_3	3.69	4.21	3.09	2.56	3.60	3.34	4.21	3.58	3.57	3.15	2.21	3.13	3.08	3.37	3.76	2.61
Cr_2O_3	b.d.	b.d.	b.d.	b.d.	b.d.	b.d.	b.d.	b.d.	b.d.	b.d.	b.d.	b.d.	b.d.	b.d.	b.d.	b.d.
Fe_2O_3	4.24	5.03	4.15	3.58	3.89	4.05	3.70	4.37	4.03	4.34	3.19	3.55	3.86	3.81	4.75	4.47
FeO	3.16	3.09	3.53	4.00	3.69	3.35	4.00	3.01	3.32	3.00	3.30	3.89	3.30	3.30	2.69	1.66
MnO	0.22	0.27	0.31	0.36	0.37	0.32	0.27	0.25	0.31	0.32	0.38	0.37	0.33	0.38	0.33	0.33
MgO	14.67	14.33	14.75	14.77	14.51	14.82	14.17	14.75	14.75	15.06	15.92	14.50	14.98	14.81	14.75	15.14
CaO	22.39	22.66	22.62	22.41	22.11	22.44	22.12	22.35	22.54	22.44	22.20	22.21	22.24	22.42	22.37	23.11
Na_2O	0.41	0.41	0.40	0.38	0.40	0.38	0.44	0.42	0.37	0.42	0.37	0.45	0.41	0.39	0.38	0.70
TOTAL	99.19	100.21	99.97	99.30	98.99	99.49	99.19	99.14	99.63	99.76	99.66	98.95	99.10	99.29	99.14	99.81
FeO_T	6.98	7.62	7.26	7.22	7.19	6.99	7.33	6.94	6.95	6.91	6.17	7.08	6.77	6.73	6.96	5.68
Cation calculation based on 6 oxygens and Fe^{2+}/Fe^{3+} adjusted to 4 cations																
Si	1.856	1.831	1.871	1.894	1.859	1.868	1.848	1.858	1.861	1.868	1.911	1.879	1.877	1.870	1.844	1.894
Al^{IV}	0.144	0.169	0.129	0.106	0.141	0.132	0.152	0.142	0.139	0.132	0.089	0.121	0.123	0.130	0.156	0.106
Total	2.000	2.000	2.000	2.000	2.000	2.000	2.000	2.000	2.000	2.000	2.000	2.000	2.000	2.000	2.000	2.000
Ti^{4+}	0.018	0.022	0.018	0.013	0.021	0.016	0.023	0.017	0.018	0.018	0.010	0.017	0.015	0.016	0.020	0.012
Al^{VI}	0.018	0.015	0.006	0.007	0.018	0.014	0.033	0.015	0.017	0.006	0.007	0.017	0.012	0.018	0.009	0.007
Cr^{3+}	0.000	0.000	0.000	0.000	0.000	0.000	0.000	0.000	0.000	0.000	0.000	0.000	0.000	0.000	0.000	0.000
Fe^{3+}	0.119	0.140	0.116	0.100	0.110	0.113	0.104	0.123	0.113	0.121	0.089	0.100	0.108	0.107	0.134	0.124
Fe^{2+}	0.099	0.096	0.109	0.125	0.115	0.104	0.125	0.094	0.103	0.093	0.102	0.122	0.103	0.103	0.084	0.051
Mn	0.007	0.008	0.010	0.011	0.012	0.010	0.009	0.008	0.010	0.010	0.012	0.012	0.010	0.012	0.010	0.010
Mg	0.816	0.791	0.815	0.821	0.810	0.822	0.789	0.820	0.817	0.832	0.877	0.809	0.833	0.822	0.821	0.832
Ca	0.895	0.899	0.898	0.896	0.886	0.894	0.885	0.893	0.897	0.891	0.878	0.890	0.888	0.894	0.895	0.913
Na	0.03	0.029	0.029	0.027	0.029	0.027	0.032	0.03	0.027	0.03	0.026	0.033	0.03	0.028	0.028	0.05
MG #	89.18	89.18	88.20	86.79	87.57	88.77	86.32	89.72	88.80	89.95	89.58	86.90	89.00	88.86	90.72	94.22

Appendix C. Table C.5 (continued)

Sample	IM-256	IM-256	IM-121	IM-121	IM-121	IM-121	IM-121	IM-121	IM-121	IM-121	IM-121	IM-121	IM-121	IM-121	IM-121	IM-121
Grain	6	6	1	1	1	1	1	2	2	2	2	3	3	3	4	4
Position	i	c	r	i	c	i	r	r	c	i	r	i	c	i	i	c
SiO_2	50.78	50.04	50.65	50.55	50.72	50.92	50.80	50.26	50.37	50.32	50.50	49.92	50.78	50.68	50.81	50.97
TiO_2	0.58	0.66	0.34	0.34	0.33	0.31	0.37	0.44	0.42	0.40	0.43	0.40	0.36	0.35	0.39	0.32
Al_2O_3	2.65	3.30	3.15	3.09	3.08	3.02	3.08	3.53	3.42	3.60	3.15	3.29	2.95	3.16	3.04	2.64
Cr_2O_3	b.d.	b.d.	b.d.	b.d.	b.d.	b.d.	b.d.	b.d.	b.d.	b.d.	b.d.	0.06	b.d.	b.d.	b.d.	b.d.
Fe_2O_3	3.22	4.04	3.15	3.71	3.10	3.17	3.12	4.06	3.51	3.37	3.32	4.36	3.14	3.58	2.73	3.15
FeO	4.26	3.99	3.01	2.44	3.08	2.98	3.22	2.70	3.11	3.21	2.87	2.38	2.94	2.69	3.59	3.09
MnO	0.36	0.33	0.08	0.09	0.14	0.13	0.11	0.15	0.11	0.14	0.15	0.14	0.15	0.12	0.20	0.17
MgO	14.83	14.44	15.30	15.44	15.38	15.36	15.28	14.90	14.96	15.05	15.22	15.12	15.46	15.38	15.16	15.52
CaO	22.14	22.17	22.97	23.16	22.78	23.10	23.01	23.24	23.06	22.85	23.06	22.99	22.95	23.08	22.66	22.74
Na_2O	0.40	0.43	0.24	0.23	0.25	0.24	0.23	0.29	0.26	0.24	0.24	0.25	0.22	0.25	0.28	0.26
TOTAL	99.22	99.4	98.89	99.05	98.86	99.23	99.22	99.57	99.22	99.18	98.94	98.91	98.95	99.29	98.86	98.86
FeO_T	7.16	7.63	5.84	5.78	5.87	5.83	6.03	6.35	6.27	6.24	5.86	6.30	5.77	5.91	6.05	5.92
Cation calculation based on 6 oxygens and Fe^{2+}/Fe^{3+} adjusted to 4 cations																
Si	1.894	1.867	1.886	1.879	1.888	1.889	1.887	1.864	1.873	1.871	1.881	1.863	1.889	1.880	1.894	1.898
Al^{IV}	0.106	0.133	0.114	0.121	0.112	0.111	0.113	0.136	0.127	0.129	0.119	0.137	0.111	0.120	0.106	0.102
Total	2.000	2.000	2.000	2.000	2.000	2.000	2.000	2.000	2.000	2.000	2.000	2.000	2.000	2.000	2.000	2.000
Ti^{4+}	0.016	0.019	0.010	0.010	0.009	0.009	0.010	0.012	0.012	0.011	0.012	0.011	0.010	0.010	0.011	0.009
Al^{VI}	0.011	0.012	0.024	0.014	0.023	0.021	0.022	0.018	0.023	0.029	0.019	0.008	0.018	0.018	0.028	0.014
Cr^{3+}	0.000	0.000	0.000	0.000	0.000	0.000	0.000	0.000	0.000	0.000	0.000	0.002	0.000	0.000	0.000	0.000
Fe^{3+}	0.090	0.113	0.088	0.104	0.087	0.088	0.087	0.113	0.098	0.094	0.093	0.122	0.088	0.100	0.076	0.088
Fe^{2+}	0.133	0.125	0.094	0.076	0.096	0.092	0.100	0.084	0.097	0.100	0.089	0.074	0.092	0.083	0.112	0.096
Mn	0.011	0.010	0.003	0.003	0.004	0.004	0.003	0.005	0.003	0.004	0.005	0.004	0.005	0.004	0.006	0.005
Mg	0.825	0.803	0.849	0.856	0.854	0.850	0.846	0.824	0.829	0.834	0.845	0.841	0.857	0.851	0.842	0.862
Ca	0.885	0.886	0.916	0.922	0.909	0.918	0.916	0.923	0.919	0.91	0.92	0.919	0.915	0.917	0.905	0.907
Na	0.029	0.031	0.017	0.017	0.018	0.017	0.017	0.021	0.019	0.017	0.017	0.018	0.016	0.018	0.020	0.019
MG #	86.12	86.53	90.03	91.85	89.89	90.23	89.43	90.75	89.52	89.29	90.47	91.91	90.31	91.11	88.26	89.98

Appendix C. Table C.5 (continued)

Sample	IM-121	IM-121	IM-121	IM-121	IM-121	IM-121	IM-121	IM-268	IM-268	IM-268	IM-268	IM-268	IM-268	IM-268	IM-268	IM-268
Grain	4	5	5	5	5	5	5	1	1	1	2	2	3	4	5	5
Position	i	i	c	i	i	i	i	i	c	r	r	c	c	c	i	i
SiO_2	50.89	50.17	49.92	50.40	50.03	51.22	50.56	50.25	49.53	50.03	49.32	49.84	48.30	48.15	49.48	48.88
TiO_2	0.34	0.42	0.41	0.41	0.44	0.31	0.37	0.66	0.55	0.48	0.58	0.51	0.69	0.76	0.51	0.63
Al_2O_3	3.00	3.69	3.40	3.39	3.62	2.74	3.44	3.68	4.18	3.75	4.40	3.84	5.12	5.36	3.61	4.73
Cr_2O_3	b.d.	b.d.	0.07	b.d.	b.d.	b.d.	b.d.	b.d.	b.d.	b.d.	b.d.	b.d.	b.d.	b.d.	b.d.	b.d.
Fe_2O_3	3.20	3.59	3.69	3.40	3.56	2.72	2.96	3.61	3.42	3.51	3.68	3.97	5.02	4.83	4.57	4.89
FeO	3.06	3.13	2.82	2.87	3.10	3.27	3.36	2.35	3.24	3.26	3.11	2.88	3.03	2.86	2.69	2.38
MnO	0.15	0.18	0.20	0.14	0.20	0.15	0.15	0.21	0.22	0.23	0.20	0.19	0.14	0.13	0.18	0.18
MgO	15.35	14.87	15.03	15.16	14.78	15.43	15.04	14.90	14.13	14.49	13.93	14.41	13.62	13.54	14.59	14.07
CaO	22.92	22.93	22.73	23.01	23.02	22.97	22.94	23.72	23.16	22.98	23.38	23.33	23.04	23.28	23.01	23.32
Na_2O	0.27	0.26	0.25	0.25	0.24	0.26	0.24	0.26	0.31	0.33	0.31	0.31	0.31	0.29	0.28	0.33
TOTAL	99.18	99.24	98.52	99.03	98.99	99.07	99.06	99.64	98.74	99.06	98.91	99.28	99.27	99.20	98.92	99.41
FeO_T	5.94	6.36	6.14	5.93	6.30	5.72	6.02	5.60	6.32	6.42	6.42	6.45	7.55	7.21	6.80	6.78
Cation calculation based on 6 oxygens and Fe^{2+}/Fe^{3+} adjusted to 4 cations																
Si	1.890	1.866	1.869	1.875	1.866	1.902	1.881	1.860	1.855	1.866	1.846	1.857	1.808	1.803	1.852	1.821
Al^{IV}	0.110	0.134	0.131	0.125	0.134	0.098	0.119	0.140	0.145	0.134	0.154	0.143	0.192	0.197	0.148	0.179
Total	2.000	2.000	2.000	2.000	2.000	2.000	2.000	2.000	2.000	2.000	2.000	2.000	2.000	2.000	2.000	2.000
Ti^{4+}	0.009	0.012	0.012	0.011	0.012	0.009	0.010	0.018	0.015	0.013	0.016	0.014	0.019	0.021	0.014	0.018
Al^{VI}	0.021	0.028	0.019	0.024	0.025	0.022	0.032	0.021	0.039	0.031	0.040	0.026	0.034	0.039	0.011	0.029
Cr^{3+}	0.000	0.000	0.002	0.000	0.000	0.000	0.000	0.000	0.000	0.000	0.000	0.000	0.000	0.000	0.000	0.000
Fe^{3+}	0.089	0.100	0.104	0.095	0.100	0.076	0.083	0.101	0.096	0.098	0.104	0.111	0.141	0.136	0.129	0.137
Fe^{2+}	0.095	0.097	0.088	0.089	0.097	0.102	0.105	0.073	0.101	0.102	0.097	0.090	0.095	0.089	0.084	0.074
Mn	0.005	0.006	0.006	0.004	0.006	0.005	0.005	0.007	0.007	0.007	0.006	0.006	0.004	0.004	0.006	0.006
Mg	0.85	0.825	0.839	0.841	0.822	0.854	0.834	0.822	0.789	0.806	0.777	0.8	0.76	0.756	0.814	0.782
Ca	0.912	0.914	0.912	0.917	0.920	0.914	0.914	0.941	0.929	0.919	0.937	0.931	0.924	0.934	0.923	0.931
Na	0.019	0.019	0.018	0.018	0.017	0.019	0.017	0.019	0.023	0.024	0.022	0.022	0.022	0.021	0.020	0.024
MG #	89.95	89.48	90.51	90.43	89.45	89.33	88.82	91.84	88.65	88.77	88.90	89.89	88.89	89.47	90.65	91.36

Appendix C. Table C.5 (continued)

Sample	IM-268	IM-268	IM-268	IM-268	IM-268	IM-268	IM-268	IM-268	IM-268	IM-268	IM-268	IM-268	IM-268	IM-268	IM-268
Grain	6	6	6	7	7	7	8	9	9	9	10	10	11	12	13
Position	r	c	i	r	c	i	c	r	c	i	c	i	c	c	c
SiO_2	49.37	48.53	48.66	48.64	49.83	49.31	49.42	49.62	47.61	49.24	49.87	49.66	50.06	49.77	49.01
TiO_2	0.56	0.70	0.66	0.70	0.56	0.60	0.63	0.50	0.86	0.64	0.52	0.58	0.52	0.49	0.68
Al_2O_3	4.12	4.88	4.80	5.01	3.89	4.36	4.44	3.88	5.94	4.55	3.92	4.16	3.78	3.99	4.79
Cr_2O_3	b.d.	b.d.	b.d.	b.d.	b.d.	b.d.	b.d.	b.d.	b.d.	b.d.	b.d.	b.d.	b.d.	b.d.	b.d.
Fe_2O_3	4.68	4.16	4.73	4.62	3.81	3.71	4.47	4.09	4.59	3.99	4.07	4.14	4.27	4.14	4.18
FeO	3.00	3.41	2.81	2.76	3.28	3.46	3.12	3.30	3.11	3.11	2.63	2.95	2.81	2.90	3.09
MnO	0.14	0.18	0.20	0.19	0.19	0.21	0.16	0.16	0.20	0.18	0.19	0.14	0.21	0.16	0.21
MgO	14.11	13.77	13.80	13.64	14.42	14.00	14.17	14.52	13.21	14.00	14.48	14.32	14.79	14.32	14.00
CaO	22.97	22.62	23.09	23.33	22.96	23.08	23.16	22.81	22.87	23.19	23.43	23.29	23.02	23.24	23.03
Na_2O	0.40	0.34	0.35	0.36	0.33	0.29	0.32	0.27	0.34	0.33	0.32	0.32	0.32	0.35	0.32
TOTAL	99.35	98.59	99.10	99.25	99.27	99.02	99.89	99.15	98.73	99.23	99.43	99.56	99.78	99.36	99.31
FeO_T	7.21	7.15	7.07	6.92	6.71	6.80	7.14	6.98	7.24	6.70	6.29	6.68	6.65	6.63	6.85
Cation calculation based on 6 oxygens and Fe^{2+}/Fe^{3+} adjusted to 4 cations															
Si	1.842	1.825	1.821	1.818	1.857	1.845	1.834	1.853	1.791	1.838	1.854	1.846	1.855	1.853	1.828
Al^{IV}	0.158	0.175	0.179	0.182	0.143	0.155	0.166	0.147	0.209	0.162	0.146	0.154	0.145	0.147	0.172
Total	2.000	2.000	2.000	2.000	2.000	2.000	2.000	2.000	2.000	2.000	2.000	2.000	2.000	2.000	2.000
Ti^{4+}	0.016	0.020	0.019	0.020	0.016	0.017	0.018	0.014	0.024	0.018	0.015	0.016	0.014	0.014	0.019
Al^{VI}	0.023	0.041	0.033	0.039	0.028	0.037	0.028	0.024	0.054	0.038	0.026	0.028	0.020	0.028	0.039
Cr^{3+}	0.000	0.000	0.000	0.000	0.000	0.000	0.000	0.000	0.000	0.000	0.000	0.000	0.000	0.000	0.000
Fe^{3+}	0.131	0.118	0.133	0.130	0.107	0.104	0.125	0.115	0.130	0.112	0.114	0.116	0.119	0.116	0.117
Fe^{2+}	0.093	0.107	0.088	0.086	0.102	0.108	0.097	0.103	0.098	0.097	0.082	0.092	0.087	0.090	0.096
Mn	0.004	0.006	0.006	0.006	0.006	0.007	0.005	0.005	0.006	0.006	0.006	0.004	0.007	0.005	0.007
Mg	0.785	0.772	0.770	0.760	0.801	0.781	0.784	0.808	0.741	0.779	0.803	0.794	0.817	0.795	0.779
Ca	0.918	0.911	0.926	0.934	0.917	0.925	0.921	0.912	0.922	0.927	0.933	0.928	0.914	0.927	0.920
Na	0.029	0.025	0.025	0.026	0.024	0.021	0.023	0.02	0.025	0.024	0.023	0.023	0.023	0.025	0.023
MG #	89.41	87.83	89.74	89.83	88.70	87.85	88.99	88.69	88.32	88.93	90.73	89.62	90.38	89.83	89.03

Appendix C. Table C.6 Electron Microprobe analyses of clinopyroxene from Nicola Group rocks.

Sample	IM-185	IM-185	IM-185	IM-185	IM-185	IM-185	IM-185	IM-185	IM-185	IM-185	IM-185	IM-185	IM-185	IM-185	IM-276	IM-276
Grain	1	1	1	1	2	2	2	2	2	2	3	3	3	3	1	1
Position	r	i	c	i	r	i	c	i	r	r	c	i	r	i	r	i
SiO_2	49.91	50.72	49.94	50.32	49.96	50.93	50.60	49.76	50.90	51.86	49.62	50.95	49.35	49.39	51.22	50.40
TiO_2	0.50	0.41	0.42	0.39	0.50	0.32	0.37	0.50	0.40	0.29	0.49	0.34	0.46	0.58	0.24	0.29
Al_2O_3	3.78	2.81	3.34	3.33	3.50	2.93	3.26	3.90	2.88	1.99	3.70	2.64	3.81	4.35	1.63	1.57
Cr_2O_3	b.d.	b.d.	0.09	b.d.	b.d.	0.13	b.d.	b.d.	b.d.	b.d.	0.07	b.d.	0.06	0.07	b.d.	b.d.
Fe_2O_3	3.18	2.94	2.93	3.11	3.62	3.08	2.62	3.65	2.81	1.92	4.04	2.91	4.05	3.93	3.67	3.83
FeO	3.94	3.10	3.76	3.70	3.78	3.36	4.31	3.63	4.16	4.41	2.84	3.26	3.25	3.07	3.87	4.42
MnO	0.19	0.17	0.15	0.17	0.16	0.24	0.22	0.16	0.17	0.20	0.14	0.17	0.20	0.20	0.54	0.46
MgO	14.20	14.67	14.49	14.51	14.24	14.98	14.50	14.12	14.70	14.81	14.27	15.23	14.23	14.31	15.98	13.69
CaO	22.75	24.18	22.67	22.93	22.85	23.05	22.64	23.02	22.93	23.70	23.74	23.01	22.76	23.09	20.98	22.78
Na_2O	0.34	0.14	0.29	0.31	0.35	0.30	0.32	0.33	0.29	0.20	0.21	0.26	0.32	0.27	0.37	0.45
TOTAL	98.79	99.14	98.08	98.77	98.96	99.32	98.84	99.07	99.24	99.38	99.12	98.77	98.49	99.26	98.50	97.89
FeO_T	6.80	5.75	6.40	6.50	7.04	6.13	6.67	6.91	6.69	6.14	6.48	5.88	6.89	6.61	7.17	7.87
Cation calculation based on 6 oxygens and Fe^{2+}/Fe^{3+} adjusted to 4 cations																
Si	1.870	1.890	1.881	1.883	1.870	1.892	1.892	1.860	1.896	1.928	1.854	1.901	1.856	1.841	1.919	1.918
Al^{IV}	0.130	0.110	0.119	0.117	0.130	0.108	0.108	0.140	0.104	0.072	0.146	0.099	0.144	0.159	0.072	0.070
Total	2.000	2.000	2.000	2.000	2.000	2.000	2.000	2.000	2.000	2.000	2.000	2.000	2.000	2.000	1.991	1.988
Ti^{4+}	0.014	0.011	0.012	0.011	0.014	0.009	0.010	0.014	0.011	0.008	0.014	0.010	0.013	0.016	0.007	0.008
Al^{VI}	0.037	0.013	0.029	0.030	0.024	0.020	0.036	0.032	0.022	0.015	0.017	0.017	0.025	0.032	0.000	0.000
Cr^{3+}	0.000	0.000	0.003	0.000	0.000	0.004	0.000	0.000	0.000	0.000	0.002	0.000	0.002	0.002	0.000	0.000
Fe^{3+}	0.090	0.083	0.083	0.087	0.102	0.086	0.074	0.103	0.079	0.054	0.114	0.082	0.115	0.110	0.103	0.110
Fe^{2+}	0.123	0.097	0.118	0.116	0.118	0.104	0.135	0.114	0.130	0.137	0.089	0.102	0.102	0.096	0.121	0.141
Mn	0.006	0.005	0.005	0.005	0.005	0.008	0.007	0.005	0.005	0.006	0.004	0.005	0.006	0.006	0.017	0.015
Mg	0.793	0.815	0.814	0.809	0.795	0.830	0.808	0.787	0.816	0.821	0.795	0.847	0.798	0.795	0.892	0.777
Ca	0.913	0.965	0.915	0.919	0.916	0.918	0.907	0.922	0.915	0.944	0.950	0.920	0.917	0.922	0.842	0.929
Na	0.025	0.01	0.021	0.022	0.025	0.022	0.023	0.024	0.021	0.014	0.015	0.019	0.023	0.02	0.027	0.033
MG #	86.57	89.36	87.34	87.46	87.08	88.87	85.68	87.35	86.26	85.70	89.93	89.25	88.67	89.23	88.06	84.64

MG# = 100•Mg/(Mg + Fe^{2+}) c=core; r=rim; i=interior

Appendix C. Table C.6 (continued)

Sample	IM-276	IM-276	IM-276	IM-276	IM-276	IM-276	IM-276	IM-276	IM-276	IM-276	IM-276	IM-276	IM-276	IM-276	IM-276	IM-276
Grain	1	1	2	2	2	2	2	2	3	3	3	3	3	3	4	4
Position	c	i	r	i	c	r	i	r	r	i	i	r	r	i	i	i
SiO_2	51.55	51.51	50.80	51.56	51.18	49.15	51.05	51.02	48.64	49.74	48.92	49.86	49.06	49.43	51.32	51.16
TiO_2	0.25	0.29	0.30	0.24	0.32	0.65	0.34	0.36	0.52	0.66	0.60	0.67	0.54	0.54	0.39	0.30
Al_2O_3	1.39	1.24	1.60	1.46	1.70	3.64	1.84	2.20	3.70	2.97	3.65	3.22	4.21	3.64	2.02	1.85
Cr_2O_3	b.d.	b.d.	b.d.	b.d.	b.d.	b.d.	b.d.	b.d.	b.d.	b.d.	b.d.	b.d.	b.d.	b.d.	b.d.	b.d.
Fe_2O_3	3.21	3.00	3.05	3.12	3.07	4.06	3.38	3.33	4.85	3.90	4.84	3.60	4.96	4.51	3.42	3.57
FeO	4.64	5.11	4.46	4.45	4.29	3.96	3.96	4.27	2.44	3.89	2.93	4.62	2.28	2.66	4.33	4.53
MnO	0.55	0.53	0.59	0.60	0.53	0.41	0.50	0.43	0.17	0.28	0.19	0.32	0.11	0.14	0.48	0.56
MgO	14.17	13.89	14.47	14.92	14.85	14.46	14.51	14.63	14.69	14.54	14.51	14.25	14.65	14.91	15.10	14.31
CaO	22.95	23.05	22.12	22.09	22.18	21.30	22.72	22.24	22.44	21.98	22.36	21.90	23.04	22.81	21.77	22.18
Na_2O	0.44	0.42	0.40	0.42	0.39	0.42	0.42	0.45	0.24	0.40	0.31	0.40	0.25	0.22	0.46	0.53
TOTAL	99.15	99.04	97.79	98.86	98.51	98.05	98.72	98.93	97.69	98.36	98.31	98.84	99.1	98.86	99.29	98.99
FeO_T	7.53	7.81	7.20	7.26	7.05	7.61	7.00	7.27	6.80	7.40	7.29	7.86	6.74	6.72	7.41	7.74
Cation calculation based on 6 oxygens and Fe^{2+}/Fe^{3+} adjusted to 4 cations																
Si	1.933	1.937	1.926	1.932	1.924	1.858	1.917	1.910	1.842	1.874	1.844	1.873	1.831	1.849	1.913	1.919
Al^{IV}	0.061	0.055	0.072	0.064	0.075	0.142	0.081	0.090	0.158	0.126	0.156	0.127	0.169	0.151	0.087	0.081
Total	1.994	1.992	1.998	1.996	1.999	2.000	1.998	2.000	2.000	2.000	2.000	2.000	2.000	2.000	2.000	2.000
Ti^{4+}	0.007	0.008	0.009	0.007	0.009	0.018	0.010	0.010	0.015	0.019	0.017	0.019	0.015	0.015	0.011	0.008
Al^{VI}	0.000	0.000	0.000	0.000	0.000	0.020	0.000	0.007	0.007	0.006	0.006	0.016	0.016	0.009	0.002	0.001
Cr^{3+}	0.000	0.000	0.000	0.000	0.000	0.000	0.000	0.000	0.000	0.000	0.000	0.000	0.000	0.000	0.000	0.000
Fe^{3+}	0.091	0.085	0.087	0.088	0.087	0.116	0.096	0.094	0.138	0.111	0.137	0.102	0.139	0.127	0.096	0.101
Fe^{2+}	0.145	0.161	0.141	0.140	0.135	0.125	0.124	0.134	0.077	0.123	0.092	0.145	0.071	0.083	0.135	0.142
Mn	0.017	0.017	0.019	0.019	0.017	0.013	0.016	0.014	0.005	0.009	0.006	0.010	0.003	0.004	0.015	0.018
Mg	0.792	0.779	0.818	0.833	0.832	0.815	0.812	0.817	0.829	0.817	0.816	0.798	0.815	0.831	0.839	0.800
Ca	0.922	0.929	0.899	0.887	0.893	0.863	0.914	0.892	0.91	0.887	0.903	0.881	0.921	0.914	0.869	0.891
Na	0.032	0.031	0.029	0.031	0.028	0.031	0.031	0.033	0.018	0.029	0.023	0.029	0.018	0.016	0.033	0.039
MG #	84.53	82.87	85.30	85.61	86.04	86.70	86.75	85.91	91.50	86.91	89.87	84.62	91.99	90.92	86.14	84.93

Appendix C. Table C.6 (continued)

Sample	IM-276	IM-276	IM-276	IM-276	IM-276	IM-276
Grain	5	5	5	6	6	6
Position	r	i	i	r	c	i
SiO_2	51.04	50.42	50.40	49.66	49.76	50.38
TiO_2	0.34	0.43	0.53	0.65	0.58	0.54
Al_2O_3	2.01	2.20	2.58	3.49	3.58	2.77
Cr_2O_3	b.d.	b.d.	b.d.	b.d.	b.d.	b.d.
Fe_2O_3	3.88	3.73	4.02	3.24	3.72	3.07
FeO	3.66	4.09	3.65	5.59	3.62	5.57
MnO	0.50	0.60	0.48	0.34	0.19	0.28
MgO	15.39	14.28	14.34	13.94	14.65	14.48
CaO	21.97	22.19	22.52	21.36	22.29	21.41
Na_2O	0.35	0.46	0.48	0.40	0.34	0.36
TOTAL	99.14	98.40	99.00	98.67	98.73	98.86
FeO_T	7.15	7.45	7.27	8.51	6.97	8.33
Cation calculation based on 6 oxygens						
Si	1.904	1.902	1.888	1.872	1.864	1.893
Al^{IV}	0.088	0.098	0.112	0.128	0.136	0.107
Total	1.992	2.000	2.000	2.000	2.000	2.000
Ti^{4+}	0.010	0.012	0.015	0.018	0.016	0.015
Al^{VI}	0.000	0.000	0.002	0.027	0.022	0.016
Cr^{3+}	0.000	0.000	0.000	0.000	0.000	0.000
Fe^{3+}	0.109	0.106	0.113	0.092	0.105	0.087
Fe^{2+}	0.114	0.129	0.114	0.176	0.113	0.175
Mn	0.016	0.019	0.015	0.011	0.006	0.009
Mg	0.856	0.803	0.801	0.784	0.818	0.811
Ca	0.878	0.897	0.904	0.863	0.895	0.862
Na	0.025	0.034	0.035	0.029	0.025	0.026
MG #	88.25	86.16	87.54	81.67	87.86	82.25

Appendix D. Table D.1 Electron Microprobe analyses of olivine from the Kamloops Lake picritic basalts.

Sample	IM-224	IM-224	IM-224	IM-224	IM-224	IM-224	IM-224	IM-225	IM-225	IM-225	IM-225	IM-225	IM-225	IM-240	IM-240	IM-240
Grain	1	1	1	1	2	2	2	1	1	1	2	2	2	1	1	2
Position	i	r	i	c	c	i	r	i	i	r	i	r	i	c	r	c
SiO_2	41.18	41.16	41.07	41.24	40.60	40.66	40.60	40.54	40.79	40.79	40.83	40.39	40.46	39.67	33.11	39.95
Al_2O_3	0.05	b.d.	0.04	0.04	0.06	0.09	0.07	0.06	0.04	0.06	0.04	0.05	0.04	0.06	0.05	0.05
Cr_2O_3	0.10	b.d.	0.07	0.08	b.d.	b.d.	b.d.	0.07	b.d.	0.00	b.d.	b.d.	b.d.	b.d.	b.d.	b.d.
FeO	7.16	7.66	8.10	6.96	9.07	9.24	9.22	8.85	8.78	9.06	9.03	8.88	8.86	10.11	10.20	10.07
MnO	0.10	0.17	0.11	0.12	0.20	0.20	0.21	0.15	0.16	0.14	0.18	0.13	0.15	0.21	0.27	0.24
MgO	51.13	50.94	50.24	51.25	49.22	49.23	49.32	49.98	49.74	49.33	49.39	49.19	49.30	48.87	49.38	48.67
CaO	0.04	0.06	0.07	0.05	0.20	0.26	0.22	0.17	0.14	0.19	0.38	0.42	0.40	0.28	0.27	0.28
NiO	0.39	0.33	0.35	0.43	0.34	0.38	0.36	0.46	0.43	0.40	0.22	0.32	0.31	0.25	0.33	0.30
TOTAL	100.15	100.32	100.05	100.17	99.69	100.06	100.00	100.28	100.08	99.97	100.07	99.38	99.52	99.45	93.61	99.56
Cation calculation based on 4 oxygens																
Si	0.997	0.997	0.999	0.997	0.997	0.996	0.995	0.990	0.996	0.998	0.998	0.995	0.995	0.983	0.887	0.988
Al	0.001	0.000	0.001	0.001	0.002	0.003	0.002	0.002	0.001	0.002	0.001	0.001	0.001	0.002	0.002	0.001
Cr	0.002	0.000	0.001	0.002	0.000	0.000	0.000	0.001	0.000	0.000	0.000	0.000	0.000	0.000	0.000	0.000
Fe^{2+}	0.145	0.155	0.165	0.141	0.186	0.189	0.189	0.181	0.179	0.185	0.185	0.183	0.182	0.209	0.229	0.208
Mn	0.002	0.003	0.002	0.002	0.004	0.004	0.004	0.003	0.003	0.003	0.004	0.003	0.003	0.004	0.006	0.005
Mg	1.845	1.840	1.822	1.848	1.802	1.797	1.801	1.819	1.811	1.800	1.800	1.806	1.807	1.805	1.973	1.795
Ca	0.001	0.002	0.002	0.001	0.005	0.007	0.006	0.004	0.004	0.005	0.010	0.011	0.011	0.007	0.008	0.007
Ni	0.008	0.006	0.007	0.008	0.007	0.007	0.007	0.009	0.008	0.008	0.004	0.006	0.006	0.005	0.007	0.006
FO %	92.3	91.9	91.1	92.4	90.0	89.8	90.0	90.9	90.5	90.0	90.0	90.2	90.3	90.2	98.6	89.7

$FO\% = 100 \bullet Mg(Mg + Fe^{2+})$ c=core; r=rim; i=interior

Appendix D. Table D.1 (continued)

Sample	IM-240	IM-241	IM-241	IM-241	IM-241	IM-241	IM-241	IM-230	IM-230	IM-230	IM-230	IM-230	IM-230	IM-230	IM-99	IM-99
Grain	2	1	1	1	2	2	2	1	1	1	1	2	2	2	1	1
Position	r	i	i	i	i	c	r	i	c	i	r	r	c	i	r	i
SiO_2	39.66	40.06	39.90	40.01	39.86	40.03	40.04	40.43	40.26	39.98	40.53	40.80	40.91	40.98	40.86	40.81
Al_2O_3	0.02	0.35	0.03	0.02	b.d.	b.d.	0.04	0.03	0.03	b.d.	0.02	0.04	b.d.	0.04	0.04	0.02
Cr_2O_3	b.d.	0.15	b.d.	b.d.	b.d.	b.d.	b.d.	b.d.	b.d.	b.d.	0.08	b.d.	b.d.	b.d.	b.d.	b.d.
FeO	10.10	11.19	10.06	10.36	10.27	10.33	10.07	9.60	9.40	9.42	9.06	7.63	7.66	7.55	8.99	9.00
MnO	0.22	0.27	0.19	0.22	0.23	0.18	0.24	0.15	0.19	0.18	0.16	0.11	0.08	0.12	0.20	0.17
MgO	48.43	46.32	48.72	48.97	48.28	48.82	48.91	48.48	48.46	48.90	49.21	50.40	50.22	50.52	50.36	50.46
CaO	0.28	1.55	0.18	0.22	0.24	0.26	0.25	0.31	0.28	0.27	0.28	0.08	0.07	0.05	0.29	0.20
NiO	0.31	0.31	0.36	0.32	0.35	0.28	0.33	0.26	0.34	0.33	0.30	0.41	0.39	0.32	0.36	0.33
TOTAL	99.02	100.20	99.44	100.12	99.23	99.90	99.88	99.26	98.96	99.08	99.64	99.47	99.33	99.58	101.10	100.99
Cation calculation based on 4 oxygen																
Si	0.987	0.992	0.988	0.985	0.990	0.988	0.987	0.999	0.998	0.991	0.996	0.997	1.001	0.999	0.990	0.989
Al	0.001	0.010	0.001	0.001	0.000	0.000	0.001	0.001	0.001	0.000	0.001	0.001	0.000	0.001	0.001	0.001
Cr	0.000	0.003	0.000	0.000	0.000	0.000	0.000	0.000	0.000	0.000	0.002	0.000	0.000	0.000	0.000	0.000
Fe^{2+}	0.210	0.232	0.208	0.213	0.213	0.213	0.208	0.198	0.195	0.195	0.186	0.156	0.157	0.154	0.182	0.182
Mn	0.005	0.006	0.004	0.005	0.005	0.004	0.005	0.003	0.004	0.004	0.003	0.002	0.002	0.002	0.004	0.003
Mg	1.797	1.711	1.799	1.798	1.788	1.796	1.798	1.786	1.790	1.806	1.803	1.836	1.831	1.836	1.818	1.823
Ca	0.007	0.041	0.005	0.006	0.006	0.007	0.007	0.008	0.007	0.007	0.007	0.002	0.002	0.001	0.008	0.005
Ni	0.006	0.006	0.007	0.006	0.007	0.006	0.007	0.005	0.007	0.007	0.006	0.008	0.008	0.006	0.007	0.006
FO %	89.9	85.5	89.9	89.9	89.9	89.8	89.9	89.3	89.5	90.3	90.1	91.8	91.5	91.8	90.9	91.1

Appendix D. Table D.1 (continued)

Sample	IM-99	IM-99	IM-99	IM-99	IM-99	IM-99	IM-99	IM-99	IM-99	Kr-07	Kr-07	Kr-07	Kr-07	Kr-07	Kr-07	Kr-07
Grain	1	1	1	1	2	2	2	2	2	1	1	1	1	1	1	1
Position	i	i	r	i	i	r	r	i	i	r	i	c	c	r	r	i
SiO_2	40.75	40.74	40.60	40.74	40.77	40.37	40.64	40.17	40.68	40.80	41.00	41.06	40.92	40.91	40.96	40.79
Al_2O_3	0.03	0.03	0.05	0.03	0.05	0.03	b.d.	0.12	0.02	0.02	0.05	0.05	0.04	0.05	0.03	0.05
Cr_2O_3	b.d.	b.d.	b.d.	b.d.	b.d.	b.d.	b.d.	0.27	b.d.	b.d.	b.d.	0.10	0.11	0.08	0.11	b.d.
FeO	8.96	8.86	8.84	8.98	8.93	9.14	9.05	9.14	8.86	8.92	8.34	8.07	7.73	7.69	7.65	7.81
MnO	0.20	0.14	0.19	0.17	0.21	0.18	0.18	0.17	0.15	0.17	0.12	0.13	0.08	0.10	0.11	0.13
MgO	50.34	50.28	50.31	49.96	49.80	49.78	49.83	48.89	50.06	50.07	50.47	50.97	51.37	51.71	51.42	51.26
CaO	0.15	0.16	0.29	0.23	0.36	0.35	0.34	0.38	0.35	0.18	0.11	0.12	0.09	0.11	0.12	0.09
NiO	0.35	0.36	0.32	0.34	0.34	0.29	0.32	0.24	0.34	0.31	0.32	0.37	0.42	0.39	0.37	0.28
TOTAL	100.78	100.57	100.60	100.45	100.46	100.14	100.36	99.38	100.46	100.47	100.41	100.87	100.76	101.04	100.77	100.41
Cation calculation based on 4 oxygens																
Si	0.990	0.991	0.988	0.992	0.993	0.988	0.992	0.991	0.991	0.993	0.995	0.992	0.988	0.986	0.989	0.989
Al	0.001	0.001	0.001	0.001	0.001	0.001	0.000	0.003	0.001	0.001	0.001	0.001	0.001	0.001	0.001	0.001
Cr	0.000	0.000	0.000	0.000	0.000	0.000	0.000	0.005	0.000	0.000	0.000	0.002	0.002	0.002	0.002	0.000
Fe^{2+}	0.182	0.180	0.180	0.183	0.182	0.187	0.185	0.189	0.180	0.182	0.169	0.163	0.156	0.155	0.154	0.158
Mn	0.004	0.003	0.004	0.004	0.004	0.004	0.004	0.004	0.003	0.004	0.002	0.003	0.002	0.002	0.002	0.003
Mg	1.823	1.823	1.825	1.815	1.809	1.817	1.813	1.798	1.818	1.817	1.827	1.836	1.850	1.857	1.851	1.852
Ca	0.004	0.004	0.008	0.006	0.009	0.009	0.009	0.010	0.009	0.005	0.003	0.003	0.002	0.003	0.003	0.002
Ni	0.007	0.007	0.006	0.007	0.007	0.006	0.006	0.005	0.007	0.006	0.006	0.007	0.008	0.008	0.007	0.005
FO %	91.1	91.1	91.2	90.7	90.4	90.8	90.6	89.9	90.9	90.8	91.3	91.8	92.5	92.9	92.5	92.6

Appendix D. Table D.1 (continued)

Sample	Kr-07	Kr-07	Kr-07	Kr-07	Kr-07	Kr-07
Grain Position	61	62	63	64	65	66
SiO_2	40.49	40.61	40.62	40.56	40.54	40.65
Al_2O_3	0.04	0.04	0.04	0.06	0.07	0.05
Cr_2O_3	0.07	b.d.	b.d.	b.d.	b.d.	0.09
FeO	8.58	8.60	8.54	8.09	8.14	8.54
MnO	0.18	0.15	0.18	0.13	0.11	0.09
MgO	50.83	50.74	50.96	50.96	51.15	50.62
CaO	0.04	0.15	0.18	0.10	0.08	0.07
NiO	0.37	0.38	0.41	0.43	0.35	0.38
TOTAL	100.60	100.67	100.93	100.33	100.44	100.49
Cation calculation bases on 4 oxygens						
Si	0.984	0.986	0.984	0.986	0.984	0.988
Al	0.001	0.001	0.001	0.002	0.002	0.001
Cr	0.001	0.000	0.000	0.000	0.000	0.002
Fe^{2+}	0.174	0.175	0.173	0.164	0.165	0.174
Mn	0.004	0.003	0.004	0.003	0.002	0.002
Mg	1.842	1.837	1.841	1.847	1.852	1.834
Ca	0.001	0.004	0.005	0.003	0.002	0.002
Ni	0.007	0.007	0.008	0.008	0.007	0.007
FO %	92.1	91.8	92.0	92.3	92.6	91.7

Appendix D. Table D.2 Microprobe analyses for clinopyroxene in the Kamloops Lake picrites.

Sample	IM-224	IM-224	IM-224	IM-224	IM-224	IM-224	IM-224	IM-224	IM-224	IM-225	IM-225	IM-225	IM-225	IM-225	IM-225	IM-225
Grain	1	1	1	1	2	3	4	4	5	1	1	1	2	2	2	3
Position	Mp-c	Mp-i	Mp-i	Mp-r	Gm	Gm	Gm-i	Gm-r	Gm	Mp-c	Mp-i	Mp-r	Mp-c	Mp-i	Mp-r	Gm
SiO_2	51.80	50.84	52.43	49.20	50.38	50.93	52.22	52.16	50.44	49.43	50.01	52.46	52.01	52.95	51.39	51.74
TiO_2	0.16	0.25	0.13	0.40	0.34	0.33	0.20	0.14	0.26	0.32	0.27	0.17	0.18	0.15	0.19	0.25
Al_2O_3	2.54	3.26	1.82	4.38	3.90	3.24	2.19	2.37	2.87	3.73	3.30	1.81	2.46	1.62	2.73	2.66
Cr_2O_3	0.94	0.62	0.90	0.07	0.32	0.48	0.74	0.94	0.13	0.44	0.26	0.47	0.92	0.85	0.75	0.68
Fe_2O_3	2.55	3.46	1.87	4.48	3.39	3.01	1.90	2.22	4.41	5.88	5.24	2.93	2.04	0.92	2.35	2.22
FeO	2.36	2.28	2.02	3.55	3.09	3.04	2.51	2.26	2.55	0.88	1.26	1.85	2.39	2.67	2.73	3.13
MnO	0.09	0.12	b.d.	0.10	0.13	0.10	0.08	0.08	0.12	0.11	0.12	0.08	0.06	0.09	0.08	0.15
MgO	16.80	16.05	17.14	14.63	16.64	16.40	16.79	16.74	16.50	15.94	16.22	17.81	16.79	17.34	16.31	16.99
CaO	22.26	22.38	22.80	21.97	20.68	21.62	22.51	22.71	21.27	22.31	22.05	21.88	22.52	22.44	22.33	21.50
Na_2O	0.26	0.28	0.23	0.29	0.26	0.25	0.28	0.27	0.27	0.31	0.33	0.26	0.25	0.23	0.25	0.22
NiO	b.d.	0.07	b.d.	b.d.	b.d.	b.d.	b.d.	b.d.	b.d.	b.d.	b.d.	b.d.	b.d.	b.d.	b.d.	b.d.
TOTAL	99.76	99.61	99.34	99.07	99.13	99.40	99.42	99.89	98.82	99.35	99.06	99.72	99.62	99.26	99.11	99.54
FeO_T	4.65	5.39	3.70	7.58	6.14	5.75	4.22	4.26	6.52	6.17	5.97	4.49	4.23	3.50	4.84	5.13
Cation calculation based on 6 oxygens and Fe^{2+}/Fe^{3+} adjusted to 4 cations																
Si	1.901	1.875	1.926	1.838	1.863	1.880	1.920	1.910	1.876	1.832	1.855	1.918	1.909	1.944	1.900	1.902
Al^{IV}	0.099	0.125	0.074	0.162	0.137	0.120	0.080	0.090	0.124	0.163	0.144	0.078	0.091	0.056	0.100	0.098
Total	2.000	2.000	2.000	2.000	2.000	2.000	2.000	2.000	2.000	1.995	1.999	1.996	2.000	2.000	2.000	2.000
Ti^{4+}	0.004	0.007	0.004	0.011	0.009	0.009	0.006	0.004	0.007	0.009	0.008	0.005	0.005	0.004	0.005	0.007
Al^{VI}	0.011	0.017	0.005	0.031	0.033	0.021	0.015	0.012	0.002	0.000	0.000	0.000	0.015	0.014	0.019	0.017
Cr^{3+}	0.027	0.018	0.026	0.002	0.009	0.014	0.022	0.027	0.004	0.013	0.008	0.014	0.027	0.025	0.022	0.020
Fe^{3+}	0.070	0.096	0.052	0.126	0.094	0.084	0.053	0.061	0.124	0.164	0.146	0.081	0.056	0.025	0.065	0.061
Fe^{2+}	0.072	0.070	0.062	0.111	0.095	0.094	0.077	0.069	0.079	0.027	0.039	0.057	0.073	0.082	0.084	0.096
Mn	0.003	0.004	0.000	0.003	0.004	0.003	0.002	0.002	0.004	0.003	0.004	0.002	0.002	0.003	0.003	0.005
Mg	0.919	0.882	0.939	0.815	0.917	0.903	0.920	0.914	0.915	0.881	0.897	0.971	0.919	0.949	0.899	0.931
Ca	0.875	0.884	0.897	0.880	0.819	0.855	0.887	0.891	0.847	0.886	0.876	0.857	0.886	0.882	0.885	0.847
Na	0.018	0.020	0.016	0.021	0.019	0.018	0.020	0.019	0.019	0.022	0.024	0.018	0.018	0.016	0.018	0.016
Ni	0.000	0.002	0.000	0.000	0.000	0.000	0.000	0.000	0.000	0.000	0.000	0.000	0.000	0.000	0.000	0.000
MG#	92.73	92.65	93.81	88.01	90.61	90.57	92.28	92.98	92.05	97.03	95.83	94.46	92.64	92.05	91.45	90.65

MG# = 100•Mg/(Mg + Fe^{2+}) c=core; r=rim; i=interior; Ph=phenocryst; Mp=microphenocryst; Gm=groundmass

Appendix D. Table D.2 (continued)

Sample	IM-222	IM-222	IM-222	IM-222	IM-222	IM-222	IM-222	IM-240	IM-240	IM-240	IM-240	IM-240	IM-240	IM-241	IM-241	IM-241
Grain	1	1	2	3	4	4	4	1	1	1	2	2	2	1	1	1
Position	Mp-i	Mp-i	Mp-c	Mp-c	Mp-r	Mp-c	Mp-i	Ph-c	Ph-i	Ph-r	Ph-r	Ph-c	Ph-i	Ph-r	Ph-c	Ph-i
SiO_2	50.56	50.67	50.37	51.32	50.53	50.54	51.14	51.17	51.00	51.15	50.59	51.81	50.88	49.28	51.72	49.32
TiO_2	0.27	0.20	0.35	0.23	0.34	0.27	0.26	0.20	0.24	0.28	0.24	0.20	0.31	0.35	0.15	0.41
Al_2O_3	3.29	3.07	3.30	2.61	3.19	3.07	2.86	2.97	3.05	3.01	3.17	2.53	3.26	3.91	2.22	4.32
Cr_2O_3	0.87	0.85	0.39	0.76	0.64	0.52	0.69	0.69	0.80	0.51	0.68	0.78	0.42	0.51	0.77	0.43
Fe_2O_3	2.75	2.95	2.82	3.13	3.92	3.58	3.43	3.73	3.79	3.45	4.23	3.31	4.31	6.07	3.57	5.56
FeO	3.04	2.48	4.00	2.22	1.62	2.16	1.62	1.62	1.51	1.91	1.35	1.33	1.28	0.42	1.06	1.02
MnO	0.11	0.00	0.11	0.08	0.11	0.13	0.11	0.07	0.05	0.07	0.07	0.11	0.11	0.09	b.d.	0.12
MgO	16.13	16.42	15.66	16.84	16.15	16.01	16.49	16.55	16.43	16.51	16.36	16.89	16.59	15.97	17.20	15.64
CaO	21.67	21.92	21.38	21.92	22.56	22.38	22.67	22.53	22.63	22.40	22.55	22.92	22.55	22.56	22.63	22.72
Na_2O	0.23	0.21	0.25	0.26	0.29	0.26	0.27	0.29	0.30	0.29	0.26	0.27	0.28	0.30	0.28	0.27
NiO	b.d.	b.d.	b.d.	b.d.	b.d.	b.d.	b.d.	b.d.	b.d.	b.d.	0.07	b.d.	b.d.	b.d.	b.d.	b.d.
TOTAL	98.92	98.77	98.63	99.37	99.35	98.92	99.54	99.82	99.80	99.58	99.57	100.15	99.99	99.46	99.60	99.81
FeO_T	5.51	5.13	6.54	5.04	5.15	5.38	4.71	4.98	4.92	5.01	5.16	4.31	5.16	5.88	4.27	6.02
Cation calculation based on 6 oxygens and Fe^{2+}/Fe^{3+} adjusted to 4 cations																
Si	1.877	1.881	1.881	1.891	1.867	1.877	1.883	1.879	1.874	1.882	1.865	1.892	1.865	1.823	1.897	1.820
Al^{IV}	0.123	0.119	0.119	0.109	0.133	0.134	0.124	0.121	0.126	0.118	0.135	0.108	0.135	0.170	0.096	0.180
Total	2.000	2.000	2.000	2.000	2.000	2.011	2.007	2.000	2.000	2.000	2.000	2.000	2.000	1.993	1.993	2.000
Ti^{4+}	0.008	0.006	0.010	0.006	0.009	0.008	0.007	0.006	0.007	0.008	0.007	0.005	0.009	0.010	0.004	0.011
Al^{VI}	0.021	0.015	0.026	0.004	0.006	0.011	0.007	0.007	0.006	0.012	0.003	0.001	0.006	0.000	0.000	0.008
Cr^{3+}	0.026	0.025	0.012	0.022	0.019	0.015	0.020	0.020	0.023	0.015	0.020	0.023	0.012	0.015	0.022	0.013
Fe^{3+}	0.077	0.082	0.079	0.087	0.109	0.100	0.095	0.103	0.105	0.095	0.117	0.091	0.119	0.169	0.098	0.154
Fe^{2+}	0.094	0.077	0.125	0.068	0.050	0.067	0.050	0.050	0.046	0.059	0.042	0.041	0.039	0.013	0.033	0.031
Mn	0.003	0.000	0.003	0.002	0.003	0.004	0.003	0.002	0.002	0.002	0.002	0.003	0.003	0.003	0.000	0.004
Mg	0.893	0.909	0.872	0.925	0.890	0.886	0.905	0.906	0.900	0.906	0.899	0.920	0.907	0.881	0.941	0.861
Ca	0.862	0.872	0.855	0.866	0.893	0.890	0.894	0.886	0.891	0.883	0.891	0.897	0.886	0.894	0.889	0.898
Na	0.017	0.015	0.018	0.019	0.021	0.019	0.019	0.021	0.021	0.021	0.019	0.019	0.020	0.022	0.020	0.019
Ni	0.000	0.000	0.000	0.000	0.000	0.000	0.000	0.000	0.000	0.000	0.002	0.000	0.000	0.000	0.000	0.000
MG#	90.48	92.19	87.46	93.15	94.68	92.97	94.76	94.77	95.14	93.89	95.54	95.73	95.88	98.55	96.61	96.52

Appendix D. Table D.2 (continued)

Sample	IM-241	IM-241	IM-241	IM-241	IM-230	IM-230	IM-230	IM-230	IM-230	IM-230	IM-230	IM-230	IM-230	IM-230	IM-230	IM-99
Grain	2	2	2	2	1	1	1	2	2	3	3	3	3	4	4	1
Position	Ph-i	Ph-i	Ph-r	Ph-i	Ph-c	Ph-i	Ph-r	Mp-i	Mp-r	Mp-c	Mp-r	Mp-i	Mp-i*	Mp-r	Mp-c	Mp-r
SiO_2	50.06	49.71	49.55	49.70	52.71	50.76	46.51	51.07	51.14	51.29	51.42	50.78	50.66	51.10	51.04	51.55
TiO_2	0.27	0.28	0.31	0.31	0.16	0.27	0.78	0.25	0.25	0.22	0.22	0.26	0.23	0.18	0.26	0.18
Al_2O_3	2.96	3.68	3.78	3.66	1.74	3.19	6.62	2.96	2.89	2.74	2.70	3.03	3.02	2.81	3.07	2.35
Cr_2O_3	0.58	0.49	0.48	0.42	0.59	0.69	0.00	0.26	0.26	0.85	0.28	0.55	0.50	0.62	0.93	0.85
Fe_2O_3	5.39	5.27	4.92	5.57	1.53	2.80	5.90	3.27	3.79	2.53	2.93	3.03	2.92	2.92	2.92	3.83
FeO	0.34	0.83	1.34	0.93	2.55	2.48	3.51	2.38	2.46	2.62	2.58	2.54	2.84	2.35	2.69	0.77
MnO	b.d.	0.11	b.d.	0.09	0.11	b.d.	0.08	b.d.	0.14	0.09	0.12	0.14	0.07	b.d.	0.12	0.10
MgO	16.44	15.91	15.80	16.08	17.43	16.20	13.27	16.51	16.38	16.55	16.70	16.64	16.42	16.32	16.38	17.20
CaO	22.82	22.66	22.45	22.42	21.99	22.14	21.52	22.17	21.99	21.93	21.78	21.35	21.32	22.18	21.81	22.68
Na_2O	0.27	0.28	0.28	0.27	0.28	0.27	0.33	0.24	0.31	0.27	0.29	0.26	0.27	0.31	0.29	0.27
NiO	b.d.	0.10	b.d.	0.09	b.d.	b.d.	b.d.	b.d.	b.d.	b.d.	b.d.	0.09	0.07	b.d.	b.d.	b.d.
TOTAL	99.13	99.32	98.91	99.54	99.09	98.80	98.52	99.11	99.61	99.09	99.02	98.67	98.32	98.79	99.51	99.78
FeO_T	5.19	5.57	5.77	5.94	3.93	5.00	8.82	5.32	5.87	4.90	5.22	5.27	5.47	4.98	5.32	4.22
Cation calculation based on 6 oxygens and Fe^{2+}/Fe^{3+} adjusted to 4 cations																
Si	1.854	1.841	1.842	1.837	1.938	1.883	1.758	1.888	1.885	1.896	1.900	1.885	1.888	1.895	1.882	1.888
Al^{IV}	0.129	0.159	0.158	0.159	0.062	0.117	0.242	0.112	0.115	0.104	0.100	0.115	0.112	0.105	0.118	0.101
Total	1.983	2.000	2.000	1.996	2.000	2.000	2.000	2.000	2.000	2.000	2.000	2.000	2.000	2.000	2.000	1.989
Ti^{4+}	0.008	0.008	0.009	0.009	0.004	0.008	0.022	0.007	0.007	0.006	0.006	0.007	0.006	0.005	0.007	0.005
Al^{VI}	0.000	0.002	0.008	0.000	0.013	0.022	0.053	0.017	0.011	0.015	0.018	0.018	0.021	0.018	0.015	0.000
Cr^{3+}	0.017	0.014	0.014	0.012	0.017	0.020	0.000	0.008	0.008	0.025	0.008	0.016	0.015	0.018	0.027	0.025
Fe^{3+}	0.150	0.147	0.138	0.155	0.042	0.078	0.168	0.091	0.105	0.070	0.082	0.085	0.082	0.081	0.081	0.106
Fe^{2+}	0.011	0.026	0.042	0.029	0.079	0.077	0.111	0.074	0.076	0.081	0.080	0.079	0.089	0.073	0.083	0.024
Mn	0.000	0.003	0.000	0.003	0.003	0.000	0.003	0.000	0.004	0.003	0.004	0.004	0.002	0.000	0.004	0.003
Mg	0.908	0.878	0.876	0.886	0.955	0.896	0.748	0.910	0.900	0.912	0.920	0.921	0.912	0.902	0.900	0.939
Ca	0.905	0.899	0.894	0.888	0.866	0.880	0.872	0.878	0.868	0.868	0.862	0.849	0.851	0.881	0.862	0.890
Na	0.019	0.020	0.020	0.019	0.020	0.019	0.024	0.017	0.022	0.019	0.021	0.019	0.020	0.022	0.021	0.019
Ni	0.000	0.003	0.000	0.003	0.000	0.000	0.000	0.000	0.000	0.000	0.000	0.003	0.002	0.000	0.000	0.000
MG#	98.80	97.12	95.42	96.83	92.36	92.09	87.08	92.48	92.21	91.84	92.00	92.10	91.11	92.51	91.56	97.51

Appendix D. Table D.2 (continued)

Sample	IM-99	IM-99	IM-99	IM-99	IM-99	IM-99	IM-99	IM-99	IM-99	IM-99	IM-99	IM-99	IM-99	IM-99	IM-99	IM-99
Grain	1	1	2	2	2	3	4	4	5	5	6	7	8	9	10	10
Position	Mp-c	Mp-i	Mp-r	Mp-c	Mp-i	Gm	Mp-c	Mp-r	Mp-r	Mp-i	Gm	Gm	Mp-i	Gm	Ph-r	Ph-i
SiO_2	51.01	52.05	48.51	51.24	51.98	49.94	51.64	51.46	50.86	50.34	48.43	50.71	52.49	49.11	50.09	51.10
TiO_2	0.17	0.15	0.38	0.19	0.17	0.34	0.17	0.17	0.31	0.17	0.40	0.29	0.21	0.37	0.27	0.24
Al_2O_3	2.67	1.85	4.59	2.79	2.21	4.02	2.18	2.28	3.02	3.05	4.60	3.01	1.79	4.22	3.42	2.57
Cr_2O_3	0.85	0.57	0.18	0.83	0.78	0.42	0.85	0.80	0.30	1.10	0.16	0.20	0.53	0.17	0.31	0.32
Fe_2O_3	3.80	3.43	6.53	3.63	3.32	5.14	3.10	3.87	4.85	4.66	6.66	4.47	3.02	5.91	5.00	4.60
FeO	1.39	1.01	1.39	1.44	1.27	1.95	1.36	1.05	1.38	0.48	0.69	2.11	1.45	1.70	1.07	1.23
MnO	b.d.	0.08	0.12	0.10	0.12	0.12	0.10	0.09	0.14	0.11	0.14	0.13	0.12	0.14	0.10	0.11
MgO	16.81	17.65	15.33	16.74	17.40	16.44	17.12	17.48	17.16	17.14	15.86	17.55	18.19	15.53	16.36	17.11
CaO	22.23	22.22	21.90	22.48	22.35	21.26	22.37	22.06	21.64	21.81	21.64	20.56	21.54	21.85	22.24	21.95
Na_2O	0.29	0.30	0.32	0.28	0.28	0.31	0.28	0.25	0.28	0.28	0.30	0.23	0.30	0.34	0.29	0.30
NiO	b.d.	b.d.	b.d.	b.d.	b.d.	b.d.	b.d.	b.d.	b.d.	b.d.	0.09	b.d.	b.d.	b.d.	b.d.	b.d.
TOTAL	99.22	99.31	99.25	99.72	99.88	99.94	99.17	99.51	99.94	99.14	98.97	99.26	99.64	99.34	99.15	99.53
FeO_T	4.81	4.08	7.27	4.71	4.26	6.57	4.15	4.53	5.74	4.67	6.68	6.13	4.17	7.02	5.57	5.37
Cation calculation based on 6 oxygens and Fe^{2+}/Fe^{3+} adjusted to 4 cations																
Si	1.882	1.911	1.806	1.882	1.900	1.837	1.902	1.889	1.865	1.858	1.803	1.870	1.917	1.824	1.854	1.880
Al^{IV}	0.116	0.080	0.201	0.121	0.095	0.163	0.095	0.099	0.130	0.133	0.197	0.130	0.077	0.176	0.146	0.111
Total	1.998	1.991	2.007	2.003	1.995	2.000	1.997	1.988	1.995	1.991	2.000	2.000	1.994	2.000	2.000	1.991
Ti^{4+}	0.005	0.004	0.011	0.005	0.005	0.009	0.005	0.005	0.009	0.005	0.011	0.008	0.006	0.010	0.008	0.007
Al^{VI}	0.000	0.000	0.007	0.003	0.000	0.011	0.000	0.000	0.000	0.000	0.005	0.001	0.000	0.009	0.003	0.000
Cr^{3+}	0.025	0.017	0.005	0.024	0.023	0.012	0.025	0.023	0.009	0.032	0.005	0.006	0.015	0.005	0.009	0.009
Fe^{3+}	0.105	0.094	0.183	0.100	0.091	0.142	0.086	0.107	0.134	0.129	0.186	0.124	0.083	0.165	0.139	0.127
Fe^{2+}	0.043	0.031	0.043	0.044	0.039	0.060	0.042	0.032	0.042	0.015	0.021	0.065	0.044	0.053	0.033	0.038
Mn	0.000	0.002	0.004	0.003	0.004	0.004	0.003	0.003	0.004	0.003	0.004	0.004	0.004	0.004	0.003	0.003
Mg	0.925	0.966	0.851	0.917	0.948	0.902	0.940	0.957	0.938	0.943	0.880	0.965	0.990	0.860	0.903	0.938
Ca	0.879	0.874	0.873	0.885	0.875	0.838	0.883	0.868	0.850	0.862	0.863	0.812	0.843	0.870	0.882	0.865
Na	0.021	0.021	0.023	0.020	0.020	0.022	0.020	0.018	0.020	0.020	0.022	0.016	0.021	0.024	0.021	0.021
Ni	0.000	0.000	0.000	0.000	0.000	0.000	0.000	0.000	0.000	0.000	0.003	0.000	0.000	0.000	0.000	0.000
MG#	95.56	96.89	95.19	95.42	96.05	93.76	95.72	96.76	95.71	98.43	97.67	93.69	95.74	94.19	96.47	96.11

Appendix D. Table D.2 (continued)

Sample	IM-99	IM-99	IM-99	IM-99	IM-99	IM-99	Kr-07	Kr-07	Kr-07	Kr-07	Kr-07	Kr-07	Kr-07	Kr-07	Kr-07	Kr-07
Grain	10	10	11	12	13	13	1	1	2	2	3	3	4	3	5	5
Position	Ph-i	Ph-c	Gm	Gm	Mp-i	Mp-i	Mp-i	Mp-i	Mp-i	Mp-i	Mp-c	Mp-i	Mp-i	Mp-r	Mp-c	Mp-i
SiO_2	52.64	51.71	49.45	48.68	52.76	51.12	51.14	51.26	51.23	50.64	50.83	51.80	52.75	52.14	50.84	52.57
TiO_2	0.15	0.16	0.34	0.43	0.16	0.28	0.22	0.25	0.19	0.22	0.19	0.17	0.16	0.12	0.20	0.14
Al_2O_3	1.63	2.23	3.81	4.70	1.72	2.86	3.04	3.14	2.91	3.29	3.14	2.14	1.78	1.98	3.32	1.94
Cr_2O_3	0.72	0.97	0.19	0.14	0.59	0.23	1.16	1.15	1.32	1.18	1.01	0.59	0.57	0.70	0.98	0.80
Fe_2O_3	2.84	3.52	5.51	6.27	2.59	3.93	2.61	2.42	2.87	3.95	3.01	3.38	1.44	2.75	3.37	2.39
FeO	1.09	1.14	1.60	2.25	1.58	2.22	2.05	2.17	1.72	1.41	1.95	1.09	2.85	1.55	1.72	1.78
MnO	0.05	0.09	0.14	0.17	0.11	0.12	0.08	0.08	0.10	0.10	0.11	0.07	0.18	0.10	0.08	0.07
MgO	17.89	17.15	16.12	15.49	17.96	17.47	16.85	16.75	17.04	17.22	16.87	18.08	18.29	18.15	16.82	17.98
CaO	22.58	22.53	21.51	21.20	21.99	20.93	21.97	22.04	22.05	21.23	21.63	21.60	20.69	21.62	21.94	21.88
Na_2O	0.25	0.29	0.31	0.31	0.30	0.24	0.23	0.26	0.22	0.28	0.23	0.23	0.24	0.17	0.24	0.22
NiO	b.d.	b.d.	b.d.	b.d.	b.d.	b.d.	b.d.	b.d.	b.d.	0.08	0.08	b.d.	b.d.	b.d.	b.d.	0.07
TOTAL	99.84	99.79	98.98	99.64	99.76	99.40	99.35	99.52	99.65	99.60	99.05	99.15	98.95	99.28	99.51	99.84
FeO_T	3.65	4.31	6.56	7.89	3.91	5.76	4.40	4.35	4.30	4.96	4.66	4.13	4.15	4.02	4.75	3.93
Cation calculation based on 6 oxygens and Fe^{2+}/Fe^{3+} adjusted to 4 cations																
Si	1.920	1.895	1.838	1.806	1.925	1.881	1.883	1.884	1.880	1.861	1.878	1.902	1.937	1.912	1.870	1.918
Al^{IV}	0.070	0.096	0.162	0.194	0.074	0.119	0.117	0.116	0.120	0.139	0.122	0.093	0.063	0.086	0.130	0.082
Total	1.990	1.991	2.000	2.000	1.999	2.000	2.000	2.000	2.000	2.000	2.000	1.995	2.000	1.998	2.000	2.000
Ti^{4+}	0.004	0.004	0.010	0.012	0.004	0.008	0.006	0.007	0.005	0.006	0.005	0.005	0.004	0.003	0.006	0.004
Al^{VI}	0.000	0.000	0.005	0.012	0.000	0.005	0.015	0.020	0.006	0.003	0.015	0.000	0.014	0.000	0.014	0.001
Cr^{3+}	0.021	0.028	0.006	0.004	0.017	0.007	0.034	0.033	0.038	0.034	0.029	0.017	0.017	0.020	0.028	0.023
Fe^{3+}	0.078	0.097	0.154	0.175	0.071	0.109	0.072	0.067	0.079	0.109	0.084	0.093	0.040	0.076	0.093	0.066
Fe^{2+}	0.033	0.035	0.050	0.070	0.048	0.068	0.063	0.067	0.053	0.043	0.060	0.033	0.088	0.047	0.053	0.054
Mn	0.002	0.003	0.004	0.005	0.003	0.004	0.002	0.002	0.003	0.003	0.003	0.002	0.006	0.003	0.002	0.002
Mg	0.973	0.937	0.893	0.857	0.977	0.958	0.925	0.918	0.933	0.943	0.929	0.990	1.001	0.992	0.922	0.978
Ca	0.882	0.884	0.857	0.843	0.860	0.825	0.867	0.868	0.867	0.836	0.856	0.850	0.814	0.849	0.865	0.855
Na	0.018	0.021	0.022	0.022	0.021	0.017	0.016	0.019	0.016	0.020	0.016	0.016	0.017	0.012	0.017	0.016
Ni	0.000	0.000	0.000	0.000	0.000	0.000	0.000	0.000	0.000	0.002	0.002	0.000	0.000	0.000	0.000	0.002
MG#	96.72	96.40	94.70	92.45	95.32	93.37	93.62	93.20	94.62	95.64	93.93	96.77	91.92	95.48	94.56	94.77

Appendix D. Table D.2 (continued)

Sample	Kr-07	Kr-07	Kr-07	Kr-07	Kr-07	Kr-07	Kr-07	Kr-07	Kr-07	Kr-07	Kr-07	Kr-07	Kr-07	Kr-07	Kr-07	Kr-07
Grain	5	6	6	7	7	7	8	8	9	9	10	10	10	10	10	10
Position	Mp-i	Mp-i	Mp-i	Mp-c	Mp-i	Mp-r	Mp-c	Mp-i	Mp-i	Mp-i	Mp-r	Mp-i	Mp-i	Mp-i	Mp i	Mp-r
SiO_2	50.78	51.52	51.67	51.90	52.04	52.69	51.97	50.78	52.16	51.03	52.30	50.85	51.35	52.05	52.28	51.20
TiO_2	0.26	0.19	0.17	0.14	0.24	0.18	0.16	0.18	0.17	0.20	0.15	0.21	0.21	0.19	0.17	0.24
Al_2O_3	3.00	2.73	2.41	2.02	1.91	1.74	1.68	2.71	1.94	2.72	2.04	3.01	2.85	2.15	1.85	2.90
Cr_2O_3	1.28	0.87	0.80	0.88	0.48	0.75	0.78	0.99	0.71	1.06	0.82	1.12	0.99	0.75	0.82	1.14
Fe_2O_3	3.48	3.44	3.56	3.34	3.40	2.57	4.29	4.59	3.13	3.45	2.77	3.66	3.03	2.79	3.16	3.15
FeO	1.28	1.22	1.02	0.66	0.96	1.71	0.10	0.31	0.97	1.09	1.41	1.18	1.63	1.46	0.94	1.50
MnO	0.10	0.08	0.08	b.d.	0.11	0.17	0.07	0.11	0.08	0.06	0.07	0.16	0.10	0.12	0.10	0.07
MgO	16.95	17.32	17.69	17.80	17.94	18.32	18.33	17.31	17.97	17.22	17.86	17.39	17.24	18.39	18.25	17.12
CaO	22.04	22.34	22.10	22.38	22.17	21.65	22.07	22.23	22.03	22.03	22.11	21.38	21.89	20.98	21.98	22.03
Na_2O	0.25	0.22	0.22	0.25	0.22	0.20	0.26	0.25	0.27	0.25	0.23	0.28	0.24	0.26	0.21	0.25
NiO	b.d.	b.d.	b.d.	b.d.	b.d.	b.d.	b.d.	b.d.	b.d.	b.d.	b.d.	b.d.	b.d.	b.d.	b.d.	b.d.
TOTAL	99.42	99.93	99.72	99.37	99.47	99.98	99.71	99.46	99.43	99.11	99.76	99.24	99.53	99.14	99.76	99.60
FeO_T	4.41	4.32	4.22	3.67	4.02	4.02	3.96	4.44	3.79	4.19	3.90	4.47	4.36	3.97	3.78	4.33
Cation calculation based on 6 oxygens and Fe^{2+}/Fe^{3+} adjusted to 4 cations																
Si	1.869	1.883	1.890	1.902	1.906	1.918	1.898	1.867	1.909	1.881	1.910	1.872	1.885	1.908	1.907	1.879
Al^{IV}	0.130	0.117	0.104	0.087	0.082	0.075	0.072	0.117	0.084	0.118	0.088	0.128	0.115	0.092	0.080	0.121
Total	1.999	2.000	1.994	1.989	1.988	1.993	1.970	1.984	1.993	1.999	1.998	2.000	2.000	2.000	1.987	2.000
Ti^{4+}	0.007	0.005	0.005	0.004	0.007	0.005	0.004	0.005	0.005	0.006	0.004	0.006	0.006	0.005	0.005	0.007
Al^{VI}	0.000	0.001	0.000	0.000	0.000	0.000	0.000	0.000	0.000	0.000	0.000	0.003	0.008	0.001	0.000	0.004
Cr^{3+}	0.037	0.025	0.023	0.026	0.014	0.022	0.023	0.029	0.021	0.031	0.024	0.033	0.029	0.022	0.024	0.033
Fe^{3+}	0.096	0.095	0.098	0.092	0.094	0.070	0.118	0.127	0.086	0.096	0.076	0.101	0.084	0.077	0.087	0.087
Fe^{2+}	0.039	0.037	0.031	0.020	0.030	0.052	0.003	0.010	0.030	0.034	0.043	0.036	0.050	0.045	0.029	0.046
Mn	0.003	0.002	0.002	0.000	0.003	0.005	0.002	0.003	0.002	0.002	0.002	0.005	0.003	0.004	0.003	0.002
Mg	0.930	0.944	0.965	0.973	0.980	0.994	0.998	0.949	0.981	0.946	0.972	0.954	0.943	1.005	0.993	0.937
Ca	0.869	0.875	0.866	0.879	0.870	0.845	0.864	0.876	0.864	0.870	0.865	0.843	0.861	0.824	0.859	0.866
Na	0.018	0.016	0.016	0.018	0.016	0.014	0.018	0.018	0.019	0.018	0.016	0.020	0.017	0.018	0.015	0.018
Ni	0.000	0.000	0.000	0.000	0.000	0.000	0.000	0.000	0.000	0.000	0.000	0.000	0.000	0.000	0.000	0.000
MG#	95.98	96.23	96.89	97.99	97.03	95.03	99.70	98.96	97.03	96.53	95.76	96.36	94.96	95.71	97.16	95.32

Appendix D. Table D.3 Electron Microprobe analyses of Cr-spinel from the Kamloops Lake picritic basalts.

Sample	IM-224	IM-224	IM-224	IM-224	IM-224	IM-224	IM-224	IM-224	IM-224	IM-224	IM-224	IM-224	IM-224	IM-225	IM-225	IM-225
Grain	1	1	1	2	2	3	4	5	5	6	7	8	9	1	2	2
Position	Mp-I	Mp-I	Mp-I	Mp-I	Mp-c	Gm	Gm	Gm	Gm	Gm	In-ol	In-ol	Gm	In-px-c	In-px-i	In-px-i
SiO_2	0.08	0.07	0.04	0.03	0.05	0.05	0.15	0.09	0.08	0.03	0.06	0.07	0.07	0.06	0.05	0.05
TiO_2	0.72	0.71	0.73	0.37	0.40	0.66	0.60	0.14	0.15	0.27	0.40	0.38	0.60	0.58	0.58	0.58
Al_2O_3	9.62	9.60	9.71	7.29	7.37	8.99	8.83	3.58	3.92	5.86	7.17	7.32	8.85	8.53	8.42	8.44
Cr_2O_3	26.66	27.11	26.06	41.44	41.26	29.50	28.70	58.14	56.28	47.61	49.46	46.00	26.65	30.60	31.38	31.11
Fe_2O_3	34.33	34.37	34.93	22.63	22.35	32.40	33.22	10.55	11.63	18.29	14.63	17.05	34.06	32.36	31.48	31.74
FeO	15.66	15.51	15.42	14.04	13.89	15.28	16.00	15.30	15.60	15.01	14.56	15.11	17.83	15.06	15.05	14.79
MnO	0.21	0.26	0.21	0.26	0.29	0.25	0.43	0.19	0.20	0.08	0.10	0.14	0.25	0.16	0.16	0.18
MgO	11.28	11.40	11.38	11.78	11.82	11.38	10.83	10.92	10.67	11.25	11.74	11.18	9.45	11.54	11.40	11.52
CaO	0.02	0.04	0.04	0.06	0.08	0.06	0.09	0.08	0.07	0.03	0.03	0.03	0.15	0.13	0.13	0.18
NiO	0.32	0.30	0.28	0.20	0.20	0.28	0.25	0.11	0.11	0.19	0.17	0.22	0.24	0.28	0.33	0.30
ZnO	b.d.	0.06	0.06	0.09	0.06	b.d.	0.09	0.06	0.05	0.07	0.10	b.d.	0.06	b.d.	0.08	0.08
TOTAL	98.90	99.43	98.86	98.19	97.77	98.85	99.19	99.16	98.76	98.69	98.42	97.50	98.21	99.30	99.06	98.97
FeO_T	46.55	46.44	46.85	34.40	34.00	44.43	45.89	24.79	26.06	31.47	27.72	30.45	48.48	44.18	43.38	43.35
Cation calculation based on 32 oxygens																
Si	0.022	0.019	0.011	0.008	0.014	0.013	0.040	0.025	0.022	0.008	0.016	0.019	0.019	0.016	0.013	0.013
Ti^{4+}	0.146	0.143	0.148	0.075	0.082	0.134	0.122	0.029	0.031	0.055	0.081	0.078	0.124	0.117	0.117	0.117
Al	3.049	3.026	3.076	2.329	2.362	2.854	2.808	1.153	1.269	1.880	2.280	2.358	2.868	2.699	2.673	2.679
Cr^{3+}	5.669	5.733	5.540	8.884	8.872	6.284	6.123	12.568	12.221	10.247	10.553	9.941	5.795	6.496	6.684	6.626
Fe^{3+}	6.948	6.917	7.067	4.618	4.574	6.567	6.745	2.171	2.404	3.746	2.971	3.507	7.049	6.539	6.381	6.433
Fe^{2+}	3.522	3.469	3.466	3.184	3.158	3.442	3.610	3.499	3.583	3.416	3.287	3.453	4.101	3.380	3.391	3.331
Mn	0.048	0.059	0.048	0.060	0.067	0.057	0.098	0.044	0.047	0.018	0.023	0.032	0.058	0.036	0.037	0.041
Mg	4.523	4.546	4.561	4.762	4.793	4.571	4.357	4.451	4.369	4.566	4.723	4.556	3.875	4.619	4.579	4.626
Ca	0.006	0.011	0.012	0.017	0.023	0.017	0.026	0.023	0.021	0.009	0.009	0.009	0.044	0.037	0.038	0.052
Ni	0.069	0.065	0.061	0.044	0.044	0.061	0.054	0.024	0.024	0.042	0.037	0.048	0.053	0.060	0.072	0.065
Zn	0.000	0.012	0.012	0.018	0.012	0.000	0.018	0.012	0.010	0.014	0.020	0.000	0.012	0.000	0.016	0.016
CR#	65.03	65.45	64.30	79.23	78.97	68.77	68.56	91.60	90.59	84.50	82.23	80.83	66.89	70.65	71.43	71.21
MG#	56.22	56.72	56.82	59.93	60.28	57.04	54.69	55.99	54.94	57.20	58.96	56.89	48.58	57.74	57.45	58.14
Fe^{2+}#	43.78	43.28	43.18	40.07	39.72	42.96	45.31	44.01	45.06	42.80	41.04	43.11	51.42	42.26	42.55	41.86
Fe^{3+}#	44.35	44.12	45.06	29.17	28.93	41.81	43.03	13.66	15.13	23.60	18.80	22.19	44.86	41.56	40.55	40.88

c=core; r=rim; i=interior; Ph=phenocryst; Mp=microphenocryst; In=inclusion (host mineral indicated)

Appendix D. Table D.3 (continued)

Sample	IM-225	IM-225	IM-225	IM-225	IM-225	IM-225	IM-225	IM-225	IM-225	IM-225	IM-225	IM-225	IM-225	IM-225	IM-225	IM-225
Grain	2	3	3	4	4	5	6	7	8	8	9	10	11	12	13	13
Position	In-px-i	Mp-i	Mp-c	In-ol-c	In-ol-i	In-ol-i	In-ol	In-ol	Mp-i	Mp-i	In-ol	In-ol	Gm	Gm	Mp-c	Mp-r
SiO_2	0.04	0.05	0.06	0.03	0.05	0.08	0.06	0.05	0.06	0.07	0.04	0.06	0.07	0.08	0.05	0.20
TiO_2	0.54	0.64	0.56	0.58	0.58	0.60	0.59	0.59	0.78	0.76	0.37	0.32	0.74	0.71	0.73	0.76
Al_2O_3	8.33	8.27	8.47	8.30	8.47	8.44	8.34	8.33	8.18	8.01	7.05	6.61	8.58	8.58	7.82	7.95
Cr_2O_3	30.79	29.58	29.71	27.92	27.14	25.98	28.95	27.34	19.96	20.76	43.57	45.39	23.03	23.24	22.16	21.53
Fe_2O_3	33.98	31.51	31.76	35.32	35.58	36.29	33.22	35.51	42.61	41.94	21.01	21.04	38.48	38.28	40.85	40.99
FeO	15.96	18.94	17.91	15.57	15.63	16.05	15.24	15.81	17.41	16.39	14.56	16.32	18.05	17.82	16.16	16.85
MnO	0.16	0.32	0.24	0.21	0.17	0.21	0.19	0.19	0.17	0.19	0.11	0.18	0.22	0.22	0.18	0.18
MgO	11.31	8.67	9.42	11.21	11.11	10.77	11.18	11.00	10.06	10.56	11.67	10.96	9.54	9.71	10.67	10.40
CaO	0.19	0.16	0.13	b.d.	b.d.	b.d.	b.d.	b.d.	0.02	0.09	b.d.	b.d.	0.05	0.02	0.02	0.04
NiO	0.26	0.25	0.28	0.30	0.30	0.32	0.31	0.30	0.39	0.36	0.26	0.22	0.34	0.36	0.37	0.41
ZnO	b.d.	0.11	0.08	b.d.	0.08	0.06	0.06	0.06	b.d.	b.d.	0.07	0.06	0.08	b.d.	0.06	0.06
TOTAL	101.56	98.50	98.62	99.44	99.11	98.80	98.14	99.18	99.64	99.13	98.71	101.16	99.18	99.02	99.07	99.37
FeO_T	46.54	47.29	46.49	47.35	47.64	48.70	45.13	47.76	55.75	54.13	33.46	35.25	52.67	52.26	52.92	53.73
Cation calculation based on 32 oxygens																
Si	0.011	0.014	0.016	0.008	0.014	0.022	0.016	0.014	0.016	0.019	0.011	0.016	0.019	0.022	0.014	0.054
Ti^{4+}	0.107	0.133	0.116	0.118	0.118	0.123	0.121	0.120	0.160	0.156	0.075	0.064	0.152	0.146	0.150	0.156
Al	2.591	2.693	2.738	2.636	2.698	2.704	2.678	2.656	2.624	2.573	2.245	2.073	2.764	2.764	2.513	2.550
Cr^{3+}	6.425	6.462	6.443	5.950	5.801	5.584	6.236	5.848	4.296	4.474	9.310	9.552	4.978	5.024	4.778	4.633
Fe^{3+}	6.748	6.551	6.555	7.163	7.238	7.423	6.811	7.229	8.727	8.603	4.272	4.214	7.915	7.876	8.382	8.396
Fe^{2+}	3.523	4.376	4.108	3.509	3.534	3.650	3.473	3.577	3.963	3.735	3.290	3.632	4.127	4.074	3.685	3.835
Mn	0.036	0.075	0.056	0.048	0.039	0.048	0.044	0.044	0.039	0.044	0.025	0.041	0.051	0.051	0.042	0.041
Mg	4.450	3.572	3.852	4.504	4.478	4.365	4.541	4.436	4.083	4.291	4.702	4.349	3.888	3.958	4.338	4.220
Ca	0.054	0.047	0.038	0.000	0.000	0.000	0.000	0.000	0.006	0.026	0.000	0.000	0.015	0.006	0.006	0.012
Ni	0.055	0.056	0.062	0.065	0.065	0.070	0.068	0.065	0.085	0.079	0.057	0.047	0.075	0.079	0.081	0.090
Zn	0.000	0.022	0.016	0.000	0.016	0.012	0.012	0.012	0.000	0.000	0.014	0.012	0.016	0.000	0.012	0.012
CR#	71.26	70.58	70.18	69.30	68.26	67.37	69.96	68.77	62.08	63.49	80.57	82.17	64.30	64.51	65.53	64.50
MG#	55.81	44.94	48.39	56.21	55.89	54.46	56.66	55.36	50.75	53.46	58.83	54.49	48.51	49.28	54.07	52.39
Fe^{2+}#	44.19	55.06	51.61	43.79	44.11	45.54	43.34	44.64	49.25	46.54	41.17	45.51	51.49	50.72	45.93	47.61
Fe^{3+}#	42.81	41.71	41.66	45.48	45.99	47.25	43.31	45.95	55.77	54.97	26.99	26.61	50.55	50.28	53.48	53.89

Appendix D. Table D.3 (continued)

Sample	IM-225	IM-225	IM-225	IM-225	IM-225	IM-225	IM-225	IM-225	IM-225	IM-225	IM-225	IM-240	IM-240	IM-240	IM-240	IM-240
Grain	14	14	15	15	15	16	16	16	17	18	19	1	1	1	1	2
Position	In-px-i	In-px-r	In-px-r	In-px-c	In-px-i	Mp-i	Mp-i	Mp-r	In-px	Gm	Gm	Ph-r	Ph-r	Ph-c	Ph-i	In-px-c
SiO_2	0.04	0.06	0.06	0.05	0.04	0.06	0.28	0.06	0.06	0.05	0.07	0.04	0.08	0.06	0.06	0.04
TiO_2	0.45	0.49	0.72	0.75	0.70	0.58	0.61	0.59	0.62	0.63	0.64	1.43	1.40	1.16	1.19	1.01
Al_2O_3	6.93	7.13	7.91	7.61	7.74	8.70	8.58	8.42	5.68	8.42	8.53	12.08	10.25	9.25	9.38	8.52
Cr_2O_3	33.70	31.59	21.06	20.31	22.83	30.68	29.76	30.60	21.19	26.52	26.60	10.82	12.02	13.65	13.63	15.91
Fe_2O_3	31.36	31.47	42.14	43.13	40.65	32.25	32.16	31.38	44.51	36.41	36.29	45.45	46.66	46.67	47.41	45.82
FeO	15.47	15.06	16.15	16.64	15.96	15.50	15.84	16.37	16.31	14.58	14.36	20.32	20.13	19.02	19.63	18.57
MnO	0.20	0.16	0.19	0.18	0.17	0.17	0.23	0.16	0.19	0.20	0.20	0.26	0.23	0.20	0.23	0.22
MgO	11.06	10.98	10.72	10.40	10.79	11.42	11.09	10.56	10.23	11.69	11.84	8.83	8.90	9.31	9.21	9.48
CaO	0.06	0.09	0.12	0.05	0.12	b.d.	0.12	0.04	0.14	0.09	0.15	0.03	0.03	b.d.	b.d.	b.d.
NiO	0.33	0.24	0.33	0.38	0.38	0.31	0.30	0.33	0.40	0.34	0.33	0.40	0.35	0.39	0.40	0.38
ZnO	0.06	b.d.	b.d.	0.06	b.d.	b.d.	0.08	b.d.	b.d.	0.05	0.06	b.d.	b.d.	b.d.	b.d.	b.d.
TOTAL	99.66	97.27	99.40	99.56	99.38	99.67	99.05	98.51	99.33	98.98	99.07	99.66	100.05	99.71	101.14	99.95
FeO_T	43.69	43.38	54.07	55.45	52.54	44.52	44.78	44.61	56.36	47.34	47.01	61.22	62.11	61.01	62.29	59.80
Cation calculation based on 32 oxygens																
Si	0.011	0.017	0.016	0.014	0.011	0.016	0.076	0.016	0.017	0.013	0.019	0.011	0.022	0.016	0.016	0.011
Ti^{4+}	0.092	0.102	0.147	0.154	0.143	0.117	0.124	0.121	0.129	0.128	0.129	0.291	0.286	0.238	0.241	0.207
Al	2.208	2.321	2.533	2.444	2.478	2.745	2.727	2.703	1.847	2.676	2.703	3.846	3.278	2.972	2.976	2.737
Cr^{3+}	7.205	6.900	4.525	4.376	4.904	6.494	6.346	6.590	4.623	5.654	5.656	2.311	2.579	2.943	2.902	3.429
Fe^{3+}	6.382	6.541	8.615	8.845	8.310	6.496	6.528	6.433	9.240	7.388	7.344	9.240	9.528	9.576	9.607	9.398
Fe^{2+}	3.497	3.480	3.670	3.791	3.627	3.470	3.572	3.728	3.763	3.287	3.230	4.590	4.569	4.338	4.421	4.232
Mn	0.046	0.037	0.044	0.042	0.039	0.039	0.053	0.037	0.044	0.046	0.046	0.059	0.053	0.046	0.052	0.051
Mg	4.459	4.522	4.343	4.225	4.370	4.558	4.459	4.288	4.208	4.700	4.747	3.556	3.601	3.785	3.697	3.852
Ca	0.017	0.027	0.035	0.015	0.035	0.000	0.035	0.012	0.041	0.026	0.043	0.009	0.009	0.000	0.000	0.000
Ni	0.072	0.053	0.072	0.083	0.083	0.067	0.065	0.072	0.089	0.074	0.071	0.087	0.076	0.086	0.087	0.083
Zn	0.012	0.000	0.000	0.012	0.000	0.000	0.016	0.000	0.000	0.010	0.012	0.000	0.000	0.000	0.000	0.000
CR#	76.54	74.83	64.11	64.16	66.43	70.29	69.94	70.91	71.45	67.88	67.66	37.53	44.03	49.75	49.37	55.61
MG#	56.05	56.51	54.20	52.71	54.65	56.78	55.52	53.49	52.79	58.85	59.51	43.65	44.08	46.60	45.54	47.65
Fe^{2+}#	43.95	43.49	45.80	47.29	45.35	43.22	44.48	46.51	47.21	41.15	40.49	56.35	55.92	53.40	54.46	52.35
Fe^{3+}#	40.41	41.50	54.97	56.46	52.96	41.28	41.84	40.91	58.82	47.00	46.77	60.01	61.93	61.82	62.04	60.38

Appendix D. Table D.3 (continued)

Sample	IM-240	IM-240	IM-240	IM-240	IM-240	IM-240	IM-240	IM-240	IM-240	IM-240	IM-240	IM-240	IM-240	IM-241	IM-241	IM-241
Grain	2	2	3	4	5	5	6	6	7	7	8	9	10	1	1	1
Position	In-px-i	In-px-i	In-px	In-px	In-px-r	In-px-r	Ph-i	Ph-c	Ph-i	Ph-r	Mp-i	In-px	In-px	Ph-i	Ph-c	Ph-i
SiO_2	0.07	0.04	0.07	0.08	0.04	0.06	0.05	0.08	0.05	0.06	0.04	0.05	0.04	0.05	0.03	0.05
TiO_2	1.22	1.03	0.96	0.84	1.08	1.06	1.41	1.26	1.52	1.61	1.20	0.70	0.70	1.70	1.64	1.63
Al_2O_3	8.62	8.63	8.73	8.36	8.96	8.83	10.40	9.69	11.95	13.61	9.40	8.26	8.32	8.93	9.62	9.67
Cr_2O_3	16.04	15.81	16.00	19.14	14.04	14.54	12.27	12.96	11.57	10.10	13.87	24.96	24.71	10.46	10.67	10.35
Fe_2O_3	45.31	45.77	45.44	43.55	46.64	47.01	48.32	46.53	44.84	44.54	46.55	38.36	38.51	49.84	48.78	48.66
FeO	18.62	18.41	18.04	17.31	19.06	18.56	21.06	19.88	20.41	20.75	19.69	16.08	16.04	20.23	19.74	19.94
MnO	0.23	0.22	0.22	0.21	0.22	0.22	0.24	0.24	0.25	0.28	0.20	0.17	0.17	0.26	0.25	0.23
MgO	9.58	9.52	9.68	10.19	9.15	9.58	8.90	8.87	8.91	8.99	9.05	10.93	10.87	8.95	9.15	9.03
CaO	0.02	0.02	0.12	0.10	b.d.	0.03	b.d.	b.d.	b.d.	0.02	b.d.	0.14	0.22	b.d.	b.d.	b.d.
NiO	0.39	0.41	0.40	0.38	0.39	0.42	0.38	0.38	0.39	0.38	0.37	0.36	0.37	0.41	0.43	0.40
ZnO	0.09	0.08	b.d.	0.06	b.d.	b.d.	b.d.	0.06	b.d.	b.d.	b.d.	b.d.	b.d.	b.d.	0.08	b.d.
TOTAL	100.19	99.94	99.66	100.22	99.58	100.31	103.03	99.95	99.89	100.34	100.37	100.01	99.95	100.83	100.39	99.96
FeO_T	59.39	59.59	58.93	56.50	61.03	60.86	64.54	61.75	60.76	60.83	61.58	50.60	50.69	65.08	63.63	63.72
Cation calculation based on 32 oxygens																
Si	0.019	0.011	0.019	0.022	0.011	0.016	0.013	0.022	0.013	0.016	0.011	0.013	0.011	0.014	0.008	0.014
Ti^{4+}	0.249	0.211	0.197	0.171	0.222	0.216	0.280	0.258	0.308	0.322	0.245	0.142	0.142	0.347	0.334	0.334
Al	2.759	2.770	2.803	2.664	2.890	2.822	3.239	3.111	3.796	4.271	3.006	2.618	2.638	2.856	3.074	3.104
Cr^{3+}	3.444	3.405	3.447	4.091	3.038	3.118	2.564	2.791	2.466	2.126	2.976	5.308	5.257	2.244	2.288	2.229
Fe^{3+}	9.260	9.381	9.318	8.860	9.605	9.595	9.610	9.538	9.095	8.925	9.506	7.764	7.799	10.178	9.953	9.972
Fe^{2+}	4.228	4.194	4.110	3.914	4.363	4.208	4.653	4.527	4.600	4.620	4.468	3.616	3.610	4.591	4.477	4.541
Mn	0.053	0.051	0.051	0.048	0.051	0.051	0.054	0.055	0.057	0.063	0.046	0.039	0.039	0.060	0.057	0.053
Mg	3.879	3.866	3.933	4.107	3.734	3.874	3.507	3.602	3.581	3.569	3.661	4.383	4.361	3.621	3.699	3.667
Ca	0.006	0.006	0.035	0.029	0.000	0.009	0.000	0.000	0.000	0.006	0.000	0.040	0.063	0.000	0.000	0.000
Ni	0.085	0.090	0.088	0.083	0.086	0.092	0.081	0.083	0.085	0.081	0.081	0.078	0.080	0.089	0.094	0.088
Zn	0.018	0.016	0.000	0.012	0.000	0.000	0.000	0.012	0.000	0.000	0.000	0.000	0.000	0.000	0.016	0.000
CR#	55.52	55.14	55.15	60.56	51.25	52.49	44.18	47.29	39.38	33.23	49.75	66.97	66.59	44.00	42.67	41.80
MG#	47.85	47.97	48.90	51.20	46.12	47.93	42.98	44.31	43.77	43.58	45.04	54.79	54.71	44.09	45.24	44.68
Fe^{2+}#	52.15	52.03	51.10	48.80	53.88	52.07	57.02	55.69	56.23	56.42	54.96	45.21	45.29	55.91	54.76	55.32
Fe^{3+}#	59.88	60.30	59.85	56.74	61.84	61.76	62.35	61.77	59.22	58.25	61.38	49.48	49.69	66.62	64.99	65.16

Appendix D. Table D.3 (continued)

Sample	IM-241	IM-241	IM-241	IM-241	IM-241	IM-241	IM-241	IM-241	IM-241	IM-241	IM-241	IM-241	IM-241	IM-241	IM-241	IM-241
Grain	1	2	2	3	3	3	4	4	5	5	5	6	7	7	8	9
Position	Ph-r	Mp-c	Mp-r	Ph-r	Ph-c	Ph-i	Ph-i	Ph-i	In-px-i	In-px-c	In-px-r	In-px-i	Mp-i	Mp-i	i	In-px-i
SiO_2	0.05	0.05	b.d.	0.04	0.04	0.04	0.04	0.05	0.04	0.06	0.05	0.06	0.04	0.03	0.03	0.05
TiO_2	1.72	1.87	1.96	1.78	1.75	1.81	2.01	1.99	1.41	1.44	1.39	1.09	3.70	3.22	3.87	1.22
Al_2O_3	9.21	7.70	7.35	9.20	9.55	9.47	8.01	8.76	9.88	10.19	10.27	9.99	3.96	4.36	2.09	9.85
Cr_2O_3	10.70	10.40	10.38	10.10	10.61	9.63	10.61	10.10	10.51	10.61	10.53	14.46	8.02	8.05	7.57	12.14
Fe_2O_3	49.17	50.35	14.37	49.41	48.88	49.65	49.22	49.42	49.07	48.58	48.32	45.60	52.95	53.59	54.40	48.12
FeO	20.15	21.01	2.55	19.89	19.92	19.98	20.69	20.83	18.53	18.74	18.61	17.98	23.16	22.63	24.64	18.59
MnO	0.25	0.27	0.31	0.23	0.24	0.24	0.23	0.25	0.25	0.26	0.25	0.21	0.33	0.29	0.34	0.25
MgO	9.02	8.26	8.04	9.12	9.18	9.11	8.53	8.62	9.77	9.71	9.63	10.04	7.47	7.61	6.25	9.78
CaO	b.d.	b.d.	b.d.	0.02	b.d.	b.d.	b.d.	0.00	0.04	0.02	0.10	0.04	b.d.	b.d.	b.d.	b.d.
NiO	0.42	0.42	0.44	0.40	0.41	0.43	0.40	0.39	0.40	0.41	0.38	0.37	0.36	0.38	0.40	0.38
ZnO	b.d.	0.07	b.d.	b.d.	0.07	0.05	b.d.	0.07	b.d.	0.06	0.06	b.d.	b.d.	b.d.	0.06	b.d.
TOTAL	100.69	100.40	45.40	100.19	100.65	100.41	99.74	100.48	99.90	100.08	99.59	99.84	99.99	100.16	99.65	100.38
FeO_T	64.39	66.31	15.48	64.35	63.90	64.66	64.98	65.30	62.68	62.45	62.09	59.01	70.80	70.85	73.59	61.89
Cation calculation based on 32 oxygens																
Si	0.014	0.014	0.000	0.011	0.011	0.011	0.011	0.014	0.011	0.016	0.014	0.016	0.011	0.008	0.009	0.013
Ti^{4+}	0.351	0.387	0.858	0.364	0.356	0.369	0.417	0.409	0.287	0.292	0.284	0.221	0.788	0.683	0.843	0.247
Al	2.943	2.499	5.045	2.952	3.045	3.029	2.605	2.819	3.153	3.243	3.283	3.177	1.322	1.449	0.713	3.129
Cr^{3+}	2.294	2.265	4.780	2.174	2.270	2.067	2.315	2.181	2.251	2.266	2.259	3.086	1.796	1.795	1.733	2.588
Fe^{3+}	10.034	10.434	6.298	10.123	9.951	10.143	10.223	10.155	10.000	9.873	9.864	9.262	11.284	11.373	11.851	9.761
Fe^{2+}	4.569	4.840	1.243	4.527	4.506	4.535	0.776	4.756	4.198	4.233	4.221	4.058	5.485	5.337	5.965	4.191
Mn	0.057	0.063	0.153	0.053	0.055	0.055	0.054	0.058	0.057	0.059	0.057	0.048	0.079	0.069	0.083	0.057
Mg	3.647	3.392	6.982	3.702	3.703	3.687	3.510	3.509	3.945	3.910	3.895	4.040	3.154	3.200	2.698	3.931
Ca	0.000	0.000	0.000	0.006	0.000	0.000	0.000	0.000	0.012	0.006	0.029	0.012	0.000	0.000	0.000	0.000
Ni	0.092	0.093	0.206	0.088	0.089	0.094	0.089	0.086	0.087	0.089	0.083	0.080	0.082	0.086	0.093	0.082
Zn	0.000	0.014	0.000	0.000	0.014	0.010	0.000	0.014	0.000	0.012	0.012	0.000	0.000	0.000	0.013	0.000
CR#	43.80	47.54	48.65	42.41	42.71	40.56	47.05	43.62	41.65	41.13	40.76	49.27	57.60	55.33	70.85	45.27
MG#	44.39	41.21	84.89	44.99	45.11	44.84	81.89	42.46	48.45	48.02	47.99	49.89	36.51	37.48	31.14	48.40
Fe^{2+}#	55.61	58.79	15.11	55.01	54.89	55.16	18.11	57.54	51.55	51.98	52.01	50.11	63.49	62.52	68.86	51.60
Fe^{3+}#	65.71	68.65	39.06	66.38	65.18	66.56	67.51	67.01	64.92	64.19	64.03	59.66	78.35	77.81	82.89	63.06

Appendix D. Table D.3 (continued)

Sample	IM-241	IM-241	IM-241	IM-241	IM-241	IM-241	IM-230	IM-230	IM-230	IM-230	IM-230	IM-230	IM-230	IM-230	IM-230	IM-230
Grain	9	9	10	10	10	11	1	1	1	1	1	2	2	3	3	4
Position	In-px-c	In-px-r	Mp-r	Mp-i	Mp-i	In-px-c	Ph-r	Ph-i	Ph-c	Ph-c	Ph-i	Gm	Gm	Mp-i	Mp-i	Gm
SiO_2	0.05	0.04	0.06	0.04	0.04	0.04	0.06	0.04	0.03	0.04	0.05	0.04	0.05	0.06	0.06	0.56
TiO_2	1.22	1.14	1.74	1.80	1.98	1.67	0.54	0.54	0.48	0.45	0.56	0.64	0.60	0.50	0.54	0.40
Al_2O_3	9.80	9.83	8.79	8.35	7.79	8.70	8.50	8.47	8.10	7.78	8.56	8.08	8.12	8.12	8.33	7.16
Cr_2O_3	12.04	12.33	10.46	10.72	10.40	10.66	30.62	30.91	33.75	35.98	30.50	26.96	26.85	30.02	30.13	32.93
Fe_2O_3	47.85	48.37	49.49	50.00	50.28	49.90	33.20	33.13	30.89	29.46	33.91	35.66	35.74	32.94	32.92	30.56
FeO	18.67	18.51	19.56	20.02	20.60	19.18	15.44	14.80	14.43	14.14	14.95	19.91	19.97	18.11	17.67	18.73
MnO	0.20	0.21	0.25	0.26	0.12	0.23	0.18	0.14	0.15	0.16	0.17	0.23	0.24	0.20	0.23	0.23
MgO	9.58	9.85	9.18	9.02	8.75	9.46	11.51	11.95	12.10	12.31	12.03	8.52	8.51	9.64	9.99	9.60
CaO	0.03	b.d.	0.05	b.d.	b.d.	0.04	b.d.	0.02	b.d.	0.02	b.d.	0.04	0.03	b.d.	b.d.	0.04
NiO	0.41	0.40	0.46	0.44	0.38	0.36	0.32	0.30	0.29	0.32	0.28	0.31	0.28	0.29	0.29	0.24
ZnO	0.07	b.d.	b.d.	b.d.	b.d.	0.05	0.08	b.d.	0.08	0.08	b.d.	0.06	b.d.	b.d.	0.06	0.07
TOTAL	99.92	100.68	100.04	100.65	100.34	100.29	100.45	100.30	100.30	100.74	101.01	100.45	100.39	99.88	100.22	100.52
FeO_T	61.73	62.03	64.09	65.01	65.84	64.08	45.31	44.61	42.22	40.65	45.46	52.00	52.13	47.75	47.29	46.23
Cation calculation based on 32 oxygens																
Si	0.014	0.011	0.016	0.011	0.011	0.011	0.016	0.011	0.008	0.011	0.013	0.011	0.014	0.016	0.016	0.151
Ti^{4+}	0.249	0.230	0.357	0.369	0.409	0.342	0.108	0.108	0.096	0.089	0.111	0.131	0.123	0.102	0.109	0.081
Al	3.131	3.114	2.828	2.681	2.519	2.789	2.665	2.651	2.535	2.423	2.661	2.595	2.609	2.596	2.647	2.281
Cr^{3+}	2.581	2.621	2.258	2.309	2.257	2.293	6.441	6.491	7.086	7.518	6.361	5.809	5.787	6.440	6.423	7.038
Fe^{3+}	9.763	9.783	10.167	10.250	10.384	10.213	6.646	6.621	6.172	5.858	6.730	7.312	7.331	6.727	6.679	6.216
Fe^{2+}	4.232	4.160	4.464	4.560	4.728	4.363	3.435	3.286	3.203	3.125	3.297	4.536	4.553	4.110	3.983	4.234
Mn	0.046	0.048	0.058	0.060	0.028	0.053	0.041	0.031	0.034	0.036	0.038	0.053	0.055	0.046	0.053	0.053
Mg	3.872	3.947	3.736	3.664	3.580	3.836	4.565	4.732	4.790	4.850	4.731	3.461	3.459	3.900	4.016	3.869
Ca	0.009	0.000	0.015	0.000	0.000	0.012	0.000	0.006	0.000	0.006	0.000	0.012	0.009	0.000	0.000	0.012
Ni	0.089	0.086	0.101	0.096	0.084	0.079	0.068	0.064	0.062	0.068	0.059	0.068	0.061	0.063	0.063	0.052
Zn	0.014	0.000	0.000	0.000	0.000	0.010	0.016	0.000	0.016	0.016	0.000	0.012	0.000	0.000	0.012	0.014
CR#	45.19	45.70	44.40	46.27	47.26	45.12	70.73	71.00	73.65	75.63	70.51	69.12	68.93	71.27	70.82	75.52
MG#	47.78	48.69	45.56	44.55	43.09	46.79	57.06	59.02	59.93	60.82	58.93	43.28	43.17	48.69	50.21	47.75
Fe^{2+}#	52.22	51.31	54.44	55.45	56.91	53.21	42.94	40.98	40.07	39.18	41.07	56.72	56.83	51.31	49.79	52.25
Fe^{3+}#	63.09	63.04	66.66	67.26	68.50	66.77	42.19	42.00	39.08	37.08	42.72	46.53	46.61	42.68	42.41	40.01

Appendix D. Table D.3 (continued)

Sample	IM-230	IM-230	IM-230	IM-230	IM-230	IM-230	IM-230	IM-230	IM-230	IM-230	IM-230	IM-230	IM-230	IM-230	IM-230	IM-99
Grain	5	6	7	8	9	9	9	9	10	10	10	11	11	12	13	1
Position	Gm	Gm	Gm	Gm	Mp-r	Mp-i	Mp-i	Mp-r	Mp-r	Mp-c	Mp-i	Mp-r	Mp-i	Mp-c	Mp-i	In-px
SiO_2	0.92	0.19	0.06	0.05	0.06	0.05	0.05	0.05	0.18	0.04	0.00	1.09	0.18	0.04	0.04	0.06
TiO_2	0.72	0.50	0.54	0.40	0.48	0.46	0.47	0.48	0.37	0.39	0.37	0.36	0.37	0.42	0.42	0.57
Al_2O_3	9.02	7.68	8.44	7.57	7.83	7.93	8.03	8.19	7.08	7.38	7.24	6.90	7.47	7.47	7.58	8.32
Cr_2O_3	22.45	30.22	29.01	33.90	32.66	34.79	34.90	33.67	39.77	44.22	42.33	37.77	39.32	40.65	40.88	25.40
Fe_2O_3	37.08	32.76	33.43	29.83	31.05	29.38	29.96	30.73	23.95	20.67	22.58	25.00	24.45	24.28	24.41	37.89
FeO	19.52	19.28	18.40	17.98	16.80	15.00	15.11	15.58	17.68	15.39	16.23	17.68	17.77	15.70	14.74	15.01
MnO	0.24	0.24	0.23	0.19	0.20	0.18	0.18	0.17	0.19	0.16	0.21	0.22	0.20	0.20	0.15	0.16
MgO	9.53	8.84	9.44	9.60	10.48	11.60	11.77	11.45	9.79	11.44	10.77	10.69	9.93	11.26	11.97	11.42
CaO	0.08	0.12	0.02	0.05	b.d.	b.d.	0.02	b.d.	0.06	b.d.	0.02	b.d.	0.02	b.d.	b.d.	0.18
NiO	0.31	0.27	0.27	0.28	0.26	0.28	0.27	0.30	0.20	0.20	0.22	0.22	0.20	0.23	0.23	0.34
ZnO	b.d.	0.11	0.08	b.d.	b.d.	0.08	0.05	0.06	0.08	0.07	0.06	0.06	0.07	0.07	0.06	b.d.
TOTAL	99.87	100.21	99.92	99.85	99.82	99.75	100.81	100.68	99.35	99.96	100.03	99.99	99.98	100.32	100.48	99.35
FeO_T	52.88	48.76	48.48	44.82	44.74	41.44	42.07	43.23	39.23	33.99	36.55	40.18	39.77	37.55	36.70	49.10
Cation calculation based on 32 oxygens																
Si	0.249	0.052	0.016	0.014	0.016	0.013	0.013	0.013	0.049	0.011	0.000	0.293	0.049	0.011	0.011	0.016
Ti^{4+}	0.146	0.102	0.110	0.082	0.097	0.093	0.094	0.096	0.076	0.078	0.075	0.073	0.075	0.084	0.084	0.116
Al	2.873	2.466	2.698	2.424	2.491	2.502	2.506	2.564	2.273	2.324	2.292	2.186	2.379	2.350	2.369	2.642
Cr^{3+}	4.797	6.510	6.223	7.285	6.972	7.365	7.308	7.073	8.566	9.342	8.993	8.027	8.401	8.581	8.571	5.412
Fe^{3+}	7.540	6.716	6.826	6.100	6.308	5.920	5.971	6.144	4.911	4.156	4.565	5.056	4.972	4.878	4.872	7.682
Fe^{2+}	4.410	4.392	4.175	4.086	3.793	3.359	3.347	3.460	4.029	3.439	3.648	3.973	4.015	3.505	3.268	3.382
Mn	0.055	0.055	0.053	0.044	0.046	0.041	0.040	0.038	0.044	0.036	0.048	0.050	0.046	0.045	0.034	0.037
Mg	3.840	3.591	3.818	3.890	4.219	4.631	4.648	4.535	3.976	4.557	4.314	4.284	4.001	4.482	4.732	4.588
Ca	0.023	0.035	0.006	0.015	0.000	0.000	0.006	0.000	0.018	0.000	0.006	0.000	0.006	0.000	0.000	0.052
Ni	0.067	0.059	0.059	0.061	0.056	0.060	0.058	0.064	0.044	0.043	0.048	0.048	0.043	0.049	0.049	0.074
Zn	0.000	0.022	0.016	0.000	0.000	0.016	0.010	0.012	0.016	0.014	0.012	0.012	0.014	0.014	0.012	0.000
CR#	62.54	72.53	69.76	75.03	73.68	74.64	74.47	73.39	79.03	80.08	79.69	78.60	77.93	78.50	78.35	67.20
MG#	46.55	44.98	47.77	48.77	52.66	57.96	58.14	56.72	49.67	56.99	54.18	51.88	49.91	56.12	59.15	57.57
Fe^{2+}#	53.45	55.02	52.23	51.23	47.34	42.04	41.86	43.28	50.33	43.01	45.82	48.12	50.09	43.88	40.85	42.43
Fe^{3+}#	49.57	42.80	43.35	38.59	40.00	37.50	37.83	38.93	31.18	26.27	28.80	33.11	31.56	30.86	30.81	48.82

Appendix D. Table D.3 (continued)

Sample	IM-99	IM-99	IM-99	IM-99	IM-99	IM-99	IM-99	IM-99	IM-99	IM-99	IM-99	IM-99	IM-99	IM-99	IM-99	IM-99
Grain	2	3	3	4	5	6	6	7	7	8	9	10	10	11	11	12
Position	In-px	In-px-i	In-px-i	In-px	In-ol	Mp-i	Mp-i	Mp-i	Mp-i	Mp-c	In-px	Mp-i	Mp-i	Mp-i	Mp-i	In-px
SiO_2	0.09	0.06	0.06	0.08	0.09	0.06	0.07	0.38	0.06	0.05	0.98	0.06	0.06	0.06	0.52	0.25
TiO_2	0.54	0.55	0.55	0.58	0.59	0.55	0.55	0.72	0.74	0.52	0.62	0.48	0.49	0.66	0.64	0.64
Al_2O_3	8.12	7.63	7.58	7.96	9.52	9.06	9.15	9.58	9.78	8.63	8.38	8.29	8.74	8.41	8.78	8.74
Cr_2O_3	23.25	26.09	26.26	25.19	19.54	29.65	29.76	24.81	25.28	31.59	26.10	34.54	33.10	22.36	23.27	22.70
Fe_2O_3	39.58	38.34	38.15	38.63	41.30	32.88	33.11	35.73	36.67	31.68	33.60	29.20	30.01	40.12	37.88	38.85
FeO	14.93	14.88	15.12	14.47	14.97	15.05	14.97	15.61	15.24	15.01	18.83	15.12	15.28	18.20	18.34	17.03
MnO	0.20	0.20	0.18	0.19	0.20	0.14	0.17	0.19	0.15	0.19	0.33	0.18	0.21	0.21	0.28	0.24
MgO	11.01	11.50	11.36	11.60	11.30	11.68	11.82	11.48	11.77	11.67	9.59	11.59	11.48	9.54	9.86	10.23
CaO	0.44	0.17	0.12	0.30	0.06	0.03	0.04	0.12	0.02	0.04	0.13	0.05	0.05	0.08	0.08	0.20
NiO	0.35	0.31	0.36	0.36	0.38	0.29	0.32	0.35	0.35	0.28	0.30	0.30	0.26	0.30	0.34	0.29
ZnO	0.05	b.d.	b.d.	0.07	0.05	b.d.	b.d.	b.d.	0.09	b.d.	0.12	b.d.	0.07	0.08	b.d.	0.08
TOTAL	98.56	99.73	99.74	99.43	98.00	99.39	99.96	98.97	100.15	99.66	98.98	99.81	99.75	100.02	99.99	99.25
FeO_T	50.54	49.38	49.45	49.23	52.13	44.64	44.76	47.76	48.24	43.52	49.06	41.39	42.28	54.30	52.42	51.99
Cation calculation based on 32 oxygen																
Si	0.025	0.016	0.016	0.022	0.024	0.016	0.019	0.102	0.016	0.013	0.267	0.016	0.016	0.016	0.140	0.068
Ti^{4+}	0.111	0.111	0.111	0.117	0.121	0.111	0.110	0.145	0.148	0.104	0.127	0.096	0.098	0.135	0.130	0.131
Al	2.607	2.421	2.408	2.527	3.052	2.856	2.866	3.029	3.056	2.718	2.692	2.610	2.751	2.693	2.794	2.796
Cr^{3+}	5.008	5.555	5.597	5.365	4.203	6.271	6.254	5.263	5.300	6.675	5.626	7.295	6.989	4.803	4.968	4.872
Fe^{3+}	8.114	7.769	7.739	7.830	8.454	6.619	6.623	7.213	7.317	6.371	6.893	5.870	6.031	8.202	7.697	7.935
Fe^{2+}	3.402	3.350	3.409	3.259	3.406	3.366	3.327	3.502	3.380	3.354	4.293	3.378	3.413	4.134	4.141	3.866
Mn	0.046	0.046	0.041	0.043	0.046	0.032	0.038	0.043	0.034	0.043	0.076	0.041	0.047	0.048	0.064	0.055
Mg	4.472	4.617	4.566	4.659	4.583	4.658	4.684	4.592	4.653	4.650	3.898	4.616	4.571	3.864	3.969	4.140
Ca	0.128	0.049	0.035	0.087	0.017	0.009	0.011	0.034	0.006	0.011	0.038	0.014	0.014	0.023	0.023	0.058
Ni	0.077	0.067	0.078	0.078	0.083	0.062	0.068	0.076	0.075	0.060	0.066	0.064	0.056	0.066	0.074	0.063
Zn	0.010	0.000	0.000	0.014	0.010	0.000	0.000	0.000	0.018	0.000	0.024	0.000	0.014	0.016	0.000	0.016
CR#	65.76	69.65	69.92	67.98	57.93	68.71	68.57	63.47	63.43	71.06	67.64	73.65	71.76	64.07	64.00	63.54
MG#	56.79	57.95	57.25	58.84	57.37	58.05	58.47	56.73	57.92	58.10	47.59	57.74	57.25	48.31	48.94	51.71
Fe^{2+}#	43.21	42.05	42.75	41.16	42.63	41.95	41.53	43.27	42.08	41.90	52.41	42.26	42.75	51.69	51.06	48.29
Fe^{3+}#	51.59	49.34	49.16	49.80	53.82	42.04	42.07	46.52	46.69	40.41	45.32	37.21	38.24	52.25	49.79	50.86

Appendix D. Table D.3 (continued)

Sample	IM-99	IM-99	IM-99	IM-99	IM-99	IM-99	IM-99	IM-99
Grain	13	14	15	16	17	18	18	18
Position	Gm	Gm	In-px	In-px	In-px	In-px-r	In-px-i	In-px-i
SiO_2	0.07	0.08	0.07	0.74	0.05	0.04	0.04	0.05
TiO_2	0.71	0.69	0.71	0.51	0.66	0.68	0.63	0.64
Al_2O_3	9.64	9.78	9.52	6.94	8.19	8.72	8.66	8.67
Cr_2O_3	24.93	25.11	21.45	27.10	23.75	24.60	26.42	26.02
Fe_2O_3	36.88	36.30	40.16	36.08	39.40	38.35	37.09	37.05
FeO	15.64	15.60	15.69	15.20	15.35	15.59	15.28	15.41
MnO	0.21	0.21	0.20	0.16	0.18	0.20	0.18	0.19
MgO	11.40	11.41	11.15	11.64	11.21	11.32	11.54	11.45
CaO	0.04	0.07	0.17	0.14	0.14	b.d.	0.04	0.02
NiO	0.33	0.30	0.34	0.34	0.35	0.34	0.38	0.32
ZnO	0.08	b.d.	0.06	b.d.	b.d.	0.06	0.07	b.d.
TOTAL	99.93	99.55	99.52	98.85	99.28	99.90	100.33	99.82
FeO_T	48.82	48.26	51.83	47.66	50.80	50.10	48.65	48.75
Cation calculation based on 32 oxygens								
Si	0.019	0.021	0.019	0.201	0.014	0.011	0.011	0.013
Ti^{4+}	0.142	0.139	0.143	0.104	0.134	0.137	0.126	0.129
Al	3.028	3.079	3.011	2.218	2.610	2.754	2.720	2.737
Cr^{3+}	5.254	5.304	4.552	5.810	5.077	5.214	5.567	5.511
Fe^{3+}	7.396	7.297	8.112	7.362	8.017	7.736	7.439	7.467
Fe^{2+}	3.486	3.484	3.521	3.448	3.471	3.494	3.405	3.452
Mn	0.047	0.048	0.045	0.037	0.041	0.045	0.041	0.043
Mg	4.530	4.544	4.462	4.706	4.519	4.524	4.585	4.573
Ca	0.011	0.020	0.049	0.041	0.041	0.000	0.011	0.006
Ni	0.071	0.064	0.073	0.074	0.076	0.073	0.081	0.069
Zn	0.016	0.000	0.012	0.000	0.000	0.012	0.014	0.000
CR#	63.44	63.27	60.19	72.37	66.05	65.44	67.18	66.82
MG#	56.51	56.60	55.89	57.71	56.56	56.42	57.38	56.98
Fe^{2+}#	43.49	43.40	44.11	42.29	43.44	43.58	42.62	43.02
Fe^{3+}#	47.17	46.54	51.75	47.84	51.05	49.26	47.30	47.52

$CR\# = 100 \bullet Cr/(Cr + Al)$

$MG\# = 100 \bullet Mg/(Mg + Fe^{2+})$

$Fe^{2+}\# = 100 \bullet Fe^{2+}/(Fe^{2+} + Mg)$

$Fe^{3+}\# = 100 \bullet Fe^{3+}/(Fe^{3+} + Cr + Al)$

APPENDIX E. Complete whole rock chemical analyses for rocks from the Iron Mask batholith.

	IM-185✓ NIC	IM-276✓ NIC	IM-251✓ PH	IM-119✓ PH	IM-257 PH	IM-265✓ PH	IM-124✓ PH	IM-242✓ PH-TZ	IM-237✓ CC	IM-171✓ CC	IM-303✓ CC	IM-27G✓ CC
SiO_2	45.2	47.8	44.8	45.7	49.5	50.2	50.4	46.7	50.3	52.6	54.4	55.2
TiO_2	0.635	0.835	1.030	0.820	0.752	0.832	0.702	0.910	0.749	0.919	0.693	0.654
Al_2O_3	5.53	16.40	17.50	16.20	19.10	16.70	18.50	17.10	19.40	17.90	18.70	18.30
Fe_2O_3	6.25	4.57	7.07	8.25	8.93	6.77	5.06	6.84	4.48	3.75	3.23	3.34
FeO	4.72	4.84	5.07	4.55	3.50	2.69	2.82	3.20	3.28	3.45	3.53	2.70
MnO	0.17	0.20	0.19	0.15	0.19	0.21	0.08	0.16	0.15	0.17	0.14	0.12
MgO	12.60	5.24	5.73	5.03	4.36	4.12	3.55	5.97	3.51	3.87	2.84	2.45
CaO	19.70	12.30	12.50	11.70	10.40	7.19	8.80	12.00	9.08	8.02	7.36	6.57
Na_2O	0.34	3.77	2.28	2.53	3.60	3.65	5.10	2.48	4.64	3.86	4.32	4.83
K_2O	0.32	0.09	1.03	1.44	1.50	3.10	0.89	1.76	1.03	2.27	2.50	1.97
P_2O_5	0.16	0.31	0.60	0.44	0.32	0.39	0.37	0.15	0.36	0.33	0.35	0.37
H_2O+	*1.2	2.6	1.9	1.5	1.3	1.6	1.9	2.1	1.2	1.6	1.0	1.4
CO_2	*1.60	0.24	0.03	0.20	0.06	0.05	0.19	0.39	0.01	0.04	0.32	0.05
SUM	98.38	99.20	99.73	98.50	99.62	97.50	98.36	99.76	98.19	98.78	99.39	97.95
LOI	2.60	2.90	1.80	1.70	1.40	2.00	2.30	2.45	1.25	1.65	1.45	1.70
Trace Elements												
Ba[1]	165	765	643	523	1182	1420	389	435	722	990	1250	1130
Ba[2]	94.20	658.51	–	503.00	–	1585.79	–	–	–	–	1441.22	1304.97
Ba[3]	–	–	800	–	1800	400	–	1400	900	1300	–	–
Rb[1]	11	5	19	32	30	52	17	45	20	40	43	33
Rb[2]	7.7	1.63	–	30.15	–	52.56	–	–	–	–	44.59	32.69
Rb[3]	–	–	20	–	50	b.d.	–	20	b.d.	60	–	–
Sr[1]	242	1000	1080	787	985	674	689	652	840	798	756	679
Sr[2]	246.58	1035.81	–	875.69	–	664.46	–	–	–	–	752.82	754.27
Sr[3]	–	–	1200	–	900	900	–	1000	900	500	–	–
Nb[1]	4	6	6	5	4	5	5	6	7	4	8	7
Nb[2]	0.22	2.41	–	1.37	–	3.12	–	–	–	–	3.17	3.04
Zr[1]	27	64	27	40	33	79	53	41	37	65	62	59
Zr[2]	13.25	54.59	–	27.17	–	37.26	–	–	–	–	23.78	17.4
Y[1]	b.d.	3	4	b.d.	b.d.	9	2	3	3	7	5	7
Y[2]	9.57	17.87	–	16.85	–	20.80	–	–	–	–	20.60	19.94
As[3]	–	–	5	–	3	12	4	-	2	6	–	–
Au[3]	–	–	6	–	b.d.	b.d.	b.d.	–	b.d.	b.d.	–	–
Ni[1]	36	20	10	19	3	7	27	18	5	7	b.d.	9
Cr[5]	212	86	33	b.d.	44	25	54	27	40	28	24	b.d.
Cr[3]	–	–	8	–	4	7	–	b.d.	b.d.	12	–	–
V[2]	324.48	316.56	–	421.23	–	289.60	–	–	–	–	206.62	177.40
Sc[3]	–	–	30.7	–	23.7	25.5	16.5	–	16.7	20.6	–	–
Sc[2]	108.15	32.66	–	25.94	–	25.30	–	–	–	–	13.24	10.43
Th[3]	–	–	b.d.	–	b.d.	2.1	0.8	[1]3	b.d.	1.5	–	[1]4
Th[2]	0.09	1.08	–	1.19	–	2.34	–	–	–	–	1.42	1.53
U[3]	–	–	b.d.	–	b.d.	1.1	0.5	–	b.d.	0.8	–	–
U[2]	0.02	0.64	–	0.55	–	1.04	–	–	–	–	0.69	0.62
Pb[1]	b.d.	4	b.d.	8	b.d.	b.d.	b.d.	b.d.	b.d.	b.d.	2	4
Pb[2]	0.25	6.87	–	1.39	–	2.44	–	–	–	–	2.51	1.51
Hf[3]	–	–	0.9	–	b.d.	2.1	b.d.	–	b.d.	2.2	–	–
Hf[2]	0.64	1.57	–	1.09	–	1.32	–	–	–	–	0.97	0.82
Cl[1]	205	138	447	343	461	241	201	268	264	245	643	469
Co[1]	36	27	33	33	27	24	22	35	22	21	21	23
Co[3]	–	–	35	–	26	22	–	32	24	25	–	–
F[4]	*175	342	410	250	359	128	290	297	438	440	402	390
Br[3]	–	–	3	–	3	1	2	–	2	1	–	–
Ga[1]	20	26	29	28	30	29	28	28	29	29	29	29
S[1]	b.d.	664	b.d.	b.d.	b.d.	b.d.	b.d.	b.d.	b.d.	b.d.	b.d.	b.d.
Sn[1]	12	8	11	12	b.d.	12	b.d.	9	b.d.	12	11	b.d.
Ti[1]	2870	4120	4960	1080	3680	3970	3410	4240	1030	4580	3360	3410
Zn[1]	54	100	83	57	42	77	36	51	48	69	43	42
Zn[3]	–	–	80	–	40	b.d.	–	50	40	60	–	–
Li[2]	8.89	15.54	–	11.29	–	11.85	–	–	–	–	10.06	8.49
Be[2]	0.28	1.50	–	0.29	–	1.68	–	–	–	–	1.02	1.55
Na[1]	–	–	18000	–	27000	27000	38000	–	37000	28000	–	–

APPENDIX E (continued)

	IM-185 NIC	IM-276 NIC	IM-251 PH	IM-119 PH	IM-257 PH	IM-265 PH	IM-124 PH	IM-242 PH-TZ	IM-237 CC	IM-171 CC	IM-303 CC	IM-27G CC
Ca%[3]	–	–	9.0	–	7.2	4.6	7.2	–	7.1	5.3	–	–
Cu[1]	b.d.	82	7	19	12	67	4	10	b.d.	25	47	15
Fe%[3]	–	–	8.38	–	6.24	6.81	5.56	–	5.7	5.2	–	–
Mo[2]	0.12	0.32	–	0.46	–	0.61	–	–	–	–	0.74	0.37
Cs[3]	–	–	2	–	1	1	1	–	1	1	–	–
Cs[2]	0.38	1.68	–	0.51	–	0.48	–	–	–	–	0.80	0.39
La[3]	–	–	8.5	–	9.2	13.1	10.0	–	9.0	11.5	–	–
La[2]	1.65	7.59	–	7.92	–	12.39	–	–	–	–	9.23	11.85
Ce[2]	5.03	16.44	–	18.61	–	26.32	–	–	–	–	19.04	24.70
Pr[2]	0.92	2.39	–	2.69	–	3.58	–	–	–	–	2.65	3.38
Nd[3]	–	–	12	–	10	14	12	–	12	12	–	–
Nd[2]	5.75	11.48	–	13.36	–	16.54	–	–	–	–	13.03	15.99
Sm[3]	–	–	3.5	–	2.5	3.6	2.7	–	3.0	3.0	–	–
Sm[2]	1.91	3.02	–	3.64	–	3.88	–	–	–	–	3.50	3.81
Eu[3]	–	–	1.4	–	0.8	1.1	0.9	–	1.5	0.8	–	–
Eu[2]	0.66	1.00	–	1.21	–	1.23	–	–	–	–	1.23	1.24
Gd[2]	2.28	3.46	–	3.97	–	4.53	–	–	–	–	4.15	4.15
Tb[3]	–	–	0.6	–	b.d.	0.6	0.5	–	0.5	b.d.	–	–
Tb[2]	0.33	0.50	–	0.56	–	0.59	–	–	–	–	0.62	0.61
Dy[2]	2.04	3.48	–	3.59	–	3.95	–	–	–	–	3.96	4.04
Ho[2]	0.39	0.67	–	0.70	–	0.78	–	–	–	–	0.80	0.81
Er[2]	1.08	1.95	–	1.82	–	2.26	–	–	–	–	2.29	2.33
Tm[2]	0.14	0.29	–	0.28	–	0.34	–	–	–	–	0.33	0.34
Yb[3]	–	–	1.6	–	1.6	2.3	1.7	–	1.8	1.9	–	–
Yb[2]	0.88	1.89	–	1.53	–	2.24	–	–	–	–	2.16	2.16
Lu[3]	–	–	0.21	–	0.21	0.34	0.26	–	0.29	0.26	–	–
Lu[2]	0.12	0.29	–	0.23	–	0.35	–	–	–	–	0.32	0.33
Ta[2]	0.12	0.27	–	0.48	–	0.31	–	–	–	–	0.57	0.75
Tl[2]	b.d.	0.03	–	b.d.	–	0.05	–	–	–	–	0.01	0.09
Bi[2]	0.04	0.12	–	b.d.	–	b.d.	–	–	–	–	b.d.	0.02
Sb[3]	–	–	0.2	–	b.d.	0.8	b.d.	–	0.2	b.d.	–	–
W[3]	–	–	36	–	66	27	44	–	37	66	–	–
*Normative Mineralogy***												
Qz	1.43	-	-	-	-	-	-	-	-	5.09	7.37	15.28
Cor	-	-	-	-	-	-	-	-	-	-	-	-
Zir	0.01	0.02	0.01	0.01	0.01	0.02	0.01	0.01	0.01	0.02	0.02	0.02
Or	1.5	0.47	5.53	7.77	7.66	14.35	4.83	9.1	5.63	12.1	12.99	9.86
Al	2.42	27.88	18.2	20.73	27.9	19.67	39.7	18.48	37.01	31.22	34.06	26.68
An	10.01	24.53	31.3	26.1	27.22	5.14	22.93	26.52	26.81	22.36	21.3	18.98
Ne	-	2.24	0.38	-	-	27.07	2.34	0.99	1.53	-	-	-
Di	59.23	27.1	21.71	23.47	15.66	20.95	14.16	22.85	12.95	11.74	7.46	6.65
Hy	7.19	-	-	3.92	26	-	-	-	-	8.1	7.6	5.03
Ol	0	6.39	10.72	-	4.9	0.66	4.17	6.59	6.1	-	-	-
Mt	8.64	7.09	11.17	13.12	10.09	6.54	8.09	8.63	7.05	5.89	4.94	4.92
Chr	0.04	0.02	0.01	-	0.01	0.01	0.01	0.01	0.01	0.01	0.01	-
He	-	-	-	-	3.34	2.69	0.01	1.79	-	-	-	-
Il	1.77	2.6	0.09	2.6	2.25	2.26	2.24	2.77	2.41	2.89	2.11	1.93
Per	-	-	-	-	-	-	-	-	-	-	-	-
Ap	0.17	0.36	0.71	0.52	0.36	0.4	0.44	0.17	0.43	0.39	0.4	0.41
Ca	7.58	1.3	0.17	1.12	0.33	0.24	1.06	2.1	0.06	0.22	1.74	0.26

[1] XRF Pressed Pellet
[2] Inductively Coupled Plasma Mass Spectrometry
[3] Neutron Activation
[4] Wet Chemical
[5] XRF Fused Pellet
* Value represent an average of two or more analyses
** Normative mineralogy calculated with measure FeO
✓ FeO measured at The University of British Columbia; others measured at a commercial laboratory

APPENDIX E (continued)

	IM-253✓ CC	IM-11✓ CC	IM-254 DYKE	IM-208✓ DYKE	IM-226 DYKE	IM-308✓ DYKE	IM-173 HY-I	IM-306 HY-II	IM-120✓ HY-III	IM-256 HY-III	IM-121✓ HY-XE	IM-268✓ HY-XE
SiO_2	56.5	61.0	55.3	46.4	50.9	49.5	41.8	43.7	41.9	42.0	45.4	40.5
TiO_2	0.656	0.404	0.629	0.796	0.887	0.878	0.954	1.020	1.010	0.844	0.706	1.150
Al_2O_3	18.30	17.70	18.40	20.20	19.00	18.90	20.70	16.40	17.60	17.80	3.90	5.48
Fe_2O_3	3.39	2.01	6.45	5.82	8.89	3.85	11.50	12.60	8.26	13.30	8.47	13.81
FeO	2.37	2.13	*2.40	4.03	3.40	3.00	–	4.70	4.98	5.30	5.88	7.64
MnO	0.17	0.09	0.18	0.18	0.20	0.13	0.13	0.21	0.18	0.24	0.15	0.18
MgO	2.18	1.47	2.52	4.35	3.67	4.43	6.49	6.54	6.69	7.22	13.40	11.20
CaO	6.19	5.13	6.57	10.90	8.44	13.60	15.40	13.20	15.30	14.90	20.00	16.70
Na_2O	5.05	4.80	4.74	3.23	4.53	3.56	1.22	1.91	1.04	1.03	0.20	0.35
K_2O	3.31	3.04	2.70	0.93	1.41	0.37	0.60	0.97	0.49	0.33	0.02	0.57
P_2O_5	0.30	0.18	0.29	0.65	0.39	0.46	0.08	0.36	0.42	0.15	0.02	0.04
H_2O+	0.9	1.0	*1.4	1.4	1.2	1.1	1.3	1.3	1.6	1.8	0.6	1.0
CO_2	0.07	0.06	*0.02	0.03	0.08	0.02	0.01	0.17	0.03	0.02	0.02	0.11
SUM	99.38	99.02	98.88	98.92	99.22	99.79	100.18	97.86	99.51	99.04	98.76	98.73
LOI	1.00	1.45	1.45	1.45	1.50	1.35	1.10	1.35	1.55	1.60	0.40	0.55
Trace Elements												
Ba[1]	1340	1700	*1355	1220	1600	263	*333	442	251	315	88	254
Ba[2]	–	2031.24	–	–	–	238.99	–	–	*207.45	–	8.33	–
Ba[3]	1800	–	1600	1600	1800	–	400	–	–	400	200	400
Rb[1]	54	37	*47	21	29	17	*10	23	16	9	5	22
Rb[2]	–	36.58	–	–	–	9.61	–	–	12.44	–	0.23	–
Rb[3]	50	–	40	b.d.	20	–	20	–	–	b.d.	20	20
Sr[1]	731	597	*647	1330	961	1180	*1145	814	1060	988	84	136
Sr[2]	–	687.48	–	–	–	1205.65	–	–	*1184.90	–	94.20	–
Sr[3]	800	–	500	1500	1000	–	900	–	–	900	b.d.	800
Nb[1]	8	5	*6	6	5	7	*4	4	4	4	6	6
Nb[2]	–	3.81	–	–	–	1.79	–	–	*0.57	–	0.24	–
Zr[1]	86	72	*79	24	41	69	*28	39	14	25	23	28
Zr[2]	–	29.62	–	–	–	21.5	–	–	*12.24	–	10.66	–
Y[1]	11	2	*2	-2	6	3	b.d.	b.d.	b.d.	b.d.	b.d.	b.d.
Y[2]	–	15.47	–	–	–	14.74	–	–	*14.14	–	6.90	–
As[3]	b.d.	–	8	b.d.	b.d.	–	b.d.	8	–	4	–	b.d.
Au[3]	b.d.	–	10	b.d.	b.d.	–	b.d.	7	–	b.d.	–	b.d.
Ni[1]	b.d.	6	*2	3	b.d.	7	*8	12	12	8	46	54
Cr[5]	20	22	23	26	25	b.d.	14	23	b.d.	22	182	52
Cr[3]	b.d.	–	b.d.	b.d.	4	–	14	–	–	3	22	3
V[2]	–	119.81	–	–	–	259.38	–	–	*481.36	–	382.35	–
Sc[3]	9.2	–	8.8	16.8	18.5	–	39.3	42.9	–	37.4	–	98.8
Sc[2]	–	5.81	–	–	–	25.49	–	–	*48.06	–	121.80	–
Th[3]	2.5	–	1.4	b.d.	[1]5	[1]2	b.d.	b.d.	[1]5	b.d.	[1]5	[1]4
Th[2]	–	2.36	–	–	–	1.38	–	–	*0.12	–	0.09	–
U[3]	1.0	–	0.8	b.d.	[1]3	–	b.d.	b.d.	–	[1]3	–	b.d.
U[2]	–	1.49	–	–		0.31	–	–	0.12	–	0.01	–
Pb[1]	b.d.	3	b.d.	b.d.	b.d.	b.d.	b.d.	b.d.	b.d.	b.d.	b.d.	b.d.
Pb[2]	–	2.56	–	–	–	1.16	–	–	*0.60	–	0.24	–
Hf[3]	2.7	–	2.1	b.d.	0.8	–	b.d.	b.d.	–	0.6	–	0.8
Hf[2]	–	1.26	–	–	–	0.87	–	–	*0.63	–	0.55	–
Cl[1]	410	308	*199	225	456	556	*338	452	421	208	261	618
Co[1]	14	22	*20	26	26	20	*36	35	16	42	54	68
Co[3]	21	–	21	31	27	–	41	–	–	55	73	46
F[4]	470	260	*380	552	474	160	492	361	280	60	57	217
Br[3]	2	–	2	2	3	–	1	2	–	3	–	3
Ga[1]	30	30	*28	29	30	28	*28	29	30	29	23	25
S[1]	b.d.	b.d.	b.d.	b.d.	b.d.	b.d.	b.d.	b.d.	b.d.	b.d.	b.d.	b.d.
Sn[1]	7	10	*8	11	8	b.d.	*10	15	8	10	9	15
Ti[1]	2720	1780	*2835	4290	4470	3400	*4490	4790	4530	3620	3150	5720
Zn[1]	55	35	*62	65	59	124	*66	69	69	124	54	76
Zn[3]	50	–	40	40	90	–	90	–	–	180	70	60
Li[2]	–	4.83	–	–	–	6.34	–	–	*9.84	–	3.23	–
Be[2]	–	1.19	–	–	–	0.76	–	–	*0.38	–	0.29	–
Na[1]	37000	–	33000	26000	32000	–	10000	15000	–	9000	–	3300

APPENDIX E (continued)

	IM-253 CC	IM-11 CC	IM-254 DYKE	IM-208 DYKE	IM-226 DYKE	IM-308 DYKE	IM-173 HY-I	IM-306 HY-II	IM-120 HY-III	IM-256 HY-III	IM-121 HY-XE	IM-268 HY-XE
Ca%[3]	5.6	–	3.5	8.0	6.0	–	11.0	8.9	–	10.0	–	11.0
Cu[1]	36	4	*62	5	12	11	*8	17	12	17	5	70
Fe%[3]	4.26	–	4.17	7.14	5.62	–	8.05	8.81	–	9.51	–	14.9
Mo[2]	–	0.67	–	–	–	0.29	–	–	0.21	–	0.22	–
Cs[3]	2	–	1	b.d.	b.d.	–	1	2	–	b.d.	–	b.d.
Cs[2]	–	0.42	–	–	–	1.42	–	–	1.02	–	0.02	–
La[3]	12.8	–	7.8	11.8	12.7	–	2.6	5.4	–	2.6	–	2.1
La[2]	–	10.31	–	–	–	7.19	–	–	*4.11	–	0.84	–
Ce[2]	–	19.98	–	–	–	13.41	–	–	*10.57	–	2.85	–
Pr[2]	–	2.55	–	–	–	1.83	–	–	*1.80	–	0.56	–
Nd[3]	14	–	9	13	15	–	6	10	–	b.d.	–	b.d.
Nd[2]	–	11.04	–	–	–	9.28	–	–	*10.29	–	3.30	–
Sm[3]	3.4	–	2.6	3.1	3.5	–	2.1	3.0	–	1.8	–	1.6
Sm[2]	–	2.65	–	–	–	2.45	–	–	*3.01	–	1.25	–
Eu[3]	1.1	–	0.9	1.0	0.9	–	0.9	1.2	–	0.6	–	0.4
Eu[2]	–	0.86	–	–	–	0.70	–	–	*1.11	–	0.43	–
Gd[2]	–	3.23	–	–	–	3.13	–	–	*3.50	–	1.46	–
Tb[3]	b.d.	–	0.5	b.d.	0.6	–	b.d.	0.6	–	b.d.	–	b.d.
Tb[2]	–	0.42	–	–	–	0.44	–	–	*0.48	–	0.23	–
Dy[2]	–	2.84	–	–	–	3.00	–	–	*3.14	–	1.46	–
Ho[2]	–	0.56	–	–	–	0.55	–	–	*0.59	–	0.27	–
Er[2]	–	1.71	–	–	–	1.62	–	–	*1.52	–	0.78	–
Tm[2]	–	0.29	–	–	–	0.24	–	–	*0.21	–	0.11	–
Yb[3]	2.4	–	2.1	1.1	1.8	–	0.9	1.8	–	0.9	–	0.8
Yb[2]	–	1.82	–	–	–	1.46	–	–	*1.20	–	0.66	–
Lu[3]	0.37	–	0.03	0.15	0.25	–	0.15	0.23	–	0.12	–	0.12
Lu[2]	–	0.26	–	–	–	0.23	–	–	*0.17	–	0.09	–
Ta[2]	–	1.19	–	–	–	0.54	–	–	*0.37	–	0.32	–
Tl[2]	–	b.d.	–	–	–	b.d.	–	–	*0.08	–	b.d.	–
Bi[2]	–	b.d.	–	–	–	0.03	–	–	*0.07	–	0.08	–
Sb[3]	b.d.	–	0.5	b.d.	b.d.	–	b.d.	0.3	–	b.d.	–	b.d.
W[3]	68	–	85	36	50	–	62	59	–	46	–	39
*Normative Mineralogy***												
Qz	3.54	31.3	9.26	-	-	-	-	-	-	-	-	-
Cor	-	-	-	-	-	-	-	-	-	-	-	-
Zir	0.02	0.02	0.02	0.01	0.01	0.02	0.01	0.01	-	0.01	0.01	0.01
Or	17.9	13.04	13.51	5.06	7.27	1.98	2.91	4.77	2.58	1.62	0.1	2.76
Al	41.46	31.27	36.01	26.5	35.45	26.97	8.99	14.24	8.29	7.66	1.47	1.85
An	16	12.9	17.73	34.86	23.84	31.15	40.44	27.67	37.23	35.63	7.87	9.56
Ne	-	-	-	0.18	-	1.88	-	-	-	-	-	0.72
Di	10.36	4.84	8.65	11.45	10.54	27.33	19.9	24.16	28.11	25.05	72.64	57.48
Hy	2.45	2.6	3.03	-	2.74	-	-	0.71	1.65	3.87	1.39	-
Ol	-	-	-	10.21	3.02	1.21	8.44	5.96	5.73	4.26	2.38	4.66
Mt	5.4	2.54	6.61	9.33	9.47	6.04	-	12.87	12.78	13.38	11.98	19.09
Chr	-	-	0.01	0.01	0.01	-	-	0.01	-	-	-	0.01
He	-	-	2.9	-	4.04	-	16.45	5.37	-	3.82	-	-
Il	2.1	1.02	1.86	1.44	2.7	2.77	0.43	2.95	3.12	2.42	2	3.27
Per	-	-	-	-	-	-	2.28	-	-	-	-	-
Ap	0.36	0.17	0.3	0.78	0.44	0.54	0.09	0.39	0.49	0.16	0.02	0.04
Ca	0.4	0.27	0.11	0.17	0.45	0.11	0.05	0.91	-	0.11	0.1	0.55

APPENDIX E (continued)

	IM-267✓ SL	IM-271 SL	IM-296✓ SL	IM-274 SL	IM-272✓ SL	IM-266✓ SL	IM-295✓ SL	IM-249 SL
SiO_2	48.1	48.7	50.0	50.5	51.8	52.3	*52.5	54.5
TiO_2	0.820	0.693	0.635	0.829	0.491	0.588	*0.678	0.668
Al_2O_3	16.70	17.70	17.70	14.90	18.40	17.80	*18.6	17.40
Fe_2O_3	5.01	9.45	4.48	9.99	3.84	3.61	4.42	8.71
FeO	4.94	4.10	5.87	4.50	3.89	3.24	3.76	4.40
MnO	0.14	0.29	0.06	0.16	0.08	0.15	*0.13	0.14
MgO	6.13	4.82	4.39	6.18	3.59	2.79	*3.03	3.96
CaO	7.39	9.01	6.11	8.81	6.78	7.02	*6.69	5.68
Na_2O	2.70	2.54	3.93	3.61	3.68	3.70	*4.02	5.73
K_2O	3.39	3.58	2.66	1.83	3.64	3.38	*3.50	1.09
P_2O_5	0.27	0.25	0.27	0.29	0.25	0.37	*0.25	0.28
H_2O+	2.2	2.3	2.2	1.6	1.4	1.9	*1.4	1.8
CO_2	0.19	0.36	0.14	0.65	0.28	2.24	*0.03	0.17
SUM	98.10	99.74	98.96	99.37	98.63	99.56	99.54	99.92
LOI	1.95	2.70	2.20	2.25	1.75	4.25	*1.48	1.75
Trace Elements								
Ba[1]	2210	1670	899	589	1460	1390	*1694	724
Ba[2]	–	–	–	–	1755.10	1717.55	2033.76	–
Ba[3]	3100	2200	1100	700	–	–	–	900
Rb[1]	64	53	53	26	64	29	*64	27
Rb[2]	–	–	–	–	67.22	29.82	64.79	–
Rb[3]	70	50	70	20	–	–	–	30
Sr[1]	487	562	704	544	537	742	*563	587
Sr[2]	–	–	–	–	539.30	754.67	562.98	–
Sr[3]	600	700	700	600	–	–	–	b.d.
Nb[1]	4	5	5	5	4	8	*6	6
Nb[2]	–	–	–	–	2.02	3.43	3.06	–
Zr[1]	51	50	65	72	50	72	*71	64
Zr[2]	–	–	–	–	37.56	68.16	55.69	–
Y[1]	b.d.	b.d.	b.d.	b.d.	b.d.	3	*4	2
Y[2]	–	–	–	–	10.74	16.96	18.22	–
As[3]	b.d.	7	*2	b.d.	–	–	–	4
Au[3]	b.d.	12	*6	b.d.	–	–	–	b.d.
Ni[1]	40	16	14	27	10	6	*4	16
Cr[5]	99	37	55	133	29	26	*13	49
Cr[3]	86	28	36	120	–	–	–	27
V[2]	–	–	–	–	194.01	216.15	220.37	–
Sc[3]	40.3	26.4	*21.4	35.9	–	–	–	20.6
Sc[2]	–	–	–	–	15.42	15.09	16.94	–
Th[3]	1.2	1.2	*1.2	1.2	–	–	–	1
Th[2]	–	–	–	–	1.02	2.23	1.46	–
U[3]	0.9	0.6	*0.85	0.6	–	–	–	0.7
U[2]	–	–	–	–	0.63	1.29	1.02	–
Pb[1]	3	b.d.	b.d.	b.d.	2	4	b.d.	5
Pb[2]	–	–	–	–	1.75	4.7	2.37	–
Hf[3]	b.d.	1.7	*1.6	1.9	–	–	–	1.7
Hf[2]	–	–	–	–	1.30	1.96	1.73	–
Cl[1]	376	193	289	330	222	259	*383	230
Co[1]	39	27	30	31	17	23	*21	15
Co[3]	47	33	34	37	–	–	–	19
F[4]	476	335	310	422	214	428	*384	284
Br[3]	2	3	*4	2	–	–	–	3
Ga[1]	24	27	25	26	29	30	*28	27
S[1]	b.d.	b.d.	b.d.	b.d.	b.d.	b.d.	b.d.	b.d.
Sn[1]	16	7	9	6	9	8	*9	b.d.
Ti[1]	3830	3620	2850	3980	2290	2620	*3032	3190
Zn[1]	53	91	34	50	39	60	*44	74
Zn[3]	40	90	b.d.	50	–	–	–	90
Li[2]	–	–	–	–	5.27	2.78	3.14	–
Be[2]	–	–	–	–	0.86	1.04	0.91	–
Na[1]	21000	20000	*30500	28000	–	–	–	43000

APPENDIX E (continued)

	IM-267 SL	IM-271 SL	IM-296 SL	IM-274 SL	IM-272 SL	IM-266 SL	IM-295 SL	IM-249 SL
Ca%[3]	5.9	6.9	*3.8	6.4	--	--	--	3.0
Cu[1]	5	18	45	48	13	52	*116	63
Fe%[3]	7.42	6.48	*7.64	7.06	--	--	--	6.11
Mo[2]	--	--	--	--	1.21	0.28	0.64	--
Cs[3]	1	b.d.	b.d.	1	--	--	--	b.d.
Cs[2]	--	--	--	--	0.72	0.10	0.32	--
La[3]	9.0	6.4	*8.1	9.8	--	--	--	5.2
La[2]	--	--	--	--	4.50	13.23	8.22	--
Ce[2]	--	--	--	--	9.31	25.85	17.67	--
Pr[2]	--	--	--	--	1.32	3.34	2.45	--
Nd[3]	11	8	*8	12	--	--	--	8
Nd[2]	--	--	--	--	6.30	14.72	11.73	--
Sm[3]	2.8	2.2	*2.2	3.2	--	--	--	2.2
Sm[2]	--	--	--	--	1.60	3.24	3.07	--
Eu[3]	0.7	0.7	*0.6	1.2	--	--	--	0.7
Eu[2]	--	--	--	--	0.56	1.08	1.11	--
Gd[2]	--	--	--	--	1.98	3.65	3.74	--
Tb[3]	0.5	b.d.	b.d.	b.d.	--	--	--	b.d.
Tb[2]	--	--	--	--	0.29	0.48	0.52	--
Dy[2]	--	--	--	--	1.97	3.15	3.45	--
Ho[2]	--	--	--	--	0.41	0.62	0.72	--
Er[2]	--	--	--	--	1.20	1.77	2.08	--
Tm[2]	--	--	--	--	0.19	0.27	0.31	--
Yb[3]	1.8	1.5	*1.8	1.9	--	--	--	2.0
Yb[2]	--	--	--	--	1.27	1.77	2.09	--
Lu[3]	0.25	0.20	*0.24	0.26	--	--	--	0.27
Lu[2]	--	--	--	--	0.20	0.28	0.30	--
Ta[2]	--	--	--	--	0.31	0.46	0.40	--
Tl[2]	--	--	--	--	0.21	-0.01	0.08	--
Bi[2]	--	--	--	--	0.05	-0.07	-0.01	--
Sb[3]	0.2	0.4	*0.2	0.2	--	--	--	0.2
W[3]	38	33	*35	55	--	--	--	29
Normative Mineralogy								
Qz	-	-	-	3.67	-	15.14	-	5.96
Cor	-	-	-	-	-	1.93	-	-
Zir	0.01	0.01	0.02	0.02	0.01	0.02	0.02	0.02
Ort	17.98	18.26	14.39	8.84	19.98	15.48	19.25	5.38
Al	21.73	19.67	32.27	26.47	30.67	25.74	33.57	42.94
An	21.01	22.7	20.85	15.56	21.29	15.1	20.93	15.48
Ne	-	-	-	-	-	-	-	-
Di	9.8	12.91	4.86	15.42	7.27		8.74	5.88
Hy	1.24	1.59	3.02	9.7	2.48	9.32	0.83	8.5
Ol	16.47	6.3	14.31	-	8.61	-	6.79	-
Mt	7.83	12.61	7.14	12.38	6.21	4.87	7.18	12.67
Chr	0.02	0.01	0.01	0.03	0.01	0.01	-	0.01
He	-	1.59	-	1.84	-	-	-	-
Il	2.56	2.07	2.01	2.36	1.58	1.59	2.21	1.95
Per	-	-	-	-	-	-	-	-
Ap	0.32	0.28	0.32	0.31	0.3	0.37	0.29	0.31
Ca	1.03	1.99	0.78	3.41	1.58	10.42	0.17	0.92

APPENDIX F. Estimates of accuracy and precision on whole rock analyses.

Precision of whole rock chemical analyses is estimated through blind replicate analyses on two rocks; IM-108, a serpentinite from the Iron Mask batholith and IM-295, a sample of Sugarloaf diorite (Table F.1). Shown in Table F.2 and Table F.3 are results of duplicate analyses used for laboratory control.

Figures F.1 to F.3 compare "accepted compositions" to compositions determined in this thesis. All error bars shown are for 1s error. Three reference materials are represented on the diagrams. One of these materials is the international standard "SY-2" and accepted values for this rock are obtained from Govindaraju (1984). The other two reference materials, "P-1" and "WP-1" are in-house standard material. "Accepted" values for P-1 and WP-1 are those established by Bartch (1993) through multiple analyses (Table F.4).

Most major and minor element concentrations fall within 1s analytical error of the accepted concentration for all three reference materials (Figure F.1). Analytical precision is better than ± 5% for these elements. Measured Na_2O and CaO concentrations in P-1 are slightly higher than accepted values.

Analytical accuracy of trace elements, represented in ppm, is generally within analytical error, but varies significantly with the analytical method used (Figure F.2). In particular, for the in-house reference material, P-1 and WP-1, both the accepted value (Bartch, 1993) and the measured concentration of a given element are dependent on the analytical method. Neutron activation (INAA) measurements of Zn and Ni are higher than XRF pressed pellet and INAA measured Rb is lower than XRF fused pellet. For both P-1 and WP-1, neutron activation and XRF fused pellet methods yield similar concentrations of Ba, Cr and Nb. For P1, Sr values from these two methods are also similar, but analyses of WP-1 estimate much lower concentrations of Sr with INAA than XRF fused pellet.

A comparison of the three analytical methods used in this study (INAA, XRF, ICP-MS) is presented in Figure F.3. Generally, XRF methods yield a greater concentration of Ba than either INAA or ICP-MS and greater values of Co than does INAA. XRF estimates lower concentrations of Nb than ICP-MS. Most of the other elements are shown to have similar concentrations independent of the analytical method and XRF and ICP-MS analyses of Rb correlate extremely well over a wide range of concentrations. Zr shows strong dependence on the method, with ICP-MS values significantly lower than XRF. This phenomenon may be due to lack of complete dissolution of zircon with the ICP-MS method. Zr concentrations reported and used in this thesis are XRF values. INAA and ICP-MS data appear to correlate fairly well, although lack of data precludes more interpretation.

APPENDIX F. Table F.1. Duplicate chemical analyses for rocks from the Iron Mask batholith and the Kamloops Lake picritic basalts with calculated analytical precision.

	IM-108								
	Iron Mask serpentinite						Mean	1s	%error
SiO_2	39.2	39.3	39.2	39.7	39.2	39.4	39.33	0.20	0.50
TiO_2	0.207	0.217	0.212	0.208	0.214	0.217	0.213	0.004	2.04
Al_2O_3	2.71	2.75	2.73	2.68	2.83	2.71	2.74	0.05	1.90
Fe_2O_3	11.00	11.00	11.00	11.10	11.00	10.90	11.00	0.06	0.57
FeO	--	--	--	--	--	--			
MnO	0.20	0.20	0.20	0.21	0.20	0.20	0.2	0.0	2.02
MgO	33.70	33.50	33.70	33.90	33.30	33.80	33.65	0.22	0.64
CaO	3.48	3.54	3.52	3.57	3.58	3.49	3.53	0.04	1.16
Na_2O	0.14	0.15	0.16	0.14	0.17	0.16	0.15	0.01	7.90
K_2O	0.58	0.57	0.57	0.55	0.55	0.57	0.57	0.01	2.17
P_2O_5	0.06	0.06	0.06	0.06	0.06	0.06	0.06	0.00	0.00
H2O+	7.40	7.40	7.40	7.40	7.30	--	7.38	0.04	0.61
CO_2	0.08	0.09	0.08	0.08	0.09	--	0.08	0.01	6.52
SUM	98.76	98.78	98.83	99.60	98.49	91.51	98.89	0.42	0.42
LOI	7.55	7.60	7.75	7.55	7.65	7.50	7.60	0.09	1.18
Trace Elements									
Ba[1]	131	142	117	128	126	--	129	9.0	7.0
Rb[1]	18	20	17	18	21	--	19	1.6	8.7
Sr[1]	13	16	16	15	14	--	15	1.3	8.8
Nb[1]	4	5	4	6	4	--	5	0.9	19.4
Zr[1]	21	21	18	21	20	--	20	1.3	6.4
Y[1]	b.d.	b.d.	b.d.	b.d.	b.d.	--			
Ni[1]	1270	1260	1260	1240	1240	--	1254	13.4	1.1
Cr[4]	2890	2860	2870	2910	3000	2880	2902	51.2	1.8
Th[1]	b.d.	b.d.	b.d.	b.d.	b.d.	--			
Cl[1]	423	386	372	399	401	--	396	19.0	4.8
Co[1]	89	94	94	93	89	--	92	2.6	2.8
F[3]	58	40	48	44	33	--	45	9.3	20.9
Ga[1]	17	16	18	16	17	--	17	0.8	5.0
S[1]	1710	1670	1670	1700	1560	--	1662	59.8	3.6
Sn[1]	10	8	12	b.d.	b.d.	--	6	5.7	94.3
Ti[1]	1190	1220	1220	1210	1210	--	1210	12.2	1.0
Zn[1]	47	51	49	50	52	--	50	1.9	3.9
Cu[1]	25	22	23	27	27	--	25	2.3	9.2
Mo[1]	3	b.d.	4	3	b.d.	--	2	1.9	93.5

[1] XRF Pressed Pellet
[2] Neutron Activation
[3] Wet Chemistry
[4] XRF Fused Pellet

APPENDIX F. Table F.1 (continued)

	IM-295 Sugarloaf diorite					Mean	1s	%error
SiO_2	52.4	52.8	52.5	52.7	52.3	52.54	0.21	0.39
TiO_2	0.680	0.685	0.674	0.671	0.674	0.677	0.006	0.83
Al_2O_3	18.60	18.70	18.60	18.60	18.50	18.60	0.07	0.38
Fe_2O_3	8.60	8.75	8.49	8.79	8.45	8.62	0.15	1.76
FeO	--	--	--	--	--			
MnO	0.13	0.13	0.13	0.13	0.13	0.13	0.00	0.00
MgO	3.00	3.03	3.00	3.17	2.97	3.03	0.08	2.60
CaO	6.66	6.75	6.66	6.75	6.62	6.69	0.06	0.88
Na_2O	4.01	4.04	4.04	4.01	4.00	4.02	0.02	0.47
K_2O	3.49	3.57	3.48	3.49	3.48	3.50	0.04	1.09
P_2O_5	0.24	0.25	0.24	0.25	0.25	0.25	0.01	2.23
H2O+	1.40	1.40	1.50	1.40	1.40	1.42	0.04	3.15
CO_2	0.03	0.03	0.02	0.02	0.03	0.03	0.01	21.07
SUM	98.82	97.14	99.33	99.98	98.80	98.91	1.05	1.06
LOI	1.50	1.50	1.50	1.45	1.45	1.48	0.03	1.85
Trace Elements								
Ba[1]	1700	1670	1710	1700	1690	1694	15.2	0.9
Rb[1]	66	64	63	64	65	64	1.1	1.8
Sr[1]	565	564	568	564	555	563	4.9	0.9
Nb[1]	7	5	6	6	7	6	0.8	13.5
Zr[1]	72	70	71	70	70	71	0.9	1.3
Y[1]	7	4	3	3	5	4	1.7	38.0
Ni[1]	b.d.	2	4	4	5	3	2.0	66.67
Cr[4]	13	13	b.d.	32	15	15	11.4	78.18
Th[1]	b.d.	3	2	4	5	3	1.9	68.7
Cl[1]	396	363	389	387	381	383	12.5	3.3
Co[1]	21	17	23	22	20	21	2.3	11.2
F[3]	378	357	402	387	397	384	17.8	4.6
Ga[1]	27	29	28	27	28	28	0.8	3.0
S[1]	b.d.	b.d.	b.d.	b.d.	b.d.			
Sn[1]	b.d.	14	8	6	7	7	5.0	71.4
Ti[1]	3040	3020	3060	3030	3010	3032	19.2	0.6
Zn[1]	44	48	42	41	46	44	2.9	6.5
Cu[1]	111	126	114	119	111	116	6.4	5.5
Mo[1]	b.d.	b.d.	b.d.	b.d.	b.d.			

[1] XRF Pressed Pellet
[2] Neutron Activation
[3] Wet Chemistry
[4] XRF Fused Pellet

APPENDIX F. Table F.2. Duplicate analyses used for laboratory control.

	IM-173		IM-185		IM-225		IM-241		IM-254		IM-296	
	Type III Iron Mask hybrid		Nicola Group lava flow		Carabine Creek picritic basalt		Watching Creek picritic basalt		Iron Mask dyke		Sugarloaf diorite dyke	
SiO_2	41.8	--	45.2	--	40.4	--	38.4	38.6	55.3	--	50.0	--
TiO_2	0.954	--	0.635	--	0.230	--	0.166	0.173	0.629	--	0.635	--
Al_2O_3	20.70	--	5.53	--	3.80	--	2.17	2.16	18.40	--	17.7	--
Fe_2O_3	11.50	--	6.25	--	2.63	--	10.30	10.40	6.45	--	11.00	--
FeO	--	--	4.72	--	5.37	--	--	--	2.40	2.40	--	--
MnO	0.13	--	0.17	--	0.17	--	0.18	0.18	0.18	--	0.06	--
MgO	6.49	--	12.60	--	31.40	--	32.60	32.90	2.52	--	4.39	--
CaO	15.40	--	19.70	--	4.72	--	5.32	5.38	6.57	--	6.11	--
Na_2O	1.22	--	0.34	--	0.09	--	0.08	0.08	4.74	--	3.93	--
K_2O	0.60	--	0.32	--	0.95	--	0.15	0.16	2.70	--	2.66	--
P_2O_5	0.08	--	0.16	--	0.11	--	0.05	0.05	0.29	--	0.27	--
H2O+	1.30	--	1.10	1.20	7.80	--	9.20	--	1.30	1.40	2.2	--
CO_2	0.01	--	1.58	1.62	0.08	--	0.36	--	0.02	0.01	0.14	--
SUM	100.18		98.31		97.75		98.98	90.08	98.83		99.10	
LOI	1.10	--	2.60	--	8.45	--	9.75	9.70	1.45	--	2.2	--
Trace Elements												
Ba[1]	334	332	165	--	213	215	226	--	1330	1380	899	--
Ba[2]	400	--	--	--	--	--	--	--	1600	--	1100	1100
Rb[1]	10	10	11	--	28	27	5	--	49	45	53	--
Rb[2]	20	--	--	--	--	--	--	--	40	--	70	50
Sr[1]	1140	1150	242	--	212	218	46	--	647	647	704	--
Sr[2]	800	--	--	--	--	--	--	--	b.d.	--	700	700
Nb[1]	5	3	4	--	5	5	5	--	6	6	5	--
Zr[1]	29	26	27	--	22	23	17	--	80	78	65	--
Y[1]	b.d.	b.d.	b.d.	--	b.d.	b.d.	b.d.	--	3	b.d.	b.d.	--
As[2]	b.d.	--	--	--	--	--	--	--	8	--	2	2
Au[2]	b.d.	--	--	--	--	--	--	--	10	--	7	b.d.
Ni[1]	9	7	36	--	1350	1380	1420	--	2	b.d.	14	--
Cr[4]	3	--	--	--	--	--	--	--	-2	--	36	39
Cr[2]	14	--	212	--	2580	--	2790	2840	23	--	55	--
S[2]	39.3	--	--	--	--	--	--	--	8.8	--	21.1	21.8
Th[1]	b.d.	b.d.	b.d.	--	b.d.	b.d.	b.d.	--	b.d.	b.d.	4	--
Th[2]	b.d.	--	--	--	--	--	--	--	1.4	--	1.3	1.1
U[2]	b.d.	--	--	--	--	--	--	--	0.8	--	0.9	0.8
Hf[2]	b.d.	--	--	--	--	--	--	--	2.1	--	1.6	1.7
Cl[1]	340	336	205	--	128	104	293	--	195	202	289	--
Co[1]	0.1	39	36	--	80	88	87	--	21	19	30	--
Co[2]	46	--	--	--	--	--	--	--	21	--	34	35
F[3]	492	--	170	180	75	--	20	--	380	380	310	--
Br[2]	1	--	--	--	--	--	--	--	2	--	4	3
Ga[1]	29	27	20	--	16	15	16	--	27	29	25	--
S[1]	b.d.	b.d.	b.d.	--	b.d.	b.d.	1120	--	b.d.	b.d.	b.d.	--
Sn[1]	9	10	12	--	10	8	7	--	7	9	9	--
Ti[1]	4490	4490	2870	--	1210	1240	746	--	2840	2830	2850	--
Zn[1]	64	68	54	--	58	61	61	--	59	64	34	--
Zn[2]	60	--	--	--	--	--	--	--	40	--	b.d.	b.d.

APPENDIX F. Table F.2 (continued)

	IM-173		IM-185		IM-225		IM-241		IM-254		IM-296	
Na[2]	10000	--	--	--	--	--	--	--	33000	--	30000	31000
Ca%[2]	11	--	--	--	--	--	--	--	3.5	--	3.5	4
Cu[1]	7	9	b.d.	--	25	25	20	--	61	62	45	--
Fe%[2]	8.05	--	--	--	--	--	--	--	4.17	--	7.49	7.78
Mo[1]	b.d.	b.d.	b.d.	--	b.d.	b.d.	b.d.	--	b.d.	b.d.	b.d.	--
Cs[2]	1	--	--	--	--	--	--	--	1	--	b.d.	b.d.
La[2]	2.6	--	--	--	--	--	--	--	7.8	--	8.1	8.1
Ce[2]	8	--	--	--	--	--	--	--	19	--	17	17
Nd[2]	6	--	--	--	--	--	--	--	9	--	9	8
Sm[2]	2.1	--	--	--	--	--	--	--	2.6	--	2.2	2.1
Eu[2]	0.9	--	--	--	--	--	--	--	0.9	--	0.5	0.6
Tb[2]	b.d.	--	--	--	--	--	--	--	0.5	--	b.d.	b.d.
Yb[2]	0.9	--	--	--	--	--	--	--	2.1	--	1.7	1.8
Lu[2]	0.15	--	--	--	--	--	--	--	0.03	--	0.23	0.24
Sb[2]	b.d.	--	--	--	--	--	--	--	0.5	--	0.2	0.2
W[2]	62	--	--	--	--	--	--	--	85	--	36	34

[1] XRF Pressed Pellet
[2] Neutron Activation
[3] Wet Chemistry
[4] XRF Fused Pellet

APPENDIX F. Table F.3. Duplicate analyses of REE and some trace elements by ICP-MS for one rock from the Iron Mask batholith and one Kamloops Lake picritic basalt.

	IM-225 Carabine Creek picritic basalt		IM-120 Type III Iron Mask hybrid	
Li	6.91	6.57	11.05	8.62
Be	0.51	0.65	0.66	b.d.
Sc	18.09	18.27	47.91	48.2
V	106.36	110.91	478.67	484.04
Rb	31.92	31.11	12.46	12.42
Sr	221.87	216.44	1190.36	1179.43
Y	4.36	4.34	14.22	14.05
Zr	10.62	11.8	12.41	12.06
Nb	0.56	0.59	0.6	0.53
Mo	0.07	0.11	0.25	0.17
Cs	0.65	0.63	1.02	1.01
Ba	142.27	138.88	204.7	210.19
La	0.99	0.99	4.04	4.18
Ce	2.32	2.39	10.5	10.64
Pr	0.35	0.34	1.77	1.82
Nd	1.87	1.78	9.98	10.6
Sm	0.6	0.53	2.98	3.04
Eu	0.21	0.17	1.11	1.11
Gd	0.75	0.72	3.42	3.58
Tb	0.11	0.11	0.49	0.47
Dy	0.78	0.82	3.22	3.06
Ho	0.17	0.15	0.58	0.59
Er	0.46	0.51	1.56	1.47
Tm	0.07	0.07	0.2	0.21
Yb	0.42	0.54	1.22	1.18
Lu	0.07	0.08	0.17	0.17
Hf	0.42	0.51	0.62	0.64
Ta	0.33	0.37	0.39	0.34
Tl	b.d.	0.23	0.14	b.d.
Pb	1.68	1.5	0.59	0.6
Bi	0.08	0.07	0.12	0.02
Th	0.18	0.23	0.13	0.1
U	0.06	0.09	0.12	0.11

APPENDIX F. Table F.4. Reproducibility on major (wt%) and trace (ppm) element composition of SY-2 and in-house standards (P-1, WP-1); accepted values are explained in text.

Element	Method	D.L.	P-1 Accepted Value Mean	1s	n	P-1 Measured Mean	1s	n	WP-1 Accepted Value Mean	1s	n	WP-1 Measured Mean	1s	n	Accepted Value SY-2	SY-2 Measured Mean	1s	n
SiO_2	XRFF	0.01	69.66	0.41	11	69.55	0.06	4	64.08	0.32	10	63.70	0.42	4	60.10	59.40	0.32	6
TiO_2	XRFF	0.01	0.404	0.013	11	0.423	0.008	4	0.520	0.013	10	0.544	0.013	4	0.14	0.17	0.02	6
Al_2O_3	XRFF	0.01	14.46	0.17	11	14.43	0.05	4	16.64	0.13	10	16.55	0.21	4	12.12	12.03	0.08	6
Fe_2O_3(T)	XRFF	0.01	3.77	0.07	11	3.81	0.08	4	4.39	0.10	10	4.39	0.12	4	6.30	6.21	0.12	6
FeO	Wet	0.1	2.01	0.07	11	2.00	0.00	2	2.32	0.06	10	2.30	0.19	3				
MnO	XRFF	0.01	0.09	0.00	11	0.09	0.00	4	0.09	0.00	10	0.09	0.00	4	0.32	0.32	0.00	6
MgO	XRFF	0.01	1.09	0.02	11	1.11	0.01	4	2.64	0.05	10	2.68	0.09	4	2.70	2.69	0.03	6
CaO	XRFF	0.01	3.58	0.07	11	3.66	0.07	4	5.14	0.07	10	5.14	0.04	4	7.98	7.94	0.05	6
Na_2O	XRFF	0.01	4.01	0.08	11	4.10	0.11	4	4.41	0.08	10	4.46	0.11	4	4.34	4.35	0.04	6
K_2O	XRFF	0.01	2.06	0.08	11	2.03	0.04	4	1.61	0.06	10	1.56	0.03	4	4.48	4.40	0.02	6
P_2O_5	XRFF	0.01	0.09	0.00	11	0.09	0.00	4	0.18	0.00	10	0.18	0.00	4	0.43	0.43	0.01	6
H_2O+	Grav	0.1	0.5	0.1	11	0.5	0.0	4	0.3	0.1	10	0.3	0.1	4				
CO_2	Grav	0.01	0.02	0.01	11	0.02	0.01	4	0.02	0.01	10	0.01	0.00	4				
SUM	Lab		99.9	0.6	11	99.9	0.2	4	100.2	0.3	10	99.7	0.7	4		98.35	0.35	2
LOI	Grav		0.5	0.1	11	0.5	0.1	4	0.3	0.1	10	0.3	0.1	4				
Ba	XRFP	20				708	7	2				607		1	460	387	52	2
Ba	INAA	100	836	92	11	900	0	2	680	92	10	675	50	4	460			
Rb	XRFP	2				48	0	2				22		1	220	209	7	2
Rb	INAA	20	37	18	11	45	7	2	22	17	10	20	8	4	220			
Sr	XRFP	2				218	16	2				737		1	275	282	7.8	2
Sr	INAA	500	250	0	11	250	0	2	525	312	10	725	171	4	275			
Nb	XRFP	2	5	2	11	8	1	4	6	2	11	8	1	4	23	25		2
Zr	XRFP	3				115	3	2	142		1	130		1	280	280	5	2
Y	XRFP	2	17	7	11	7	4	4	5	5	11	1	0	4	130	124	12	2
As	INAA	2	1	0	11	1	0	2	1	0	10	1	0	4				
Au	INAA	5	2	1	11	2	0	2	2	0	10	2	0	4				
Ni	XRFP	2	1	1	11	2	1	4	35	1	10	35	3	4				
Cr	INAA	2	126	8	11	150	0	2	62	5	10	64	4	4				
Cr	XRFF	10	106	53	11	143	11	4	58	20	10	82	9	4	12	30	11	6
S	XRFP	50	20	0	11	20	0	4	20	0	10	20	0	4				
Sc	INAA	0.1	10.6	0.3	11	11.8	0.1	2	9.6	0.5	10	9.3	0.3	4				
Th	XRFP	2				4	3	2	1		1	2		1				
Th	INAA	0.5	3.9	0.3	11	4.4	0.2	2	1.9	0.2	10	1.8	0.1	4				
U	INAA	0.5	1.5	0.2	11	1.7	0.1	2	0.9	0.2	10	0.8	0.1	4				
Pb	XRFP	2	5	3	11	6	2	4	5	3	10	4	3	4				
Hf	INAA	0.5	3.5	0.5	11	3.9	0.2	2	3.2	0.4	10	3.0	0.3	4				
Cl	XRFP	50	79	44	11	136	34	4	241	27	10	283	29	4				

APPENDIX F. Table F.4 (continued)

Element	Method	D.L.	P-1 Accepted Value Mean	P-1 Accepted Value 1s	P-1 Accepted Value n	P-1 Iron Mask Mean	P-1 Iron Mask 1s	P-1 Iron Mask n	WP-1 Accepted Value Mean	WP-1 Accepted Value 1s	WP-1 Accepted Value n	WP-1 Iron Mask Mean	WP-1 Iron Mask 1s	WP-1 Iron Mask n	Accepted Value SY-2	SY-2 Iron Mask Mean	SY-2 Iron Mask 1s	SY-2 Iron Mask n
Co	XRFP	2				12	1	2				12		1				
Co	INAA	1	9	1	11	10	1	2	15	1	10	13	1	4				
F	Wet	20	205	45	11	227	27	4	275	48	10	294	21	4				
Br	INAA	1	2	1	11	2	1	2	3	1	10	2	1	4				
Ga	XRFP	3				24	1	2				29		1				
Sn	XRFP	5				5	4	2				6		1				
Ti	XRFP	5				2035	7	2				2680		1				
Zn	XRFP	2	50	2	11	50	3	4	61	8	10	57	3	4				
Zn	INAA	40	76	66	11	75	7	2	70	25	10	53	22	4				
Na	INAA	100	27636	674	11	31000	0	2	30800	1476	10	30000	816	4				
Ca	INAA	0.5	3	0	11	2	0	2	4	1	10	3	0	4				
Cu	XRFP	2	2	2	11	4	4	4	7	4	10	9	2	4				
Fe	INAA	0.05	2.60	0.10	11	2.80	0.09	2	2.93	0.16	10	2.83	0.13	4				
Mo	XRFP	2	1	0	11	1	0	4	1	0	10	1	0	4				
Cs	INAA	1	1	1	11	2	1	2	1	1	10	1	0	4				
La	INAA	0.5	13.3	0.9	11	14.7	0.2	2	13.8	1.1	10	13.6	0.5	4				
Ce	INAA	3	26	2	11	31	1	2	27	3	10	28	1	4				
Nd	INAA	5	11	1	11	13	0	2	12	1	10	13	1	4				
Sm	INAA	0.1	2.3	0.2	11	2.8	0.0	2	2.5	0.4	10	2.7	0.1	4				
Eu	INAA	0.2	0.8	0.1	11	0.8	0.2	2	0.9	0.2	10	1.0	0.2	4				
Tb	INAA	0.5	0.3	0.2	11	0.4	0.3	2	0.2	0.1	10	0.2	0.0	4				
Yb	INAA	0.2	2.1	0.1	11	2.5	0.1	2	1.2	0.1	10	1.2	0.1	4				
Lu	INAA	0.05	0.35	0.02	11	0.42	0.02	2	0.19	0.02	10	0.18	0.02	4				
Sb	INAA	0.2	0.2	0.1	11	0.3	0.1	2	0.1	0.0	10	0.1	0.1	4				
W	INAA	3	1	1	11	1	0	2	1	0	10	1	0	4				

D.L. - Detection Limit
XRFF - XRF Fused Pellet
XRFP - XRF Pressed Pellet
INAA - Neutron Activation
n - Number of Analyses

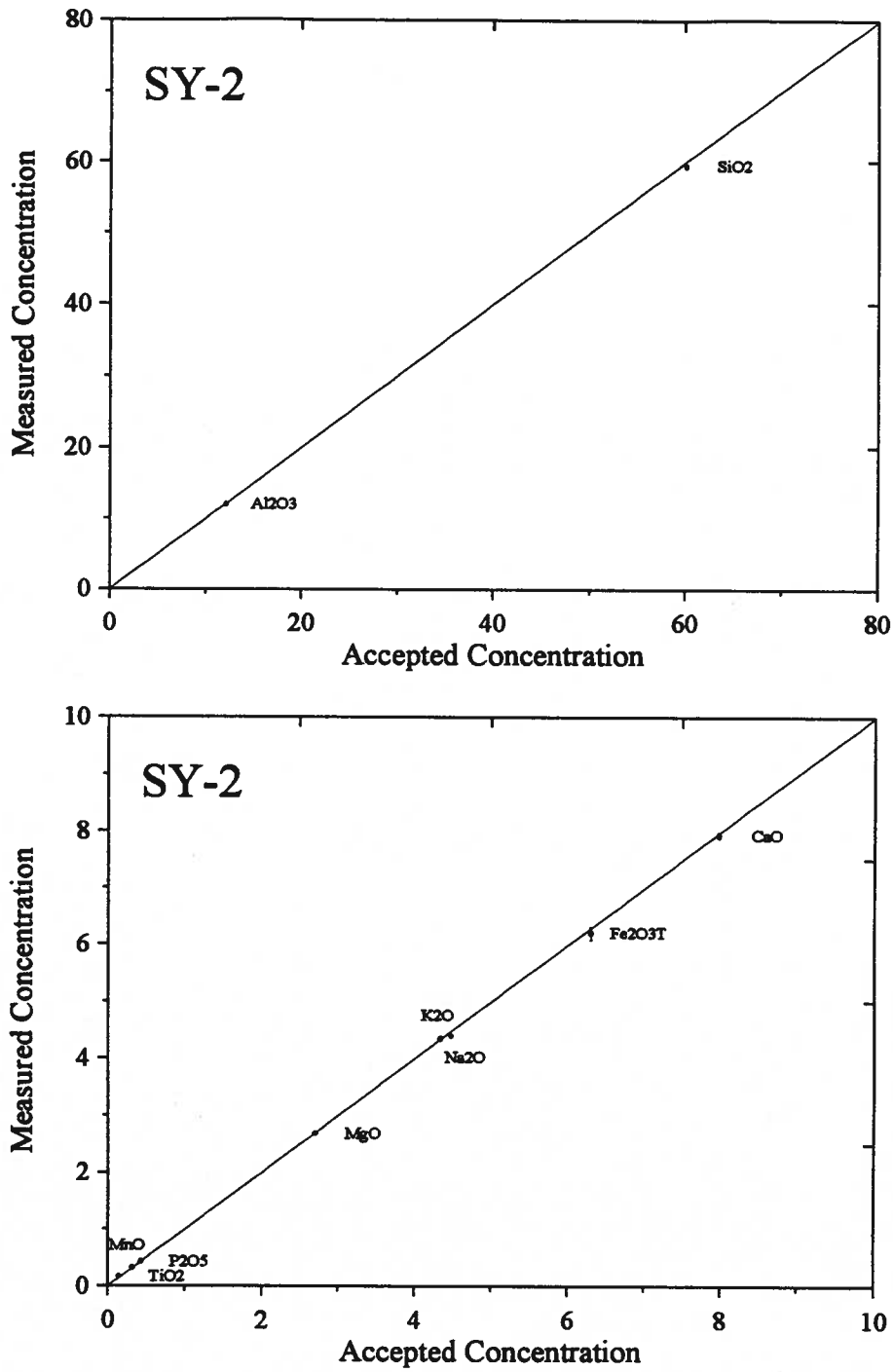

Figure F.1a. Accepted concentration *vs* measured concentration for major element determinations on International Standard SY-2. Error bars are 1s; accepted values from Govindaraju (1984).

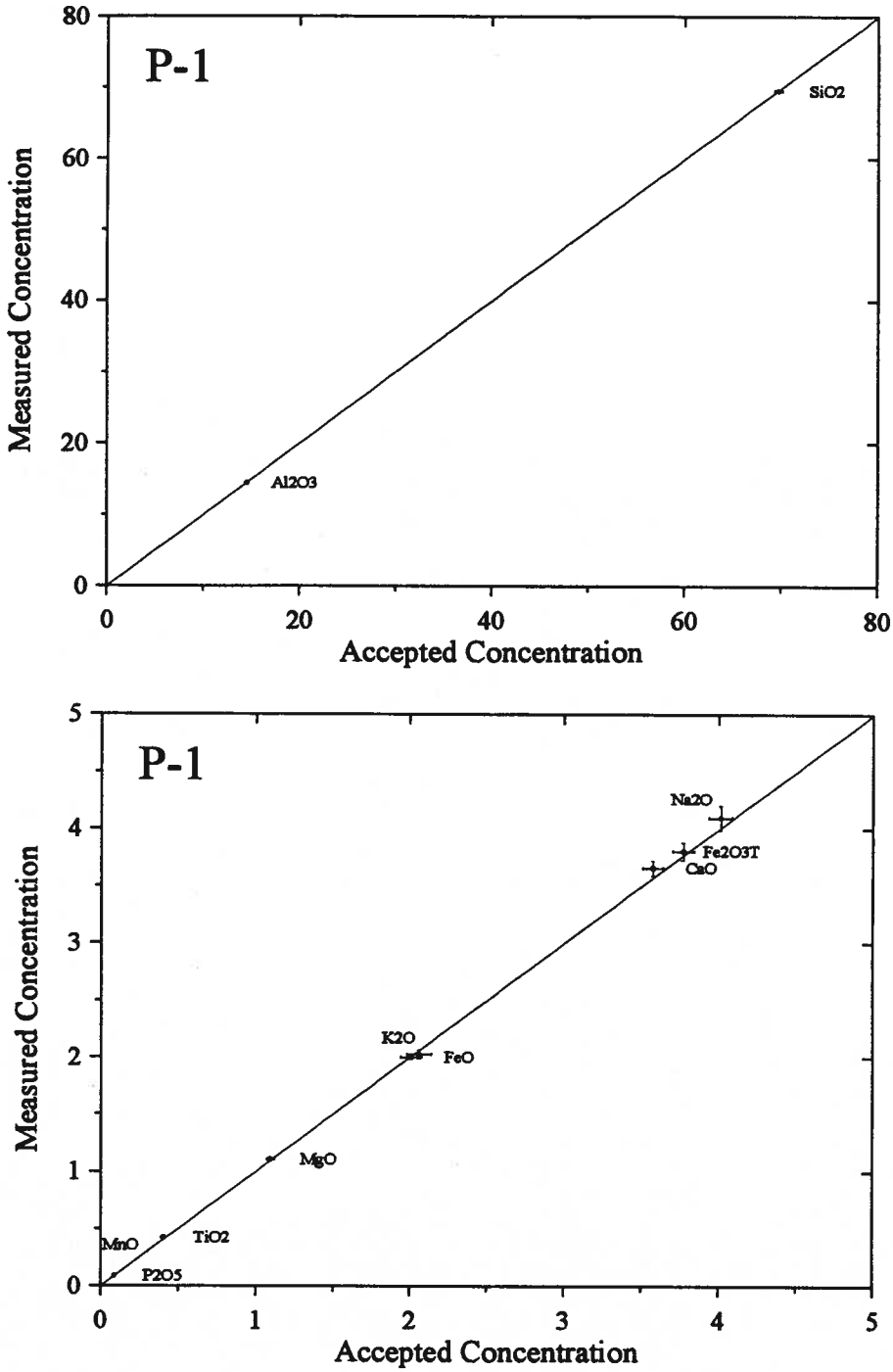

Figure F.1b. Accepted concentation *vs* measured concentration for major element determinations on in-house standard P-1. Error bars are 1s; accepted values from Bartch (1993).

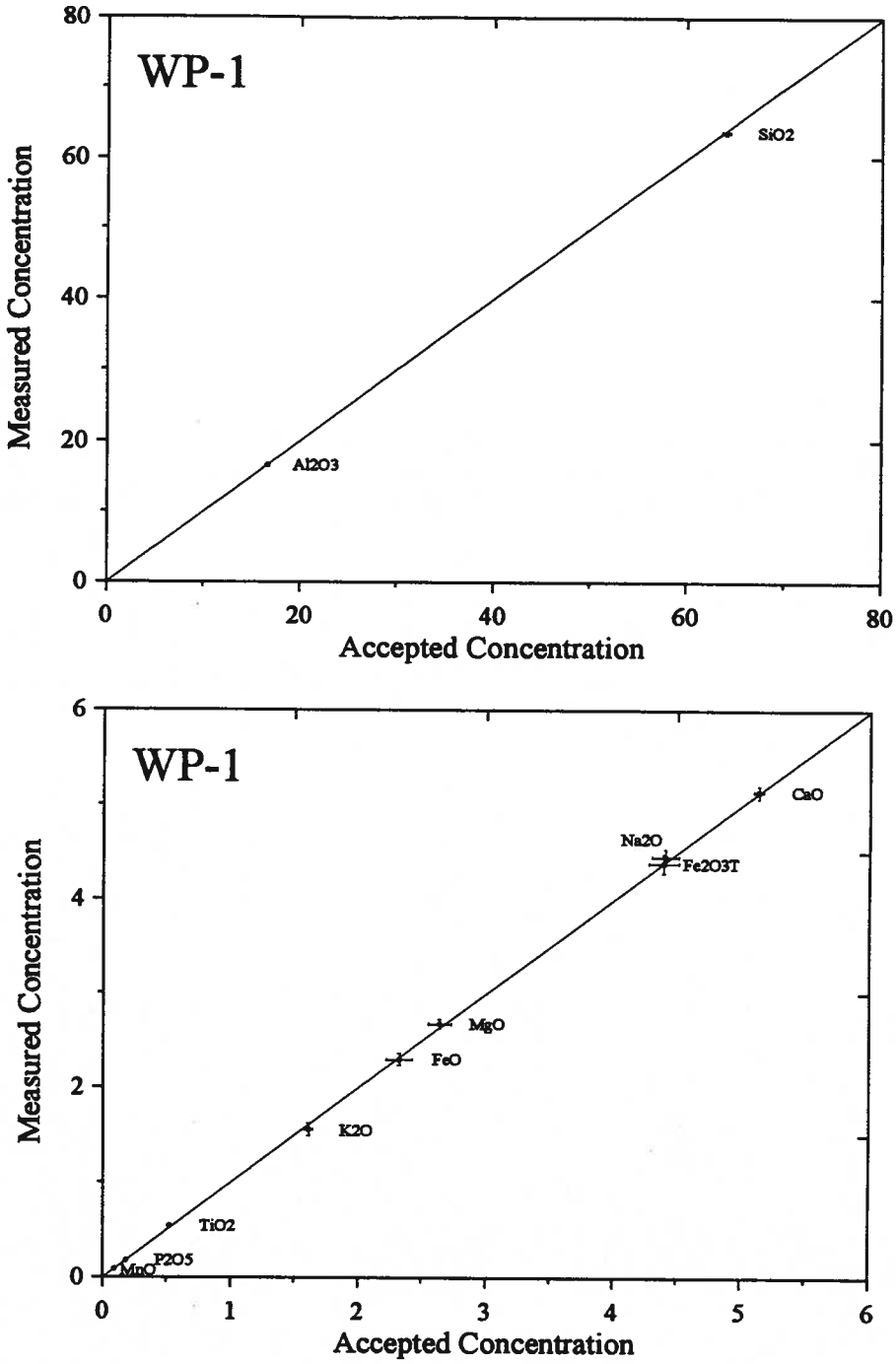

Figure F.1c. Accepted concentation *vs* measured concentration for major element determinations on in-house standard WP-1. Error bars are 1s; accepted values from Bartch (1993).

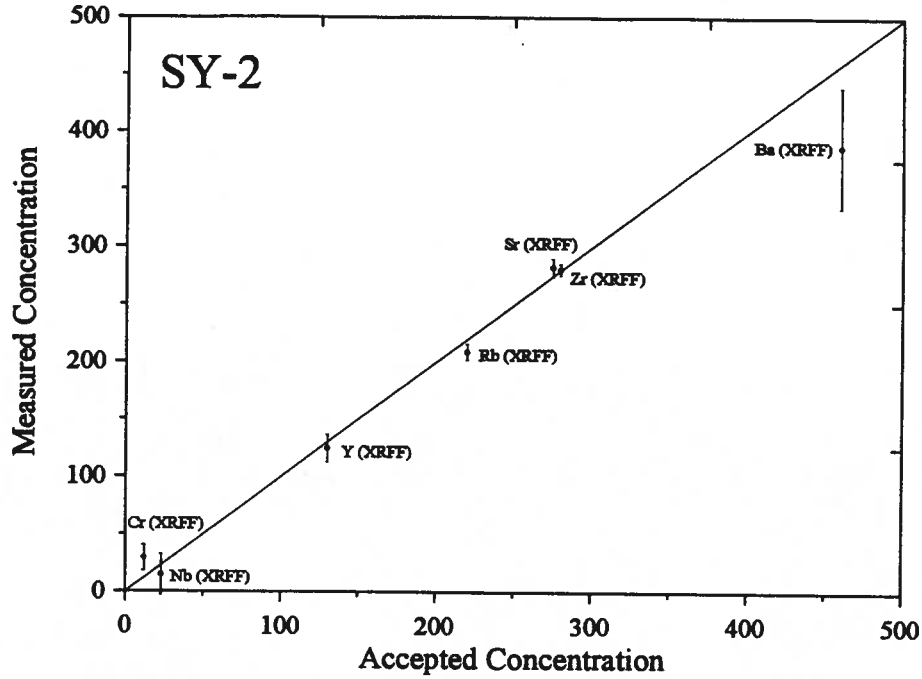

Figure F.2a. Accepted concentration *vs* measured concentration for trace element determinations on International Standard SY-2. Error bars are 1s; accepted values from Govindaraju (1984).

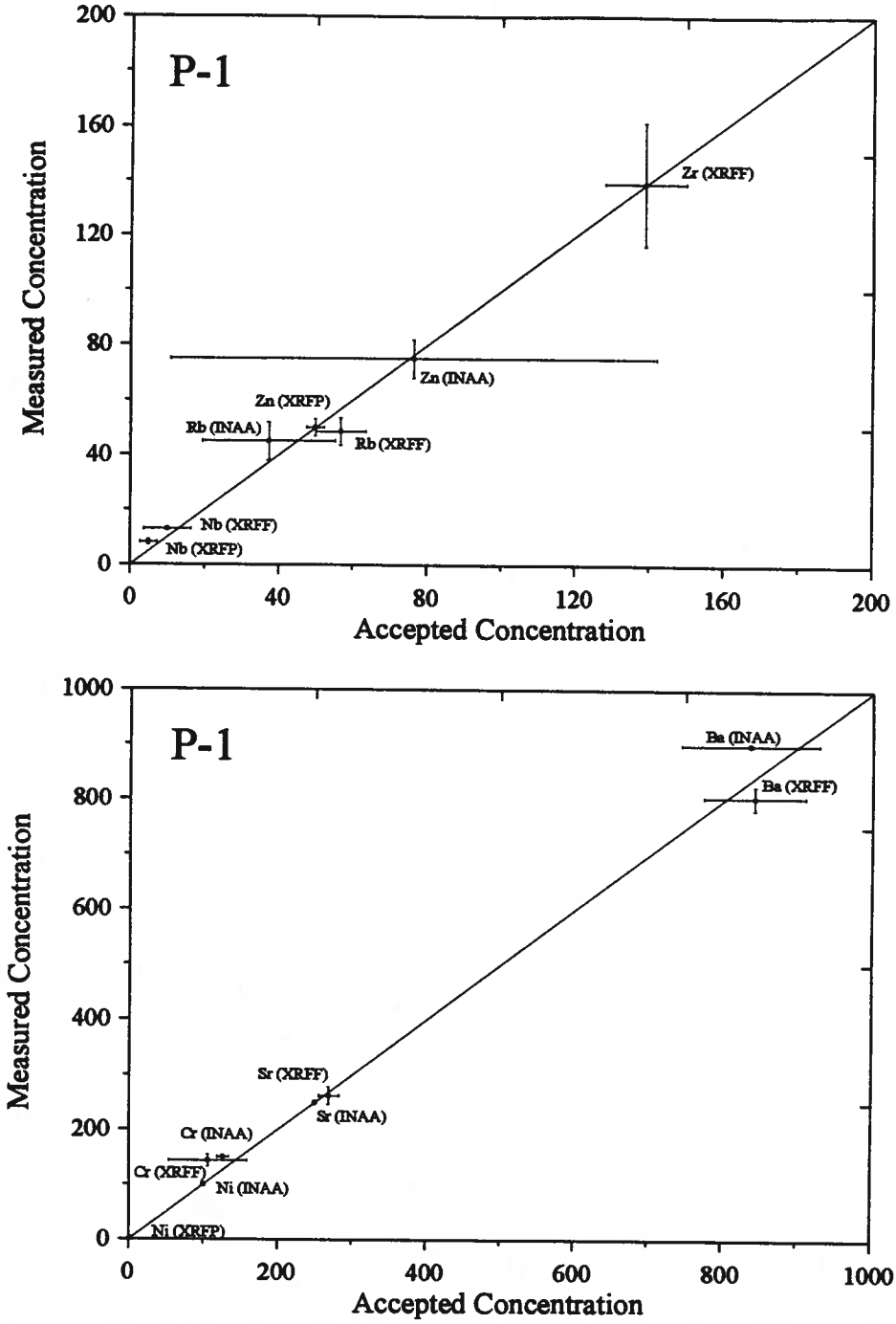

Figure F.2b. Accepted concentration *vs* measured concentration for trace element determinations on in-house standard P-1. Error bars are 1s; accepted values from Bartch (1993).

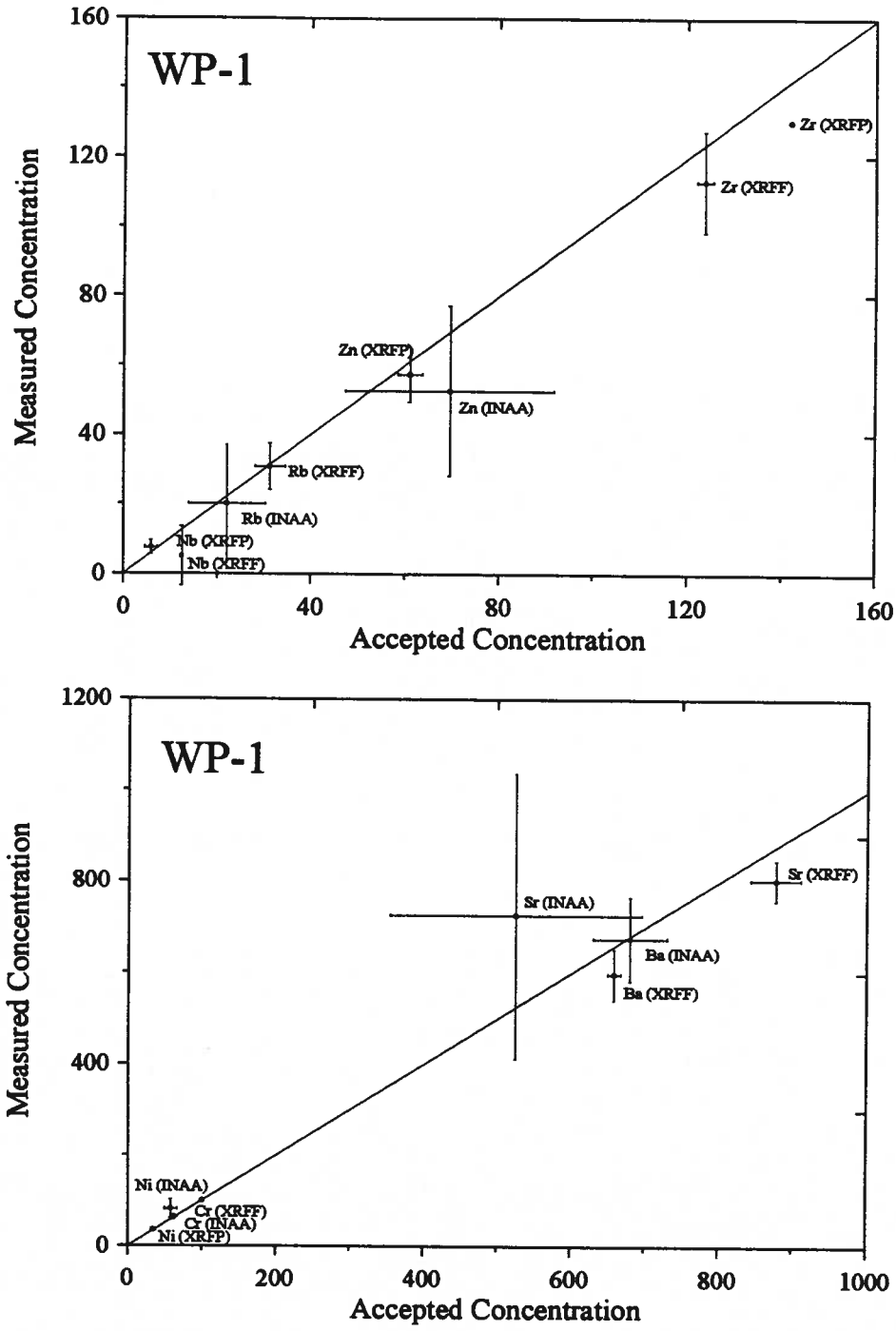

Figure F.2c. Accepted concentration *vs* measured concentration for trace element determinations on in-house standard WP-1. Error bars are 1s; accepted values from Bartch (1993).

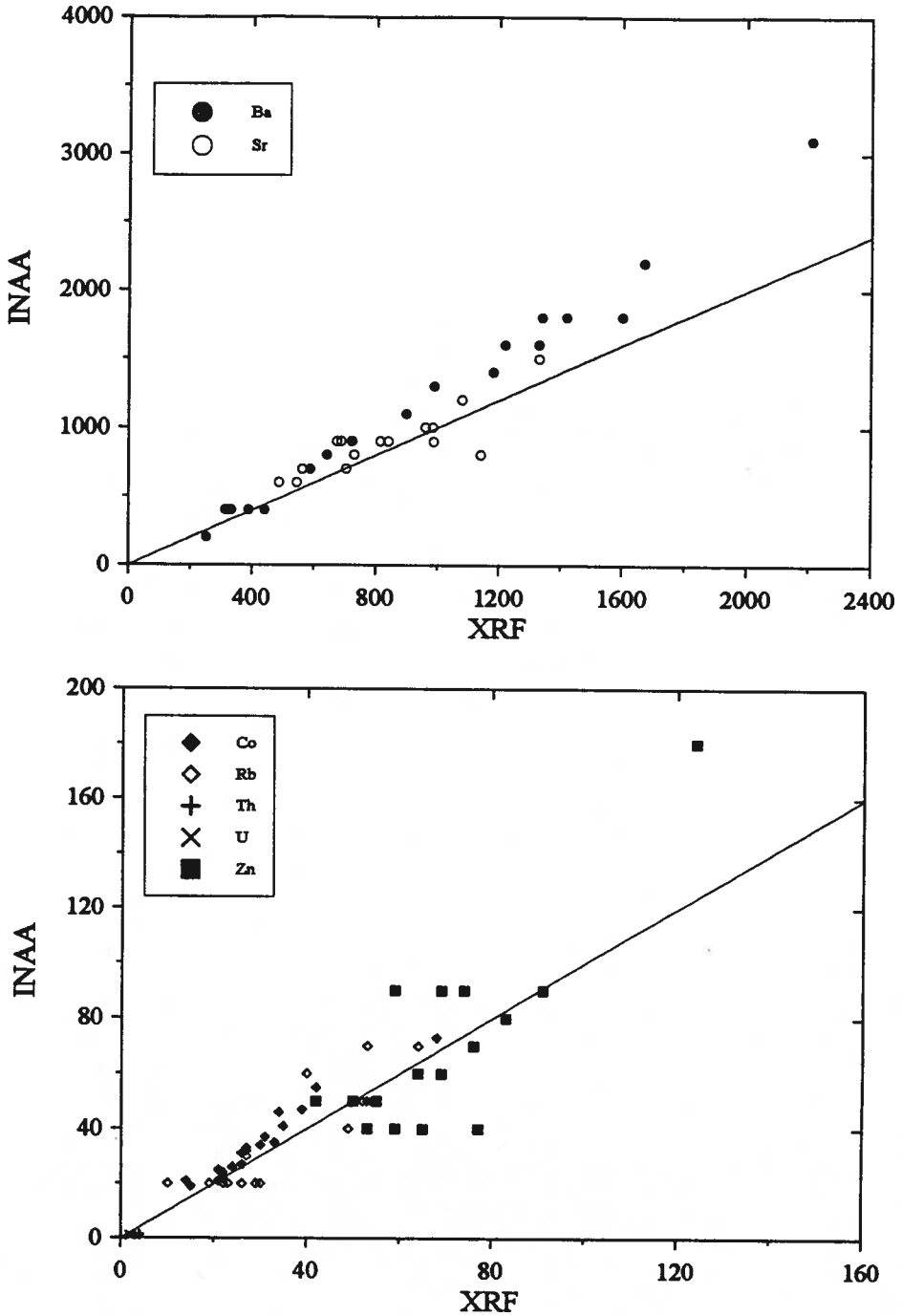

Figure F.3a. XRF *vs* INAA analytical techniques for trace element determinations.

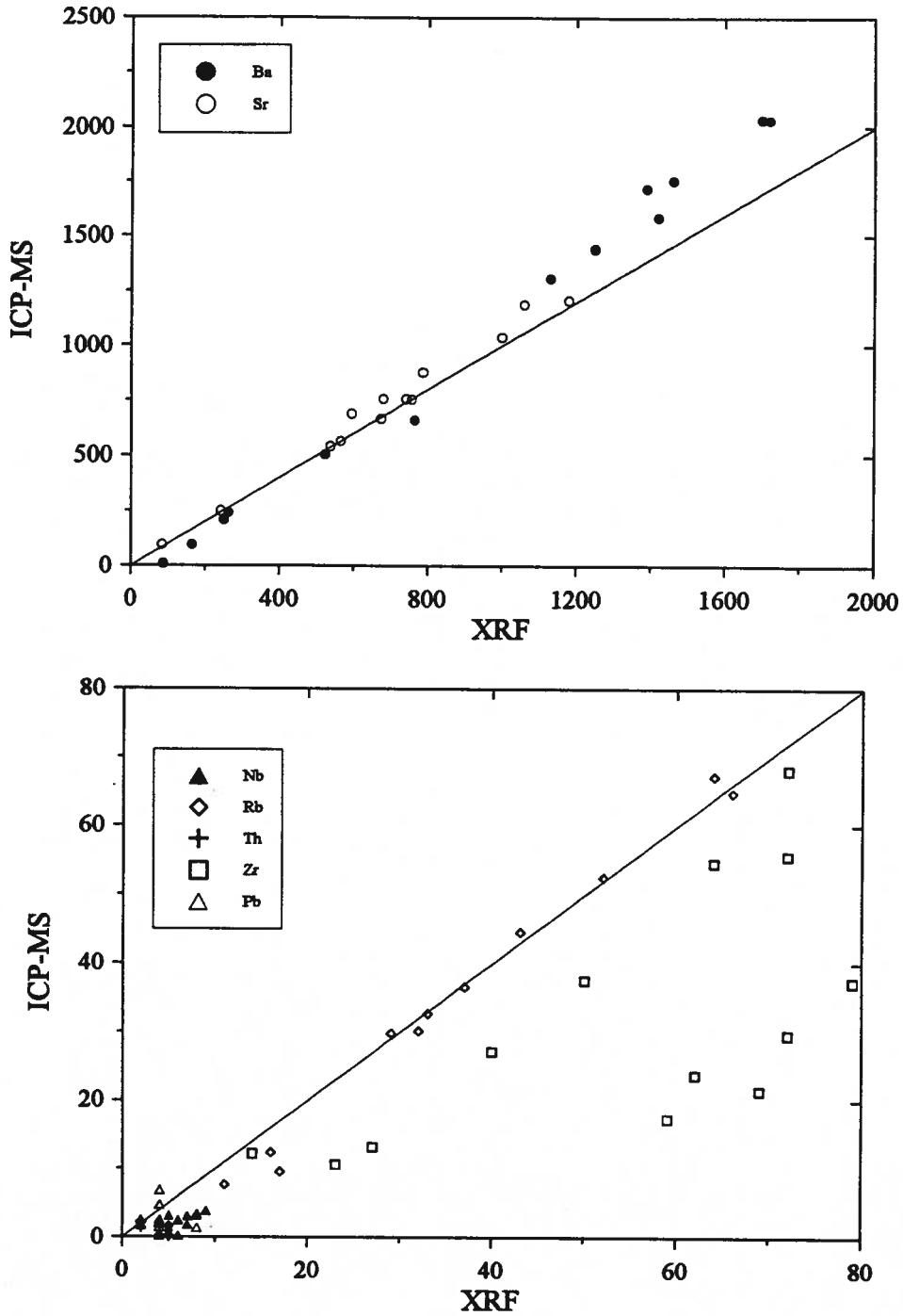

Figure F.3b. XRF *vs* ICP-MS analytical techniques for trace element determinations.

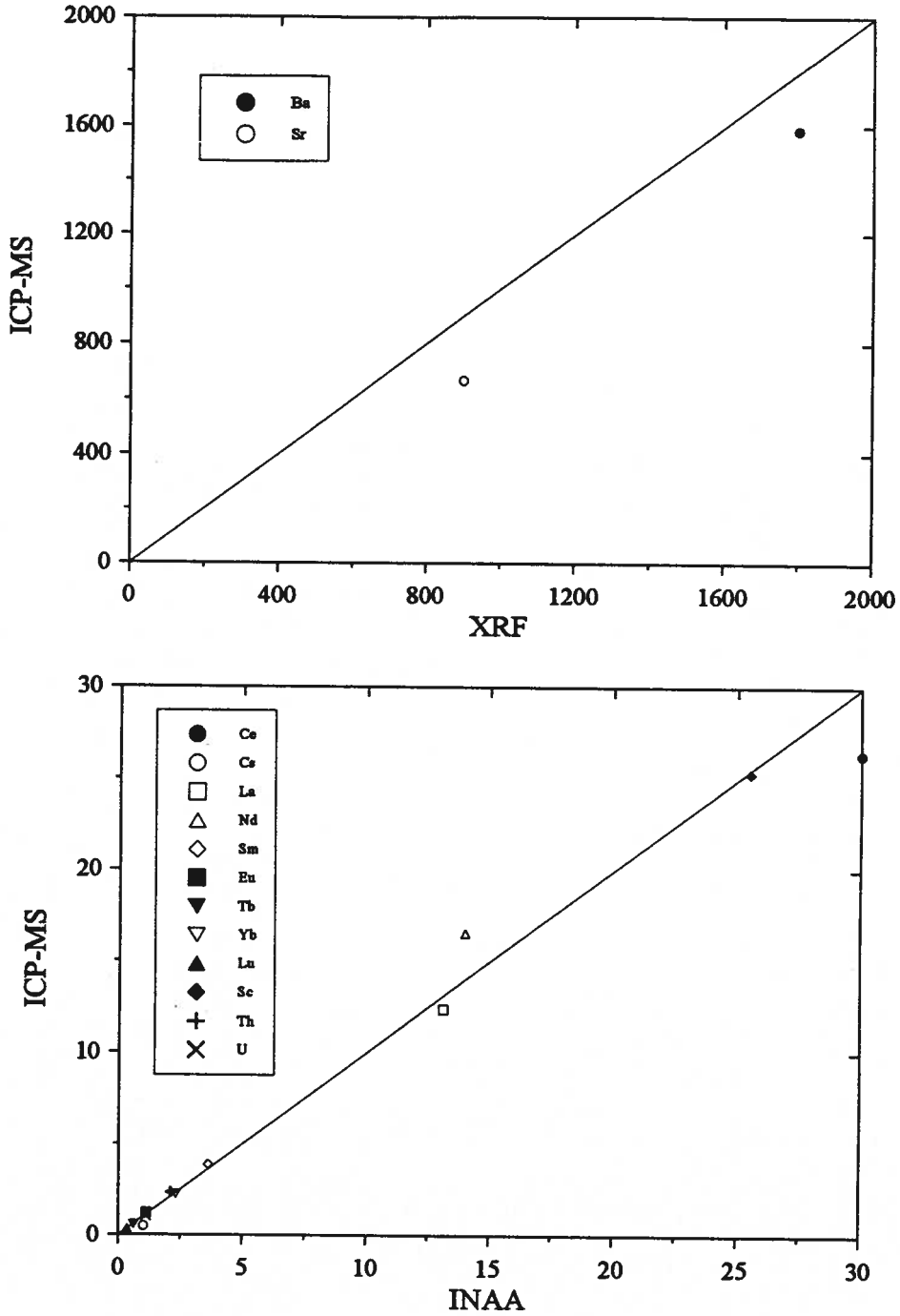

Figure F.3c. INAA *vs* ICP-MS analytical methods for trace element determinations.

APPENDIX G. Rock preparation and analytical methods.

G.1 POWDER PREPARATION

Samples selected for geochemical analyses were processed at the University of British Columbia. Clean samples of approximately $6cm^2$ were crushed to less than 1cm in a jaw crusher. Rock chips were hand sorted to ensure no weathered surfaces, fracture surfaces or alteration veinlets were included. The finest material was discarded. These chips were pulverized to approximately -200 mesh in a tungsten carbide shatterbox using a minimal amount of time to prevent oxidation of the rock. The powder was sieved through 200 mesh nylon fiber. The above procedures were repeated until approximately 0.4l of powder was obtained. The fractions were homogenized and then split and submitted to commercial analytical laboratories.

G.2 ANALYTICAL METHODS

Major, minor and trace element concentrations were determined at XRAL laboratories in Don Mills, Ontario. Major elements and most minor and trace elements were determined by XRF Pressed Pellet. Some trace and rare earth elements were determined by neutron activation. For sample and element specific details, see Appendices E and F.

Some trace and all rare earth elements concentrations were determined the University of Saskatchewan on an Elan-5000 inductively coupled plasma mass spectrometer (ICP-MS) following the procedure described by Jenner et al. (1990). Duplicate analyses are given in Appendix F.

Some FeO measurements were made at the University of British Columbia. A maximum FeO wt% was estimated for each sample. Ammonium meta-vanadate (NH_4VO_3) was added to approximately 0.500g of -200 mesh sample in the ratio of 0.01g NH_4VO_3 for each 1.0g of estimated FeO. NH_4VO_3 was

measured to 5 decimal places of accuracy. This mixture was dissolved in HF acid. After dissolution, the sample was transferred to a flask containing approximately 50ml boric acid and 150ml H_2O by repeated rinsing of the dissolution container with cold H_2SO_4 and H_2O. A few drops of barium diphenylamine sulphonate solution was added to the flask to produce a distinct purple colour. This solution was then titrated with ferrous ammonium sulphate until the colour changes to apple green. Blanks were also run at regular intervals for use as standards. FeO in the sample is calculated by:

$$\%FeO = \frac{61.42}{R} \bullet \frac{(V - v'T)}{t}$$

where v' = wt of NH_4VO_3 in standard
t = titrant of standard
R = wt of sample
V = wt of NH_4VO_3 with sample
T = titrant of sample

The wt% FeO in the sample is calculated from:

$$Fe_2O_3 = Fe_2O_3\ (Total) - FeO^*$$

where FeO* = Fe_2O_3 equivalent FeO.